



UNIVERSITY OF IOANNINA
SCHOOL OF SCIENCES AND TECHNOLOGIES
DEPARTMENT OF MATERIALS SCIENCE AND ENGINEERING

Computational modelling of parametric stent design
in human atherosclerotic arteries

Georgia Karanasiou

A thesis submitted to University of Ioannina in partial fulfillment
of the requirement for the degree of

Masters in Engineering

Department of Materials Science and Engineering,

University of Ioannina

Month 9 Year 2018

Director of Research: Prof. Dimitrios I. Fotiadis



ΕΛΛΗΝΙΚΗ ΔΗΜΟΚΡΑΤΙΑ
ΠΑΝΕΠΙΣΤΗΜΙΟ ΙΩΑΝΝΙΝΩΝ
ΠΟΛΥΤΕΧΝΙΚΗ ΣΧΟΛΗ
ΤΜΗΜΑ ΜΗΧΑΝΙΚΩΝ ΕΠΙΣΤΗΜΗΣ ΥΛΙΚΩΝ
ΠΡΟΓΡΑΜΜΑ ΜΕΤΑΠΤΥΧΙΑΚΩΝ ΣΠΟΥΔΩΝ
«ΠΡΟΗΓΜΕΝΑ ΥΛΙΚΑ»

ΜΕΤΑΠΤΥΧΙΑΚΗ ΔΙΑΤΡΙΒΗ

Γεωργία Καρανάσιου

ΤΙΤΛΟΣ ΜΕΤΑΠΤΥΧΙΑΚΗΣ ΔΙΑΤΡΙΒΗΣ
ΥΠΟΛΟΓΙΣΤΙΚΗ ΠΑΡΑΜΕΤΡΙΚΗ ΜΟΝΤΕΛΟΠΟΙΗΣΗ
ΕΚΠΤΥΞΗΣ ΕΝΔΟΠΡΟΘΕΣΗΣ ΣΕ ΠΡΑΓΜΑΤΙΚΕΣ ΑΡΤΗΡΙΕΣ

ΙΩΑΝΝΙΝΑ, 2018

Εσώφυλλο:

Η παρούσα Μεταπτυχιακή Διατριβή εκπονήθηκε στο πλαίσιο των σπουδών για την απόκτηση του Μεταπτυχιακού Διπλώματος Ειδίκευσης στην εξειδίκευση:

Βιοϋλικά και Βιοιατρική Τεχνολογία

που απονέμει το Τμήμα Μηχανικών Επιστήμης Υλικών του Πανεπιστημίου Ιωαννίνων.

Εγκρίθηκε τηναπό την εξεταστική επιτροπή:

ΟΝΟΜΑΤΕΠΩΝΥΜΟ

ΒΑΘΜΙΑ

.....Επιβλέπων

Δημήτριος Φωτιάδης

- 1. Δημήτριος Φωτιάδης**, Καθηγητής του ΤΜΕΥ της Πολυτεχνικής Σχολής του Παν/μίου Ιωαννίνων, Επιβλέπων
- 2. Λεωνίδα Γεργίδης**, Επίκουρος Καθηγητής του ΤΜΕΥ της Πολυτεχνικής Σχολής του Παν/μίου Ιωαννίνων, Επιβλέπων
- 3. Λάμπρος Μιχάλης**, Καθηγητής Καρδιολογίας του Πανεπιστημιακού Γενικού Νοσοκομείου Ιωαννίνων

ΥΠΕΥΘΥΝΗ ΔΗΛΩΣΗ

"Δηλώνω υπεύθυνα ότι η παρούσα διατριβή εκπονήθηκε κάτω από τους διεθνείς ηθικούς και ακαδημαϊκούς κανόνες δεοντολογίας και προστασίας της πνευματικής ιδιοκτησίας. Σύμφωνα με τους κανόνες αυτούς, δεν έχω προβεί σε ιδιοποίηση ξένου επιστημονικού έργου και έχω πλήρως αναφέρει τις πηγές που χρησιμοποίησα στην εργασία αυτή."

(Υπογραφή υποψηφίου)

ACKNOWLEDGMENTS

The end of this beautiful journey, the writing of this thesis fulfills me with great feelings since I was not alone in this journey, but I had the support of professors, colleagues and friends. At this point, I would like to express my sincere gratitude to anyone that has contributed in this way to this endeavor.

First of all, I would like to express my sincere thanks to my supervisor, Prof. Dimitris Fotiadis, Professor, Dept. of Materials Science and Engineering, University of Ioannina, who with a profound scientific background on medical informatics has opened a new window on understanding the basic principles of biological systems and biomaterials and the application of information technology in medicine. His continuous trust and support at all stages of my research career is invaluable.

The support of the members of the three-member Advisory Committee of the dissertation, namely Professor Lamrpos Michalis and Professor Leonidas Gergidis on the main research topics of the dissertation, was valuable and lasting. The contribution of Professor Lambros Michalis was decisive from the outset and throughout this research, both at a professional and personal level.

My valuable collaboration with the Harvard-MIT Biomedical Engineering Center (Edelman Lab) Harvard-MIT Group members and mainly with Professor Elazer Edelman, who guided me whenever willingly and was always available for fruitful and constructive discussions that greatly enhanced our synergy.

I would like to thank my colleagues Dr. Giorgos Rigas, Dr. Nick Tachos, Dr. Antonis Sakellarios, Dr. Lambros Athanasios and Kosta Stefanou with whom I collaborated and shared my parallel research interests. Furthermore, I would like to thank Dr. Evanthia Tripoliti for advising me and urging me to continue my effort and for being always beside me in every step. Also, I want to thank my colleagues and friends from the Medical Technology & Intelligent Information Systems Unit (MedLab) for their excellent cooperation and the creation of a very pleasant working environment.

Finally, I thank my family for the over-understanding, the moral support and their unremitting encouragement throughout this time.

This work was part funded by the project “SMARTool - Simulation Modeling of coronary ARtery disease: a tool for clinical decision support, Horizon2020, GA 689068” and the project “InSilc- In-silico trials for drug-eluting BVS design, development and evaluation, Horizon2020, GA 777119”.

I would also like to express my sincere thanks to Rontis Corporation S.A., which has provided me with useful information on the stent and for the excellent cooperation we have had.

ΕΥΧΑΡΙΣΤΙΕΣ

Ολοκληρώνοντας αυτό το όμορφο ταξίδι, η συγγραφή αυτής της ενότητας μου δίνει ιδιαίτερη χαρά, γνωρίζοντας ότι στην πορεία αυτή δεν ήμουν μόνη, αλλά είχα την υποστήριξη αξιόλογων καθηγητών, συναδέλφων αλλά και φίλων. Στο σημείο αυτό θα ήθελα να εκφράσω την ειλικρινή ευγνωμοσύνη μου γιατί ο καθένας συνέβαλλε με τον τρόπο του σε αυτήν την προσπάθεια.

Αρχικά, θα ήθελα να ευχαριστήσω θερμά τον επιβλέποντα καθηγητή μου κ. Δημήτρη Φωτιάδη, ο οποίος με βαθύ επιστημονικό υπόβαθρο σε θέματα ιατρικής πληροφορικής μου άνοιξε ένα νέο παράθυρο σε πολύ ενδιαφέρουσες αναζητήσεις για την κατανόηση των βασικών αρχών λειτουργίας των βιολογικών συστημάτων και των βιοϋλικών και την εφαρμογή της πληροφορικής στην ιατρική. Η συνεχής εμπιστοσύνη και υποστήριξη σε όλα τα στάδια της ερευνητικής μου διαδρομής είναι ανεκτίμητη.

Η διακριτική στήριξη των μελών της Τριμελούς Επιτροπής παρακολούθησης της διατριβής, δηλ. του Καθηγητή κ. Λάμπρου Μιχάλη και του Επίκουρου Καθηγητή κ. Λεωνίδα Γεργίδη σε θέματα κυρίως ερευνητικών κατευθύνσεων της διατριβής ήταν πολύτιμη και διαρκής. Η συμβολή του Καθηγητή κ. Λάμπρου Μιχάλη ήταν καθοριστική από την αρχή και καθόλη την διάρκεια της έρευνας αυτής, τόσο σε επαγγελματικό όσο και προσωπικό επίπεδο. Σημαντικό ρόλο στην εκπόνηση της παρούσας διατριβής έπαιξε και η συνεργασία μου με τα μέλη της ομάδας του Κέντρου Βιοϊατρικής Τεχνολογίας στο Harvard-MIT (Harvard-MIT Biomedical Engineering Center, or Edelman Lab) και κυρίως του Καθηγητή κ. Elazer Edelman, ο οποίος με καθοδηγούσε όποτε χρειαζόταν με προθυμότητα και ήταν πάντα διαθέσιμος για πλούσιες και εποικοδομητικές συζητήσεις που ενισχύαν σε μεγάλο βαθμό την μεταξύ μας συνέργεια. Θα ήθελα επίσης να εκφράσω τις θερμές ευχαριστίες μου στην εταιρεία Rontis Corporation S.A., η οποία μου διέθεσε πολύτιμες πληροφορίες σχετικές με τα stent καθώς και για την άψογη συνεργασία που είχαμε.

Θα ήθελα να ευχαριστήσω τους συνεργάτες μου Δρ. Γιώργο Ρήγα, Δρ. Νικόλαο Τάχο, Δρ. Αντώνη Σακελάριο, Δρ. Λάμπρο Αθανασίου και κ. Κώστα Στεφάνου με τους οποίους συνεργάστηκα και μοιράστηκα παράλληλη ερευνητική πορεία. Περαιτέρω, θα ήθελα να ευχαριστήσω την Δρα. Ευανθία Τριπολίτη και τον Καθηγητή Θεμιστοκλή Έξαρχο που με συμβούλευαν και με παρότρυναν να συνεχίσω την προσπάθεια μου και ήταν πάντα δίπλα μου σε κάθε μου βήμα. Επίσης, να ευχαριστήσω όλους τους

συνεργάτες και φίλους μου από την Μονάδα Ιατρικής Τεχνολογίας & Ευφών Πληροφοριακών Συστημάτων (MedLab) για την άψογη συνεργασία αλλά και την δημιουργία ενός ιδιαίτερα ευχάριστου εργασιακού περιβάλλοντος.

Τέλος, ευχαριστώ την οικογένειά μου για την υπέρμετρη κατανόηση, την ηθική συμπαράσταση και υποστήριξη που έδειξαν όλο αυτό το διάστημα αλλά και την αγάπη τους που μου εξασφάλισε συνθήκες ηρεμίας.

Η παρούσα εργασία χρηματοδοτήθηκε στα πλαίσια του Ευρωπαϊκά Χρηματοδοτούμενου Προγράμματος “SMARTool - Simulation Modeling of coronary ARTery disease: a tool for clinical decision support, Horizon2020, GA 689068” και “InSilc- In-silico trials for drug-eluting BVS design, development and evaluation, Horizon2020, GA 777119”.

TABLE OF CONTENTS

Chapter 1: Introduction	1
1.1 Cardiovascular disease	1
1.2 Imaging modalities	7
1.3 Treatment options for coronary atherosclerosis	15
1.4 Angioplasty, stenting and by-pass	16
1.5 Evolution of coronary stenting	16
1.6 Considerations in relation to stenting	19
1.7 Mechanisms or restenosis.....	19
1.7.1 Pathophysiology of restenosis	20
1.7.1.1 The early phase: endothelium injury and inflammatory response.....	21
1.7.1.2 Granulation tissue formation	22
1.7.1.3 Tissue remodelling phase	22
1.7.2 Thrombosis.....	22
1.7.2.1 Pathophysiology and factors implicated in stent thrombosis.....	23
1.8 Objective of the thesis	24
1.8.1 Thesis structure.....	24
Chapter 2: Stent Coronary Market.....	27
Chapter 3: Stents and desirable characteristics.....	31
3.1 Properties of an ideal coronary stent	31
3.2 Expansion	32
3.3 A materials perspective	33
3.3.1 Properties of SS316	34
3.3.2 Properties of Pt–Ir alloys	34
3.3.3 Properties of Tantalum	35
3.3.4 Properties of Co–Cr alloy.....	35
3.3.5 Properties of Ti.....	35
3.3.6 Properties of Ni–Ti.....	35
3.4 Stent design	36
3.5 Fabrication method.....	37
Chapter 4: Evaluation of coronary stents.....	39
4.1 Regulations and approval process	39
4.2 <i>In vitro</i> mechanical testing	41
4.3 <i>In vitro</i> studies	42
4.4 Animal Models	44
4.5 Clinical Studies.....	44
4.6 <i>In silico</i> testing	46
Chapter 5: Stent modelling	47
5.1 Finite Element Method	47
5.2 Review of stent deployment modelling	52
5.2.1 Free expansion of stents	52
5.2.2 Simulation of stent deployment in arterial segments.....	62
5.2.2.1 Idealized arterial segments	62
5.2.2.2 Patient Specific arterial segments.....	70
Chapter 6: Effect of stent design and material on stent deployment	75
6.1 Description of the Computational model.....	75
6.1.1 Creation of the stent model.....	76
6.1.1.1 Creation of the 3D stent design	76
6.1.1.2 Constitutive behavior of stent material.....	76
6.2 Creation of the arterial model.....	77
6.2.1 Creation of the 3D reconstructed artery.....	77
6.2.1.1 3D Coronary Artery Reconstruction Using IVUS and Angiography	77
6.2.2 Constitutive behavior of the artery	78

6.3	Boundary Conditions and loading	82
6.4	Mesh Sensitivity	82
6.5	Effect of stent material	85
6.5.1	Results of Model A.....	86
6.5.2	Results of Model B.....	91
6.5.3	Results of Model C.....	96
6.6	Effect of stent design	101
6.6.1	Results of Model D.....	102
6.6.2	Results of Model E	107
Chapter 7: Discussion and Conclusions.....		113
7.1	Discussion of results.....	113
7.1.1	Comparative analysis of stent material.....	114
7.1.2	Comparative analysis of stent design	119
Chapter 8: Limitations and future work		125
Chapter 9: References		129
A. APPENDIX		142
A1.	Detailed list of clinical trials in coronary stenting [135].	142
A2.	Stent design	175
A3.	Mesh sensitivity.....	178

List of Figures

Figure 1: Overview of cardiovascular disease and other diseases [24].	2
Figure 2: Overview of coronary arteries [26].	3
Figure 3: Structure of the arterial wall [26].	3
Figure 4: Stages of Atherosclerosis [30].	5
Figure 5: Imaging modalities in atherosclerosis [38].	7
Figure 6: Invasive coronary angiography before and after stent placement [42].	8
Figure 7: Reconstruction of arterial segment based on X-ray coronary angiography [44].	9
Figure 8: Segmentation process: (i) the acquired image, (ii) inner wall, outer wall and calcified plaques segmentation [61].	11
Figure 9: Images of intravascular ultrasound (IVUS).	13
Figure 10: Images of Optical coherence tomography (OCT).	13
Figure 11: Fusion of IVUS and angiography [70].	14
Figure 12: Pathway leading to restenosis after stent implantation [97].	20
Figure 13: Global Coronary Stents Market Revenue, 2013 and 2020 ([116], [117]).	28
Figure 14: Closed vs Open cell stent design [137].	37
Figure 15: Overview of some commercially available stents.	37
Figure 16: Process for obtaining CE marking for stent scaffolds.	41
Figure 17: (a) Longitudinal compression testing. (b) Radial compression testing, (c) 3-point bending, (iv) torsion stent testing	42
Figure 18: Process for FEA.	49
Figure 19: Examples of linear (left) and quadratic (right) elements.	50
Figure 20: Von Mises stress and equivalent plastic deformation at the inflation pressure of 0.5 MPa and after the load removal ([139]).	55
Figure 21: Representation of the FEMs.	75
Figure 22: Representation of the 3D arterial reconstruction based on IVUS and angiography imaging data.	78
Figure 23: Illustration of the model used in mesh sensitivity analysis.	83
Figure 24: Von Mises stress (MPa) distribution after stent deployment on the arterial part II with: (a) mesh A, (b) mesh B, (c) mesh C and, (d) mesh D.	85
Figure 25: Von Mises stress (MPa) distribution in the inner arterial wall for Model A.	86
Figure 26: Von Mises stress (MPa) distribution in the outer arterial wall for Model A.	87
Figure 27: Von Mises stress (MPa) distribution in different cross sections along the area where the stent was deployed (Model A).	87
Figure 28: Von Mises stress (MPa) distribution for the stent (Model A) in the unloading phase.	88
Figure 29: Von Mises stress (MPa) distribution for the stent (Model A) from the loading till the unloading phase.	89
Figure 30: Von Mises stress percentage volume distribution for stent and artery of Model A (P=1.8 MPa).	90
Figure 31: Von Mises stress percentage volume distribution for stent and artery of Model A (P=0 MPa).	90
Figure 32: Plot of pressure vs radial deformation for node 2 (node existing in the stent middle cross-section) for stent (Model A).	91
Figure 33: Von Mises stress (MPa) distribution in the outer arterial wall for Model B.	92
Figure 34: Von Mises stress (MPa) distribution in the inner arterial wall for Model B.	92
Figure 35: Von Mises stress (MPa) distribution in different cross sections along the area where the stent was deployed (Model B).	93
Figure 36: Von Mises stress (MPa) distribution for the stent (Model B) in the unloading phase.	94
Figure 37: Von Mises stress (MPa) distribution for the stent (Model B) from the loading till the unloading phase.	94

Figure 38: Von Mises stress percentage volume distribution for stent and artery of Model B (P=1.8 MPa).....	95
Figure 39: Von Mises stress percentage volume distribution for stent and artery of Model B (P=0 MPa).....	95
Figure 40: Plot of pressure vs radial deformation for node 2 (node existing in the stent middle cross-section) for stent (Model B).....	96
Figure 41: Von Mises stress (MPa) distribution in the outer arterial wall for Model C.....	97
Figure 42: Von Mises stress (MPa) distribution in the inner arterial wall for Model C.....	97
Figure 43: Von Mises stress (MPa) distribution in different cross sections along the area where the stent was deployed (Model C).....	98
Figure 44: Von Mises stress (MPa) distribution for the stent (Model C) in the unloading phase.....	99
Figure 45: Von Mises stress (MPa) distribution for the stent (Model C) from the loading till the unloading phase.....	99
Figure 46: Von Mises stress percentage volume distribution for stent and artery of Model C (P=1.8 MPa).....	100
Figure 47: Von Mises stress percentage volume distribution for stent and artery of Model C (P=0 MPa).....	100
Figure 48: Plot of pressure vs radial deformation for node 2 (node existing in the stent middle cross-section) for stent (Model C).....	101
Figure 49: Von Mises stress (MPa) distribution in the outer arterial wall for Model D.....	103
Figure 50: Von Mises stress (MPa) distribution in the inner arterial wall for Model D.....	103
Figure 51: Von Mises stress (MPa) distribution in different cross sections along the area where the stent was deployed (Model D).....	104
Figure 52: Von Mises stress (MPa) distribution for the stent (Model D) in the unloading phase.....	104
Figure 53: Von Mises stress (MPa) distribution for the stent (Model D) from the loading till the unloading phase.....	105
Figure 54: Von Mises stress percentage volume distribution for stent and artery of Model D (P=1.8 MPa).....	105
Figure 55: Von Mises stress percentage volume distribution for stent and artery of Model D (P=0 MPa).....	106
Figure 56: Plot of pressure vs radial deformation for node 2 (node existing in the stent middle cross-section) for stent (Model D).....	107
Figure 57: Von Mises stress (MPa) distribution in the outer arterial wall for Model E.....	108
Figure 58: Von Mises stress (MPa) distribution in the inner arterial wall for Model E.....	108
Figure 59: Von Mises stress (MPa) distribution in different cross sections along the area where the stent was deployed (Model E).....	109
Figure 60: Von Mises stress (MPa) distribution for the stent (Model E) in the unloading phase.....	110
Figure 61: Von Mises stress (MPa) distribution for the stent (Model E) from the loading till the unloading phase.....	110
Figure 62: Von Mises stress percentage volume distribution for stent and artery of Model E (P=1.8 MPa).....	111
Figure 63: Von Mises stress percentage volume distribution for stent and artery of Model E (P=0 MPa).....	111
Figure 64: Plot of pressure vs radial deformation for node 2 (node existing in the stent middle cross-section) for stent (Model E).....	112
Figure 65: Von Mises stress (MPa) distribution in the inner arterial wall for Model A, Model B and Model C.....	115
Figure 66: Von Mises stress (MPa) distribution in the outer arterial wall for Model A, Model B and Model C.....	115
Figure 67: Von Mises stress percentage volume distribution for the artery (Model A, Model B, Model C) (P= 0 MPa, deflation phase).....	115

Figure 68: Von Mises stress (MPa) distribution for the stent from the loading till the unloading phase (Model A, Model B, Model C).....	117
Figure 69: Von Mises stress percentage volume distribution for the stent (Model A, Model B, Model C) (P= 0 MPa, deflation phase).	118
Figure 70: Plot of pressure vs radial deformation for node 2 (node existing in the stent middle cross-section) for stent (Model A, Model B, Model C).....	118
Figure 71: Principal stress in the inner arterial wall in the region of stent deployment.	120
Figure 72: Principal stress percentage volume distribution for the artery (Model D, Model E) (P= 0 MPa, deflation phase).	121
Figure 73: Von Mises stress percentage volume distribution for the artery (Model D, Model E) (P= 0 MPa, deflation phase).	121
Figure 74: Von Mises stress (MPa) distribution for the stent from the loading till the unloading phase (Model D, Model E).	122
Figure 75: Von Mises stress percentage volume distribution for the stent (Model D, Model E) (P= 0 MPa, deflation phase).	123
Figure 76: Plot of pressure vs radial deformation for node 2 (node existing in the stent middle cross-section) for stent (Model D, Model E).....	123

List of Tables

Table 1: Human atherosclerotic lesions classification [14].	5
Table 2: Terms of different types of human atherosclerotic lesions in pathology [37].	6
Table 3: Overview of coronary artery reconstruction approaches based on X-ray angiography data [43].	9
Table 4: Eight Approved Bare-Metal and Coated (Drug-Free) Metal Coronary Artery Stents.	17
Table 5: Features of Four Approved DES [87].	18
Table 6: Potential Mechanisms of Stent Thrombosis.	23
Table 7: Key metrics for coronary stents in 10 major markets.	27
Table 8: Stent materials and properties.	34
Table 9: Overview of FDA approved coronary stents.	36
Table 10: Stent fabrication processes.	38
Table 11: Animal models used in coronary stenting.	44
Table 12: Element types in stress analysis.	49
Table 13: Details of finite element types.	50
Table 14: Details of FEMs.	76
Table 15: Stents designs and associated geometric characteristics.	76
Table 16: Material properties of stents.	76
Table 17: Material properties of the arterial wall used in the Mooney-rivlin material model.	82
Table 18: Arterial geometry and stent dimensional characteristics (Model A).	83
Table 19: Details of finite element meshes.	84

List of abbreviations

BRS	Bioresorbable Scaffolds
BX	Balloon- expandable
CABG	Coronary Artery Bypass Grafting
CAC	Coronary Artery Calcification
CAD	Coronary Artery Diseases
CCTA	Coronary Computed Tomographic Angiography
CF	Constant expansion Force
Co–Cr	Cobalt-Chromium
CVD	Cardiovascular disease
DALY	Disability-Adjusted Life Years
DES	Drug eluting Stents
ECs	Endothelial cells
EI	Expected Improvement
FEA	Finite Element Analysis
FEM	Finite Element Model
GBD	Global Burden of Disease
ICA	Invasive Coronary Angiography
ISR	In Stent Restenosis
IVUS	Intravascular ultrasound
LCA	Left Coronary Artery
LDL	Low Density Lipoprotein
LPV	Loaded by a Pressure Variant
LRD	Loaded by a Radial Displacement
Mg	Magnesium
MPC	multipoint constraint elements
MRA	Coronary Magnetic Resonance Angiography
MRI	Magnetic Resonance Imaging
Ni–Ti	Nickel-Titanium
NURBS	Non-uniform rational basis-splines
OCT	Optical coherence tomography
PCI	PCI
PLLA	Poly-L lactide
PTCA	Percutaneous Transluminal Coronary Angioplasty
R&D	Research and Development
RCA	Right Coronary Artery
RUC	Repeated Unit Cell
SMA	Shape Memory Alloys
SMC	Smooth Muscle Cell
SX	Self-expandable
Ta	Tantalum
VRF	Variable Radial Force

ABSTRACT

The biomechanical behaviour of coronary stents after their implantation is of great interest to interventional cardiologists and biomedical engineers, since in-stent restenosis (ISR), which is related to the arterial wall injury, is a serious adverse event. Several factors can affect ISR, such as the stent design and the materials used for the stent scaffold, therefore various research teams have been investigating the mechanical performance of stents through the utilisation of computational approaches.

The interest of the researchers has been initially focused on examining the free-stent expansion, investigating the stent behavior during and after deployment, ignoring the presence of other components, such as the surrounding arterial wall. Among the parameters, which were examined, were the stent foreshortening, the dogboning, the recoil and the stent diameter [1], [2]. The effect of stent design was also examined, in terms of number, width and length of individual stent cells for different commercially available stent designs [1], [3], [4]. Later, the arterial wall was also included in the analysis towards investigating the stent and arterial wall response. However, those studies have been mostly accounted on the utilisation of idealised geometries for the arterial wall. These studies have analysed the mechanical behavior of the stent, in terms of deformation, stress and strain, while for the new generation of stents, additional parameters were included, such as the behavior of the stent coating [5], the drug-release and degradation mechanisms. The arterial wall was modelled as an idealised cylindrical vessel, while the plaque had a parabola-shape. The arterial wall was assumed to be straight or curved, while stent expansion was achieved either as a pressure- or a displacement driven approach [6], [138], [7]. Different types of stent materials were used in the computational analysis and were compared in terms of stresses and strain [8], [9], [10], [11]. The effect of stent design was also investigated. Specifically, the stent diameter [12], the geometry of the bridges [13], the strut spacing [14] and the thickness [15], the stent angle and length [2], [16], the shape of the circumferential rings and links [17] were examined. Even if those simplified approaches have assisted in understanding the stenting mechanics, there was an imperative need in modeling the 3D arterial morphology in a more realistic way and including the patient-specific characteristics. To accomplish this, information from different imaging modalities (MRI, angio, IVUS, OCT) of a particular patient's vasculature were used [18]. Those studies shed the light on the importance of representing the arterial wall and plaque

components, not as a single layer structures [14], [19], [20], but taking into consideration the composition of the tissue. In such studies, different parameters were investigated, such as the stent material properties [21], the stent design [18], [22], the stent-balloon interaction [23], stent design and the tissue material properties.

To achieve stent implantation success, scientific discoveries and technologies should be translated into practical applications. It is evident that in interventional cardiology, percutaneous cardiovascular intervention has been transformed from a quirky experimental procedure to a therapeutic approach for patients with cardiovascular disease. Inherent in the application of stent technology is the preclinical testing using animal and the clinical testing with humans. However, a further understanding could be achieved through the complementary information from *in silico* experiments. This thesis aims to investigate and evaluate the effect of stent design and materials through the utilization of realistic and patient specific arterial geometries. It is an attempt to provide insight on the key factors that could affect the success of the interventional process through the analysis of the design and material parameters that play a significant role. This is achieved through the creation of five different *in silico* models that are compared in terms of stress and deformation distribution in the arterial wall and stent components. Three different materials for the stent scaffold (CoCr, SS316L, PtCr) and two stent designs (stent with thick vs stent with thin struts) are used in the *in silico* experiments. The innovation of the current study lays on the inclusion and incorporation of patient specific characteristics and arterial morphology that enables the replication and reproduction real clinical scenarios.

In detail, eight chapters are included:

Chapter 1 provides an overview of cardiovascular disease, atherosclerosis and treatment options focusing on stenting. The evolution of coronary stenting and the main considerations during this interventional procedure, the mechanisms and the pathophysiology implicated in ISR and thrombosis are described.

Chapter 2 presents an analysis of the stent market, the key players in the coronary stent industry as well as the predictions for the market potential.

Details on the stents desirable characteristics and on the properties from the materials perspective are provided in Chapter 3. A categorization of the stents based on the

geometry and the two main categories of stents available in the market are also presented.

Chapter 4 presents the process of stent evaluation, that is currently followed, describing the regulatory framework, the approval process, the *in vitro* mechanical testing, the animal and the finally the clinical studies.

Chapter 5 provides a comprehensive literature review of the computational approaches in coronary stent modeling. More specifically, modeling studies on stent free expansion and expansion in idealized and patient specific arterials segments are analysed.

Chapter 6 describes the main steps that were followed to create the Finite Element Models (FEM) that were used in the current analysis. Specifically, information on the stent design and the 3D arterial reconstruction are presented accompanied with the method for the meshing approach. The boundary conditions and the loading which are used as well as the governing equations are presented. Then the two main approaches; the creation of the FEM models with different stent design and materials is performed and the relevant results are presented in terms of deformation and stress distribution in the stent scaffold and in the vascular tissue.

Chapter 7 presents the conclusions obtained from the analysis and the comparison of the representative stent materials (Model A, Model B and Model C) and the representative stent designs (Model D and Model E). The analysis focuses on assessing the effect of design and material on stent expansion, stress distribution and occurred arterial stresses during the deployment process inside a reconstructed diseased arterial segment. It is revealed that the stent of Model A exhibits higher arterial stresses in the arterial wall followed by Model B and Model C. For all models (Model A, Model B, Model C), stent expansion affects the inner arterial layer. As far as the distribution of the arterial stress in different stress ranges is concerned, it is demonstrated that: (i) the percentage of arterial stress in the stress range of 0-0.15MPa is higher for the arterial wall of Model B, (ii) the percentage of arterial stress in the stress range of 0.15-0.30MPa is slightly higher for the arterial wall of Model C, (iii) the percentage of arterial stress in the stress range over 0.3 is higher for Model A. In addition: (i) the percentage of the von Mises stress for the stent of Model B in the stress range of 0-200MPa is higher compared to Model A and Model C, (ii) the percentage of the von Mises stress for the stent of Model C in the stress range of 200-400MPa is higher followed by the stent of

Model B and the stent of Model A, (iii) the percentage of the von Mises stress for the stent of Model A in the stress range over 400MPa is higher compared to the stent of Model B and the stent of Model C. Model D (Model_thin) and Model E (Model_thick) have been designed with a strut thickness of 0.0702 mm and 0.0774 mm respectively. The Principal stresses for the inner arterial wall are depicted for Model_thin and Model_thick in different views. Higher arterial stresses are located behind the region where the stent was expanded and more specifically in the region of stenosis. The slightly highest stresses in the arterial wall are observed for Model_thick compared to Model_thin. However, from the different views, it is evident that the areas of the inner arterial wall affected from higher stresses are more in the model with the thick struts. Specifically, it is demonstrated that: (i) the percentage of arterial principal stress in the stress range of 0-0.3 MPa is higher for Model D (67.5%) compared to Model E (66.5%), whereas the percentage of arterial principal stress in the stress range over 0.3MPa is higher for Model E with the thicker struts compared to Model D with the thinner struts. Both stent models follow the same deformation pattern, while for all pressures, in Model D (thin struts) higher von Mises stresses occur compared to Model E (thick struts). Regarding the percentage volume of each stent model belonging to different stress ranges: (i) 62.5% percentage of the total von Mises stress belongs to the stress range of 0-200MPa for Model D and 71.28% for Model E respectively, (ii) the highest percentage in the stress range over 200MPa belongs to Model D (37.5%).

Chapter 8 provides an overview of the limitations of the current thesis in terms of the materials properties used, the assumption of the homogeneity of the arterial wall and the lack of the direct experimental validation of the computational results.

ΠΕΡΙΛΗΨΗ

Η συμπεριφορά που παρουσιάζουν τα στεντ κατά την διάρκεια της έκπτυξης τους αλλά και κατά την παραμονή τους εσωτερικά του ενδοαγγειακού τοιχώματος έχει αποτελέσει αντικείμενο μελέτης και έρευνας τα τελευταία χρόνια και έχει προσελκύσει το ενδιαφέρον των επεμβατικών καρδιολόγων αλλά και των ερευνητών. Αυτό οφείλεται κυριώς στο γεγονός ότι η διαδικασία έκπτυξης αλλά και η εν δυνάμει τοποθέτηση του στεντ δύναται να συνοδεύεται από ανεπιθύμητες βλάβες, όπως η επαναστένωση του αυλού. Το φαινόμενο αυτό προκαλείται και είναι αποτέλεσμα πολλών παραγόντων που δρούν αθροιστικά όπως το υλικό του στεντ καθώς και λοιπά σχεδιαστικά χαρακτηριστικά, όπως το μήκος του στεντ, το πάχος του συνδέσμου, κλπ. Η ανάπτυξη του τομέα της τεχνολογίας οδήγησε στην ανάδειξη και χρήση υπολογιστικών μεθόδων, μέσω των οποίων παρέχεται η δυνατότητα μελέτης και ανάλυσης πλήθους προβλημάτων. Κατά αυτόν τον τρόπο, πολλές ερευνητικές ομάδες βασιζόμενες στην μέθοδο των πεπερασμένων στοιχείων και χρησιμοποιώντας κατάλληλα υπολογιστικά εργαλεία μελέτησαν την συμπεριφορά του στεντ κατά την έκπτυξη του. Αρχικά το ενδιαφέρον των ερευνητών επικεντρώθηκε στην ανάλυση της συμπεριφοράς του στεντ θεωρώντας ότι δεν έρχεται σε επαφή με τον αυλό (ελεύθερη έκπτυξη). Οι παράμετροι που μελετήθηκαν ήταν η μείωση του μήκους του στεντ, η διάμετρος του και η «υποχώρηση» από την αρχική του παραμορφωμένη κατάσταση [1], [2]. Επίσης μελετήθηκε η επίδραση των σχεδιαστικών λεπτομερειών, όπως ο αριθμός, το πάχος και το μήκος κάθε «κελιού» του στεντ [1], [3], [4]. Αργότερα, στις μελέτες που έγιναν, ενσωματώθηκε και το αρτηριακό τοίχωμα δεδομένου ότι υπήρχε η ανάγκη να μελετηθεί η επίδραση που έχει το στεντ στο εσωτερικό του αυλού αλλά και στο αρτηριακό τοίχωμα γενικότερα. Σε αυτές τις μελέτες, το αρτηριακό τοίχωμα προσομοιαζόταν με έναν ομοιογενή κύλινδρο με συγκεκριμένο πάχος ο οποίος εφερε εσωτερικά μια παραβολικής μορφής τρισδιάστατη μορφολογία, την αθηρωματική πλάκα. Αν και οι ανωτέρω παραδοχές εξιδανίκευαν την πραγματικότητα, παρήχαν ταυτόχρονα την δυνατότητα να έχουμε μια ποιοτική εκτίμηση για τις τάσεις και τις παραμορφώσεις που δεχόταν το τοίχωμα κατά την διάρκεια της έκπτυξης του στεντ αλλά και κατά την παραμονή του εσωτερικά του τοιχώματος [6], [138], [7].

Στις διάφορες μελέτες που έγιναν χρησιμοποιήθηκαν διαφορετικά υλικά για τα στεντ με στόχο την σύγκριση των επαγόμενων τάσεων και παραμορφώσεων [8], [9], [10], [11]. Επίσης διερευνήθηκε η επίδραση που επιφέρει ο διαφορετικός σχεδιασμός του

στεντ, όπως η διάμετρος [12], η γεωμετρία των γεφυρών [13] η απόσταση του ορθοστάτη [14] το πάχος [15], η γωνία και το μήκος του στεντ [2], [16], [17]. Μολονότι οι ανωτέρω απλοποιημένες προσεγγίσεις συνέβαλαν στην κατανόηση της μηχανικής στεντ, υπήρξε επιτακτική ανάγκη να μοντελοποιηθεί η τρισδιάστατη αρτηριακή μορφολογία με πιο ρεαλιστικό τρόπο και να ενσωματωθούν στα υπολογιστικά μοντέλα τα ειδικά χαρακτηριστικά του κάθε ασθενή.

Για να επιτευχθεί αυτό, χρησιμοποιήθηκαν πληροφορίες από διαφορετικές απεικονιστικές εξετάσεις (MRI, angio, IVUS, OCT) [217]. Κατά αυτόν τον τρόπο δόθηκε η δυνατότητα να συμπεριληφθούν τα συστατικά του αρτηριακού τοιχώματος και οι διάφοροι τύποι της αθηρωματικής πλάκας [185], [183], [101]. Η τρισδιάστατη ανακατασκευή του αρτηριακού τοιχώματος από την σύξευξη διαφόρων απεικονιστικών εξετάσεων προσέδωσε στα μοντέλα μια προσωποποιημένη προσέγγιση, ενσωματώνοντας εξατομικευμένα μορφολογικά χαρακτηριστικά, θεωρώντας όλα τα στρώματα του αρτηριακού τοιχώματος, και λειτουργώντας ως δίαυλος για την προώθηση και ανάδειξη της προσέγγισης της εξατομικευμένης ιατρικής [18]. Σε αυτές τις μελέτες, μελετήθηκε η επίδραση διαφόρων παραγόντων, όπως το υλικό του στεντ [21], τα σχεδιαστικά χαρακτηριστικά του στεντ [18], [22] και η μορφολογία του τοιχώματος [23].

Αυτή η εργασία αποσκοπεί στη διερεύνηση και αξιολόγηση της επίδρασης του υλικού και των σχεδιαστικών χαρακτηριστικών του στεντ κάνοντας χρήση τρισδιάστατων αρτηριών ανακατασκευασμένων από απεικονιστικές εξετάσεις. Η εργασία περιλαμβάνει 8 κεφάλαια.

Το 1^ο Κεφάλαιο παρουσιάζει μια ανασκόπηση σχετικά με την κλινική προσέγγιση και πιο συγκεκριμένα την αιτία ανάπτυξης της καρδιαγγειακής νόσου, των παραγόντων που συντελούν στην δημιουργία της αθηροσκλήρωσης, στις διαθέσιμες θεραπευτικές μεθόδους, εστιάζοντας στην τοθέτηση του στεντ και στους μηχανισμούς και την παθοφυσιολογία που εμπλέκονται στην επαναστένωση του στεντ και την δημιουργία θρόμβωσης.

Το 2^ο Κεφάλαιο εστιάζει στην ανάλυση της αγοράς στεντ αλλά και στις προβλέψεις που υπάρχουν για την δυναμική της αγοράς για τα επόμενα χρόνια.

Στο 3^ο κεφάλαιο, παρουσιάζονται οι διαφορετικοί τύποι στεντ που υπάρχουν, η κατηγοριοποίηση τους, καθώς και τα επιθυμητά χαρακτηριστικά και οι ιδιότητες τους. Το 4^ο Κεφάλαιο παρουσιάζει την διαδικασία που ακολουθείται από τον σχεδιασμό του στεντ μέχρι την προώθηση του στην αγορά, περιγράφοντας το υπάρχον ρυθμιστικό πλαίσιο, τις διαδικασίες αξιολόγησης και έγκρισης, τις *in vitro* μηχανικές δοκιμές που πραγματοποιούνται στα στεντ, τις μελέτες που γίνονται στα ζώα και τις κλινικές μελέτες.

Στο 5^ο Κεφάλαιο παρουσιάζεται μια αναλυτική βιβλιογραφική ανασκόπηση των υπολογιστικών προσεγγίσεων στη μοντελοποίηση των στεντ.

Το 6^ο Κεφάλαιο περιγράφει τα κύρια βήματα που ακολουθήθηκαν για τη δημιουργία των Μοντέλων Πεπερασμένων Στοιχείων που χρησιμοποιήθηκαν στην συγκεκριμένη εργασία. Συγκεκριμένα, παρουσιάζονται πληροφορίες σχετικά με το σχεδιασμό των στεντ και την τρισδιάστατη αρτηριακή ανακατασκευή, τις συνοριακές συνθήκες και την φόρτιση για την έκπτυξη του στεντ καθώς και τις εξισώσεις που επιλύθηκαν. Στη συνέχεια, αναλύεται η επίδραση του υλικού αλλά και των σχεδιαστικών χαρακτηριστικών των στεντ και συγκρίνονται οι παραμορφώσεις και οι τάσεις στα στεντ και στον αρτηριακό τοίχωμα.

Το 7^ο Κεφάλαιο παρουσιάζει την ανάλυση των αποτελεσμάτων και τα συμπεράσματα που προέκυψαν από την σύγκριση τριών στεντ με διαφορετικά υλικά (Μοντέλο Α, Μοντέλο Β και Μοντέλο C) και δύο στεντ με διαφορετικά σχεδιαστικά χαρακτηριστικά (Μοντέλο D και Μοντέλο E). Η ανάλυση επικεντρώνεται στην εκτίμηση της επίδρασης των σχεδιαστικών χαρακτηριστικών και του υλικού του στεντ, κατά την διάρκεια της έκπτυξης του, στην κατανομή των επαγόμενων τάσεων και παραμορφώσεων τόσο στο στεντ όσο και στο αρτηριακό τοίχωμα. Τα αποτελέσματα δείχνουν ότι το στεντ του Μοντέλου Α προκαλεί υψηλότερες αρτηριακές τάσεις στο αρτηριακό τοίχωμα σε σχέση με το Μοντέλο Β και το Μοντέλο C. Για όλα τα Μοντέλα (Μοντέλο Α, Μοντέλο Β, Μοντέλο C), η έκπτυξη του στεντ επηρεάζει την εσωτερική επιφάνεια του αρτηριακού τοιχώματος. Όσον αφορά την κατανομή της αρτηριακής τάσης σε διαφορετικές περιοχές τάσεων, αποδεικνύεται ότι: (α) το ποσοστό αρτηριακής τάσης στην περιοχή τάσεων 0-0.15 MPa είναι υψηλότερο για το αρτηριακό τοίχωμα του Μοντέλου Β, (β) το ποσοστό αρτηριακής πίεσης στο εύρος τάσης 0,15-0,30MPa είναι ελαφρώς υψηλότερο για το αρτηριακό τοίχωμα του μοντέλου C, (γ) το ποσοστό

αρτηριακής τάσης στην περιοχή τάσεων πάνω από 0,3 είναι υψηλότερο για το μοντέλο A. Επιπλέον, το ποσοστό των επαγόμενων τάσεων: (α) για το στεντ του Μοντέλου B διάστημα 0-200MPa είναι υψηλότερο σε σύγκριση με το Μοντέλο A και το Μοντέλο C, (β) για το στεντ του Μοντέλου C στο διάστημα 200-400MPa είναι υψηλότερο σε σχέση με το Μοντέλο B και το Μοντέλο A, (γ) για το στεντ του Μοντέλου A για τάσεις πάνω από 400 MPa είναι υψηλότερο σε σύγκριση με το στεντ του Μοντέλου B και το στεντ του Μοντέλου C.

Τα μοντέλα D (Model_thin) και Model E (Model_thick) έχουν σχεδιαστεί με πάχος αντηρίδας 0.0702 mm και 0.0774 mm αντίστοιχα. Η ανάλυση δείχνει ότι παρουσιάζονται υψηλότερες αρτηριακές τάσεις πίσω από την περιοχή όπου εκπτυχθηκε το στεντ και πιο συγκεκριμένα στην περιοχή της στένωσης. Οι ελαφρώς υψηλότερες τάσεις στο αρτηριακό τοίχωμα παρατηρούνται για το Model_thick σε σύγκριση με το Model_thin. Επίσης για το μοντέλο με το μεγαλύτερο πάχος αντηρίδας έχουμε μεγαλύτερο ποσοστό υψηλών τάσεων. Συγκεκριμένα, αποδεικνύεται ότι: (α) το ποσοστό της βασικής αρτηριακής τάσης στην περιοχή τάσεων 0-0,3 MPa είναι υψηλότερο για το Μοντέλο D (67,5%) σε σύγκριση με το Μοντέλο E (66,5%), ενώ το ποσοστό των κύριων αρτηριακών τάσεων στο εύρος τάσης πάνω από 0,3MPa είναι υψηλότερο για το Μοντέλο E με τις παχύτερες αντηρίδες σε σύγκριση με το Μοντέλο D με τις λεπτότερες αντηρίδες. Και τα δύο μοντέλα στεντ ακολουθούν το ίδιο μοτίβο παραμόρφωσης, ενώ για όλες τις πιέσεις, στο Μοντέλο D εμφανίζονται υψηλότερες τάσεις von Mises σε σύγκριση με το Μοντέλο E. Αναφορικά με τον ποσοστιαίο όγκο κάθε μοντέλου στεντ που ανήκει σε διαφορετικές περιοχές τάσεων: (α) ποσοστό 62,5% της συνολικής τάσης von Mises ανήκει στην περιοχή τάσεων 0-200MPa για το Μοντέλο D και 71,28% για το Μοντέλο E αντίστοιχα, (β) το υψηλότερο ποσοστό στην περιοχή στρες πάνω από 200MPa ανήκει στο μοντέλο D (37,5%).

Το 8^ο Κεφάλαιο παρουσιάζει τις παραδοχές που λάβαμε υπόψιν για την εκπόνηση της συγκεκριμένης μελέτης σχετικά με τις ιδιότητες των υλικών, την ομοιογένεια του αρτηριακού τοιχώματος και την μη δυνατότητα επικύρωσης των αποτελεσμάτων και σύγκρισής τους με πειραματικά αποτελέσματα και παρουσιάζει τα πεδία στα οποία θα επικεντρωθεί η μελέτη μας στο μέλλον με στόχο την περαιτέρω εμβάθυνση και κατανόηση των μηχανισμών που δημιουργούνται κατά την έκπτυξη του στεντ και την συσχέτιση εκείνων των χαρακτηριστικών του στεντ που θα πρέπει να λαμβάνονται υπόψιν κατά την φάση του σχεδιασμού και δημιουργίας του.

Chapter 1: Introduction

- 1.1 Cardiovascular disease
 - 1.2 Imaging modalities
 - 1.3 Treatment options for coronary atherosclerosis
 - 1.4 Angioplasty, stenting and by-pass
 - 1.5 Evolution of coronary stenting
 - 1.6 Considerations in relation to stenting
 - 1.7 Mechanisms or restenosis
 - 1.8 Objective of the thesis
-

1.1 Cardiovascular disease

Cardiovascular disease (CVD) is a chronic disease that affects the circulatory system, which mainly involves the heart and/or the blood vessels. CVD includes coronary artery diseases (CAD), such as angina and heart attack, which are related to atherosclerosis. CVD is a major health and economic burden in Europe and worldwide (Figure 1). The prevalence of this disease classifies it, in the leading causes of death worldwide. The 2013 Global Burden of Disease (GBD) study estimates that CVD causes 17.3 million deaths globally and 4 million deaths in Europe each year. This disease is different among gender. Specifically, the mortality rate is higher in women (49%) compared to men (40%) (Figure 1).

There also exist differences in the prevalence of CVD between the European countries; 1.3 million deaths observed in the EU-15 countries, 1.9 million deaths observed in the EU-28 countries and 2.1 million deaths in non-EU member countries. The associated costs, direct and indirect, are inevitable high with an increase in the hospitalization rates for the majority of EU and non-EU countries. According to WHO, the highest rate of

hospitalisation is in UK accounting for 6276 hospital admissions for CVD (per 100 000 population) [24].

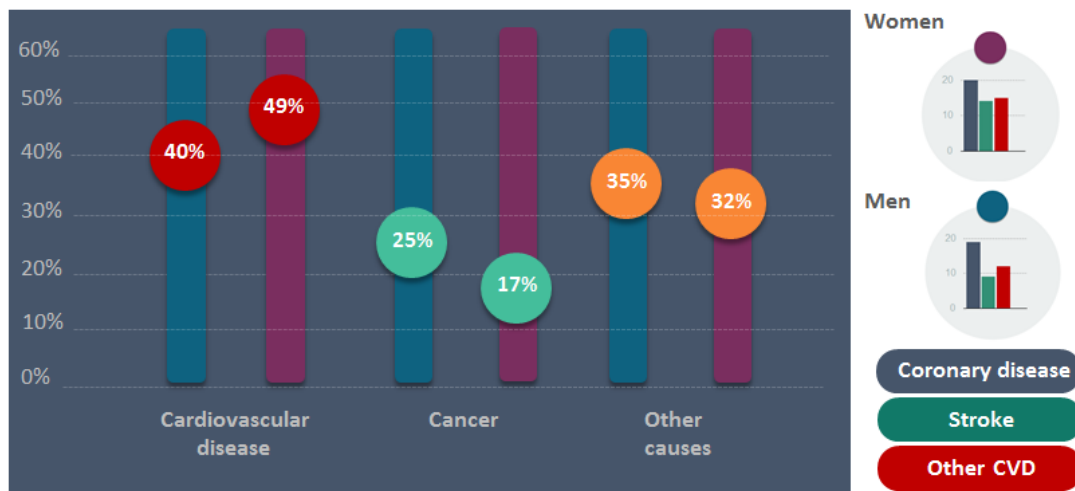


Figure 1: Overview of cardiovascular disease and other diseases [24].

Heart and Coronary arteries

Coronary circulation concerns the supply of oxygen-rich blood and nutrients to the myocardium, which is the muscle tissue of the heart. From an engineering perspective, the heart is a pump which delivers the oxygenated blood to all parts of the body including the heart muscle. This healthy oxygenated blood delivery to the heart is vital for ensuring its normal operation. Coronary arteries are predominant delivery vessels that supply blood to the heart and are classified as: (i) Left Coronary Artery (LCA) and, (ii) Right Coronary Artery (RCA). The LCA branches are classified as: (i) Circumflex artery, (ii) Left Anterior Descending artery (LAD), which provides blood to the left atrium, side and back of the left ventricle, and the front and bottom of the left ventricle and the front of the septum, respectively. The RCA branches are classified as: (i) Right marginal artery, (ii) Posterior descending artery, and provide blood to: (i) right atrium, (ii) right ventricle and, (iii) bottom portion of both ventricles and back of the septum. An illustration of the position of these arteries relative to the heart is presented in Figure 2.

Each of these arteries, in their normal healthy state, is composed of three distinct layers: (i) intima, (ii) media, and (iii) adventitia [25] (Figure 3). The intima is the inner layer of the artery and consists of a single layer of endothelial cells existing in the arterial wall and resting on a thin basal membrane. There also exists a subendothelial layer with a varying thickness according to the location, age and disease. In general, in the healthy

arteries of young people, this subendothelial layer does not exist. In young people, the intima layer is very thin and does not have a significant contribution to the mechanical performance of the arterial wall. However, this intima thickness stiffens with age. In addition, pathological changes of the intima are associated with atherosclerosis.

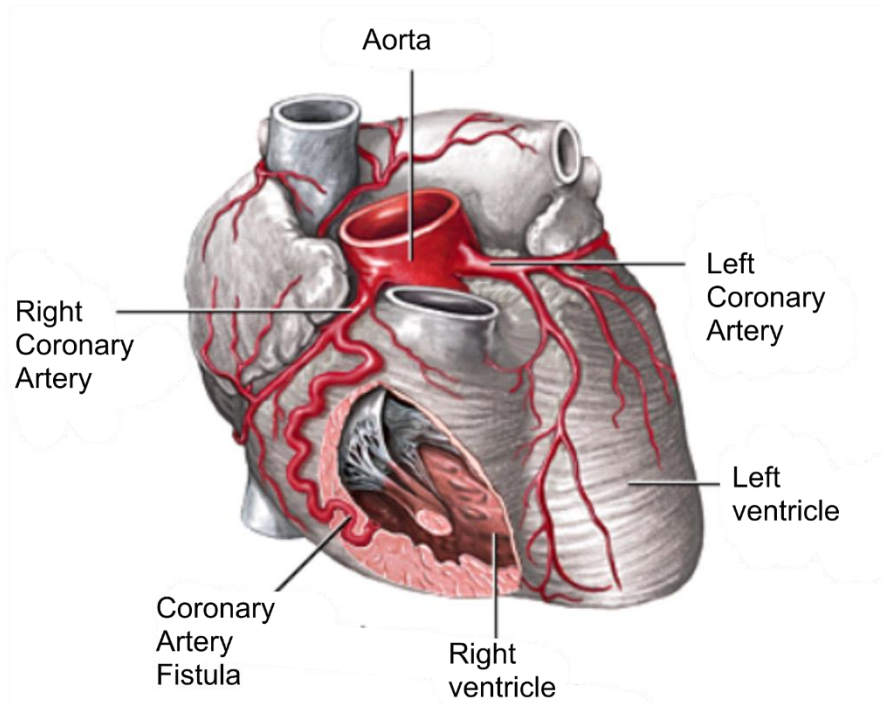


Figure 2: Overview of coronary arteries [26].

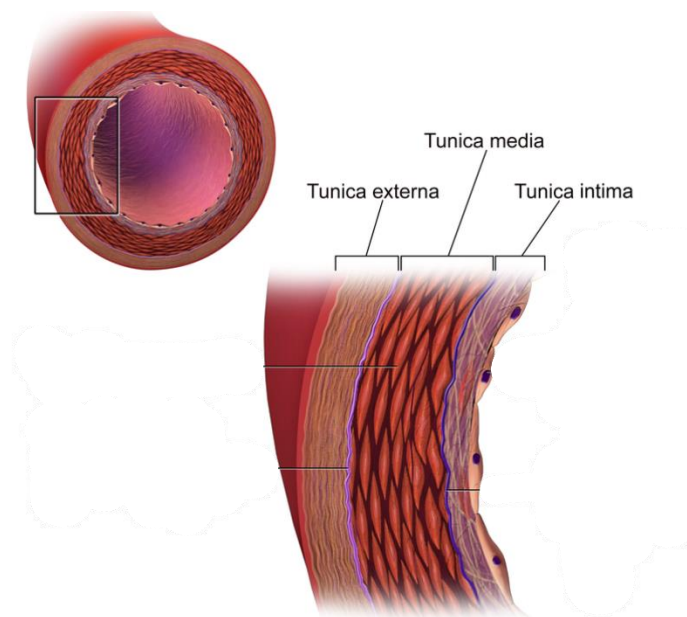


Figure 3: Structure of the arterial wall [26].

The media is the middle arterial layer and is composed by a complex three-dimensional (3D) network of smooth muscle cells (SMCs), elastin and collagen fibrils. The elastin layer separates the media into a varying number of concentrically fiber-reinforced medial layers. The intima and adventitia layers are separated from media by the internal elastic lamina and external elastic lamina, respectively. The adventitia is the outermost layer of the artery and is composed of fibrocytes and fibroblasts that form a fibrous tissue. The adventitia thickness strongly depends on the type and function of the blood vessel. The adventitia contributes significantly to the stability of the arterial wall.

Atherosclerosis

Atherosclerosis is an inflammatory vascular pathology in which the atheromatous plaque builds up inside the arteries [27] (Figure 4). The endothelium, which is the cellular layer lining the inner surface of the blood vessels, acts as a permeability barrier for protecting the healthy arterial wall from potential antagonistic substances in the blood. The onset of inflammation, increases the endothelial permeability and enables the accumulation of plasma proteins (Low-density lipoprotein (LDL)) in the endothelium [28]. Once the LDL is trapped in the endothelium, its oxidation takes place, which positively contributes to the inflammatory response of the endothelium. In parallel, the monocytes are deposited on the site of the inflammation, transmigrate through the endothelium, where their differentiation results into macrophages and uptake of oxidized LDL. This rapid uptake of oxidized LDL contributes to the transformation of the macrophages into foam cells. Next, the apoptosis and necrosis of foam cells result in the formation of the atherosclerotic plaque. The proliferation and migration of SMC from the medial layer of the arterial wall [29] contribute to the protrusion of the lesion into the lumen.

Atherosclerosis is among the main causes of death in the western world. A significant narrowing of the arterial lumen occurs and induces oxygen deficiency in the heart or in the brain. In addition, another complication is the atherosclerotic plaque rupture, which potentially blocks the blood downstream. In case the blood flow to the heart is restricted and limited, the portion of the heart muscle supplied by this artery becomes necrotic; known as myocardial infarction or heart attack. There are certain risk factors that can induce damage in the arterial endothelium and can trigger atherosclerosis [31], such as: (i) high blood pressure [32], (ii) high cholesterol levels [33] (iii) smoking [34], (iv)

obesity [35], (v) lack of physical activity [36]. The human atherosclerotic lesions can be histological classified to the categories described in Table 1 and Table 2 [37].

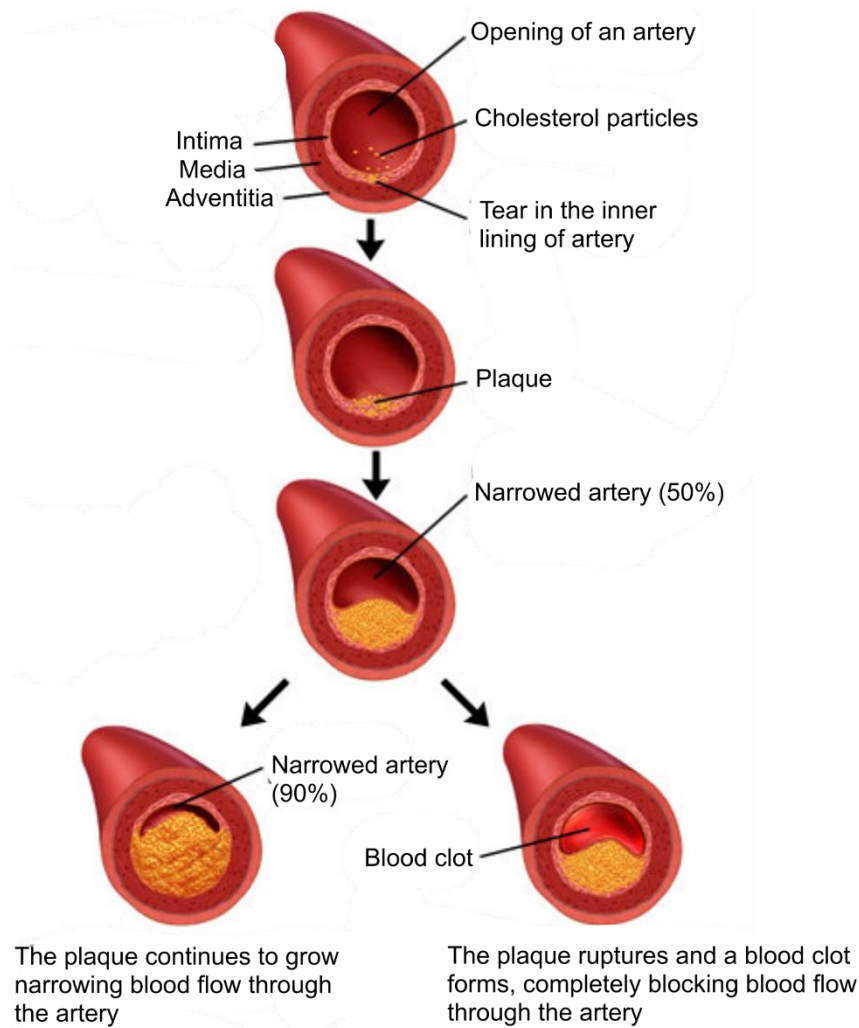


Figure 4: Stages of Atherosclerosis [30].

Table 1: Human atherosclerotic lesions classification [14].

Nomenclature and main histology	Sequences in progression	Main growth mechanism	Earliest onset	Clinical correlation
Type I (initial) lesion, isolated macrophage foam cells		Growth mainly by lipid accumulation	from first decade	Clinically silent
Type II (fatty streak) lesion, mainly intracellular lipid accumulation			from third decade	
Type III (intermediate) lesion, type II changes & core of extracellular lipid				

Type IV (atheroma lesion) Type II changes & core of extracellular lipid				Clinically silent or overt
Type V (fibroatheroma) lesion , lipid core & fibrotic layer, or multiple lipid cores & fibrotic layers, or mainly calcific, or mainly fibrotic		Accelerated smooth muscle and collagen increase	from fourth decade	
Type VI (complicated lesion) , surface defect, hematoma- hemorrhage, thrombus		thrombosis, hematoma		

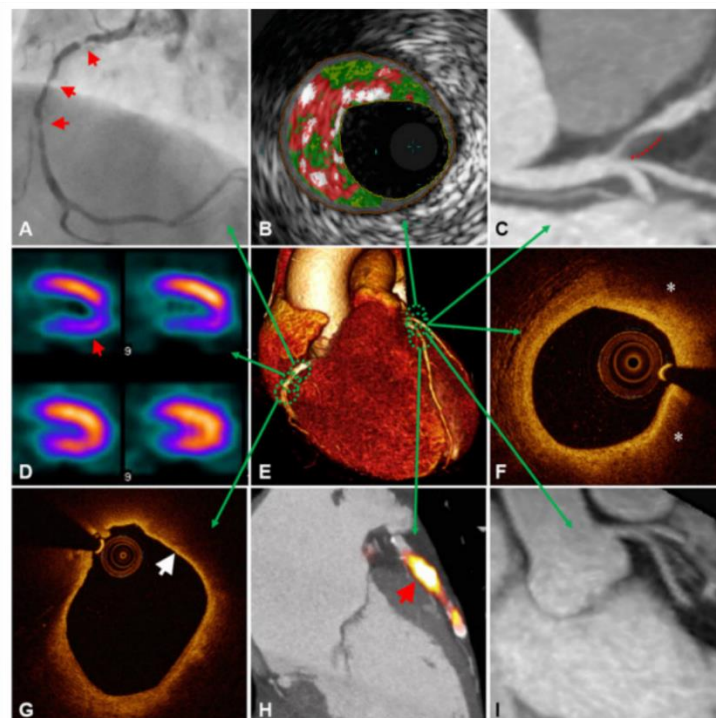
Table 2: Terms of different types of human atherosclerotic lesions in pathology [37].

Terms for Atherosclerotic Lesions in Histological Classification		Other terms for the Same Lesions Often Based on Appearance with the Unaided Eye	
Type I lesion	Initial lesion	N/A	Early lesions
Type IIa lesion	Progression-prone type II lesion	Fatty dot or streak	N/A
Type IIb lesion	Progression-resistant type II	N/A	N/A
Type III lesion	Intermediate lesion (preatheroma)	N/A	N/A
Type IV lesion	Atheroma	Atheromatous plaque	N/A
Type Va lesion	Fibroatheroma (type V lesion)	Fibrolipid plaque	N/A
		Fibrous plaque, plaque	N/A
Type Vb lesion	Calcific lesion (type VII lesion)	Calcified plaque	Advanced lesions
Type Vc lesion	Fibrotic lesion (type VIII lesion)	Fibrous plaque	Raised lesions
Type VI lesion	Lesion with surface defect, and/or hematoma – haemorrhage, and/or thrombotic deposit	Complicated lesion, Complicated plaque	Advanced lesions

Specifically, Type I and II lesions, usually called as early lesions, occur mainly in infants and children. Type III lesions evolve after the adolescence. Their composition is the same as the one between early and advanced lesions. Type IV is considered advanced and presents a disruptive intimal structure. Type IV lesions appear from the third decade on, whereas type V and VI lesions appear after the third decade of life. The underlying mechanisms of Type V and VI lesions progress are different from those existing in Types I through IV. In type IV lesions, an extensive accumulation of extracellular lipid localized in the lipid core takes place. In type V lesions: (i) fibrous in addition to lipid cores results in fibroatheroma (Type Va), (ii) the calcification of a fibrolipid lesion is Type Vb, (iii) fibrous tissue with or without lipid and minimal or no calcium is fibrotic lesion (Type Vc).

1.2 Imaging modalities

Advances in imaging technology have provided a wide range of diagnostic tools for characterizing the atherosclerotic plaques *in vivo* [38] (Figure 5).



A. X- Ray angiography
 B. Virtual histology intravascular ultrasound (VH-IVUS)
 C. Computed tomographic (CT) angiography
 D. Single-photon emission computed tomography (SPECT)
 E. 3D volume rendered CT whole-heart image
 F. Optical Coherence Tomography (OCT) image
 G. OCT image of a lipid-rich coronary plaque displaying thin overlying fibrous cap
 H. Fused ^{18}F -NaF positron emission tomography (PET)-CT image
 I. 3-T magnetic resonance (MR) contrast-angiography

Figure 5: Imaging modalities in atherosclerosis [38].

Atherosclerosis imaging modalities includes a variety of already established and experimental methods and techniques. In general, these techniques are used to detect not only the anatomic and physiological characteristics of the arterial tissue, but also to provide critical information on plaque composition.

Invasive coronary angiography

For CAD diagnosis, the invasive coronary angiography (ICA) is the gold-standard anatomic atherosclerosis imaging technique [39, p.] (Figure 6). This imaging modality enables the visualisation of the coronary vessels through the injection of a radiopaque contrast material [40]. It involves the insertion of a pre-shaped catheter, via a peripheral arterial sheath, for injecting radio-opaque contrast under X-ray fluoroscopy. ICA has a high-diagnostic (superior spatial, 0.1–0.2 mm) and temporal (10ms resolution) accuracy, which is incomparable to the available non-invasive techniques; therefore, it is the best technique for determining and evaluating the severity of luminal occlusion. However, even if X-ray coronary angiography has evolved since its first introduction five decades ago, it has several limitations [41]. X-ray coronary angiography includes the complex 3D/4D structure of the contrast filled coronary arteries by 2D X-ray projections, which can be degraded by imaging artifacts. A large amount of 3D/4D information of the coronary arteries is not retained mainly due to the projection operation; the effect of the suboptimal projection angles, the vessel overlap, tortuosity, foreshortening and eccentricity could result in underestimating the severity of the stenosis and consequently in selecting an inappropriate stent size [41].

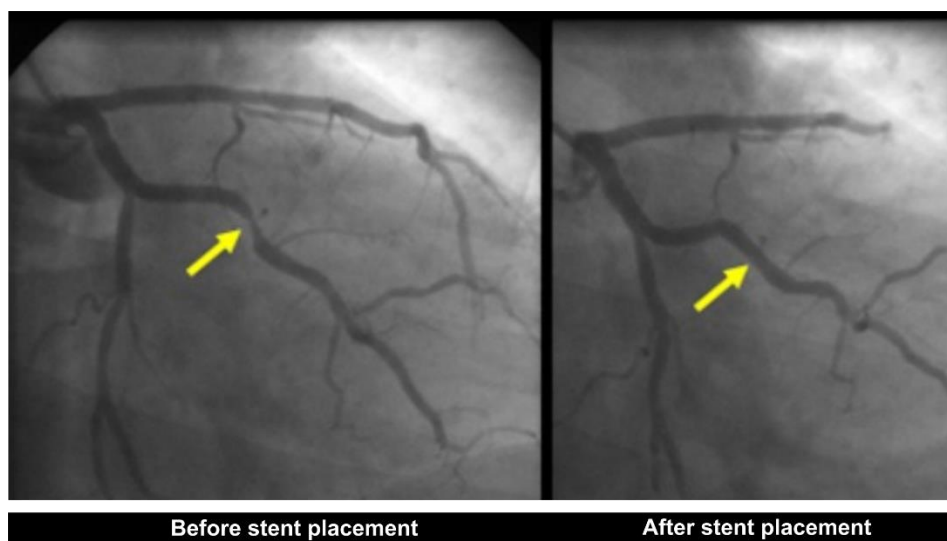


Figure 6: Invasive coronary angiography before and after stent placement [42].

Due to the advances in the C-arm based angiography systems, several types of X-ray coronary angiography exist; single plane, biplane, rotational and dual-axis rotational coronary angiography [43]. The availability of the diverse X-ray coronary angiography strategies enabled the creation of several 3D reconstruction algorithms, [44] (Figure 7).

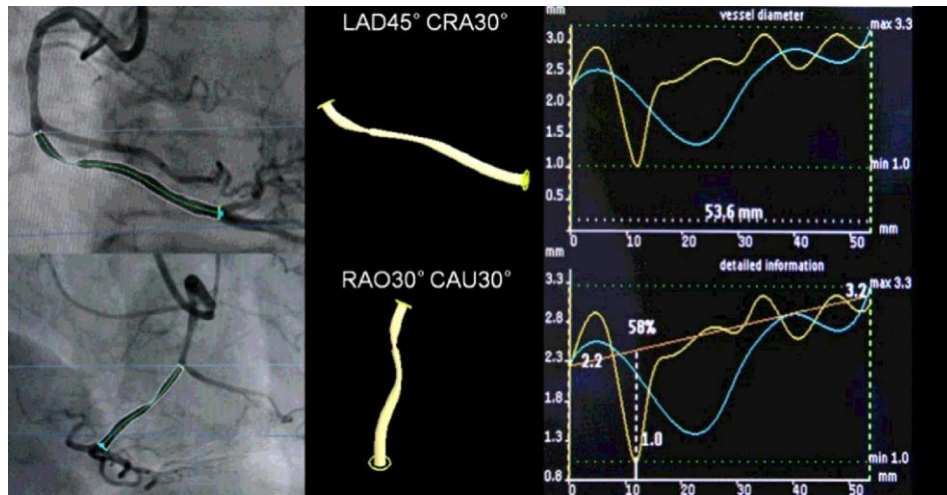


Figure 7: Reconstruction of arterial segment based on X-ray coronary angiography [44].

In Table 3, an overview of model-based coronary artery reconstruction methods from X-ray angiography is provided.

Table 3: Overview of coronary artery reconstruction approaches based on X-ray angiography data [43].

Reference	Breath-hold	Additional input	Calibration	3D reconstruction
Sarry <i>et al.</i> [45]	+	CLs (2)	+	Fourier deformable model with PEE
Cañero <i>et al.</i> [46]	+	CLs (2)	+	ACM with PEE
Zheng <i>et al.</i> [47]	N/A	Corresponding 2D points (2)	Opt. of ext. params	Calibration opt. followed by ACM with PEE and temporal energy
Yang <i>et al.</i> [48]	N/A	CLs (2)	Opt. of ext. & int. params	ACM with BPEE & calibration opt. iteratively
Chen <i>et al.</i> [49]	N/A	CLs (2)	Opt. of ext. params	Calibration opt. followed by epipolar matching + triangulation

Hoffmann <i>et al.</i> [50]	N/A	CLs (2)	Opt. of ext. params	Calibration opt. followed by epipolar matching + triangulation
Chen <i>et al.</i> [51]	N/A	CLs (2)	Opt. of ext. params	Calibration opt. followed by epipolar matching + triangulation
Shechter <i>et al.</i> [52]	+	CLs (2)	+	Used
Andriotis <i>et al.</i> [53]	N/A	Corresponding 2D points (2)	Opt. of ext. params	Calibration opt. followed by epipolar matching + triangulation
Fallavollita <i>et al.</i> [54]	–	CLs (2)	–	Reliable point matching & bundle adjustment, iteratively
Jandt <i>et al.</i> [55]	+	–	+	Segment from back-projected vesselness response
Jandt <i>et al.</i> [56]	+	–	+	N/A
Yang <i>et al.</i> [57]	N/A	CLs (2)	–	Epipolar matching & bundle adjustment, iteratively
Liao <i>et al.</i> [58]	+	CLs (4–5)	+	Graph-cut based sparse stereo
Liu <i>et al.</i> [59]	N/A	CLs (3)	+	Graph-cut based sparse stereo

Coronary Computed Tomographic Angiography

Coronary Computed Tomographic Angiography (CCTA) is a useful first-line diagnostic method for examining patients with symptoms of angina. CCTA is an accurate test with high sensitivity to detect anatomically CAD when compared with invasive angiography. CCTA is performed in combination with coronary artery calcification (CAC) imaging, which is a risk stratification approach for providing an

estimation of the disease progress and risk of future events [60]. For the 3D arterial and plaque morphology reconstruction, the methodology includes the following steps: (i) pre-processing of the raw images, (ii) rough estimation of the lumen/ outer vessel wall borders and approximation of the vessel's centerline, (iii) adaptation (manual) of plaque parameters, (iv) extraction of the lumen centerline, (v) detection of the lumen/ outer vessel wall borders and calcium plaque area, and (vi) construction of the 3D surface [61] (Figure 8).

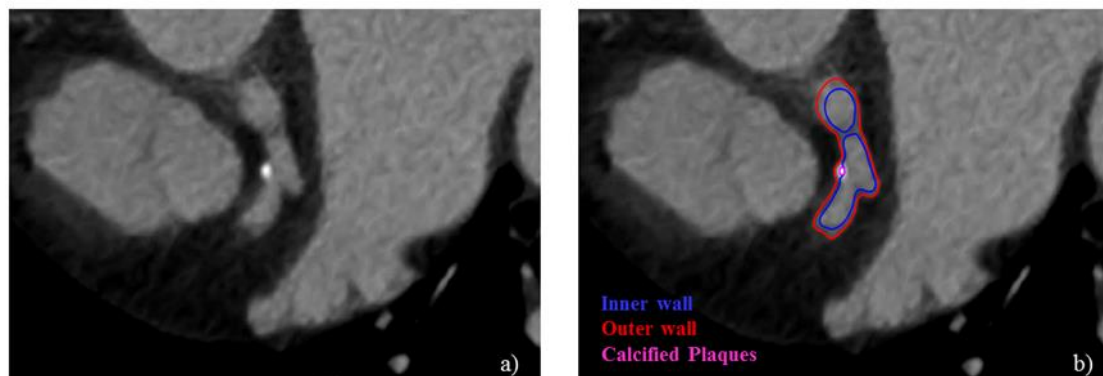


Figure 8: Segmentation process: (i) the acquired image, (ii) inner wall, outer wall and calcified plaques segmentation [61].

Magnetic Resonance Angiography

Even if X-ray coronary angiography is the gold standard for the CAD diagnosis, both in Europe and in USA, several limitations are related to this imaging modality: invasiveness, high cost, exposure of the patient to ionizing radiation. The last years, the need of a cost-effective, non-invasive, patient -friendly approach has resulted in the introduction of Magnetic Resonance Angiography (MRA) as an emerging non-invasive alternative for the coronary arteries visualization [62], [63].

MRA is a cost-effective imaging approach with a high spatial resolution and high soft-tissue contrast. In addition, it has the ability to create any image plane in three dimensions. No exposure in harmful ionizing radiation is also an advantage of this technique.

However, even if MRA provides superior soft-tissue characterization compared with CTA, this technique is challenging because of the arising motion artefacts during the extended acquisition time and also due to the difficulties to obtain satisfactory contrast-to-noise ratio, spatial resolution, and volumetric coverage. Despite the aforementioned

challenges, MRA is a rapidly emerging imaging modality, which can provide reliable images of the proximal and mid-vessels.

MRA enables the visualisation of the proximal segments of the coronary arteries with a great accuracy (nearly 100 %). Superior results are obtained with the LAD and the RCA. The visualization of the LCX is of lower quality and for a shorter course [64]. MRA angiography presents several advantages over CTA [65]: (i) the patient is not exposed to ionizing radiation, therefore, it is suitable for evaluating the coronary arteries in children/ young adults, since the risk for cancer from radiation exposure is higher in these groups, (ii) can assess the arterial lumen of the coronary artery and provide better diagnostic performance, even in a segment with heavily calcified plaque and, (iii) the arterial visualization is enabled without the need of contrast agents.

Intravascular Coronary Imaging

Intravascular coronary imaging with ultrasound (IVUS) (Figure 9), optical coherence tomography (OCT), and near infrared-spectroscopy (NIRS) can provide useful and detailed information for the composition of the atherosclerotic plaque. Gray-scale IVUS is not able to differentiate the individual plaque components, however virtual histology (VH)-IVUS can detect the presence of necrotic core, dense calcium, fibrous, and fibrofatty plaque with high accuracy [66].

OCT is an invasive imaging technique which produces high resolution intracoronary images. It has the same general operation principle with IVUS, however OCT is based on infrared light, not ultrasound [67]. OCT can differentiate the fibrous, calcified, or lipid-rich plaque and identify thin-cap fibroatheroma (Figure 10). It can also recognize intraluminal thrombus [68]. Near-infrared spectroscopy (NIRS) uses diffuse reflectance near-infrared light in order to create a chemogram of vessel wall components. It is a technique based on the detection of varied absorption and scattering patterns [23]. Despite the fact that NIRS can identify lipid, which is an underlying high-risk plaque in human arteries, its major limitation is that it cannot provide any structural information on the plaque.

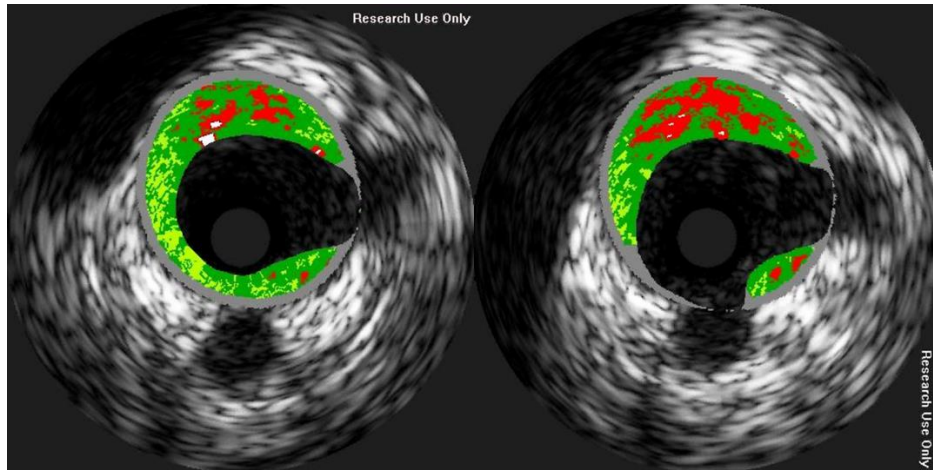


Figure 9: Images of intravascular ultrasound (IVUS).

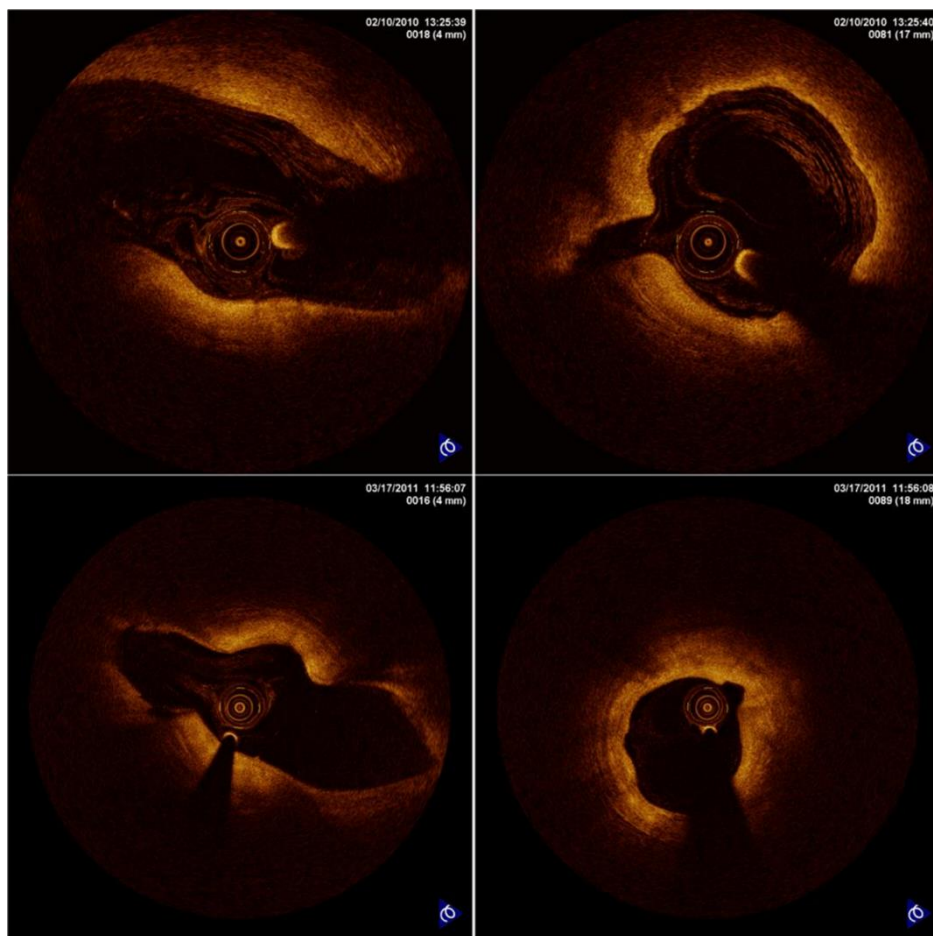


Figure 10: Images of Optical coherence tomography (OCT).

Fusion of intravascular ultrasound and angiography

Through the fusion of IVUS and the angiography and the application of a specific segmentation algorithm, the 3D reconstruction of a coronary artery can be achieved [69]. Specifically, the segmentation algorithm is utilised for detecting the ROI in the

IVUS. A cubic B-spline is used for the catheter path in each biplane projection. Each B-spline curve is swept along the normal direction of its X-ray angiographic plane forming a surface. A 3D curve, which represents the reconstructed path, is the result of the intersection of the two surfaces. The detected ROIs in the IVUS images are positioned perpendicularly onto the path and a sequential triangulation algorithm is used for computing their relative axial twist. An efficient algorithm is used for estimating the absolute orientation of the first IVUS frame.

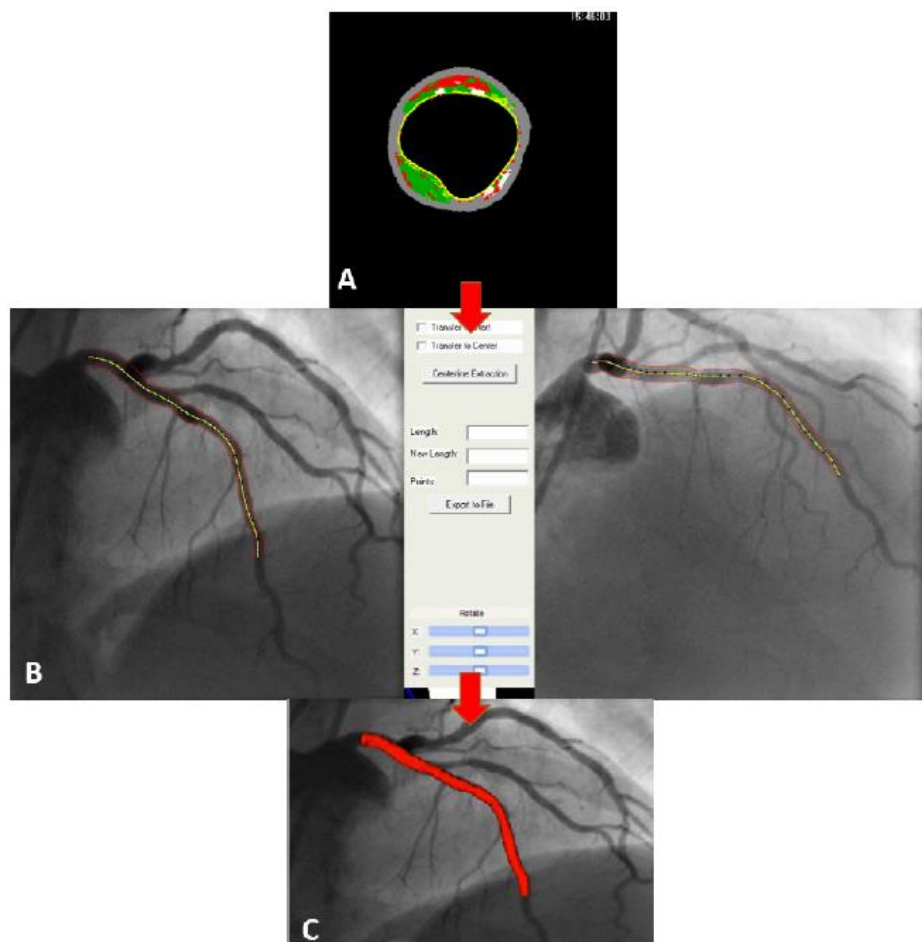


Figure 11: Fusion of IVUS and angiography [70].

Next-generation intravascular ultrasound and optical coherence tomography

High-definition intravascular ultrasound

The high-definition IVUS has the advantage of relatively deep imaging penetration, which is a key element for the conventional IVUS, and offers an improved higher resolution image with IVUS at a higher frequency. High-definition (60-MHz) IVUS

can provide superior axial resolution (<40 vs. 100mm), faster catheter pullback speeds (10 vs. 0.5 mm/ s) and rapid image acquisition (60 vs. 30 frames/s) compared with conventional IVUS. In addition, high-definition-IVUS has additional benefits over OCT; greater tissue penetration and vessel wall visualisation. Furthermore, high-definition-IVUS systems can utilize more imaging data for developing an image, improving the dissections, overlapping stent struts and thrombus detection, which in turn can be beneficial for improved treatment decisions [71].

Polarization-sensitive optical coherence tomography

Polarization-sensitive OCT is a new imaging technique that enables the quantification of collagen and SMCs in atherosclerotic plaques. Polarization-sensitive-OCT can estimate the polarization state of backscattered light and detect tissue birefringence, such as collagen. A stable plaque is related with high collagen content, thicker collagen fibres and large numbers of SMCs. On contrary, contrast, unstable plaques are associated with lower collagen content, thinner collagen fibres and fewer SMCs. Polarization-sensitive-OCT can estimate the local retardation, which is the change of the polarization states along depth, and provides valuable information on critical plaques [72].

1.3 Treatment options for coronary atherosclerosis

Currently, the pharmacological treatment of atherosclerosis is based on lipid lowering combined with anti-inflammatory therapies. However, these therapies cannot fully inhibit the progress of atherosclerosis, since their maximum efficacy is only 30% - 40% [73]. Based on the fact that the immunological system plays a significant role in atherosclerosis development, the inclusion of anti-inflammatory and immunomodulatory strategies has become a reality with very promising results [74].

Coronary Artery Bypass Grafting (CABG) is an “open-heart surgery, in which a section of a blood vessel is grafted from the aorta in order to bypass the blocked section of the coronary artery and improve the blood supply to the heart. In 1910, Alexis Carrel was the first to describe CABG [75] and it was in the late of 1930s, when cardiac surgery became more feasible. In 1960’s, the first successful human coronary artery bypass operation was performed [76], while currently the number of CABG is declining from a peak of 519,000 operations in 2000 to approximately 300,000 cases in 2012 [77].

1.4 Angioplasty, stenting and by-pass

Today the gold standard for treating atherosclerotic coronary vessels is Percutaneous transluminal coronary angioplasty (PTCA). The first PTCA was performed by Andreas Gruntzig in 1977, as an alternative form of CABG [78]. PTCA includes the insertion of a catheter, with a small inflatable balloon on the end, within the narrowed coronary artery and the inflation of the balloon which pushes outward, compresses the plaque and expands the surrounding wall of the artery. This process results in widening the arterial lumen and restoring the blood flow.

Coronary artery stents are tubular metal scaffolds, which are positioned in the stenotic region through a balloon catheter, usually after angioplasty, and are expanded to provide scaffolding support and prevent arterial recoil. After this process, the scaffold remains inside the artery as a permanent part (for non- degradable stents). An ideal stent deployment process requires an expansion, which is sufficient enough to open the vessel obstructions and in parallel causes minimal arterial damage [79], since ISR can be a result of unsuccessful stent implantation, including arterial wall over-stretch and injury, incomplete stent expansion or fracture of the stent struts.

1.5 Evolution of coronary stenting

The objective of a coronary stent is to maintain the vessel patency. The deployed stent should provide in parallel several characteristics, such as good biocompatibility, flexibility, strong radial force, deliverability, low thrombogenesis and low rates of neointimal hyperplasia. Bare metal stents (BMS) were the first devices utilised for coronary stenting. Even though these devices reduced the rates of restenosis compared with balloon angioplasty, ISR and arterial re- narrowing were observed in 20%-30% of the lesions [80].

Sigwart *et al.* [81] implanted, in 1986, the first WALLSTENT® (Schneider AG, Bülach, Switzerland), a self- expanding Nitinol stent. The Palmaz-Schatz stent (Johnson & Johnson, New Brunswick, NJ, USA) was developed late in 1987 and it was the first BX stainless steel stent. However, a major issue with the BMS was the high incidence of ISR [82]. There have been significant improvements in the design and material of BMS over the past decade, including the utilization of new alloys, such as cobalt-chromium and platinum chromium, as well as newer materials that allow the manufacture of stents with lower profile, pushability and trackability and thinner struts,

preserving however the radial strength. Some characteristics of some BMSs are presented in Table 4.

Table 4: Eight Approved Bare-Metal and Coated (Drug-Free) Metal Coronary Artery Stents.

Stent	Manufacturer	Material(s)	Design Characteristics
Bare-Metal Designs			
ACT-One®	Progressive Anangioplasty Systems, Menlo Park, CA	Ni-Ti alloy (Nitinol)	Tubular-slotted design; diameter: 4 mm; length: 17 mm; balloon-expandable
GFX®	Applied Vascular Engineering, Santa Rosa, CA	316 stainless steel	Corrugated-ring design; diameter: 3 mm; length: 12 mm
InFlow™	InFlow Dynamics, Munich, Germany	316 stainless steel	Tubular-slotted design; diameter: 3 mm; length: 15 mm
MULTI-LINK™	Advanced Cardiovascular Systems/Guidant, Santa Clara, CA	L-605 CoCr alloy	Corrugated-ring design; diameter: 2.5, 2.75, 3.0, 3.5, 4.0 mm; thickness: 0.091–0.124 mm; length: 8–28 mm; balloon-expandable
NIR®	Medinol Ltd., Tel Aviv, Israel	316 low-carbon steel; gold	Cellular (7- or 9-cell) design; diameter: 2–5 mm; thickness: 0.10 mm; length: 9–32 mm; balloon-expandable
Palmaz-Schatz	Johnson & Johnson, Interventional Systems, Warren, NJ	316 stainless steel	Tubular-slotted design; diameter: 3.5 mm; length: 9–15 mm; self-expandable
Coated (Drug-Free) Metal Designs			
Biodiv Ysio™ AS	Biocompatibles Cardiovascular, Inc., San Jose, CA/Abbott Labs	316L stainless steel	Tubular-slotted design; diameter: 2.0, 2.5 mm; thickness: 0.05–0.09 mm; length: 15 mm; balloon-expandable

Rithron-XR®	Biotronik GmbH, Berlin, Germany	316L stainless steel	Slotted design; balloon- expandable
-------------	------------------------------------	-------------------------	---

The need for repeat revascularisation secondary to restenosis was the main limitation of BMS implantation. Apart from acting as a vascular scaffold, stents can act as a drug delivery system, the so called drug-eluting stents (DES). DESs consist of a metallic stent, a polymer-based drug delivery platform and a pharmacological agent. The aim of DES technology is to minimize the vascular inflammation and the cellular proliferation and consequently reduce ISR. The introduction of DES has contributed to a reduction of restenosis and a decrease in revascularisation procedures. Studies such as RAVEL [83], SIRUS [84], and TAXUS IV [85] clearly demonstrated a reduction of angiographic restenosis, while the efficacy of DES in reducing ISR was also confirmed by a number of larger clinical studies for different indications [86]. Second-generation DES, consisted of thinner stent struts and more biocompatible polymeric coatings with reductions in drug load. These scaffolds were designed to overcome the limitations of the first-generation DES. Some characteristics of some DES are given in Table 5.

Table 5: Features of Four Approved DES [87].

Stent	Manufacturer	Material(s)	Eluted Drug	Design Characteristics
CYPHER™	Cordis Corp., Miami Lakes, FL	316L stainless steel	Sirolimus	Slotted design; balloon- expandable
TAXUS™, Express ² ™	Boston Scientific Corp., Natick, MA	316L stainless steel	Paclitaxel	Slotted design; length: 16, 24, or 32 mm; thickness: 2.5, 3.0, or 3.5 mm; balloon- expandable
Endeavor	Medtronic, Santa Rosa, CA	CoCr alloy	Zotarolimus	Low profile; strut thickness: 0.091 mm
Dexamet™	Abbott Vascular Devices, Redwood City, CA	316L stainless steel	Dexamethasone	Tubular-slotted design; thickness: 0.05– 0.09 mm; length: 15 mm

Due to the permanent irritation of metallic stents in the coronary arteries and the subsequent undesirable processes on the vascular biology, bioresorbable scaffolds (BRS), a novel and challenging therapeutic option has appeared. The concept of BRS

to support the vascular integrity during the percutaneous coronary intervention (PCI), followed by the release of antiproliferative drugs and a controlled scaffold degradation that restores vasoreactivity and function, has been proven to be a potential solution to the limitations raised by the current metallic stents [88], [89], [90]. In Appendix A1, an overview of clinical studies involving BMSs and DESs are presented.

1.6 Considerations in relation to stenting

Even if the widespread use and the advancements in the R&D technology enabled the advent of a variety of different stent devices, the success of cardiovascular stents implantation has been limited in some cases by adverse clinical outcomes. ISR, or a re-narrowing of a previously treated arterial vessel due to excessive tissue growth, is one of the main complications following stent implantations. It has been estimated that restenosis requiring revascularization occurs in 20% of patients [91]. In order to reduce restenosis, DES have been developed. Despite the fact that DES have reduced the incidence of restenosis compared to BMS, restenosis rates as high as 10% [92], [93] are still a reality. In addition, the inhibition of SMC growth, results in the growth or migration of endothelial cells from the stent struts [94], [95] and this lack of a layer of endothelial cells over stent struts increases the possibility of late stent thrombosis. Even if the incidence of late stent thrombosis is only 1%, it can cause high incidents of acute myocardial infarction, approximately in 40-70% of cases.

1.7 Mechanisms of restenosis

Restenosis is a process that occurs after mechanical injury, such as in the case of balloon angioplasty and stent implantation. The positioning of a conventional BMS, through the utilization of a balloon, initiates a variety of reactions including re-endothelialization of the surface, crushing, and lifting of the atherosclerotic plaque from the underlying arterial wall, and tearing and stretching of the medial wall, with eventual neointimal growth, as a general healing response (Figure 12).

The first reaction to the mechanical injury by stent implantation is the activation of the platelets and the formation of thrombus, accompanied by inflammatory reaction, even if dual antiplatelet therapy is followed. However, to note that, in case of dual antiplatelet therapy absence, the extent of platelet deposition is significantly higher. This is followed by the activation of chemokines and cytokines, which result in the

proliferation and migration of SMCs within the media and the intima, which in turn results in intimal thickening and the surrounding extracellular matrix (ECM), with or without the progression to restenosis [98]. To understand the underlying mechanisms of restenosis following stent implantation, animal studies have been instrumental in elucidating the process of remodelling and its contribution to restenosis [99].

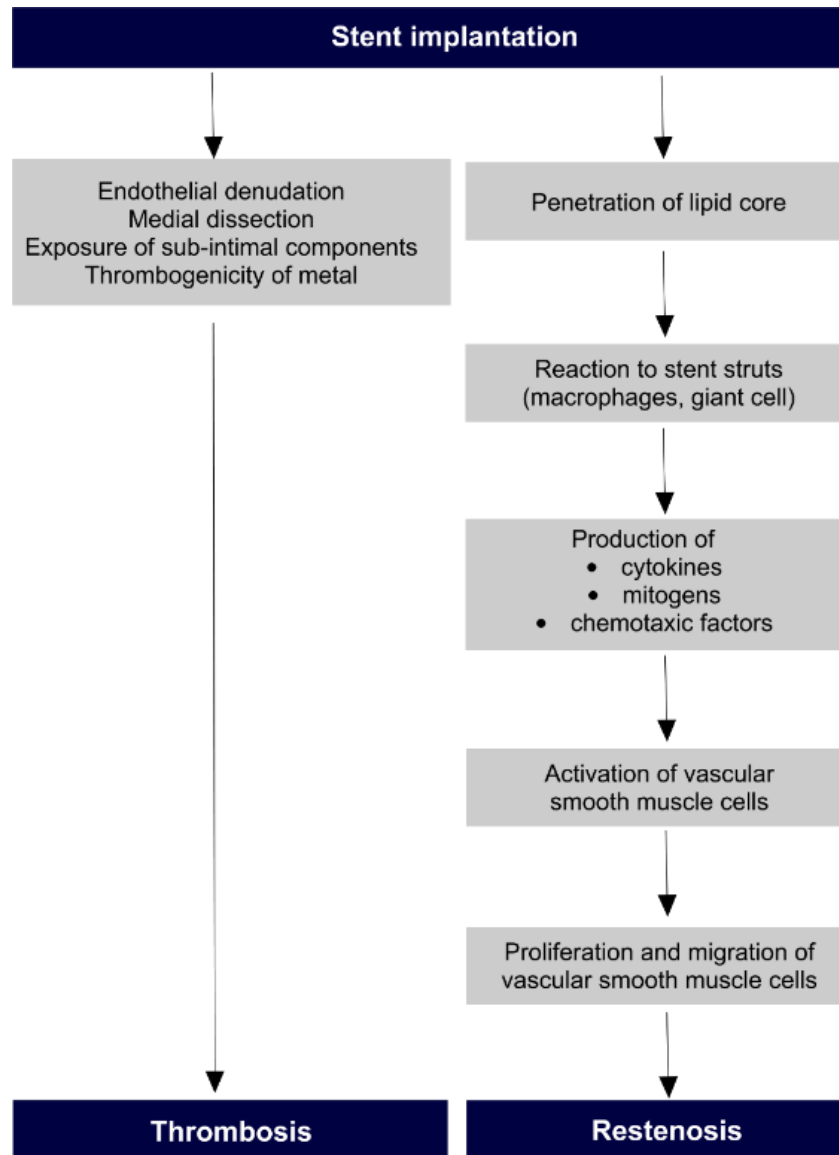


Figure 12: Pathway leading to restenosis after stent implantation [97].

1.7.1 Pathophysiology of restenosis

Restenosis, an exaggerated response, is defined as 75% cross-sectional luminal area narrowing of the stented area due to neointimal tissue caused by SMCs and proteoglycan-collagenous matrix presence. There is a difference in the time course of re-endothelialization and neointimal growth after stent deployment between animals,

such as pigs, rabbits and human coronary arteries [95], [100]. For instance in animal models, the peak of neointimal growth is observed at 28 days after BMS implantation, whereas this process takes place in humans after 6–12 months following stent implantation [100]. In animal models with normal underlying media, restenosis is not a common response and is observed only in case there is a severe injury with tearing and a profuse inflammatory response to the underlying wall. The animal model that can more closely reproduce and simulate the human disease is the porcine coronary artery model, however, the rate of healing in porcine models are very rapid with greater proliferation compared to human models.

1.7.1.1 The early phase: endothelium injury and inflammatory response

In the early phase after stent implantation, endothelial cells (ECs) are partially or totally destroyed and promote the activation and aggregation of platelets, the infiltration of circulating leucocytes, and the release of growth factors and cytokines [101], [98], [102].

The early process after BMS implantation is related to the endothelium injury [103] and can be divided into the following phases: (i) endothelial denudation, (ii) re-endothelialization, and/or (iii) neo-endothelium [98]. Infact, the response to coronary stent implantation concerns the complete to partial destruction of the EC layer, which initiates the thin thrombus layer formation that covers the vascular and stent surface, whereas the complete coverage of the neointima by the vascular ECs takes place several weeks after. The endothelium injury and the placement of stent, which is a foreign in the arterial environment, results in the activation of platelets and their accumulation at the site of the lesion, with recruitment of circulating leucocytes [98]. The interaction of leucocyte–platelet is critical for the initiation and progress of neointimal formation. According to recent studies, the inflammation post stenting is a very critical process observed also in animal models, using specific antibodies to leucocytes (CD45), macrophages (CD14), and monocytes (CD115). In human studies, a strong correlation has been shown between an early chronic inflammation and intimal thickening in stented coronary arteries [104].

1.7.1.2 Granulation tissue formation

The ECs proliferate and migrate over the injured arterial areas, while the fibrin clot is replaced by the SMCs and the macrophages. The newly developed vascularized tissue contains macrophages, which are responsible for the phagocytosis of cell debris and the secretion of growth factors chemokines and cytokines. The macrophages promote the inflammatory response, but in collaboration with platelets and ECs assist in secreting the growth factors.

1.7.1.3 Tissue remodelling phase

The hallmark of this phase is the modification of the SMCs, which are activated by the growth factors/cytokines as a result of the injured endothelium and media, platelets, and infiltrated inflammatory cells as well as by the compressive forces created in the vessel wall by the stent positioning and expansion along with the low shear stress-induced by stent struts. The SMCs migrate and proliferate from the media towards the intima. The proliferation of the SMCs in the media and the subsequent migration into the intima requires the transition of SMCs from a contractile to a synthetic phenotype with the eventual ECM deposition in the intima [105]. The ECM plays an important role due to the cells interaction that influence the wound adhesion, migration, proliferation, and remodelling. The first phase of the matrix formation includes the formation of the “provisional matrix”, which is created by plasma proteins, such as fibrin, fibrinogen, and fibronectin [106]. Then, the ECM allows the macrophages and SMCs to adhere and initiate the repair process. Collagens also adversely affect the SMCs by arresting its proliferation and eventually leading in altered contractile forces with a subsequent SMC apoptosis and cell loss. These processes are closely interconnected and difficult to be separated in sequential phases.

1.7.2 Thrombosis

Stent thrombosis is a serious issue and results from the occlusion of the endoprosthetic lumen by thrombus and is a process with a wide chronological spectrum that may occur immediately after stent implantation to years after implantation. Stent thrombosis can be categorized among the most serious complications of PCI, therefore its incidence and prevalence has been examined very closely. The stent thrombosis rates have paralleled the evolution of stents and antiplatelet agents. Even if there is a debate about

whether randomized controlled trials can accurately reflect and reproduce the “real-world” data applicable in clinical practice, several research studies have examined stent thrombosis and a variety of clinical trials have been conducted focusing on this process.

1.7.2.1 Pathophysiology and factors implicated in stent thrombosis

Again, as in ISR, the endothelium also plays a pivotal role in the pathogenesis of stent thrombosis. The exposure of the arterial wall to the offending agent contributes to the stereotypical response of neointimal formation and in intimal thickening [107]. This is primarily initiated by the proliferation of SMCs due to a multitude of histochemical reactions.

The mechanisms underlying stent thrombosis are multifactorial and can be classified to patient-specific factors, procedural factors (including stent selection), and post-procedural factors (type and duration of antiplatelet therapy) [108] (Table 6). Stent thrombosis occurs more often in patients with acute coronary syndromes, diabetes mellitus and chronic kidney disease [109]. In addition, another factor that has been strongly correlated to stent thrombosis is the premature discontinuation of dual-antiplatelet therapy within 6 months [110].

Table 6: Potential Mechanisms of Stent Thrombosis.

Potential Mechanisms of Stent Thrombosis	
Patient-related factors relating to increased thrombogenicity	
Smoking	Diabetes mellitus
Chronic kidney disease	Acute coronary syndrome presentation
Thrombocytosis	Thrombocytosis
Lesion-based factors relating to rheology/thrombogenicity within stents	
Diffuse coronary artery disease with long stented segments	Diffuse coronary artery disease with long stented segments
Bifurcation disease	Bifurcation disease
Stent-related factors	
Poor stent expansion	Edge dissections limiting inflow or outflow
Strut fractures	Development of neoatherosclerosis within stents with new plaque rupture

One of the most commonly implicated factors of stent thrombosis is the type of the implanted coronary stent. Despite the fact that DES is more prone to stent thrombosis, and BMS have high rates of ISR rates, this is a very simplistic fact since there is a great degree of crossover in the pathological mechanisms responsible for both entities. According to Stone *et al.* [111], who conducted a pooled data analysis from nine (9) double-blind trials with patients randomly receiving a BMS or a first-generation DES,

the 4-year rates of stent thrombosis were higher in the DES group of patients compared to the BMS groups, however the results were statistically insignificant. After one year, these stent thrombosis higher rates in the first-generation DES groups achieved statistical significance, suggesting that the post implantation timing of stent thrombosis is critical and must be taken into consideration for understanding the role of device-related risk factors. The procedural factors related to stent thrombosis include the selection of the stent (BMS, DES, BRS) and the degree of stent expansion and positioning to the arterial wall [108]. The stent design, material, and coatings can influence the onset of thrombogenicity. Kolandaivelu *et al.* [112] showed that thick-strutted (162 μm) stents caused 1.5-fold more thrombogenicity than thin-strutted (81 μm) devices ($P < 0.001$) in porcine coronary arteries. Tada *et al.* [113] showed that thin-strut DES improved stent strut coverage rates compared to thick-strut DES at 6–8 months follow-up.

1.8 Objective of the thesis

The aim of this thesis is to evaluate the effect of stent design and material on stent deployment using the Finite Element Method. This parameter analysis could be applicable to BX stents in a variety of materials. The assessment of the stress state within the arterial wall and the scaffolding performance of the device is the main interest of this thesis.

This work also introduces the importance of personalised medicine. It enters the realm of utilising patient specific characteristics for evaluating the stent. This differentiation from the current approaches that focus on idealised geometries and do not take into account the individual arterial morphology could be considered as a fundamental innovation.

1.8.1 Thesis structure

In Chapter One, an overview of cardiovascular disease, atherosclerosis and treatment options focusing on stenting is presented. In detail, the evolution of coronary stenting and the main considerations during this interventional procedure, the mechanisms and the pathophysiology implicated in ISR and thrombosis are described.

Chapter Two provides an analysis on the stent market, the key players in the coronary stent as well as the predictions for the market potential in the future.

Details on the stents desirable characteristics and on the properties from the materials perspective is provided in Chapter Three. A detailed description of the categorization of stents based on the geometry and the two main categories available in the market is also described.

Chapter Four presents the process of stent evaluation that is currently followed, with reference to the regulatory framework, the approval process, the *in vitro* mechanical testing performed in stents, the animal and the finally the clinical studies.

Chapter Five provides a comprehensive literature review of computational approaches in coronary stent modeling. More specifically, the modeling approaches on stent free expansion and expansion in idealized and patient specific arterials segments are presented.

Chapter Six describes the main steps that were followed to create the FEM models used in the current analysis. Specifically, information on the stent design and the 3D arterial reconstruction are presented accompanied with the method for meshing that was followed. The boundary conditions and the loading that are used as well as the governing equations are provided. Then the two main approaches, the creation of the FEM models with different stent design and materials, is performed and the relevant results are presented in terms of deformation and stress distribution in the stent scaffold and in the vascular tissue.

Chapter Seven provides a comparison and an evaluation of the FEM with the representative stent materials (Model A, Model B and Model C) and the three representative stent designs (Model D and Model E). The comparisons focus on assessing the effect of design and material on stent expansion, stress distribution and occurred arterial stresses during the deployment process inside a reconstructed diseased arterial segment.

Chapter Eight provides an overview of the limitations of the current thesis in terms of the materials properties used, the assumption of the homogeneity of the arterial wall and the lack of the direct experimental validation of many of the computational results created.

Chapter 2: Stent Coronary Market

Since the first stent development and implantation, a variety of different stent designs have been proposed by the Stent Biomedical Industry, with variations in design, materials and technology. Coronary stents can be utilized for a variety of indications in CAD, such as de novo lesions, small-vessel disease, bifurcation lesions, tortuous and narrow lesions. Coronary stents can improve the clinical outcomes for these indications, and improve the quality of life for patients.

Currently, stent implantation has become the gold standard in the treatment of occluded by atherosclerosis arteries. Specifically, in 2011, the global market of coronary stent devices reached €7 billion with a prediction of approximately €15.2 billion by the end of 2024 [114], [115]. In Table 7, the key metrics for coronary stents in 10 major markets (US, France, Germany, Italy, Spain, UK, Japan, Brazil, China, and India) is presented [116], whereas the distribution per country for the actual and expected sales of coronary is depicted in Figure 13.

Table 7: Key metrics for coronary stents in 10 major markets.

Coronary stents market, key metrics in 10 major markets (2013-2020)	
2013 coronary stents market sales (\$m)	
US	\$2,065.3
EU	\$573.1
APAC	\$2,123.3
Brazil	\$124.0
Total	\$4,885.7m
2013 Global market sales by type of stent (\$m)	
Drug-eluting Stents (DES)	\$4,335.6m
Bare metal Stents (BMS)	\$530.1m
Pipeline assessment (Stage of clinical development)	
Number of stents in the early development stage	4
Number of stents in the preclinical stage	13
Number of stents in the early clinical stage	6
Number of stents in the late clinical stage	5
Key events (2013-2020)	Level of impact
(2013) Boston Scientific receives FDA approval for Promus PREMIER everolimus-eluting platinum-chromium (Pt-Cr) stent	1
(2013) Approval and launch of next generation DES, such as BioFreedom (Biosensors International) and Coroflex ISAR (B.Braun) in the EU	2
(2013) Elixir Medical Corporation receives a CE mark for the DESolve bioabsorbable stent (BAS) in the EU	2

(2014) MicroPort Scientific Corporation receives approval for Firehawk (first drug-eluting coronary stent in China)	2
(2014) Approval and launch of STENTYS sirolimus self-expanding stent	1
(2015) Commercial launch of the CE-Marked DESolve 100, a novolimus-eluting, thin strut BAS, in the EU	1
(2015-2016) Expected commercial launch of BAS, such as DREAMS by Biotronik and Fantom by REVA Medical, in the EU	2
(2016-2017) Commercial launch of Absorb BVS in the US and APAC, including in Japan and China	3
(2019-2020) Expected commercial launch of BAS, such as DREAMS by Biotronik and Fantom by REVA Medical, in the US	2
Expected 2020 Coronary Stents Market Sales (\$m)	
US	\$1.849.9m
EU	\$555.2m
APAC	\$3.023.5m
Brazil	\$187.8m
Total	\$5.616.4m

Source: Global Data

EU = France, Germany, Italy, Spain, UK

APAC = Asia-Pacific Ocean (Japan, China, India)

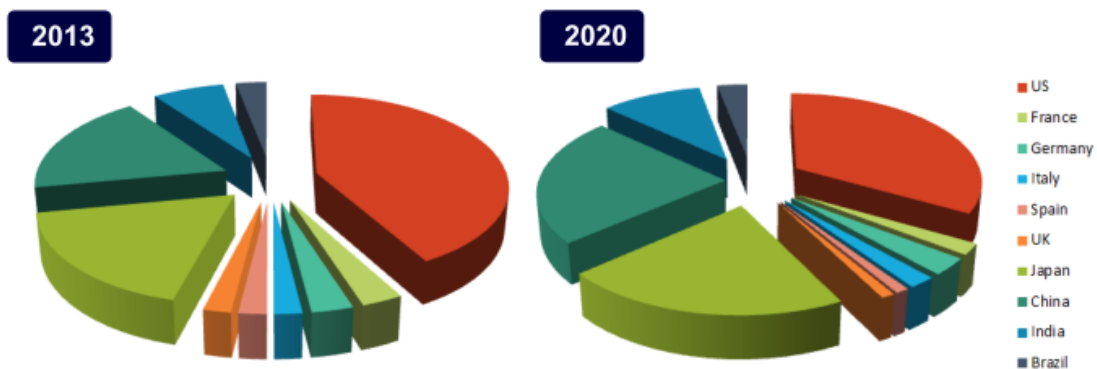


Figure 13: Global Coronary Stents Market Revenue, 2013 and 2020 ([116], [117]).

The application of stents has been widely adopted in the clinical practice and has been linked with improved patient outcomes. Specifically, a variety of BMS and DES exist providing the ability to interventional cardiologists to choose among a handful of stents. DES currently dominate the coronary market and account for nearly 90% of the total stent market. Based on this large market potential and given the high prevalence of CAD in the Europe and worldwide, the Stent Biomedical Industry has paid much attention on the R&D and the commercialization of innovative DES systems. This larger market of DES stents is a result of the extensive clinical expertise of the

Interventional Cardiologists in using these stents, accompanied with the improved outcomes and the reduction in the need of repeating stenting. In case a patient is not a good candidate for being provided a DES, a BMS is implanted. The coronary stents market is a vast and dynamic market with numerous players consisting of large, mid-size, and small companies that develop different types of coronary stents to target various indications. However, the coronary stents market is controlled by a few key players, including Abbott Vascular, Boston Scientific, Medtronic, etc. Other companies such as Rontis, B. Braun, Sahajanand Medical, Technologies and MicroPort Scientific Corporation could be potential competitors to the large stent companies since they develop innovative coronary stent platforms.

Chapter 3: Stents and desirable characteristics

- 3.1 Properties of an ideal coronary stent
 - 3.2 Expansion
 - 3.3 A materials perspective
 - 3.4 Stent design
 - 3.5 Fabrication method
-

Stents can be broadly categorized to BMS, DES and BVS. BMS consist only of metal, and they can also include a biocompatible polymer coating. On the other hand, DES have a drug coating, which is usually bound within a polymer. The drugs that are most commonly used are sirolimus and paclitaxel, which are anti-proliferative, interfere with the cell growth/division cycle [117] and assist in reducing restenosis. BVS are made up of biodegradable materials which gradually degrade in approximately 12 months after the stent implantation. BVS may also include a drug coating. Preliminary results have shown promising results related to the inflammatory response to BVS.

3.1 Properties of an ideal coronary stent

A stent can be considered as ideal if it is easy delivered, provides an adequate arterial support, and reduces the associated risk of restenosis and thrombosis, both in the short and long term. Even if the adverse effects of stent implantation are easy to understand, the definition and evaluation of the stent performance is a challenging task. In engineering terms, the following criteria have been defined as the key criteria that each stent should meet and fulfil to ensure the post-stenting improved outcomes.

- **Radial strength.** This is one of the key objectives of stent implantation since high radial strength is necessary to provide an adequate arterial support.

- **Flexibility.** This is a prerequisite for any stent and concerns how easily the stent can be positioned in the stenotic site in arteries which can be highly curved and tortuous.
- **Crimping on the balloon.** Usually stents are crimped on a folded balloon towards a good deliverability into the artery. Failure to maintain this feature could result in the slipping of the stent off the balloon in a blood vessel.
- **Radiovisibility.** This is the ability of the X-ray attenuation caused by stent material and the ability to absorb X-ray or reduce the permeation. This characteristic is very important since the interventional cardiologists should be able to observe the implanted stent and evaluate the success of the implantation process.
- **Conformability.** This requirement is related to the ability of the stent to conform to the arterial shape, especially in stenosed tortuous sites, where the straightening of the stented artery is not desirable.
- **Good apposition.** The stent should be in a uniform contact with the arterial wall upon deployment. Underexpansion or underdeployment of stents have been identified early on as a risk factor. In case there is lack of contact between the stent struts and the underlying intima, or if one or more struts project into the arterial lumen, undesirable physiological effects, such as ISR and ST can be caused.
- **Biocompatibility.** Different metals, such as polymer coatings, have been evaluated in animal models and subsequently in patients to improve the biocompatibility of metallic stents and reduce the onset of physiological immune responses.

3.2 Expansion

Based on the mode of delivery, stents can be classified to balloon- expandable (BX) and self-expandable (SX). BX stents are manufactured in crimped state and expanded by inflating a balloon. SX are manufactured at the vessel diameter, are crimped and deployed when the constraint is removed. BX are made of metal, usually stainless steel (316L), or other alloys, such as platinum-chromium or cobalt-chromium, that can plastically deform with the balloon inflation. SX are made of shape memory alloys (SMA), such as Nickel-Titanium (Nitinol, Ni-Ti), and expand autonomously after their

release. Nitinol is the most common material for self-expandable stents; Ni–Ti advantages are the optimal superelastic material properties and the excellent biocompatibility performance [118]. The response of Ni–Ti stents depends on the thermo-elastic reversible transformation between two crystallographic structures with different mechanical and physical properties: (i) austenite, where the unit cell is more ordered and stable at temperatures above A_f (martensite to austenite transformation finish temperature), and (ii) martensite, where the unit cell is less ordered and stable at temperatures below M_f (austenite to martensite transformation finish temperature) [119].

3.3 A materials perspective

Since 1987, when the first stainless steel stent was introduced, the materials used for coronary stents have evolved and expanded rapidly. In order to fulfil the requirements and the clinical drivers of stent implantation and achieve an improvement of the stent's performance, manufacturers invested heavily in R&D focusing on the materials and surface technologies [120].

BX stents should be able to withstand plastic deformation and preserve the required size once deployed. On the other hand, SX stents, should present sufficient elasticity in order to be compressed and then expand in the target lesion [12]. The characteristics and properties of an ideal stent have been in detail presented in section 3.1. Generally, stents should have: (i) low profile and be able to be crimped on the balloon catheter supported by a guide wire; (2) sufficient expandability ratio; after the stent is inserted at the target lesion and after the inflation of the balloon, the stent should sufficiently expand and conform to the arterial wall (iii) good radial hoop strength and negligible recoil; after the stent implantation, it should be able to overcome the imposed by the arterial wall forces and not collapse, (iv) adequate flexibility; stents should be flexible enough to be guided through atherosclerotic arteries with small diameters, (v) enough radiopacity/MRI compatibility, in order to allow the clinicians to assess the *in vivo* location of the stent; (vi) resistance to thrombus formation to be compatible with blood and not promote platelet adhesion and deposition, and (vii) drug delivery capacity to carry the drug and prevent restenosis. In general, among the most common materials used for stent manufacturing are: (i) 316L stainless steel (SS316), (ii) platinum–iridium (Pt–Ir) alloy, (iii) tantalum (Ta), (iv) nitinol (Ni–Ti), (v) cobalt–chromium (Co–Cr)

alloy, (vii) titanium (Ti), (viii) pure iron (Fe), and (x) magnesium (Mg) alloys (Table 8).

Table 8: Stent materials and properties.

Metal	Elastic Modulus (GPa)	Yield Stress (MPa)	Tensile strength (MPa)	Density (g/cm ³)
316L Stainless Steel (ASTM F138 and F139; annealed)	190	331	586	7.9
Tantalum (annealed)	185	138	207	16.6
Cp – Titanium (F67; 30% cold worked)	110	485	760	4.5
Nitinol	83 (Austenite phase)	195-690 (Austenite phase)	N/A	
	28-41 (Martensite phase)	70-140 (Martensite phase)	N/A	
Cobalt- Chromium	210	448-648	951-1220	9.2
Pure iron	211.4	120-150	180-210	7.87
Mg alloy (WE43)	44	162	250	1.84

3.3.1 Properties of SS316

SS316 is the most commonly used metal for stents, both for BMS and coated stents. SS316 is among the most preferred materials, due to the well-suited mechanical properties accompanied with excellent corrosion resistance characteristics. However, it has a certain limitation that concerns the release of ions from the metal surface. Specifically, the release of nickel, chromate, and molybdenum ions from SS316 stents may induce local immune response and inflammatory reactions, which are linked to intimal hyperplasia and in-stent restenosis [121].

3.3.2 Properties of Pt–Ir alloys

Stents made from Pt–Ir alloy show excellent radiopacity [122] and enable the 3D visualisation of the lumen using MRI. Pt–Ir alloys have an excellent corrosion resistance [123], however they have poor mechanical properties [124]. Although they reduce the onset of thrombosis and neointimal proliferation, they have a higher recoil percentage (16%) than the SS316 stents (5%) [125]. However, the artifacts from Pt–Ir alloy in MRI are lower than those of SS316 stents.

3.3.3 Properties of Tantalum

Ta presents good corrosion resistance due to the highly stable surface oxide layer [126], which prevents the electron exchange between the metal and the adsorbed biological tissue. Ta is used as a coating on SS316 surfaces to improve corrosion properties and enhance the biocompatibility [127]. Ta is an MRI compatible material, and due to its non-ferromagnetic properties does not produce significant artifacts [128]. Although Ta is biocompatible and superior to SS316 [129], the commercial availability of Ta stents is lower than SS316 stents.

3.3.4 Properties of Co–Cr alloy

Co–Cr alloys are used for manufacturing coronary stents. Co–Cr alloys show excellent radial strength as a result of their high elastic modulus. Co–Cr alloys have the ability to deliver ultra-thin struts with increased strength, which is one of the most critical parameters in stent design. Additionally, these stents are radiopaque as well as MRI-compatible.

3.3.5 Properties of Ti

Ti is applied in several biomedical fields, such as in orthopedic and dental implants, due to the excellent biocompatibility and the enhanced corrosion resistance. Ti has a high yield strength in approximately the same range with Co–Cr, however it has lower tensile strength that increases the probability of failure when expanded to stresses beyond their yield strengths, which is a normal condition in BX stent deployment. Due to these inadequate mechanical properties, Ti is not commonly used for making stents, however Ti-nitride-oxide coating on SS316, such as the one used in the Titan stent (Hexacath, France) [130], or other Ti alloys, such as Ni–Ti, is extensively used in stent manufacturing.

3.3.6 Properties of Ni–Ti

Ni–Ti consists of 49.5–57.5 at% nickel, while the remaining is Ti [131]. It is used in the development of SX stents, due to its shape memory characteristics. At room temperature, these stents have a smaller diameter, whereas an expansion to their present diameter is performed at body temperature. Ni–Ti is plastically deformed at room temperature, the so called martensitic phase, and crimped on to the delivery system.

After its implantation, a recovery in its original shape is performed (austenite phase) and then it conforms to the arterial wall, due to the increase in the temperature inside the body. Although Ni–Ti is considered as a corrosion resistant material, several studies report a release of nickel ions and other toxic effects to the arterial tissue [132]. To overcome this barrier, appropriate processes are followed, such as by plasma-immersion ion implantation [48], nitric acid treatments [49], heat treatments [50], and electropolishing [50], that focus on reducing the nickel concentration on the surface [47], [48]. In addition, to improve the corrosion resistance, the Ni–Ti stents can be coated with materials, such as Ti nitride, polyurethane and polycrystalline oxides. An overview of some stents approved by the FDA is presented in Table 9.

Table 9: Overview of FDA approved coronary stents.

FDA approved coronary stents		
Stent name	Manufacturer	Bare stent material
BiodivYsio™ AS	Biocompatibles Cardiovascular Inc. CA	316L stainless steel
BeStent™ 2	Medtronic	316L stainless steel
CYPHER™	Cordis Corporation	316L stainless steel
Multi-link vision™	Guidant Corporation	L-605 Cobalt Chromium alloy
NIRflex™	Medinol Ltd	316L stainless steel
TAXUS™ Express2™	Boston Scientific Corporation	316L stainless steel
Liberté™ Monorail™	Boston Scientific Corporation	316L stainless steel
Rithron-XR	Biotronik GmbH	316L stainless steel

3.4 Stent design

The categorization of stents according to their geometry is one of the most interesting aspects of stent design. A variety of different stent designs are currently available in the market. In general, commercially available stents can be classified to two main categories: (i) closed-cell and open cell design, with differences in the type of connection, such as peak to peak or valley to valley (Figure 14).

Typically, the number and arrangement of bridge connectors differentiate the two stent designs. A variety of clinical studies have been conducted focusing on the evaluation of these two different stent types design, such as the one of Sciahbasi *et al.*, who showed that the implantation of a closed cell stent design is associated with better coronary angiographic flow after stenting [133]. Most stents are manufactured from wire or tubing. Wire stents are used for SX stents, while laser cutting from tubing is used for

BX stents. The stent design process should take into account several conflicting mechanical requirements; (i) good radial support for achieving significant elastic recoil in deployment, (ii) a design that achieves a minimum crimped diameter sacrifices structural strength, (iii) stiff design assures secure arterial contact but may invoke arterial damage. In order to achieve the optimal balance of strength and flexibility, different stent designs have been created. The commercially available stent geometries (Figure 15) are subjected to strict patent claims, therefore, the manufacturer’s detailed information related to the stent geometry is usually not publically available.

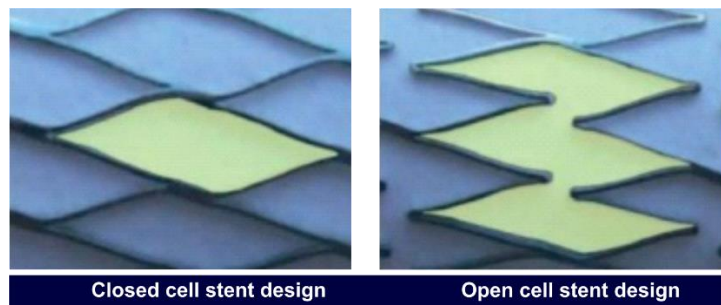


Figure 14: Closed vs Open cell stent design [137].

To accurately represent the stent design, a microscope or micro-Computer Tomography is required. The micro-CT strategy enables the creation of a precise 3D reconstruction of both the stent and balloon directly from the CT-scans. These stent dimensions can be used to build a 3D CAD stent model.

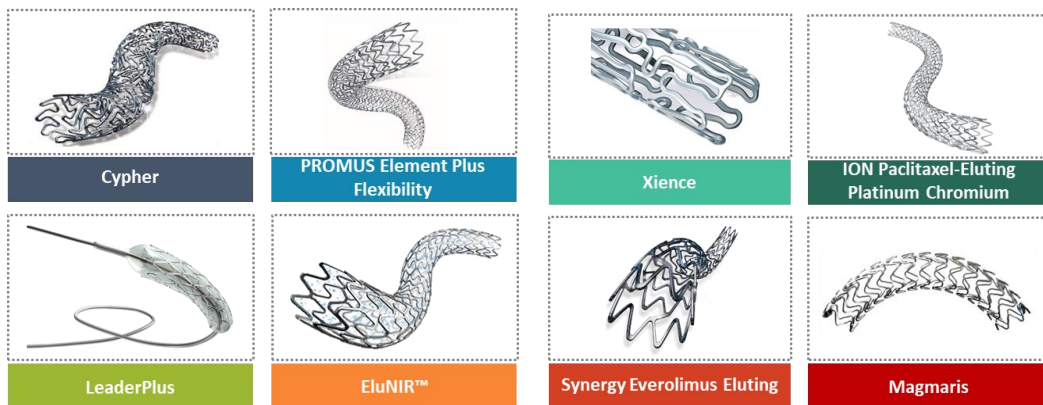


Figure 15: Overview of some commercially available stents.

3.5 Fabrication method

Depending on the stent type, different fabrication methods exist for stent manufacturing, including bottom-up strategies, such as 3D printing and solvent casting and top-down fabrication approaches, such as laser machining, molding, electroforming [134]. The multitude of fabrication modalities are presented in Table 10.

Table 10: Stent fabrication processes.

Fabrication Process	Materials		Field of application	
	Metals	Polymers	Industry	Academia
Nd:YAG Laser*	✓	x	✓	✓
Feintosecoiid Laser	✓	✓	✓	
Compression Molding	✓	✓		✓
Photochemical Etching	✓	✓	✓	✓
Electroforming	✓		✓	✓
Sputter Coating	✓			✓
Micro Electro Discharge	✓			✓
Lithography	✓	✓		✓
Fused Deposition Modeling		✓		✓
Solvent Casting		✓		✓

*Nd:YAG Laser = neodymium:yttrium-aluminum-garnet

Chapter 4: Evaluation of coronary stents

- 4.1 Regulations and approval process
 - 4.2 In vitro mechanical testing
 - 4.3 In vitro studies
 - 4.4 Animal Models
 - 4.5 Clinical Studies
 - 4.6 *In silico* testing
-

4.1 Regulations and approval process

The evaluation for the EU market approval of coronary stents falls under the Medical Device Directive 93/42/EEC [135] and the 2007/47/EC directive [136]. According to these, the medical devices are categorised, taking into consideration the risk they can cause to the patients, to four groups (I/IIa/IIb/III) [137]. Stents belong in class III and therefore “explicit prior authorization with regard to conformity” is required. Therefore, in order to meet the essential requirements and be released in the market, the CE marking is necessary. The specific requirements for the assessment of coronary stents should be in compliance with:

- Council Directive 93/42/EEC concerning medical devices, last amended by Directive
- 2007/47/EC of the European Parliament and of the Council.
- EMEA/CHMP/EWP/110540/2007: Guideline on the clinical and non-clinical evaluation during the consultation procedure on medicinal substances contained in drug-eluting (medicinal substance-eluting) coronary stents.

- EN 14299:2004 Non active surgical implants – Particular requirements for cardiac and vascular implants – Specific requirements for arterial stents.
- EN 12006-3:1998 Non-active surgical implants – Particular requirements for cardiac and vascular implants – Part 3: Endovascular devices.
- EN ISO 10993 Biological evaluation of medical devices.
- EN ISO 14155-1:2003 Clinical investigation of medical devices for human subjects – Part 1: General requirements.
- EN ISO 14155-2:2003 Clinical investigation of medical devices for human subjects – Part 2: Clinical investigation plans.
- EN ISO 14630:2005 Non-active surgical implants – General requirements.
- EN ISO 14971:2007 Medical devices – Application of risk management to medical devices.
- GHTF SG5 N2R8:2007 Guidance on clinical evaluation.
- ISO/DIS 25539-2 Cardiovascular implants – Endovascular devices – Part 2: Vascular stents.
- MEDDEV 2.1/3 (2001) Interface with other directive – Medical devices/medicinal products.
- MEDDEV 2.7.1(2003) Evaluation of clinical data: A guide for manufacturers and notified bodies.
- MEDDEV 2.12-2 (2004) Guidelines on post market clinical follow-up.

Inevitable, the EU process for stent device regulation is less onerous compared to the processes in other biomedical invasive implants. This is advantageous for the patients in terms of timely access to important stent innovations. However, a variety of concerns exist related to the thoroughness of stents evaluation. At the same time, the current approval process for stent devices and clinical trials, in Europe, is fragmented and asks for considerable improvement.

The stent biomedical industry and the development pipelines for coronary stents present significant differences depending on the type of stent (design, material, drug coating, etc), but have the same essential components and serve the same need; to design and develop a medical device which will improve the outcomes for the patient's health, minimize the presence of side effects, have low development costs and achieve shorter time for being introduced in the market. Currently, the stent biomedical industry for

coronary stents includes the following phases: (i) pre-clinical assessment, including *in vitro* mechanical testing and animal studies, (ii) clinical assessment for efficacy, and (iii) post-market analysis.

The objective of the CE marking is to show that the stent is safe and that it meets the intended by the manufacturer performance. Specifically, in order to receive the coronary stent approval, the manufacturer should employ a Notified body, which has to review the technical dossier, to test the stent samples, and to assess the non-clinical and clinical assessment evidence. In addition, the stent manufacturer must perform some randomized clinical trials, and in case the results are satisfactory, then the certificate and the CE mark can be obtained [138]. The approval process that is currently followed for medical devices is presented in Figure 16.

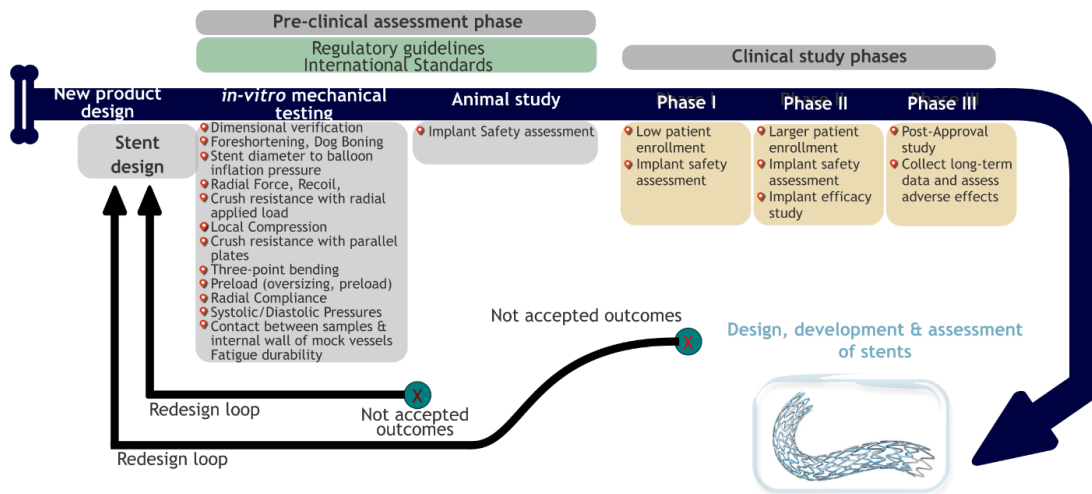


Figure 16: Process for obtaining CE marking for stent scaffolds.

4.2 *In vitro* mechanical testing

All stent manufacturers have to perform standard mechanical stent testing (Figure 17). Specifically: (i) Dimensional verification - Profile/diameter test ISO 25539. This test defines the maximum diameter along the sections of the stent to assess the dimensional compatibility between the stent and the arterial lesion. (ii) Foreshortening ISO 25539. This test defines the length to diameter relationship of the stent, the unconstrained length in case of a SX stent and the stent thickness. (iii) Stent diameter to balloon inflation pressure ISO 25539. This test determines the relationship between the stent diameter and the inflation pressure. (iv) Dog Boning ISO 25539. This test evaluates the difference between the diameter of the stent and those of the proximal and distal ends of the balloon, when the implant is expanded under the maximum inflation pressure.

(v) Radial Force ISO 25539. This test determines the force produced by a self-expanding stent, in relation to the stent diameter under expansion and compression. (vi) Recoil ISO 25539. This test quantifies the percentage by which the stent diameter decreases from its expanded diameter to its relaxed diameter. The recoil measurements are performed proximal, center and distal to the stent. (vii) Crush resistance with radial applied load ISO 25539. This test determines the load/deformation characteristics of the stent, under a circumferentially uniform radial load. (viii) Local Compression ISO 25539. The purpose of this test is to determine the deformation of the stent in response to a localized compressive force, and assess whether the stent recovers its original shape after testing. (ix) Crush resistance with parallel plates ISO 25539. This test determines the required load, which can cause buckling or deflection corresponding to at least 50% diameter reduction, and the required load which can cause a permanent deformation or fully stent collapse. (x) Three-point bending ASTM F2606. This test provides guidelines for characterizing the BX stent and the stent flexibility by the utilization of three-point bending procedures.

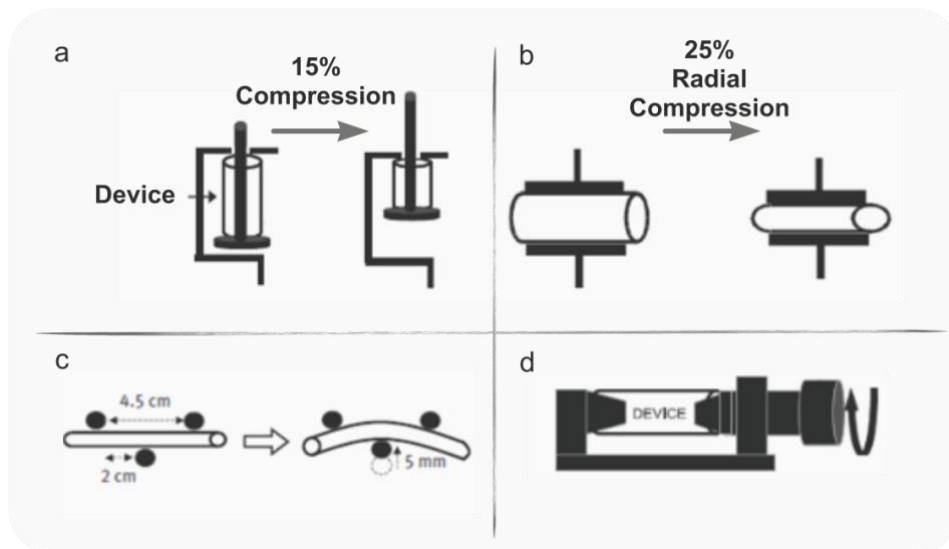


Figure 17: (a) Longitudinal compression testing. (b) Radial compression testing, (c) 3-point bending, (iv) torsion stent testing.

4.3 *In vitro* studies

Several experimental works have been conducted to study the deformation, the fatigue and biomechanical performance of coronary stents. Some of these experiments have been performed in a simulated body environment, such as in the study of Nam *et al.* [139], who evaluated the deformation of SS316L stents with and without Si-incorporated diamond-like carbon coating. The results demonstrated that the uncoated

steel is less ductile and more vulnerable to fracture than the coated one. The dynamic deformation of coronary stents was studied by Zhou *et al.* [140], who used a sequence of microscopic photos to examine the deformation of the sample. The arterial recoil after expansion was studied for 11 metal stents showing that the radius-thickness ratio is a significant factor for the initial imperfections. The multi-buckling performance depended on both material and design features, showing that in case the structure is designed with sudden change of local stiffness, multi buckling is more likely to appear. Vassilev *et al.* [141] examined the stent deformation in coronary bifurcations. The experimental test-bed consisted of an elastic arterial model with a diameter of 3.5 mm and side branches with a diameter of 3.5 mm and 2.75 mm, respectively. Two Chopin (Balton, Warsaw, Poland) stents were implanted in the mock up vessels, followed by balloon redilation and kissing balloon. The results revealed an elliptical cross-sectional shape of the proximal portion and a circular cross-sectional for the distal portion. In general, the balloon redilation resulted in the lateral displacement and opening of the stent cell, both in the proximal and distal portions. Some years later, Pitney *et al.* [142] analysed the stent deformation and fracture caused by post-dilation balloon catching, which was a phenomenon observed when non-compliant balloon for post stenting redilation was used. For this study, clinical and bench tests were performed in parallel. The results showed that approximately 1.8% of stents exhibited separation after post-stenting redilation, a process caused by the balloon catching. In the bench test, 50% of the cases showed balloon catch when provocative manoeuvres were applied, while this incidence was reduced to 20%, when provocative manoeuvres were not applied.

Lately, Zhao *et al.* [143] performed an experimental investigation of the stent–artery interaction. Specifically, the stent implantation inside the artery analogue was captured by two high-speed cameras. The surface strain maps on the stented tube were evaluated with a 3D digital image correlation technique and the strain history illustrated three stenting phases: (i) balloon inflation, (ii) pressurization, and (iii) deflation. The surface strain distributions along one axial path were examined at different time points to evaluate the stent–vessel interactions. The results showed that balloon expansion process is affected by the external loadings from both the stent and the artery analogue.

4.4 Animal Models

Animal models of coronary stent implantation provide insight for the feasibility, safety and efficacy of stent deployment [144]. Animal testing can be performed in: (i) small (mouse, rat), (ii) medium (rabbit) and (iii) large (pig, sheep, dog, primate) species, with the porcine model to be the most useful, practical and adaptable (Table 11). The porcine model has been used for understanding and evaluating the stent performance and in particular for capturing the biology of vascular interventions and healing.

Table 11: Animal models used in coronary stenting.

	Vessel	Size (mm)	Expense	Similarity to human	Commonly used
Pig	Coronary	3-3.5	++	++	++
Dog	Coronary	3.5-4.0	+++	++	+
Primate	Coronary	3.0-4.0	++++	+++	
Sheep	Coronary	3.0-4.0	++	++	

A standard endpoint in animal models is the angiographic assessment that provides the ability to compare and evaluate the pre- and post- deployment images in terms of lumen diameter, % stenosis, and late lumen loss. The available imaging options are IVUS, OCT and NIRS. Micro-CT is also a powerful approach, especially for reconstructing and capturing the complete stent/artery relationships. After the implantation of the stent to the animal model, a detailed assessment is followed in different time points: (i) early time points (3–7 days) after stenting for obtaining information regarding the thrombotic risk, (ii) within 1–2 weeks, the normal coronary arteries of pigs endothelialise rapidly, (iii) in day 28, the neointimal hyperplasia is quantitated towards providing useful information for the different stents, (iv) two or more late time points, such as in 90, 180 and 360 days, should also be checked to detect long-term effects, including neointimal hyperplasia and endothelial coverage, fibrin deposition, calcification, inflammation, etc. (v) three-month follow-up is usually acceptable for the initiation of the investigational device exemption clinical trials assuming that no adverse findings are present at this time and that vascular responses are no worse than earlier time points.

4.5 Clinical Studies

The side effects associated with the coronary stent implantation are presented and highlighted in several case reports [145]. These reports mostly address the issue of stent failure and the associated implications for the patients, such as chest pain, restenosis

and thrombosis. The presence of these complications varies from few days to months after the deployment.

Such incidence is reported in Kang *et al.* [146], according to whom a very early stent fracture occurred two days after implantation of two DES Cypher stents, on a 76 years old male with a history of hypertension, smoking and diabetes. A complete stent fracture was observed on a 44 years old male after approximately twenty two months of Cypher implantation [147]. The same group showed a fracture on a Zoratalimus eluting stent after five months of deployment in a right coronary artery due to high vessel tortuosity. Late failure of a Cypher sirolimus stent and a bare metal Multi-Link stent was reported by Okamura *et al.* [148], in a 73 years old woman with hypertension, diabetes mellitus and hypercholesterolemia, after eight months of deployment. These failures were caused by the stent fracture at the region of maximum arterial bending and tension. A retrospective review of 530 patients with angiographic follow-up over a 32-month period showed a percentage of 1.9% stent fractures [149].

Another retrospective analysis of PCI on 3920 patients with DES over 12 months was performed by Shaikh *et al.* [150]. ISR was reported in 188 cases, while stent fracture was observed in 35 (18.6%) out of the 188 cases. To note that this study included only cases with severe stent fracture, excluding mild (single strut fractures) and moderate stent fracture (more than one strut but without clear separation of fractured stent segments).

In brief, according to an extensive analysis performed in the registry of clinical trials, approximately: (i) 47% of the trials focus on the evaluation of a single stent, (ii) 53% of the trials focus on the comparison of different type of stents or stenting techniques. More specifically, the safety and efficacy of the stents are evaluated in terms of the clinical device, procedural success and clinical outcomes. The stents are tested in straight and bifurcated arteries following different implantation strategies. The comparison is performed in terms of the effect of: (i) stent design (length, strut thickness, diameter, etc), (ii) type of drug and pharmacokinetics performance (e.g. release, absorption), (iii) short and long term outcomes (rate of stent strut coverage and uncovered stents, risk of fracture due to overdilation, ISR), (iv) type of vessel (long lesions and/or dual vessels, number of stenosis, plaque composition), (v) patient-specific categories (gender, presence of diabetes, heart transplantation), (vi) changes in

the heart flow after stent insertion and wall shear stress distribution, (vii) stent scaffolding shape and malaposition, (viii) type of biodegradable polymer, (viii) two stent versus one stent technique.

4.6 *In silico* testing

Nowadays, the only conclusive way to guarantee the safety and efficacy of a coronary stent is to test it *in vitro* in the laboratory, and then on living organisms, initially on animals (*in vivo*) and then on humans (clinical evaluation/trial). As described, the *in vitro* mechanical testing includes the testing of the constituent permanent metals and polymers, the compression and flexural testing, as well as the pulsatile durability testing. The preclinical evaluation is an essential process in the development of coronary stents. Even if the clinical trial methodology and practice have been improved enormously over the last years, many key issues have been left unmet.

Specifically, due to the hugely complex nature of human diseases, there is a significant difference between individuals with an inevitable variability in the anatomy and the pathology of the diseased arteries. Therefore, it is quite usual that a coronary stent performs exceptionally well in controlled laboratory experiments and pre-clinical studies, but presents several issues (failure, ISR, ST) during or after clinical trials. In addition, whilst clinical trials provide useful insight related to the safety or effectiveness of the coronary stent, in case of failure during clinical trials, it may be abandoned, even if a small modification and improvement could resolve the issue. This mainly leads in an “all-or-nothing” mind-set in the Stent Biomedical Industry, where the objective of the research and development investment virtually asks from the biomedical company to focus only on how to reduce the risk of the coronary stents. This in turn strangles innovation, decreases the number of new coronary stents presented to the market every year, while in parallel increases the development costs. One has to agree that there is ample room for improving the complete development chain of coronary stent and improve the patient outcomes. During last decade, there has been a huge investment in information technology and *in silico* modelling for the development of biomedical products. *In silico* technologies are of great value, and could answer several difficult questions, such as: “How does the stent behave after implantation?”, “What are the changes that we could implement in a stent design in order to achieve improved patient outcomes?”.

Chapter 5: Stent modelling

5.1 Finite Element Method

5.2 Review of stent deployment modelling

5.1 Finite Element Method

Several problems in science and in the field of biomedical engineering, including the stent implantation, include complicated systems of differential equations which are too difficult to be solved due to their complex geometry. Finite element analysis (FEA) has evolved over the last three decades and is related to breaking up a continuum into discrete, coupled components that approximate the overall solution. Specifically, the domain of interest is split into non-overlapping coupled components, which are called elements.

FEA enables the examination and analysis of a continuum with geometries of high complexity through the utilization of the finite elements, which can be formulated with arbitrary shape. This allows the representation of the continuum without the need for the actual geometry simplification. Finite elements are used to perform specific analysis in various engineering applications, especially in biomedical engineering design. The use of FEA allows the assessment of a proposed design in terms of safety and effectiveness and assists in meeting the required specifications *a priori* of the design manufacturing. FEA plays an important role in the creation of product prototypes since it provides accurate and reliable results and assists in decision making.

Early studies indicate that the accuracy of a FEA relies on the element's geometry, geometry distortion, such as iso-parametric elements, shape function, principles and laws used in developing the governing equation and the material which is used. Several

materials are currently available; therefore, a detailed examination for the selection of the most suitable element needs to be followed.

For the 1D analysis, certain elements can be used to solve the analysis. The available research results show that for the 2D analysis, bilinear quadrilateral elements are better compared to simple linear triangular elements, in terms of meshing capabilities and accuracy. However, the accuracy of the simple linear triangular element could be enhanced through the utilisation of higher order elements, but this may lead to the “mesh-locking problem”, which is a key drawback of triangular element [151]. H-p adaptive techniques have been introduced for increasing the accuracy of the finite element method. It was found that quadrilateral elements are more accurate compared to the triangular elements when the newly formulated h-p adaptive technique was used [152]. As far as the 3D analysis is concerned, hexahedron elements could be better compared to tetrahedron elements, however both quadratic hexahedron and tetrahedron elements have similar performance and accuracy.

The behaviour of the phenomena that need to be examined can be represented with mathematical models (approximate models), which are based on specific principles and laws. Several principles exist which can be used to formulate the finite elements. The principle of static equilibrium (direct method) is used for phenomena, which can be described by simple governing equation, the theorem of Castigliano and the principle of minimum potential energy are applied for more complicated elastic structural problems. Higher mathematical principles (variational methods) are used to express FEA for phenomena described by more complex mathematical model, which involve derivative terms. There are several variational methods, such as Galerkin, Ritz, collocation, and least-squares methods [3].

Once the approximate model is developed using the principles and the laws as described above, shape functions are applied to complete the finite element formulation. The general equation for a single finite element is the following:

$$[k]\{q\} = \{Q\} \tag{5.1}$$

The elements are represented by a linear combination of polynomial functions with undetermined coefficients, which form the approximate numerical solution to the governing differential equations. The nodes that are located on the elements represent

the undetermined coefficients. The solution is found on the modes through the polynomial functions and appropriate boundary conditions. The continuous solution derives from the combination of the assumed algebraic polynomials.

To achieve an accurate solution, the elements must be kept as small as possible. This results in an approximation defined by a larger number of equations, which in turn increases with every increase in the number of elements used. However, the differential equations are converted to many algebraic equations, which makes the problem more complicated. Even if the FEA has initially been resolved with personally written computer programs to perform the analysis, currently many commercial softwares are available for simulating the physical problem and eliminating the need for an individual code. The methodology and the different steps which are followed in the FEA are presented in Figure 18.

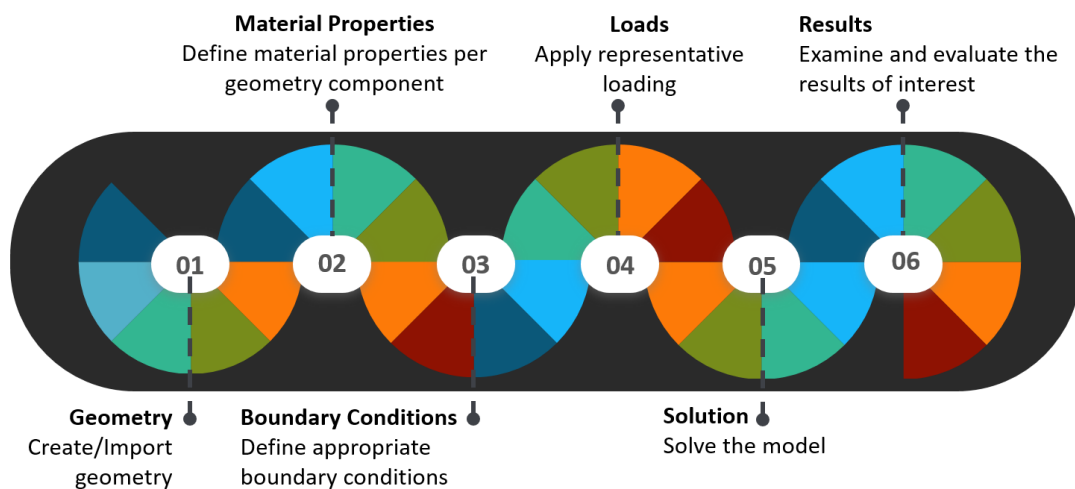
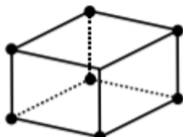
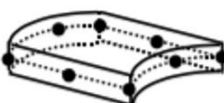
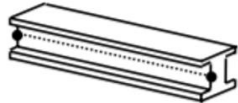
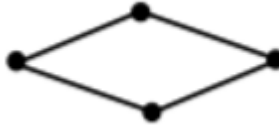


Figure 18: Process for FEA.

One of the considerations in the creation of the finite element model is the type of the element type to be used. Table 12 shows the element types that are usually used in a stress analysis.

Table 12: Element types in stress analysis.

Element types in stress analysis			
			
Continuum (solid) elements	Shell elements	Beam elements	Rigid elements

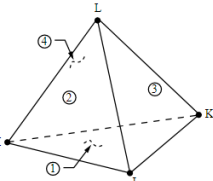
The key difference between these element families is the type of geometry that each family assumes. The fundamental variables which are calculated during the analysis are the degrees of freedom. The number of nodes that each element has, determines the order of interpolation over that element. When the degrees of freedom are calculated at the element's nodes, the same variables are defined at any other point in the element through interpolation from the nodes. For elements with nodes only at their corners, the linear interpolation is utilised between the nodes, making the elements linear or first-order. Elements with mid-side nodes are second-order elements and use quadratic interpolation (Figure 19).



Figure 19: Examples of linear (left) and quadratic (right) elements.

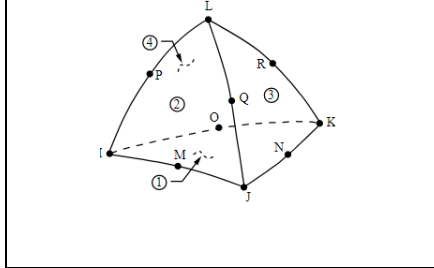
In general, three groups of elements exist; line elements for 1D analysis, planar elements for 2D analyses and solid elements for 3D analyses. Each of these groups includes various types of elements. For instance, bar and spring element are specific elements categorised under line elements. In particular cases, specific elements are used. There are also other elements which can be for any cases, by adopting the governing equation according to the specific problem. Such elements are triangular and rectangular elements, which are general planar elements. In the current analysis the following element types are used: (i) Solid 285, (ii) Solid 187, (iii) Conta174, (iv) Targe170, (v) Surf154 and (vi) Combin14. More details of those elements are depicted in Table 13.

Table 13: Details of finite element types.

Element type	Details
	<p>Lower-order 3-D, 4-node mixed u-P element. Solid 285: (i) has a linear displacement behavior. (ii) is suitable for modeling irregular meshes, (iii) is defined by four nodes and has four degrees of freedom at each node, (iv) has plasticity, hyperelasticity, creep, stress stiffening, large deflection, and large strain capabilities, (v) is capable of simulating deformations of nearly incompressible elastoplastic materials, nearly</p>

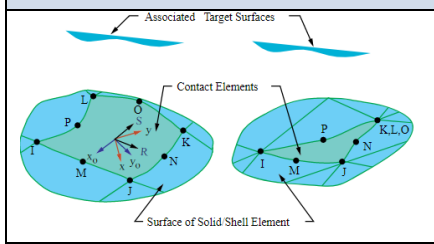
incompressible hyperelastic materials, and fully incompressible hyperelastic materials.

Solid 187



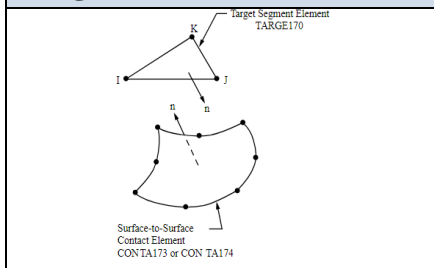
Higher order 3-D, 10-node element. It is defined by 10 nodes with three degrees of freedom at each node: translations in the nodal x, y, and z directions. The element has: (i) plasticity, (ii) hyperelasticity, (iii) creep, (iv) stress stiffening, (v) large deflection, and (vi) large strain capabilities.

Conta174



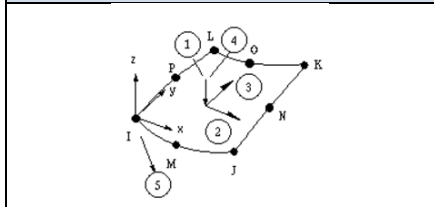
Conta174 is used to represent contact and sliding between 3D surfaces and a deformable surface defined by this element. Conta174 element is used in 3D structural and coupled-field contact analyses for both pair-based contact and general contact.

Target170



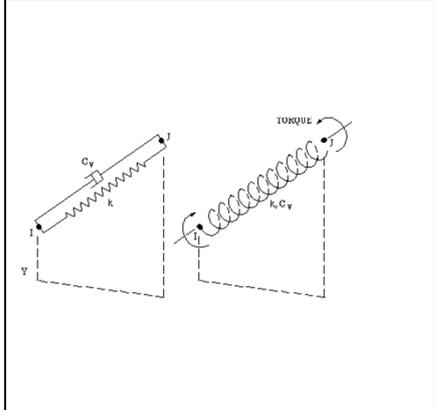
Target170 is used to represent various 3D "target surfaces for the associated contact elements. The contact elements themselves overlay the solid, shell, or line elements describing the boundary of a deformable body and are potentially in contact with the target surface, defined by TARGET170.

Surf154



Surf154 is used in various load and surface effect fields. It may be overlaid onto an area face of any 3-D element. Surf154 is applicable to 3D structural analyses, in which various loads and surface effects could exist simultaneously.

Combin14



Combin14 has longitudinal or torsional capability in 1D-, 2D-, or 3D applications. The longitudinal spring-damper option is a uniaxial tension-compression element with up to three degrees of freedom at each node (translations in the nodal x, y, and z directions). No bending/torsion is considered. The torsional spring-damper option is a purely rotational element with three degrees of freedom at each node (rotations about the nodal x, y, and z axes). No bending/axial loads are considered.

5.2 Review of stent deployment modelling

5.2.1 Free expansion of stents

Several computational studies have focused on examining the mechanical behaviour of stents and investigating the deformation of a stent during the deployment, based on the evaluation of major effects that occur, such as the recoil and dogboning. Recoil is related to the reduction of the stent diameter due to the resistance of the arterial wall, and is a result of balloon deflation following the stent expansion. Dogboning, on the other hand, takes place during the expansion and concerns the unequal expansion of stent middle section and ends and can cause high levels of stress on the arterial walls and lead in the tissue damage. Specifically, dogboning and recoiling effects can be defined by the following equations [153]:

$$\text{Dogboning} = \frac{(d_e - d_m)}{d_m} \times 100\% \quad (5.2)$$

where d_e and d_m is the mean diameter at the ends of the stent and the diameter in the middle of the stent after deflation, respectively.

$$\text{Recoiling} = \frac{(d_o - d_1)}{d_o} \times 100\% \quad (5.3)$$

where d_o and d_1 is the diameter in the middle of the stent at maximum pressure and after deflation respectively.

Dumoulin *et al.* [154] focused on the mechanical behaviour of a stent during and after implantation. More specifically, the recoil, fatigue life and collapse of the BXstent were investigated. A repeating unit cell of the Palmaz-Schatz design was expanded through the application of a pressure to the inner surface. Their results on expansion and intrinsic recoil showed that apart from the shape and mechanical properties, its performance highly depends on the deployment magnitude. The team of Chua *et al.* investigated the stent expansion using the FEM. Tan *et al.* [155] investigated and compared two different stents in terms of expansion performance; the Freedom stent and the Palmaz-Schatz stent. They focused on evaluating the effect of stent design and the presence of a calcified plaque. The increase in the wire diameter and the elastic modulus by 150% resulted in the need of imposing an increased inflation pressure. In addition, the incompressible plaque coming into contact with the mid portion of the

stent resulted in an abrupt distortion (Freedom stent) and an hour-glass deformity (PalmaZ-Schatz stent). Etave *et al.* [156] examined the mechanical characteristics of two different stents, each of which is representative of its type; a tubular stent (PalmaZ-Schatz stent- TS1) and a coil stent (Freedom stent). The required deployment pressure for the expansion of the Freedom stent was lower compared to the pressure required for the PalmaZ-Schatz stent. In addition, in the Freedom stent, when the deployment diameter exceeded 4.5 mm, a sudden increase in the pressure was observed; reaching 8 atm at a diameter of 5 mm. In addition, the thickness of the struts had a significant role. Specifically, for the deployment of the modified with the thicker struts PalmaZ-Schatz (TS2), a 6.5 times greater pressure was required. The TS1 stent was also more flexible compared to the TS2 stent. The TS1 stent could also be deformed by 10% at compressive pressures of between 0.7-1.3 atm, while the TS2 stent was deformed to the same extent at 8.5–20 atm. The shortening of the stent was also different; TS1 undergone shortening between 0%- 11%, and TS2 between 0% -8%.

Migliavacca *et al.* [1] examined the influence of the thickness, the metal-to-artery surface ratio, the longitudinal and radial cut lengths of a typical diamond-shaped stent on its mechanical performance and compared the response of different stent models under different internal pressure. The study simulated the stent expansion and the partial recoil under balloon inflation and deflation. The results showed higher radial and longitudinal recoil, but a lower dogboning for a stent with a low metal-to-artery surface ratio. The stent performance in terms of foreshortening, longitudinal recoil and dogboning was also influenced by the stent thickness.

In 2002, Chua *et al.* [3] performed a FEA for predicting the stent diameter and the foreshortening under the application of different speeds of pressure, ignoring the presence of the balloon. Their analysis indicated that the maximum potential diameter can only be achieved under moderate pressure speed applied on the inner surface of the stent. The authors stated that smaller and lower pressure speeds are expected to result in greater potential diameter, but it may also introduce gross buckling of the stent, which is undesirable. In contrast, higher pressure speeds will result in higher stresses in the stent. Higher pressure speed generated higher stent stress but lower radial displacement. Chua *et al.* [157] also performed a non-linear finite element simulation towards examining the interaction between the slotted tube PalmaZ-Schatz stent and the balloon during stent expansion. The ends of the stent were free to allow its expansion and

shortening, while the ends of balloon were fully tethered and only the radial expansion was allowed. The results showed that as the stent expands, the stress is gradually increased. It was also observed that in the four corners and the middle of the cells and in the bridging struts higher stresses are present. This is attributed to the fact that during expansion the struts are pulled apart from each other and develop a rhomboid shape of cells and when there is no room for storing the applied forces, the weakest section collapses. One year later, Chua *et al.* [4] investigated the effect of design parameters, such as the number, width and length of individual stent cells on the deployment performance of the Palmaz – Schatz stent. It was shown that the number, width and length of the stent cells had a minor influence on the expanded diameter and stent foreshortening, however a major effect was observed on the rate of elastic recoil, which decreased as the number of cells and the regularity of their distribution was increased. The same year, Petrini *et al.* [158] compared the flexibility of two next-generation Johnson & Johnson stents (Carbostent and Bx-Velocity) in their unexpanded and expanded configurations. To study the stents flexibility in both unexpanded and expanded configurations, at the extremities of each stent, a fixed angular rotation was applied. The results demonstrated a different response for the two stents. Specifically, a higher degree of flexibility was observed for the Bx-Velocity stent, while lower levels of flexibility were obtained for both stents in their expanded state. McGarry *et al.* [159] followed a computational micromechanics approach based on the crystal plasticity theory for the analysis of the mechanical performance of stents. Specifically, the crystal plasticity theory incorporated both the microstructure and the microscale deformation mechanisms and provided a representation of the stent strut face-centered cubic grain structure and the anisotropic crystallographic plasticity that occurs during large strain deformation.

Migliavacca *et al.* [153] studied the expansion of the coronary Cordis BX Velocity stent and examined: (i) the distal and central radial recoil, (ii) the longitudinal recoil, (iii) the foreshortening, and (iv) the dogboning effects. The results of the FEA were compared to experimental measurement of stent expansion using an optical extensometer. The inflation pressure (1.2MPa) was equal for the experiment and simulation. The von Mises stress and equivalent plastic deformation at the inflation pressure of 0.5 MPa and after the load removal were obtained (Figure 20). More interesting was the correlation between the central diameter and the inflating pressure. Specifically, when the inflation

pressure reached the value of 0.2 MPa, a rapid stent expansion was achieved, whereas at higher pressures, a less pronounced diameter increment was observed. This behaviour can be attributed to the fact that the stent rings behave as a cantilever under flexion; with small applied pressure, the structure undergoes large deformations. The elastic recoil was examined for the stent middle position the after expansion, at a pressure of 0.5 MPa. The experimentally and the simulated recoil was 1.1% and 1.2% respectively. In addition, both experiment and simulation had high plastic deformation at the U-bends of the sinusoidal struts.

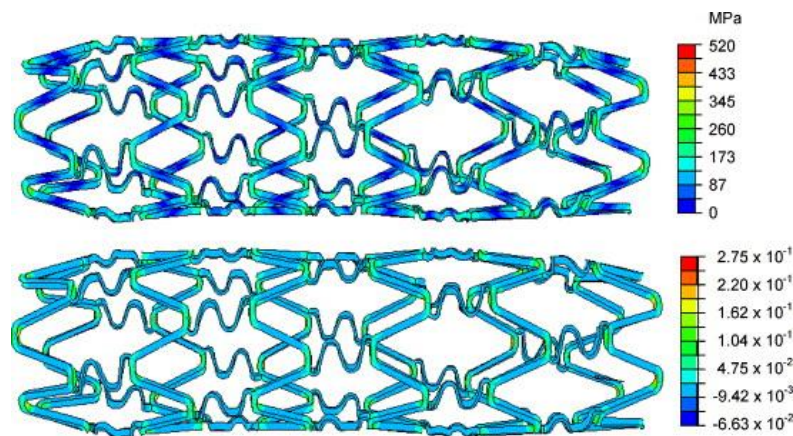


Figure 20: Von Mises stress and equivalent plastic deformation at the inflation pressure of 0.5 MPa and after the load removal ([139]).

The same year, Walke *et al.* [160] performed a computational analysis of the SS316L Genesis stent to determine the stent diameter as a function of the pressure. In parallel to the computational analysis, experiments were also performed. The results of the experiments, that were in a very good agreement with the results of the FE analysis, showed that the stent enlargement process is not proportional to the pressure inside the balloon and that an abrupt increase of the stent diameter was detected when a critical value of the balloon pressure was exceeded.

Mori *et al.* [161] performed an experimental and a 2D analysis with two cells and one link for investigating the deformation mode and resistance under the longitudinal compressive load. The results showed that the deformation resistance from the numerical analysis was highly associated with the bending stiffness measured with the bending test, showing the usefulness of their analysis in evaluating the relationship between stent flexibility and design parameters.

Hall *et al.* [162] presented results from a comparative study of six different numerical models using variations of 3D solid and 2D shell and beam elements. The stent expansion was achieved through a displacement-driven approach upon a cylindrical analytical surface. It was observed that all element types had a similar response despite the difference in the numerical models dimensionality. In addition, the beam elements were able of predicting similar maximum and minimum values of stress and strain at identical locations on the stent with significant low computational requirements.

Wang *et al.* [117] performed a FEA to evaluate the effect of the stent strut width and balloon length on the transient behaviour of two stents. For the representation of the balloon geometry, an idealised cylinder was used, in the inner surface of which the pressure load was applied. It was shown that the variation of the proximal and distal strut width and the balloon length had a great effect on stent dogboning.

Wu *et al.* [163] examined the longitudinal flexibility of the Nirflex stent based on two models. The first model concerned the bending of a single unit. The second model was related to the whole stent bending to two equal and opposite moments at each end. The results showed that in the single unit cell bending the deformation is concentrated in just one of the two struts. For the whole stent, as expected, the middle section of the S-shaped stent was less deformed, providing evidence for the effect of stent length.

Mortier *et al.* [164] incorporated the folding pattern of the balloon in the stent deployment modeling. Specifically, the authors developed a numerical model of the CYPHER™ stent combined with a realistic trifolded balloon. The effect of several parameters (balloon length, folding pattern, and relative position of the stent and balloon catheter) were investigated. The validation of the modeling approach were in good agreement with the manufacturer data. This parametric analysis revealed that the length of the balloon and the folding pattern highly influence the uniformity and the symmetry of the stent expansion. In addition, it was shown that small positioning inaccuracies could have an impact on the stent expansion, a parameter that should be taken into consideration during the stent placement in order to decrease the endothelial damage.

To examine the stent-balloon interaction, Ju *et al.* [165] created three different FE models: (i) the panel model, (ii) the repeated unit cell (RUC) model (iii) the RUC with a free end (RUC+) model, and studied the expansion of a Palmaz-Schatz stent.

According to the results, the RUC model had a similar expansion (4.8 mm in diameter) and von Mises stress (286 MPa) compared to those (diameter of 4.6 mm and von Mises stress of 286 MPa) in the study of Chua *et al.* It was also shown that RUC provided a very good prediction of the middle section stent deformation. However, the results failed in predicting the deformation for the ends of the stent. In contrast, the RUC+ method provided satisfactory predictions for both the inner and distal stent segments.

To fully understand the mechanical performance of stents, Park *et al.* [166] performed the modeling of transient non-uniform balloon-stent expansion. Since then, the majority of the computational studies considered the modelling of the balloon expansion by applying a uniform radial internal pressure. To fully understand the mechanical characteristics of the stent, the consideration of the realistic modeling of transient non-uniform balloon-stent expansion is necessary; therefore, the authors compared seven commercially available stents: (i) Palmaz-Schatz, (ii) Tenax, (iii) Coroflex, (iv) MAC Standard, (v) MAC Q23, (vi) MAC Plus and RX Ultra, (vii) Multi-Link. The stents were evaluated in terms of flexibility, foreshortening, dogboning, radial stiffness, longitudinal and radial recoil and coverage area. Flexibility was evaluated by the following bending equation of a simple canti-lever beam:

$$EI = \frac{PL^3}{3\delta} \quad (5.4)$$

where EI is the bending stiffness, P is the pressure, L is the stent length and δ is the deflection.

Radial stiffness which evaluates how much well the stent can support the arterial wall after stent deployment was calculated as in (5.5).

$$Radial\ Stiffness = P_{initial} EV \quad (5.5)$$

where $P_{initial}$ is the initial pressure and EV is the Eigenvalue.

The radial recoil that shows the degree of stent contraction after removing the balloon was calculated as in (5.6)

$$Radial\ Recoil = \frac{(R_{load} - R_{unload})}{R_{load}} \times 100\% \quad (5.6)$$

It is important to reduce the coverage area between the stent and the arterial wall in order to prevent the restenosis. Coverage area was examined as in (5.7).

$$\text{Coverage area} = \frac{\text{Surface of stent}}{\text{Area of artery}} \quad (5.7)$$

All stents showed similar expansion performance, apart from the Palmaz- Schatz stent. The Tenax stent had excellent flexibility characteristics and coverage area, whereas the MAC was excellent in foreshortening, in longitudinal, radial recoil and radial stiffness. The analysis of the results are in agreement with Wang *et al.* [167] and Migliavacca *et al.* [1] and show that foreshortening, longitudinal, radial recoil and dogboning are higher in stents with closed unit cells compared to stents with opened unit cells, indicating that the utilization of stents consisted of opened unit cells may inhibit side effect caused by foreshortening, recoil or dogboning. Depending on the stent length, an actual stent consists of four to six unit cells in the circumferential direction, and from 6 to 18 in the axial direction. Donnelly *et al.* [168] adopted the 2D unit cell approach, in which the identification and discretization of the smallest repeating structure of the stent was performed. A similar method had been successfully followed by McGarry *et al.* [159]. The results revealed that the unit cell method provides a more conservative estimation of stent performance compared to the complete 3D model, especially in what concerns the radial recoil and the maximum post-recoil stress. However, the authors stated that the 2D approach is acceptable for achieving a simple and efficient comparison of different stent designs.

The same year, Xia *et al.* [169] performed a FEA following a general RUC approach for examining the performance of BX stents with different types of closed cells (Palmaz-Schatz type and with V- or S-shaped links). The RUC approach is advantageous since less computational time is required to achieve the same analysis accuracy as with larger models since the existing periodicities in the stent can be directly represented by the application of the periodic boundary conditions. The results show that even if the V- and S-stents are easier to expand compared to the Palmaz-Schatz stent, there is noticeable foreshortening of the S-stent and V-stent.

De Beule *et al.* [170] compared the transient behaviour of a Bx-Velocity stent following three different expansion modeling strategies: (i) application of a pressure directly on the inner stent surface, (ii) application of a displacement-driven condition on the inner

balloon surface, (iii) application of a pressure on the inner surface of a tri-folded catheter balloon. The results were validated with pressure–diameter data from the manufacturer’s and it was revealed that the inclusion of the balloon and more specifically the presence of the folded balloon ensured a very good agreement between the predicted and the manufacturers’ measurements.

Stent foreshortening or dogboning can induce a vascular injury, resulting in the restenosis of the coronary artery. Lim *et al.* [171] suggested potential design parameters towards reducing the possibility of restenosis risk through a comparative study of seven commercial stents (Palmaz-Schatz PS153, TenaxTM, MAC Standard, MAC Q23, MAC Plus, Coroflex, RX Ultra Multi-link). All stents were considered to be made of 316L stainless steel, while the balloon was assumed to be made of high-density polypropylene. Three steps were followed for the transient non-uniform balloon simulation: (i) free expansion of the stent, until the initial radius of the balloon reached the value of the initial inner radius of the stents, (ii) examination of dogboning to a diameter of 3 mm, which is the typical inner diameter of a coronary artery (iii) investigation of stent foreshortening after the balloon removal.

The results for all stents showed that foreshortening and dogboning were higher in stents with closed unit cells connected by straight-line, and lower in stents with opened unit cells connected by bend-shaped link structures. These findings indicate that the utilisation of a stent with opened unit cells connected by bend-shaped link structures could prevent restenosis caused by foreshortening or dogboning. These findings were also supported by Park *et al.* [166].

Following the study of Xia *et al.* [169], Ju *et al.* [172] applied the following three models for the analysis of Palmaz-Schatz stents and stents of sinusoidal types: (i) Panel model, which reduces the size of the numerical model from the full without losing the computational accuracy (ii) RUC, which provided satisfactory results for the inner part of the stent apart from the two ends, (iii) RUC+ (RUC with a free end), which provided accurate results for both the inner and the distal ends of the stent. One of the main conclusions of this study was that the utilization of a RUC with a free end could capture the dogboning behaviour as well as the inner stent region using specific boundary conditions.

Lim *et al.* [171] analysed the deployment characteristics of several stents during free expansion. The aim of the study was to identify potential stent design parameters capable of reducing the possibility of ISR driven by foreshortening and dog-boning. 3D numerical models of seven commercially available stents and a tri-folded catheter balloon were considered in the study. Interestingly, the catheter balloon was discretised using a number of shell elements and the expansion of each stent was achieved through a volume control process. Validation of this approach was performed by comparing predicted pressure–diameter relationships to experimental data reported in the literature. Similar expansion profiles were observed for each stent, and predicted rates of foreshortening and dog-boning were measured. The authors noted that rates of foreshortening and dog-boning were generally higher among stents comprising closed unit cells connected by straight-line link elements as opposed to open unit cells connected by bend-shaped link structures.

Li *et al.* [2] followed a “bottom-up” approach for the shape optimization of the mechanical properties of the Mac Stent. The findings showed an improvement in the dogboning effect from 9.06 to 0.40 (initial to optimal design). Pochrzast *et al.* [173] performed a comparison between the performance of the stainless steel (Cr-Ni-Mo) and the CoCr-W-Ni alloy stent. The FEA was based on the utilization of the Josonics Flex stent; a single-layer, slotted tube stent. For the stent expansion, an internal pressure of 0.5 atm was applied. The results of the numerical analysis showed that the stent stresses in both stents were localized in the inner region of the bends. After exceeding the expansion pressure of 2.96 atm, a sudden increase of the stent’s diameter (up to $d = 4$ mm) took place. The CoCr-W-Ni stent performed exceptionally with very good expansion characteristics, showing that this alloy could be used as an alternative alloy for the JOSONICS Flex stent.

Wu *et al.* [163] performed a FEA following a bending method towards studying the stent flexibility. Through the application of the multipoint constraint elements (MPC), the bending moment was uniformly applied to the stent. However, the limitation of this study was that the stent crimping and expansion were not considered. Tamaredi *et al.* [174] investigated the effect of the stent thickness and cross-link width on the deployment performance of the stent and showed that the stent thickness reduction results in a subsequent reduction in the loads required for its expansion. In addition, it

was shown that the change of the cross-link width did not have any effect on the load-deformation nor in the stent dogboning performance.

In 2010, the FDA released guidelines for the medical device industry. The document included several key clinically-relevant functional attributes, such as stress/strain, fatigue resistance, radial strength and expansion recoil, in which the FDA is interested for the assessment of the future new stent approvals. Taking this into account, Hsiao *et al.* [175] followed the parametric stent design concept and demonstrated that this approach can assist in the design and analysis of a new stent shortening the stent development cycle. The results showed that: (i) the crown radius is a critical parameter for the equivalent plastic strain and the expansion recoil, (ii) the strut width and strut thickness are the most critical parameters for the radial strength and the fatigue safety factor respectively, (iii) the radial strength alters with the stent design. Specifically, an increase of 30% in the strut width increased in turn the radial strength by 61%.

Park *et al.* [176] investigated the crimping and expansion deformation behaviors in the Cobalt-Chrome alloy SCM-10 stent (DSI, Yangsan-city, Korea). Specifically, the thicknesses of stent strut were 70, 80, 90 and 100 μm , the inner diameter was 1.8 mm, and the length was 18.188 mm. It was noticed that the maximum stress increases proportional to the strut thickness increase, due to the increase in the material strength. In addition, with an increased stent expansion, the inner angle of the strut increased as well.

Ciekot *et al.* [177] examined the design characteristics that a stent should have in order to minimize the dogboning effect. The decision variables were the stent thickness and the inflation pressure. In addition, some constrains were also used: (i) the shortening did not exceed 2%, (ii) the arterial wall thickness ranged between 0.2 - 0.3 mm, (iii) the inflation pressure was between 0.4- 0.7 MPa. The optimization analysis showed that the lowest value of stent diameter growth (17%) appears for the stent thickness of 0.29 mm and for the pressure 0.7 MPa. The required expansion pressure (0.4MPa) for the wall thickness of 0.2 mm was lower than for the wall thickness of 0.3 mm (0.7MPa).

Roy *et al.* [178] focused on the *in silico* modelling of six commercially available stents: (i) Palmaz-Schatz stent, (ii) Cypher Stent, (iii) S670 Stent, (iv) Driver Stent, (v) Taxus Express Stent and (vi) Element Stent using eight different stent materials. The results indicate that the minimum von Mises stress is developed in the strut connector of the

Element Stent. In the Driver, Element and Taxus Express stents, there is a non-uniform stress distribution, while the maximum displacement is observed in the center of the stent unit cells. As far as the materials are concerned, tantalum, elgiloy and magnesium are more susceptible for developing high stresses whereas the cobalt-chromium alloys show a better performance.

The majority of the commercially available stents are interfaced with non-degradable polymer coatings. However, several adverse clinical effects could result from a coating failure: (i) increased risk of thrombosis, (ii) altered drug delivery, (iii) release of toxic ions deriving from the metallic platform leading to an inflammatory response [179]. The effect of the coating on stent expansion characteristics was studied in an uncoated and a coated stent [180]. The results showed that both stents reached the same maximum diameter and developed the maximum stress values in the same regions. The only noticeable difference was that the coated stent had a higher residual stress, possibly due to the property mismatch between the stent and the coating. A contradictory study of a polymer-coated DES with a platform of Pt-enhanced alloy (Pt–Cr steels) and a poly(lactic-co-glycolic) acid (PLGA) coating showed that the curved areas (link) were subjected to high stress in the coating; stress distribution with double peaks slightly off the strut center were higher along the inner area of the stent than the outer [5]. The evaluation of the mechanisms underlying coating delamination is also vital [180]. Debonding occurs mainly in the high strain plastic hinge regions, while the initiation depends on the material, the thickness of the coating and the curvature of the hinge. Stiff and thick coatings on plastic hinges of high curvature debond at lower level of stent expansion, while the earliest buckling of the coatings is seen in the vicinity of the geometric discontinuity, revealing the importance of eliminating the coating in high curvature and discontinuity regions [180].

5.2.2 Simulation of stent deployment in arterial segments

5.2.2.1 Idealized arterial segments

Auricchio *et al.* [181] presented results from an analysis that investigated the performance of the Palmaz–Schatz stent in terms of elastic recoil, foreshortening and metal-to artery-ratio surface ratio when deployed in an idealised stenotic artery. The artery was modelled as an idealised cylindrical vessel and included a parabola-shaped plaque. To achieve stent expansion, a pressure was applied in the inner stent surface.

This analysis represents one of the first attempts to analyse the stent expansion within a stenotic artery based on the finite element method.

Chua *et al.* [6] carried out a FEA to assess the deployment characteristics of the Palmaz–Schatz stent when deployed within an idealised stenotic artery and evaluated the degree of induced arterial stresses. The artery was modelled as a cylinder with a parabola-shaped plaque. Stent expansion was achieved through the same method employed by Auricchio *et al.* [138]. The results showed that the highest arterial stresses are those that coincide with locations at which most plaque ruptures occur. Regarding the stent deployment characteristics, the maximum stent diameter under expansion within the stenotic artery was less than the maximum stent diameter achieved during stent free expansion.

Ballyk *et al.* [182] evaluated the effect of stent oversizing on the induced arterial stress and examined the “stress threshold” for the development of neointimal hyperplasia. A 3D hyperelastic numeric model was utilised to analyse the nonlinear behavior of the artery during stent deployment. Initially, an axial prestretch of 10% and an arterial pressure (mean) of 100 mm Hg were applied, followed by the Palmaz-Schatz stent expansion to a diameter 30% greater than that the arterial. The arterial wall stresses with percentage diameter inflation was associated with the known distribution of stent-induced neointimal hyperplasia. The results revealed that initially the stent ends, then the stent cross-links and the stent struts, and finally the bare area between the stent struts exceeded the threshold. The peak of the stress concentrations increased exponentially with stent expansion, showing the importance of minimal stent overexpansion and the need of designing novel stents that conform to peak stress reduction.

Wu *et al.* [7] evaluated the biomechanical impact of a study-specific stent when expanded within both a straight and a curved stenotic artery. An idealised cylinder with a parabola-shaped plaque was used for the straight artery, whereas the curved artery was modelled in an identical way with a curvature in a toroidal coordinate system. The authors followed an approach for activating and deactivating the contact elements, while the stent expansion was realized through a displacement-driven boundary condition. In the case of the curved artery, the stent failed to follow the curved arterial shape and caused the arterial straightening, which in turn induced high stresses in the plaque and in the arterial wall.

Biodegradable polymers are the most promising materials for stent scaffolds [183], [184]. Fully expandable polymeric biodegradable stents initially provide a support to the arterial wall as scaffolds to prevent the mechanic recoil after deployment. In approximately 6 months, the arterial remodelling enters the stable phase, therefore no substantial scaffolding is needed. Subsequently, it is anticipated that stents dissolve after 6 months and leave behind the vessel without pro-inflammatory substances. During this process, the polymers slowly soften, allowing the high arterial stresses to disappear [185]. Among the critical concerns for polymeric biodegradable stents are their mechanical performance and their interaction with the arterial wall during and after deployment. Agrawal *et al.* [8] was the first that assessed the *in vitro* performance of the Duke biodegradable stent which was made of Poly-L lactide (PLLA). This team showed that in order to achieve satisfactory results from a biodegradable stent, a careful balance between the mechanical properties of the PLLA and the stent design should be achieved. Nuutinen *et al.* [9] performed *in vitro* tests of a woven fibre polymeric braided stent which was subjected to radial compression. The performance of those stents was not as good as the one of stent metals, and the collapse pressure was lower, even in the case of the thicker PLLA fibres.

Biodegradable Magnesium stents exhibit different mechanical properties compared to Stainless Steel (SS) stents: (i) much lower ultimate elongation, indicating that the excessive strain during expansion needs to be avoided, and (ii) lower elastic modulus (25% of SS), resulting in the need of more material (widening stent strut) to provide adequate scaffolding. However, more material could result in strain increase during expansion. In addition, the degradation time, mainly controlled by both uniform and stress corrosion processes, requires at the same time an increase in mass and a reduction in maximum stress during scaffolding, requirements that contradict each other. Based on the aforementioned prerequisites, Wu *et al.* [186] developed a morphing procedure and evaluated four different designs that varied at the end and the middle of the curved parts and the middle of the straight parts. The increase of mass distribution in struts (by 48%) resulted in decreasing the: (i) principal stress (by 29%) and (ii) maximum principal strain (by 14%). This novel stent improved scaffolding, implying that changes of mass distribution along the strut may be useful for enhancing the development of innovative and effective stents, especially for low ductility materials.

Lally *et al.* [19] investigated the mechanical behaviour of stents in order to determine the interaction between the stent and the artery. In this study, two different stent were used; the S7 (Medtronic AVE) and the NIR (Boston Scientific) stent. The analysis of stresses in the stented arterial wall indicated that the S7 stent caused lower stress compared to the NIR stent. These findings were in a good agreement with the observed clinical restenosis rates, which showed that higher restenosis rates occur in the NIR stent compared to the S7 stent.

Liang *et al.* [187] simulated the stent deployment under the balloon inflation and deflation. The results showed that the distal end of the stent may injure the arterial wall since high stresses were concentrated in the contacting region between the stent and the plaque. Bedoya *et al.* [14] investigated the effects of the different stent designs parameters on the arterial stress and the radial displacement achieved by the stent. The stent models represented a sample of the commercially available stents. Each stent was expanded in a homogeneous arterial model. Among the designs, which were evaluated, those with large axial strut spacing, blunted corners, and higher amplitudes in the ring segments caused high circumferential stresses over smaller areas of the artery's inner surface compared to all other configurations. The dominant parameter was the axial strut spacing. All stent designs with a small stent strut spacing induced higher stresses over larger areas compared to stent with large strut spacing. The increase of either the radius of curvature or the strut amplitude resulted in smaller areas with high stresses. At larger strut spacing, the sensitivity to radius of curvature was larger compared to the small strut spacing. The results suggested that stent designs with large axial strut spacing, blunted corners at bends, and higher amplitudes induced smaller arterial regions to high stresses, and preserved a radial displacement that could be sufficient enough for restoring the adequate flow.

Even if computer-aided topology optimization is a relatively new approach, it has received unprecedented attention by several research teams [188], [189]. Timmins *et al.* [190] developed an algorithm for stent design optimization taking into account the wall stress, lumen gain and cyclic deflection. An optimization approach was developed based on the Lagrangian interpolation elements with weighting coefficients. Varying the weighting coefficients resulted in stent designs that prioritize one output over another. The accuracy of the algorithm was validated through FEM.

Takashima *et al.* [191] performed a comparative study of both experimental and mathematical simulation for evaluating the stress distribution in the stent-artery contact area. Two kinds of link stents (M1 and M2) and two kinds of artery models (cylinder model and stenosis model) were used in these experiments. Stent expansion was achieved by inflating a balloon in the radial direction until reaching an inner stent diameter of 3 mm. The results showed that: (i) the contact area, between a stent with a high number of cells and links and the artery, were distributed over the whole surface of the stent for both modeling approaches, (ii) the contact area ratios were larger in the experimental than in the computational model.

Timmins *et al.* [192] investigated the influence of the stent design and the stiffness of the atherosclerotic plaque on the arterial wall. The artery was modelled as an axisymmetric idealized diseased vessel. The plaque assumed to have a hyperelastic behavior and was modeled with a 0.5, 1.0, and 2.0 times as stiff as the stiffness of the arterial wall. The results showed that the stress in the arterial wall was affected by the stent design and the material characteristics of the atherosclerotic plaque and more specifically was influenced by the stiffer plaques.

Xiang *et al.* [16] and Li *et al.* [2] created parametric geometric models for achieving stent optimization with parameters the stent angle and length. Even if those approaches were an important step towards improving the stent design, this parameterization lacks of possible rich variation in shape.

FE modeling may also provide significant information related to the fatigue resistance and the radial flexibility of metallic stents. Non-uniform rational basis-splines (NURBS) provide high precision and overall flexibility in defining curves; for a defined number of parameters and allow optimization including an extensive range of shapes than direct parameterization [193]. Kelliher *et al.* [194] was the first that directly used the NURBS parameters as design variables showing a wide range of different shapes deriving from a single geometric model. Their results, however, included only the parametric explorations of the design rather than full optimization.

Zahenmanesh *et al.* [15] examined the influence of stent strut thickness on the stresses within the arterial wall. This study was based on the ISAR-STEREO clinical trial [195], which compared the restenosis outcome for two stents with the same design but with different strut thickness. The analysis of the arterial stresses showed that the higher

expansion diameter of the Mlinkthin stent caused higher stresses in the plaque tissue, which was in contact with the stent. Another finding was that a thinner strut stent invokes considerably lower stresses in the arterial wall when expanded to the same initial diameter as a thicker strut stent and lower stresses when expanded to the same diameter as a thicker.

Pericevic *et al.* [196] investigated the influence of the plaque composition on the arterial overstretching and the arterial injury after stent deployment. An idealised FEM was created and investigated the influence of hypercellular, hypocellular and calcified plaque types and increased stent inflation pressures on the arterial wall and the plaque components. It was shown that the type of the atherosclerotic plaque had a significant influence on the arterial stresses. Higher arterial stresses were observed for the cellular plaques, whereas the stiffer plaques played a protective role, since they reduced the arterial stress for a specific inflation pressure.

Early *et al.* [197] developed a FEM of the stent-artery interaction. Initially stent expansion was modeled, followed by bending through a displacement boundary condition to the artery. It was shown that high stresses occur at the proximal/distal ends of the stent. Since high stress and arterial injury are linked with restenosis, these results suggested that this mechanical environment could be the main cause of high restenosis rates.

Capelli *et al.* [198] studied the mechanical effect of five different BX stent designs. The analysis took into account the process of balloon inflation and deflation. The arterial stresses and the tissue prolapse within the stent cells were assessed and compared for the different stent designs.

Pant *et al.* [199] performed a geometry parameterisation for a Cypher (Cordis Corporation, Johnson & Johnson co.) stent and explored the functionality of sequential circumferential rings connected by 'n' shaped links. Each stent performance was evaluated, among other, in terms of acute recoil, arterial stresses and flexibility. Their methodology and the obtained results were adopted by several optimisation studies and could be used for the development of a family of stents with increased resistance to ISR.

Pant *et al.* [17] followed a Gaussian process modelling approach to parameterize the stent geometry, by varying the shape of the circumferential rings and links and assessed the stent recoil, stress distribution and flexibility. It was shown that the large values of strut width combined with small axial lengths of circumferential rings are optimal for minimizing the average stresses. In addition, it was demonstrated that a larger amplitude of the links with minimum curved regions is required for improving the stent flexibility and the average stresses.

Garcia *et al.* [12] evaluated the influence of the stent geometrical parameters on the radial force and based on the outcomes of the analysis designed a new stent towards improving the stent-arterial wall interaction. In the modelling, the commercially available Acculink stent model was used. The parameters taken into account were the radial and circumferential strut thickness and the initial stent diameter. The force needed for the stent radial expansion for the different values of each geometrical variable and the relevant effect on healthy and diseased arterial wall were assessed. The results showed a notable decrease of the contact pressure over the inner arterial wall in healthy areas by the variable radial force compared to the constant expansion force.

The dogboning is an important indicator for assessing the stent expansion quality. Due to the presence of nonlinear function of the geometrical parameters and pressure loads required for the stent expansion, the evaluation of the structural optimization of the stent can be computationally expensive. However, there exist some approximation models, such as the Kriging model [200] that can be used for constructing global approximations for stent optimization. Li *et al.* [201] utilized an optimization method based on the Kriging surrogate model to reduce the stent dogboning in the expansion process. Specifically, the named expected improvement, which is an infilling sampling criterion, was used to balance the local and global searches in the optimization iteration. Four element models of stent dilation were used to examine the stent dogboning rate: (i) Loaded by a Radial Displacement (LRD) model, which is loaded by a radial displacement on the inner balloon surface (artery and plaque included), (ii). Linear Parameter Varying (LPV) model, which is the same as LRD model with a time-related pressure (artery and plaque included), (iii) LPC model, which was loaded by a constant pressure (artery and plaque included) (v) SMPV model, which followed the same loading scenario with LPV model, without including artery and plaque. The results

showed that the LPV and SMPV model can be used for stent optimization and can significantly decrease the dogboning effect.

Azaouzi *et al.* [13] studied the behavior of the stent in terms of flexibility, torsion and expansion focusing on the effect of the stent “bridges”. The geometry of the bridges plays an important role and should be taken into consideration in the phase of stent design. In general, during stent insertion within tortuous blood vessels, the latter is subjected to a variety of mechanical loading such as: bending, torsion as well as residual stresses as a result of the balloon expansion. The analysis of the four stent designs revealed that the most flexible stents for both bending and torsion are the symmetric N-Shaped and the unsymmetrical V-shaped bridges. In addition, the symmetric V-shaped bridge stent had the lowest flexibility.

Imani *et al.* [202] investigated the effect of the stent design on the arterial wall utilizing the Palmaz-Schatz, the Xience V and the NIR stent. This comparative study showed that the Palmaz-Schatz stent caused 15.6% and 7.6% higher stresses in the arterial wall compared to the Xience V stent and NIR stent, respectively. The results suggested a direct association between ISR and the stresses in the arterial wall, since the Palmaz-Schatz stent exhibited the highest restenosis rate in the performed clinical trials.

The recent FEA on metallic stents performed by Schiavone *et al.* [203] confirmed that the stent design is a key factor for controlling stent expansion and the associated arterial stresses. Specifically, open-cell design shows to expand easier and has a higher recoiling compared to the closed-cell design. The dogboning is higher for the slotted tube design and the open-cell sinusoidal design, but there is a significant reduction when the design is strengthened with longitudinal connective struts. After stent deployment, the maximum von Mises stress are located at the U-bends of the stent cell struts, and there is varying magnitude depending on the material and the severity of plastic deformation. The associated stresses in the atherosclerotic plaque are distinctly different for the different stent designs and materials, both in terms of distribution and size. In addition, the composition of the plaque strongly affects the stent and modifies the induced on the plaque stresses.

Clune *et al.* [204] used the NURBS control parameters to extend the range of stent designs. They used a method based on the control parameters, as optimization design variables, achieving significant geometric variation compared to previous stent

parameterizations. In addition, this team introduced the Goodman plot-based measure of fatigue resistance to the optimization problem, considering that the fatigue resistance and its association to other performance indicators is important for maximizing the stents safety.

Schiavone *et al.* [205] compared the performance of the Xience metallic stent and the Elixir bioresorbable polymeric stent. The models included the stent, the balloon and the artery and the stent deployment pressure-driven approach was followed. The Xience stent showed a higher expansion rate compared to the Elixir stent. The diameter of the Elixir stent was smaller since a higher recoil occurred. During the crimping process, reduced expansion, increased dogboning and decreased vessel stresses were observed. The polymeric stent induced lower stresses in the artery which was beneficial, however this analysis highlighted the challenge for polymeric stents to match the performance of metallic stents.

The comparison and evaluation of different stent designs has gained great interest [206]. Schiavone *et al.* [10] studied four stents inside a realistic artery; two stents made of SS316 and two made of Cobalt–Chromium (CoCr) alloy. Co–Cr stents experienced higher stresses compared to SS316 stents. However, all stents presented the dogboning effect provoking higher stress concentration to the ends of the plaque. A similar comparative study, [207] investigating the performance of five BX and a SX stent, demonstrated that different levels of arterial stress and strain concentrations exist. The SS316 stents induced larger strain on the arterial walls compared to the CoCr stents, mainly due to the higher stiffness of the CoCr stents and the corresponding thinner struts. The Ni–Ti stent induced less arterial stress and strain which might be attributed to the lower stiffness of the Ni–Ti alloy. Even if in these arterial models a stenosis was included, they did not account for the effect of the severity of stenosis or its material properties. These parameters were later examined in a comparative study conducted by Conway *et al.* [11].

5.2.2.2 Patient Specific arterial segments

A literature review on the recently published numerical approaches reveals that the majority of computational models developed in recent years consider the arterial wall and the plaque component as homogeneous and single-layer structures [14], [19], [20]. Several computational models assume the arterial wall as isotropic, which is a

simplified approach since experiments have revealed the cylindrically orthotropic behavior of both non-diseased [208], [209], [210] and diseased arterial tissues [211]. In addition, only few studies include 3D realistic geometries [212]. Even if those simplified approaches have contributed in understanding the stenting mechanics, there was an imperative need in modeling the 3D morphology in a more realistic way, capturing and approaching the patient-specific characteristics. In order to accomplish this, the utilising of multi-imaging for a particular patient's vasculature is required.

An overview of the modelling approaches and how the arterial wall was defined in each of them is presented below. Liang *et al.* [187] included the balloon component in a stent deployment simulation, however the arterial wall was simplified and assumed as an idealised cylinder. A more detailed approach was tried from Holzapfel *et al.* [18] who modelled the arterial geometry utilising eight different tissue models from high-resolution MRI. Kioussis *et al.* [213] investigated which is the optimal stent design for specific clinical criteria. This study improved the numerical results of stenting by taking into account the interaction of stents with the atherosclerotic lesions. Specifically, the arterial wall was assumed as a non-homogeneous solid and consisted of four different tissue components, while the constitutive material models captured their nonlinear, anisotropic behaviour. The stent was parameterized and two modified designs were generated. The balloon was modelled through an orthotropic model and its expansion was achieved through the application of an internal pressure. The balloon-stent and artery interaction was solved as a 3D contact problem. In addition, to model the fissuring and dissection of the plaque under dilation, two tears were incorporated in the undeformed arterial wall configuration. The outcomes of the simulations showed that the inclusion of the tears at the intima caused an alteration in the stress environment in the stenosis. Specifically, the mechanical load was carried by the intima, the non-diseased media, and the adventitia. However, the highest stresses were observed at the tears region, revealing that the induced injury due to stenting was still located in the dissection site and did not spread over the lesion, which is in agreement with the recent study of Gasser *et al.* [214].

Gijsen *et al.* [22] performed a stent deployment in a 3D reconstructed coronary artery. The 3D arterial model was based on the fusion of biplane angiography and IVUS. The stent strut thickness varied and authors investigated the stent stresses and the induced stresses on the arterial wall. The results showed that higher arterial stresses are observed

behind the stent struts as well as in regions of the thin arterial wall. The maximum stent strut stresses were located near the connecting parts between the stent struts. In addition, the authors showed that the decrease of the strut thickness resulted in the reduction of the arterial damage without significantly increasing the strut stresses.

Mortier *et al.* [215] compared three different second generation DESs and their effect on the arterial wall of a coronary bifurcation with a (highly) curved main vessel. A new method was used for the creation of the 3D bifurcation model using *in vivo* patient-specific angiographic data. The different layers of the arterial wall and the anisotropic behavior of these layers were modeled through the utilisation of a novel algorithm. The proposed simulation strategy deployed the stent in the curved main branch through the insertion of a folded balloon catheter. Stent deployment induced high arterial stresses and therefore a modified stent using a parametric model was developed for reducing the arterial injury while preserving a sufficient radial strength.

Zahedmanesh *et al.* [23] focused on investigating the mechanics of balloon–stent interaction and shed light on the difficulties of folded balloon geometries creation. Specifically, the authors created a folded balloon model which was later used for the numerical deployment of a stent in a patient specific arterial geometry. The reconstruction of the patient derived model was based on digitised 3D angiography images. Stent deployment was achieved by the application of the inflation pressure to the stent (Model A) and in the realistic balloon (Model B). The analysis illustrated that the inclusion of the balloon is imperative to accurately model the stent deformation and stresses. On the other hand, the direct application of the pressure to the stent inner surface could be used for estimating the stresses in the arterial wall allowing the numerical modelling within complex arterial geometries.

Gervaso *et al.* [216] simulated three different modelling approaches to assess the stent-free expansion and the stent expansion inside an idealised artery. The different stent expansion modelling approaches were achieved by: (i) applying a uniform pressure on the inner stent surface, (ii) expanding a cylindrical surface with displacement control (iii) including a deformable balloon. The results showed differences in the free and confined-stent expansions which were attributed to the different expansion techniques and revealed that the inclusion of the balloon is essential for estimating the arterial injury during stent expansion.

For a particular stenotic artery, the optimal intervention strategy varies and depends on several factors such as the stent type, the strut thickness, the stent cell geometry as well as the stent-arterial wall radial mismatch. Holzapfel *et al.* [18] proposed a methodology in which several parameters varied, in order to evaluate the difference within the arterial wall before and after stent implantation. For describing the material behavior of the artery and the atherosclerotic plaque, eight different vascular tissues were considered. The latter captured the typical anisotropic and nonlinear behaviour that the arterial tissue and plaque have. The 3D stent models: ((i) the Multi-Link-Tetra™ stent (Guidant), (ii) the NIROYAL™ Elite stent (Boston-Scientific) and (iii) the InFlow™-Gold-Flex stent (InFlow Dynamics)) were parameterized so as to allow the creation of new designs by varying some parameters in the stent geometry.

A large number of biomaterials are available for stent manufacturing. Tamaredi *et al.* [21] performed a computational analysis for evaluating the effect of different stent materials on the biomechanical performance of the stent deployment in different patients. The Palmaz-Schatz stent geometry was utilized for quantitatively predicting the effect of the mechanical properties of the selected biomaterials on the stent and the coronary artery. This study is considered important since it provides the knowledge for understanding the role of stent materials and the induced biomechanical responses to the arterial wall.

Chapter 6: Effect of stent design and material on stent deployment

-
- 6.1 Description of the Computational model
 - 6.2 Creation of the arterial model
 - 6.3 Boundary Conditions and loading
 - 6.4 Mesh Sensitivity
 - 6.5 Effect of stent material
 - 6.6 Effect of stent design
-

6.1 Description of the Computational model

The computational model includes a reconstructed artery from patient specific data and a stent scaffold that is in its unexpanded configuration (Figure 21).

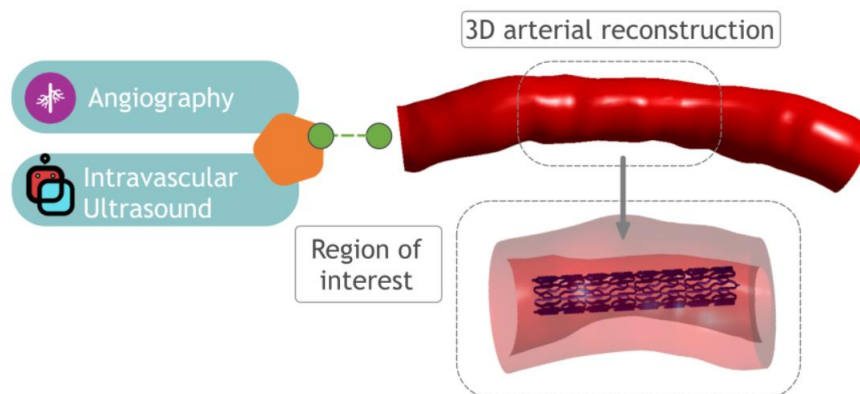


Figure 21: Representation of the FEMs.

ANSYS 14.5 (Ansys Canonsburg, PA) is used for the FEM development and for the post processing of the results [217]. Five different FEM are created. In each model, the reconstructed artery is the same. The difference lays in the stent materials (Model A, Model B, Model C) and stent design (Model D, Model E) used.

An overview the FEM is presented in Table 14. Model A, Model B and Model C include the arterial geometry with stents of CoCr, SS316L and PtCr materials respectively. The stent design (Stent design I) is based on the design of the commercially available LeaderPlus stent (Rontis Corporation S.A., Zug, Switzerland [218]). Model D and Model E are based on the stent design I with specific alterations in the strut thickness.

Table 14: Details of FEMs.

	Stent design	Stent material
Model A	Stent design I	CoCr
Model B	Stent design I	SS316L
Model C	Stent design I	PtCr
Model D	Stent design II	CoCr
Model E	Stent design III	CoCr

6.1.1 Creation of the stent model

6.1.1.1 Creation of the 3D stent design

As described, the design of the stent was based on the design of LeaderPlus stent from Rontis Corporation S.A., Zug, Switzerland [218]. The company provided the geometrical pattern of the stent and then the 3D stent design was achieved through the process presented in Appendix A2. For the design purposes, the Solidworks software was used. Details on the different stent designs are provided in Table 15.

Table 15: Stents designs and associated geometric characteristics.

Stent	Length (mm)	Din	Strut thickness (mm)
Model A	7.55	1.26	0.0810
Model D	7.55	1.26	0.0702
Model E	7.55	1.26	0.0774

6.1.1.2 Constitutive behavior of stent material

As presented in Table 14, three different stent materials (CoCr, SS316L, PtCr) were used in Model A, Model B and Model C respectively. The elastic behaviour of all stents was considered to be linear and isotropic in terms of finite deformation stress and strain measures. More details on the material properties are provided in Table 16. The material model used in Model A, Model D and Model E is CoCr.

Table 16: Material properties of stents.

Stent Material Properties	Model A	Model B	Model C
Material	CoCr	SS316L	PtCr
Elastic modulus (MPa)	232000	193000	200000
Yield strength (MPa)	414	360	355
Tensile strength (MPa)	738	675	834
Poisson's ratio	0.32	0.3	0.32

6.2 Creation of the arterial model

6.2.1 Creation of the 3D reconstructed artery

To represent the physical domain in the modelling approaches, the utilisation of a geometry (1D/2D/3D) parts is essential. In any physical problem, the geometry plays a key role, and this is a characteristic which in turn affects the accuracy of the simulation results. In the same manner, in stent deployment the accurate representation of the arterial segments of the arterial trees is of paramount importance. In the current study, the arteries were reconstructed employing the key imaging modalities for the visualisation of the circulatory system; IVUS and angiography. In the following sections, the methodology that was used for the 3D reconstruction of the artery based on the fusion of IVUS and angiography is presented.

6.2.1.1 3D Coronary Artery Reconstruction Using IVUS and Angiography

The coronary artery reconstruction was performed through the employment of a validated methodology that is based on the combination of angiographic and IVUS data [219]. In brief, the IVUS catheter (Atlantis SR 40 MHz, Boston Scientific Corporation, Natick, MA, USA) was advanced to the distal RCA and angiographic images, after contrast agent injection, from two orthogonal views, were used. The IVUS catheter was moved through an automated pullback device, at a constant speed of approximately 0.5 mm/sec. The data were initially digitized and were further processed. After the detection of the lumen and media-adventitia borders in the end-diastolic images of the IVUS sequence, they were perpendicularly positioned onto the 3D catheter path, which is the outcome of two end-diastolic angiographic images. To determine the orientation of the IVUS frames onto the path, efficient algorithms were employed. The output of the aforementioned process was two point clouds; (i) the lumen and, (ii) media adventitia wall. In Figure 22, the output of the described reconstruction method is presented.

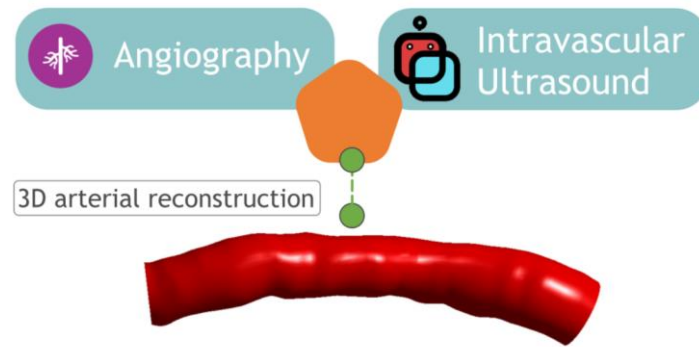


Figure 22: Representation of the 3D arterial reconstruction based on IVUS and angiography imaging data.

6.2.2 Constitutive behavior of the artery

The biomechanical behavior of the arterial wall has been a subject of research with a great knowledge generated by the experiments of Cox *et al.* [220], [221] and Dobrin *et al.* [222], [223]. Arteries have a highly nonlinear behavior, alike most soft tissues, with a progressive stiffening under increased loads. They also show an increased circumferential stiffening, when the axial stretch is increased. To note that the required axial force to preserve the vessel stretched to a constant length at physiological pressures is approximately zero, when this is the *in vivo* length. This demonstrates that the artery does not undertake any axial load *in vivo*, which is advantageous in terms of energy reinforcing the optimal operation.

The arterial wall heterogeneity is also taken into account by assuming distinct layers; the individual layers are modelled as homogeneous. This is explained by the regularity of each arterial layer composition [224], which is also confirmed by mechanical tests [225].

Maltzahn *et al.* [226] was the first that quantified the nonlinear mechanics of the arterial wall taking into consideration its layered structure. The same group, some years later, performed multiaxial tests in bovine carotids, with and without the adventitia. Their results suggested that both layers are anisotropic and stiffer in the axial direction.

Some preliminary results of the mechanical data on the mechanical response of the individual layers were published by Vito *et al.* [227]. This team used the canine aorta and performed uniaxial experiments in the circumferential and axial directions of the adventitia and media-intima. They concluded that both the adventitia and media were

isotropic with adventitia being stiffer. However, later, following Patel *et al.* [228], the same authors showed that the media was cylindrically orthotropic.

Based on the aforementioned studies, it is evident that the media and adventitia behave differently. The stress-strain behaviour of both layers, has similarities in what regards high loads. In contrast, for lower loads, the media is stiffer. This could potentially be attributed to the fibrillary collagen, being present in adventitia, which is wavy, and can be considered to be unloaded. When the stretch increases, the collagen fibers are stretched and the stiffness of the tissue is rapidly increasing. On the other hand, in the media, the SMC along with the elastin and collagen contribute to the load-bearing capacity of the vessel, allow the rapid stiffening.

Layer-specific data representing the behavior of the arterial vessels is scarce since the layer separation is a very complex process and raises also ethical considerations. Holzapfel *et al.* [229] published some data related to the heterogeneity of the arterial wall layers' behaviour. From the results it is evident that young arteries do not experience a sudden stiffening (both layers) as aged arteries do. For the media, this could be explained from the fatigue induced fracture of elastic laminae, while for the adventitia the reason behind this could be the increased cross-linking among collagen fibers, due to the remodeling process.

Modelling of Arterial Tissues

From the biomechanical point of view, for the evaluation of the mechanical performance of the arterial vessels, the creation and utilization of the respective constitutive equations, determined by experiments, should be followed. One of the simplest experiments, which can be applied on an arterial vessel is the uniaxial extension test. The arterial wall stress-stiffening response deviates from the law of Hooke provided that the Hooke's law is only applied on linear elastic materials. Additionally, once arteries are subject to cyclic varying strain, a hysteresis loop in the stress-strain curve is shown in each cycle. This hysteresis loop is reduced with succeeding cycles and is stabilised after a number of cycles.

For the mechanical characterisation and the development of the constitutive model only the steady state stress-strain is used with the first number of cycles applied to obtain steady state called preconditioning cycles [230].

One significant property of the arterial tissue is the presence of water, which is incompressible. Specifically, the arterial wall is composed of approximately 70% water. Incompressibility is an important parameter which is utilised in the constitutive models for arteries and is related to the conservation of volume; the product of the principal stretches in a sample should be equal to one.

$$\lambda_1\lambda_2\lambda_3 = 1 \quad (6.1)$$

The first theory for the study of the mechanics of rubber-like materials was developed by Mooney *et al.* [231] and was later extended by the Treloar *et al.* [232] and Rivlin *et al.* [233], [234].

Puglissi *et al.* [235] studied the arterial elasticity based on the approach of rubber-like materials. This theory assumed a strain energy density function, W , for the material as a function of principal stretches $(\lambda_1, \lambda_2, \lambda_3)$ or the stretch invariants (I_1, I_2, I_3) . Rubberlike materials, which can undergo large elastic deformations without being permanent deformed are called hyperelastic materials. Hyperelastic constitutive equations are strain energy density functions for hyperelastic materials. Arteries exhibit some hysteresis under cyclical loads and cannot be assumed as perfect hyperelastic materials. However, according to Fung *et al.* [236], the behaviour of soft tissue does not depend strongly on the strain rate and the behaviour could be modelled through hyperelastic models, if the loading and unloading were treated separately as elastic. This is the pseudo-elasticity concept which was first introduced by Fung *et al.* [236] provided that the theory of viscoelasticity was more difficult to implement than the theory of elasticity. For a hyperelastic material:

$$S_{ij} = \frac{\partial W}{\partial E_{ij}} = 2 \frac{\partial W}{\partial C_{ij}} \quad (6.2)$$

where S_{ij} , E_{ij} , C_{ij} are the components for: (i) second Piola-Kirchhoff stress tensor, (ii) Green-Lagrangian strain tensor, (iii) Cauchy-Green deformation tensor.

A variety of strain energy functions have been approached to fit the experimental stress-strain data obtained for different materials since each function is suitable for certain material behaviours. For the stress-strain relationship of arteries, Fung *et al.* [236] used the following exponential strain energy function:

$$W = \frac{1}{2}c(e^Q - 1) \quad (6.3)$$

$$\begin{aligned} Q = & c_1 E_{11}^2 + c_2 E_{22}^2 + c_3 E_{33}^2 + 2c_4 E_{11} E_{12} + 2c_5 E_{22} E_{33} + 2c_6 E_{22} E_{33} \\ & + c_7 (E_{12} + E_{21}) + c_8 (E_{23} + E_{21}) + c_8 (E_{23} + E_{32}) \\ & + c_9 (E_{13} + E_{31}) \end{aligned} \quad (6.4)$$

where c, c_1 and c_9 are the material parameters obtained by fitting to the experimental stress-strain data and $E_{11} - E_{13}$ are the Green-Lagrangian strain tensor components.

In parallel, several polynomial forms of the strain energy functions have been used to model the arterial tissue and biomaterials. Such a polynomial form is the Mooney-Rivlin model:

$$W = \pi \sum_{i,j}^{\infty} c_{ij} (I_1 - 3)^m (I_2 - 3)^n, a_{\infty} = 0 \quad (6.5)$$

where c_{ij} and I_1, I_2 are the material constants and the stretch invariants for the material respectively ($I_3=0$, for incompressible materials).

$$I_3 = \lambda_1^2 \lambda_2^2 \lambda_3^2 \quad (6.6)$$

$$I_2 = \lambda_1^2 \lambda_2^2 + \lambda_1^2 \lambda_3^2 + \lambda_2^2 \lambda_3^2$$

$$I_1 = \lambda_1^2 + \lambda_2^2 + \lambda_3^2$$

Additionally, many polynomial strain energy density functions have been used for modelling the hyperelastic materials, such as the Ogden [237]:

$$W = \sum_{p=1}^N \frac{2\mu_p}{\alpha_p} (\lambda_1^{\alpha_p} + \lambda_2^{\alpha_p} + \lambda_3^{\alpha_p} - 3) \quad (6.7)$$

where μ_p, α_p , are material constants.

The aforementioned models are phenomenological models, which means that they are mathematical equations coming from the fitting to the experimental stress-strain data of the materials. Even if the Ogden model is very capable of fitting to stress-strain data obtained from soft tissue and rubber like materials, it is important that the hyperelastic constants are defined with high precision since there is a highly sensitive model response to the constants [238].

Another approach in modelling the soft tissue is the utilisation of mechanistic models which are informed by the structure of the material and study the tissue as a heterogeneous material. In this case, the model parameters are not just curve fitting constants but they also have a physiological meaning. Such a model was proposed by Holzapfel *et al.* [239], which considers the arterial wall as a heterogenous material composed by a homogeneous ground matrix and two families of collagen fibres dispersed in the matrix at a specific angle and symmetric with respect to one another. Taking into account that the model considers two families of collagen fibres, the anisotropy of the arteries can be captured.

In the current thesis, the arterial tissue was assumed homogeneous and a hyper-elastic material model proposed by Mooney-Rivlin *et al.*, defined by the following polynomial form [29], was used

$$W(I_1, I_2, I_3) = \sum_{p,q,r=0}^n c_{ij} (I_1 - 3)^p (I_2 - 3)^q (I_3 - 3)^r \quad (6.8)$$

where the strain invariants I_1, I_2, I_3 , are the material constants as defined in previous section. The material properties of the arterial wall are presented in **Table 17**.

Table 17: Material properties of the arterial wall used in the Mooney-rivlin material model.

Arterial Material Properties	Arterial hyperelastic coefficients				
	C10	C01	C20	C11	C30
	0.0189	0.00275	0.08572	0.5904	0

6.3 Boundary Conditions and loading

For stent expansion, the boundary conditions imposed on the stent were those suggested by Gervaso *et al.* [216]. More specifically, a pinned boundary condition was applied at the arterial ends, while three nodes in the middle section of the stent were allowed to expand only radially to avoid rigid movement. For the stent-artery contact, a surface-to-surface frictional contact was selected. To achieve stent expansion, a pressure-driven approach was followed. Specifically, pressure was applied in the inner stent surface in three distinct phases: (i) loading (P=0 to 1.8MPa), (ii) holding (P=1.8MPa constant) and, (iii) unloading (P=1.8 to 0MPa).

6.4 Mesh Sensitivity

In finite element approaches, it is important to include mesh refinement and increase the number of nodes of the model towards determining the degree of change of the

solutions of primary and secondary variables. Ideally, the mesh refinement is performed until there is no change in the solution between primary and secondary variables. The mesh sensitivity study has been carried out using Model A. Figure 23 shows the finite element geometry used in the mesh sensitivity study. The arterial geometry and the stent dimensional characteristics are presented in Table 18.

Table 18: Arterial geometry and stent dimensional characteristics (Model A).

Arterial Geometry	Dimensional characteristics		
	<i>Max Inner Diameter (mm)</i>	<i>Min Inner Diameter (mm)</i>	<i>Length (mm)</i>
	4.40	2.26	30
Stent geometry	<i>Inner diameter (mm)</i>	<i>Thickness (mm)</i>	<i>Number of rings</i>
	1.26	0.081	8

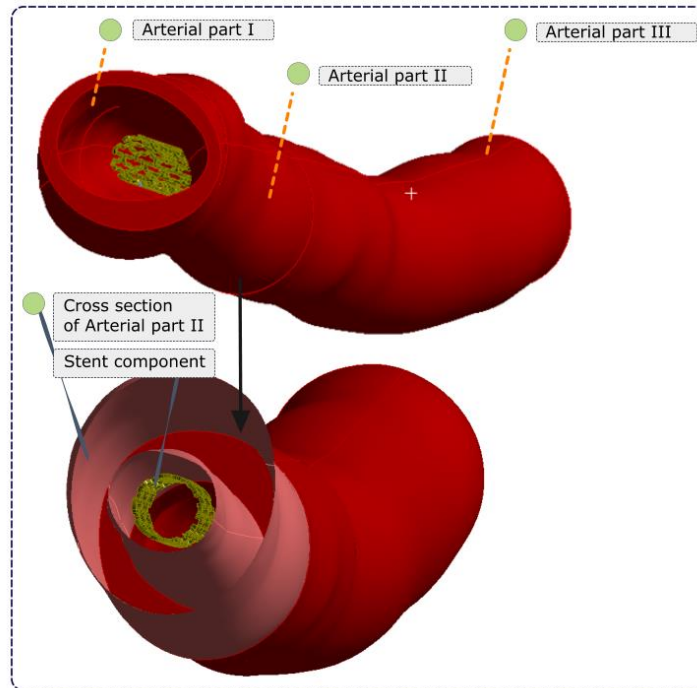


Figure 23: Illustration of the model used in mesh sensitivity analysis.

For the stent, four different finite element meshes (Mesh A, B, C and D) were used and compared. The arterial wall was meshed using lower-order 3-D, 4-node mixed u-P element elements with reduced integration (type SOLID285) and higher order 3-D, 10-node element (SOLID187). SOLID187 has a quadratic displacement behaviour and is well suited for modeling irregular meshes, as those produced from 3D reconstructed models. The mesh density of the artery was studied by varying the number of element size of the arterial wall (arterial part I-III). Details of the finite element meshes are

depicted in Table 19. The stress distribution for the different meshes is shown in Figure 24. The convergence criterion was that the maximum von Mises stresses converges within 5%. This was obtained with Mesh D, relative to the Mesh C. Therefore, Mesh D was selected for the analysis. More details of the Mesh are included in Appendix A3.

Table 19: Details of finite element meshes.

Mesh	Type of Elements	No of elements	Element Midside Nodes
Mesh A	Solid 285	267702	All dropped
	Conta174		
	Targe170		
	Surf154		
	Combin14		
Mesh B	Solid 285	611367	All dropped
	Conta174		
	Targe170		
	Surf154		
	Combin14		
Mesh C	Solid 285	258373	Stent -kept nodes/ Artery dropped
	Solid 187		
	Conta174		
	Targe170		
	Surf154		
	Combin14		
Mesh D	Solid 285	203557	Stent -kept nodes/ Artery dropped
	Solid 187		
	Conta174		
	Targe170		
	Surf154		
	Combin14		

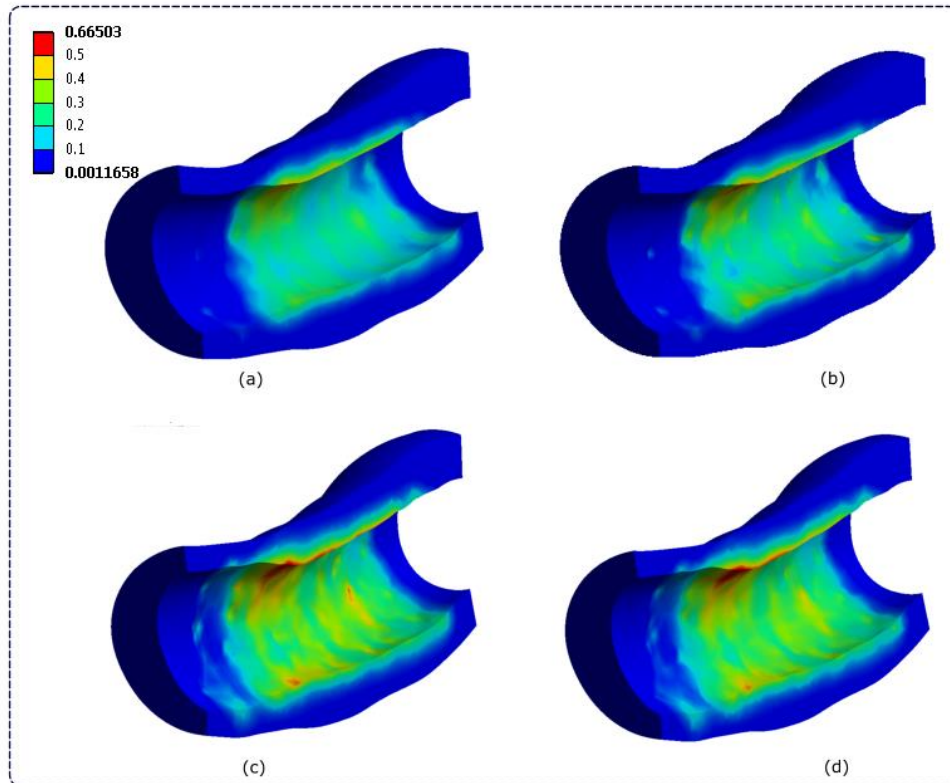


Figure 24: Von Mises stress (MPa) distribution after stent deployment on the arterial part II with: (a) mesh A, (b) mesh B, (c) mesh C and, (d) mesh D.

6.5 Effect of stent material

The results of the simulations performed in this study show that the material properties of the stent influence the resulting stress field imposed on the arterial wall. Specifically, areas of high stress are indicative of the areas in which an adverse biological response is likely to occur. From the analysis of the models the following parameters are examined:

- **Von Mises stress in the arterial wall.** More specifically, the von Mises stress is presented in the inner and outer arterial wall of the deployment area, in the arterial region of interested (ROI) and in cross-sections perpendicular to the stent axis. In addition, the distribution of the von Mises stress of the arterial region of interest in different stress ranges is reported.
- **Von Mises stress in the stent scaffold.** More specifically, the von Mises stress is presented in different time points of the stent inflation and deflation. In addition, the distribution of the von Mises stress of the stent scaffold in different stress ranges is reported.

- **Stent directional deformation.** The behavior of a specific node existing in the middle section of the stent scaffold is analysed in terms of directional deformation during the different loading phases.

6.5.1 Results of Model A

In this section, the results for Model A are presented. More specifically, in Figure 25 and in Figure 26, the von Mises stresses in the inner and the outer wall are depicted. In general, as expected, the area where the stent expands suffers from high stresses. It is observed that higher stresses occur in the intimal arterial area where the severity of the plaque was greatest. Specifically, the maximum von Mises in the inner arterial wall stress is approximately 0.64MPa. Regarding the outer arterial wall, the stress distribution and the stress concentration is less, reaching a maximum stress of approximately 0.17MPa. In addition, stress peaks can be locally observed behind the stent struts.

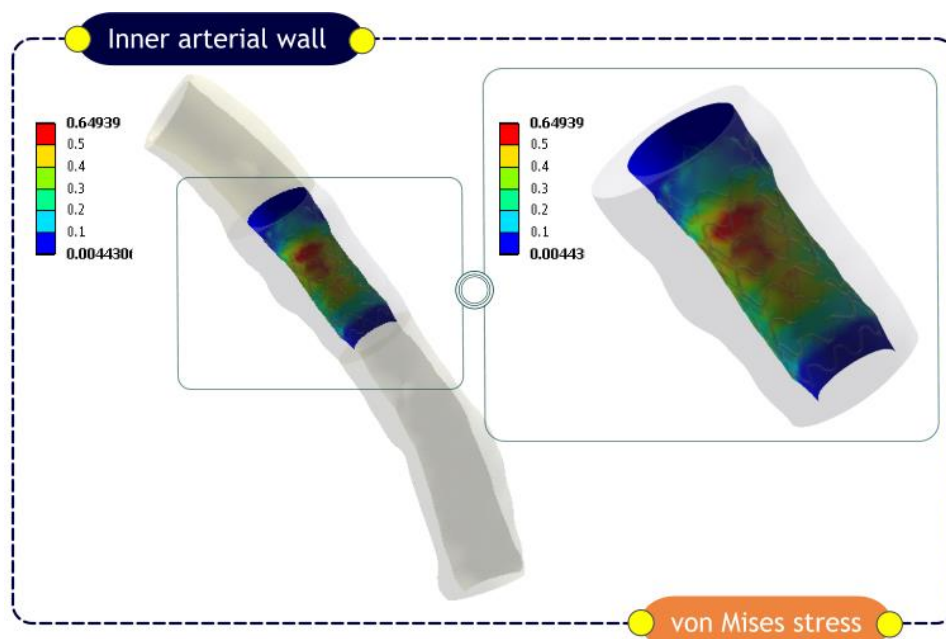


Figure 25: Von Mises stress (MPa) distribution in the inner arterial wall for Model A.

To evaluate the effect of stent deployment along the arterial segment, six (6) different cross sections were created (Figure 27). Specifically, these cross sections were perpendicular to the stent longitudinal axis, starting from the one end till the other. Generally, the stress decreases when moving from the lumen to the outer wall from all cross sections. It is observed that the highest stress occurs in section 3, followed by sections 2, 4 and 5.

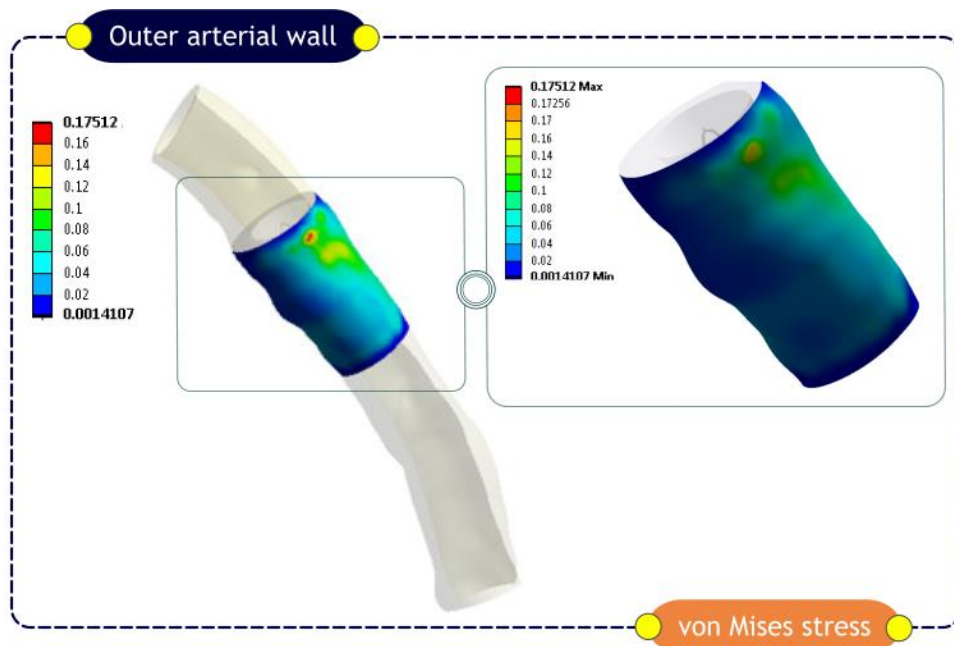


Figure 26: Von Mises stress (MPa) distribution in the outer arterial wall for Model A.

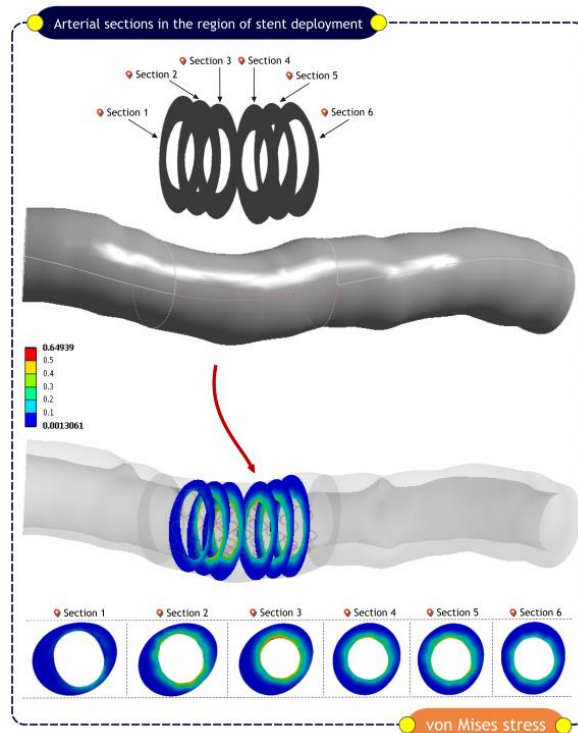


Figure 27: Von Mises stress (MPa) distribution in different cross sections along the area where the stent was deployed (Model A).

The stresses in the stent struts are shown in Figure 28. In general, the stent expansion is affected by the degree of stenosis. It is observed that the stent does not follow a uniform expansion; the ends of the stent are expanded more than the middle stent area.

Locally, highest stresses are depicted near the connection of the stent struts. The peak stresses in these areas reach approximately 736MPa.

In order to evaluate the effect of the inflation pressure and the consequent stent stresses, the distribution in six different loading phases were analysed (Figure 29): (i) Inflation phase – P=1MPa, P= 1.5MPa and P=1.8MPa, (ii) Deflation phase - P=1.5MPa, P= 1MPa and P=0MPa. In the inflation phase, the stent stress has a stress of 681MPa (P=1MPa), which is increased to 736MPa (P=1.5MPa), reaching a maximum stress of 749MPa for P=1.8MPa. On the contrary, when the inflation pressure is decreased the stent stress decreases as well and reaches a value of 432 MPa (P=1MPa). However, when the pressure is totally removed from the inner stent surface the von Mises stress increases and reaches the value of 735MPa.

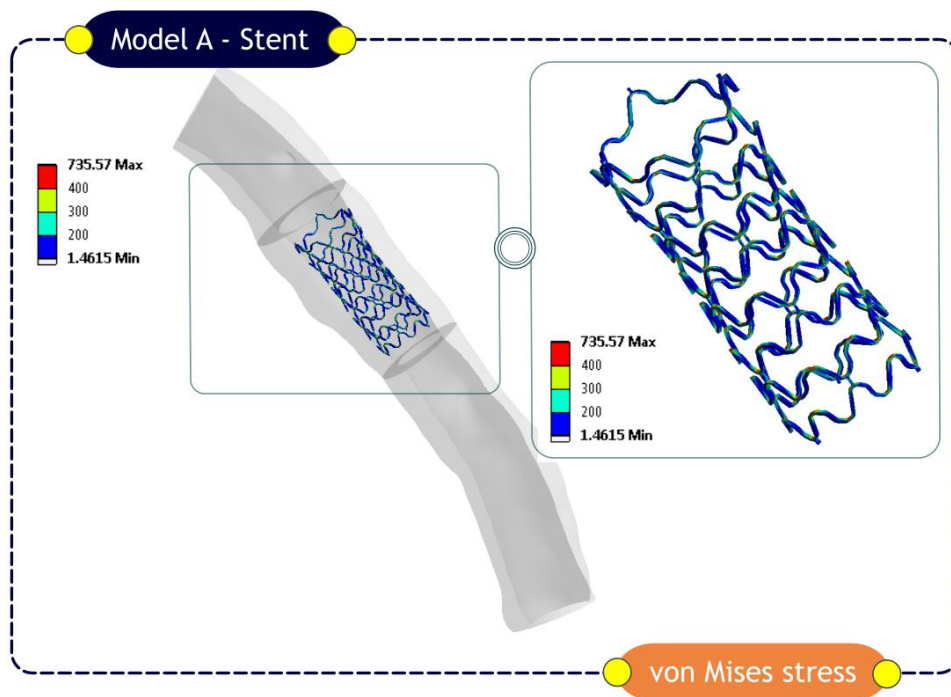


Figure 28: Von Mises stress (MPa) distribution for the stent (Model A) in the unloading phase.

Figure 30 shows the stress distribution for the stent and the artery under the inflation pressure of 1.8MPa. It is observed that the percentage of stent volume is approximately: (i) 62.05% for the stress range 0-200MPa, (ii) 31.18% for the stress range 200-400MPa and, (iii) 6.15% for the stress range over 400MPa. Similarly, the arterial stress is approximately: (i) 70.47% for the stress range 0-0.15MPa, (ii) 17.89% for the stress range 0.15-0.30MPa, (iii) and 7.68% in total for the stress range 0.3-0.45MPa.

Figure 31 shows the stress distribution for the stent and the artery under the deflation phase ($P=0$). It is observed that the percentage of stent volume is approximately: (i) 73.98% for the stress range 0-200MPa, (ii) 20.83% for the stress range 200-400MPa and, (iii) 5.19% for the stress range over 400MPa. Similarly, the arterial stress is approximately: (i) 83.35% for the stress range 0-0.15MPa, (ii) 13.01% for the stress range 0.15-0.30MPa, (iii) and 3.64% over the range of 0.3.

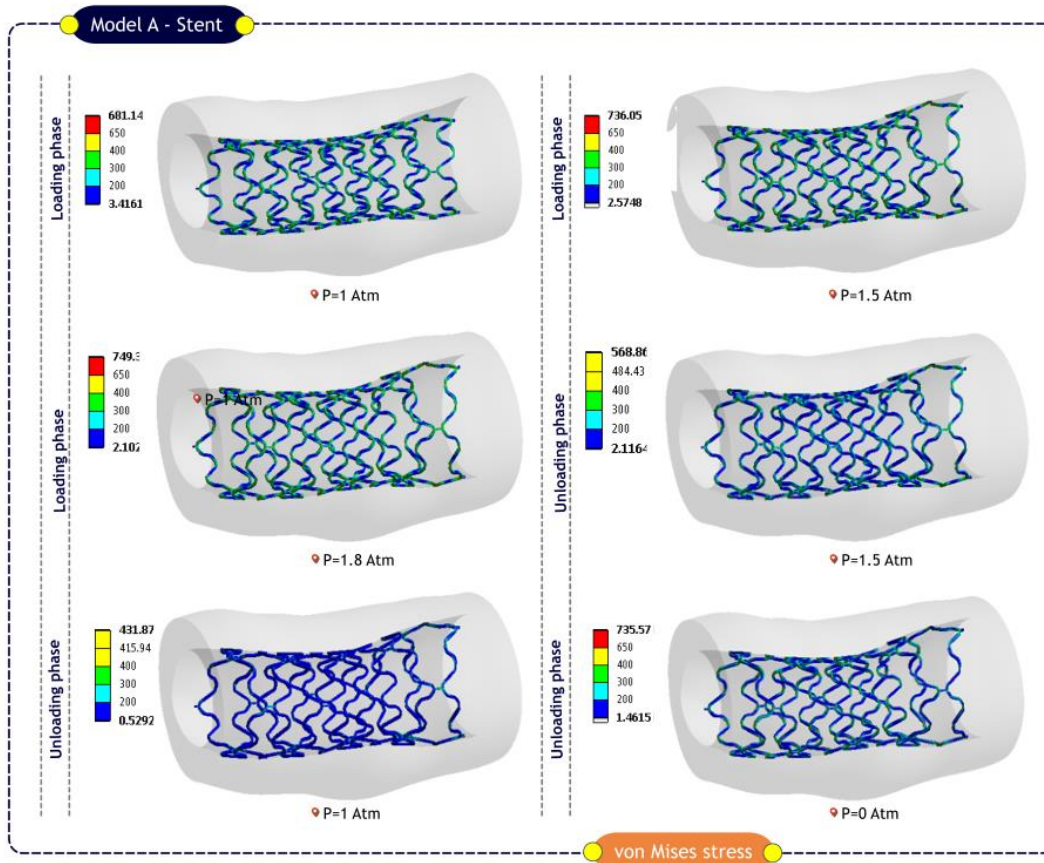


Figure 29: Von Mises stress (MPa) distribution for the stent (Model A) from the loading till the unloading phase.

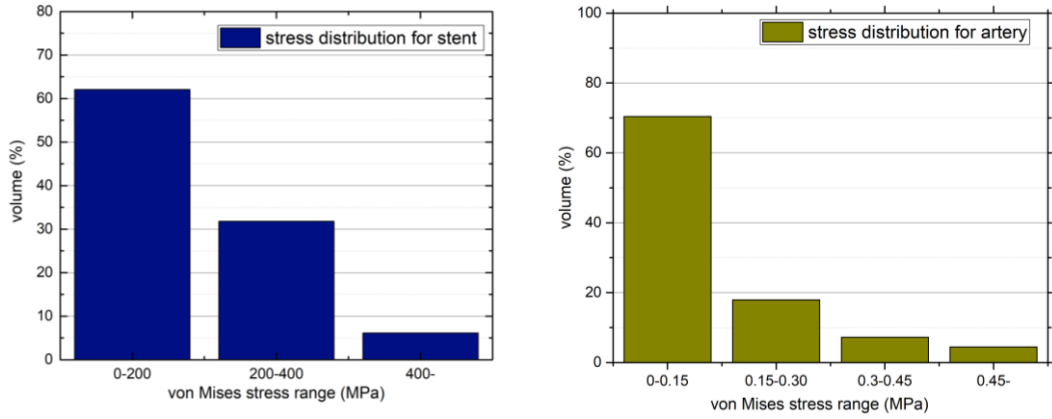


Figure 30: Von Mises stress percentage volume distribution for stent and artery of Model A (P=1.8 MPa).

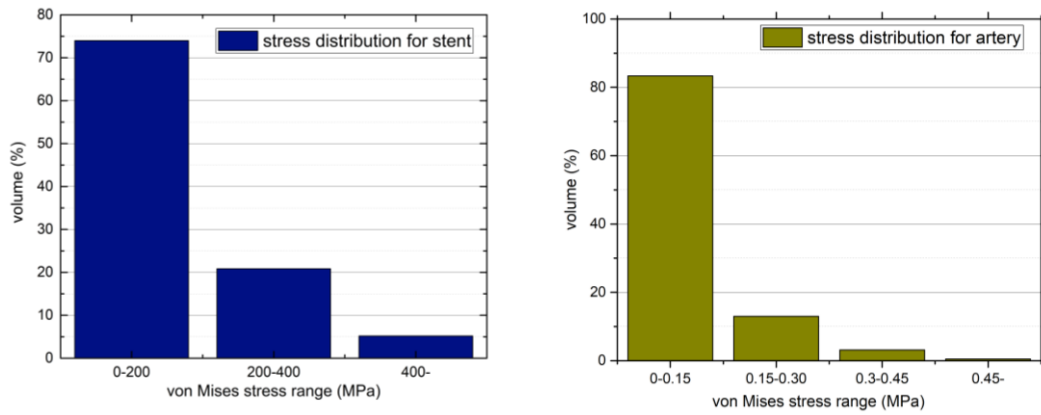


Figure 31: Von Mises stress percentage volume distribution for stent and artery of Model A (P=0 MPa).

To better understand the mechanical performance of the stent, the expanded radius against the expanding pressure was evaluated, for node 2 of the central stent cross section (Figure 32). We observe that the rate of increment of the stent radius is not proportional to the inflation pressure. The stent radius increased slowly at inflations pressure lower than 0.5 MPa and far more rapidly and significantly thereafter - plateauing at 0.66 mm at 1.8 MPa (t=18). When the pressure is removed, a stent contraction is observed as a consequence of the reduced pressure. The maximum radius achieved for the central node of Model A is 0.66 mm, whereas the final radius achieved for the node 2 is 0.59mm.

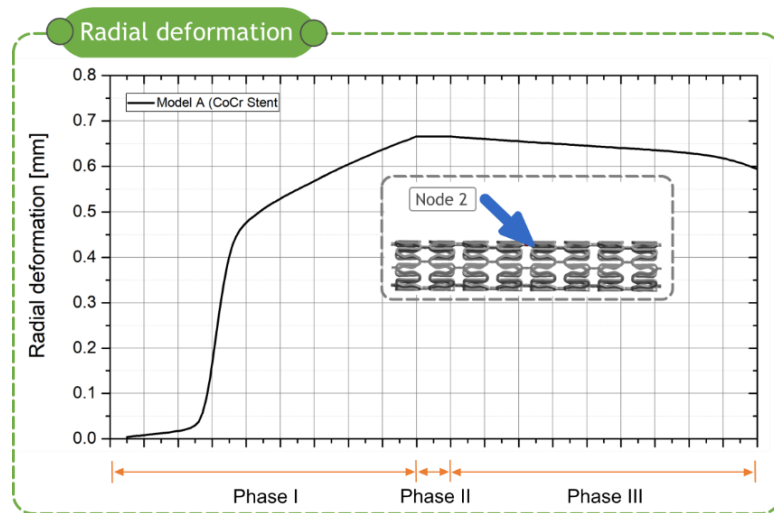


Figure 32: Plot of pressure vs radial deformation for node 2 (node existing in the stent middle cross-section) for stent (Model A).

6.5.2 Results of Model B

In this section, the results for Model B are presented. More specifically, Model B has the same geometrical characteristics for both the arterial wall and the stent, as those included in Model A. The only difference is the utilization of a different material for the stent. More specifically, the SS316L material is used.

In Figure 33 and Figure 34, the von Mises stresses in the inner and the outer wall are depicted. In general, as expected, the area where the stent expands suffers from high stresses. It is observed that higher stresses occur in the intimal arterial area where the severity of the plaque was greatest. Specifically, the maximum von Mises in the inner arterial wall stress is approximately 0.62MPa. Regarding the outer arterial wall, the stress distribution and the stress concentration is less, reaching a maximum stress of approximately 0.20MPa. In addition, stress peaks can be locally observed behind the stent struts.

To evaluate the effect of stent deployment along the arterial segment, six (6) different cross sections perpendicular to the stent longitudinal axis were used (Figure 35). It is observed that the stress decreases when moving from the lumen to the outer wall from all cross sections. More specifically, the highest stress occurs in section 3, followed by sections 2, 5 and 4.

The stresses in the stent struts of Model B are shown in Figure 36. As expected, the stent expansion is affected by the degree of stenosis and does not follow a uniform expansion. Again the ends of the stent are expanded more than the middle stent area. In

general, highest stresses are observed near the connection of the stent struts with a peak of approximately 658MPa.

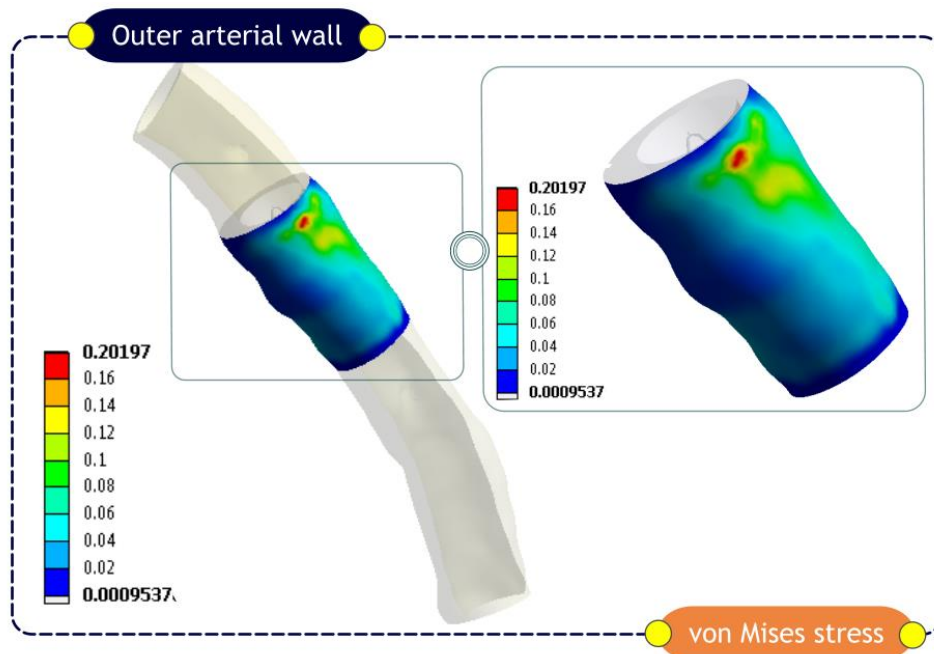


Figure 33: Von Mises stress (MPa) distribution in the outer arterial wall for Model B.

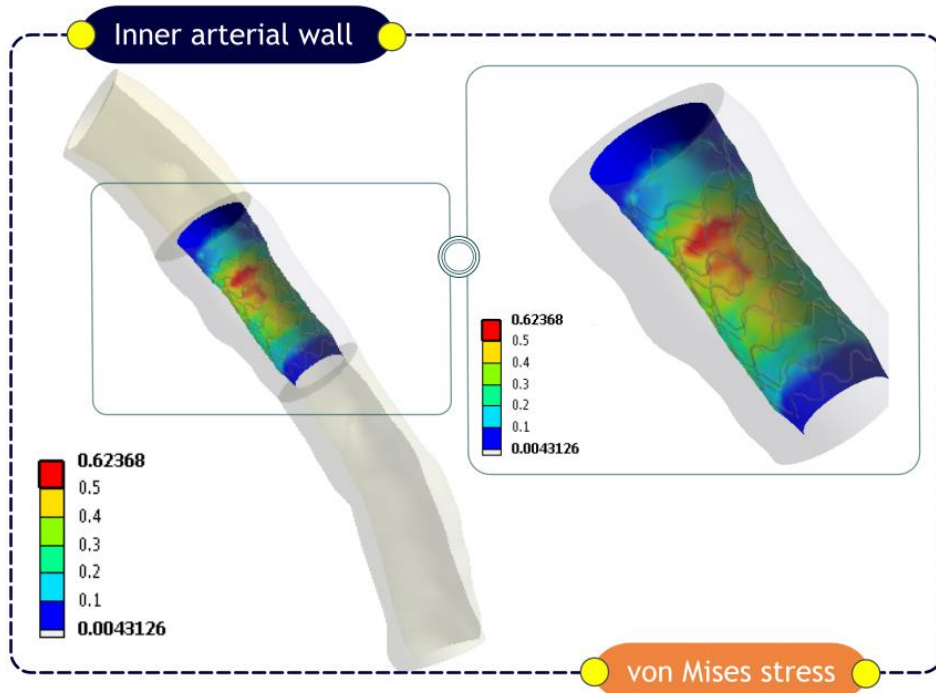


Figure 34: Von Mises stress (MPa) distribution in the inner arterial wall for Model B.

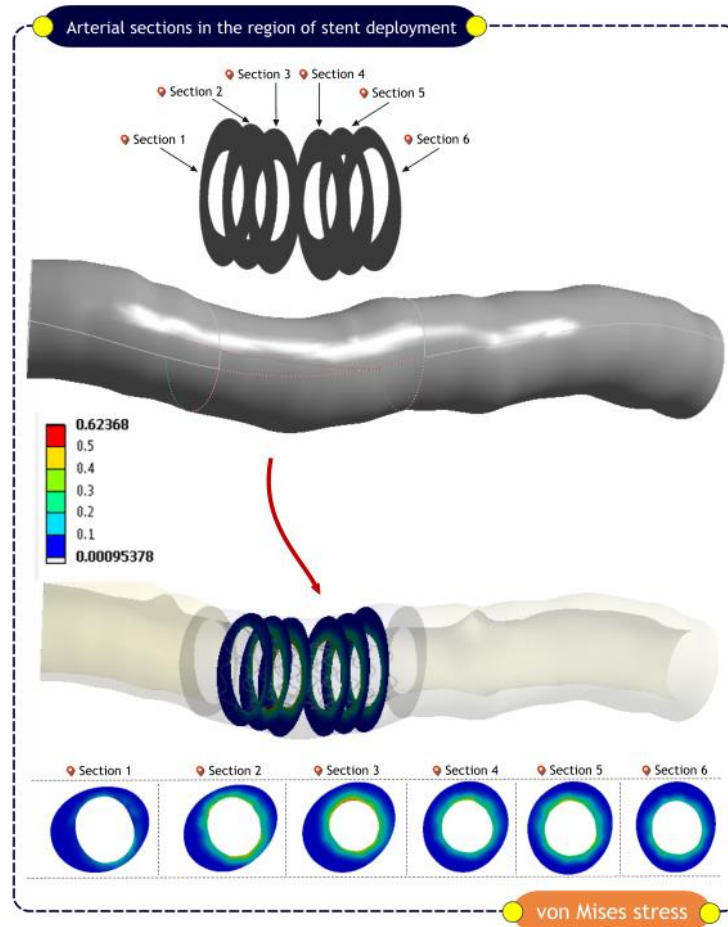


Figure 35: Von Mises stress (MPa) distribution in different cross sections along the area where the stent was deployed (Model B).

To assess how inflation pressure affects the developing in the stent stresses, the distribution in six different inflation phases was analysed (Figure 37): (i) Inflation phase – $P=1\text{MPa}$, $P= 1.5\text{MPa}$ and $P=1.8\text{MPa}$, (ii) Deflation phase - $P=1.5\text{MPa}$, $P= 1\text{MPa}$ and $P=0\text{MPa}$. In the inflation phase, the stent stress has a stress of 621MPa ($P=1\text{MPa}$), which is increased to 660MPa ($P=1.5\text{MPa}$), reaching a maximum stress of 673MPa for $P=1.8\text{MPa}$. On the contrary, when the inflation pressure is decreased the stent stress decreases as well and reaches a value of 409MPa ($P=1\text{MPa}$). However, when the pressure is totally removed from the inner stent surface the von Mises stress increases and reaches the value of 658MPa .

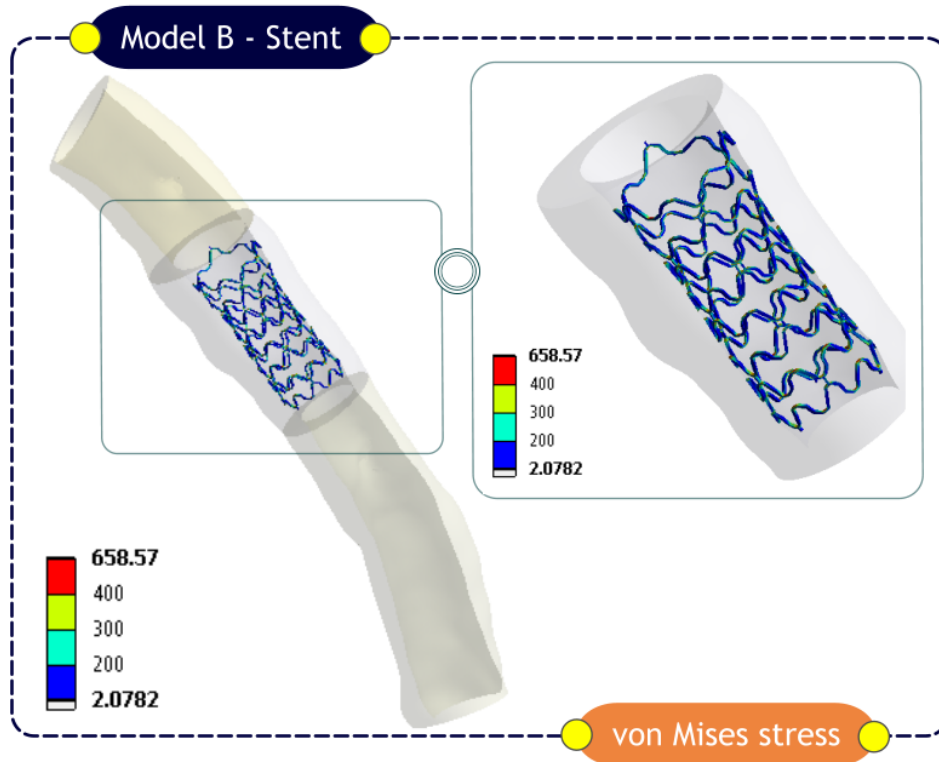


Figure 36: Von Mises stress (MPa) distribution for the stent (Model B) in the unloading phase.

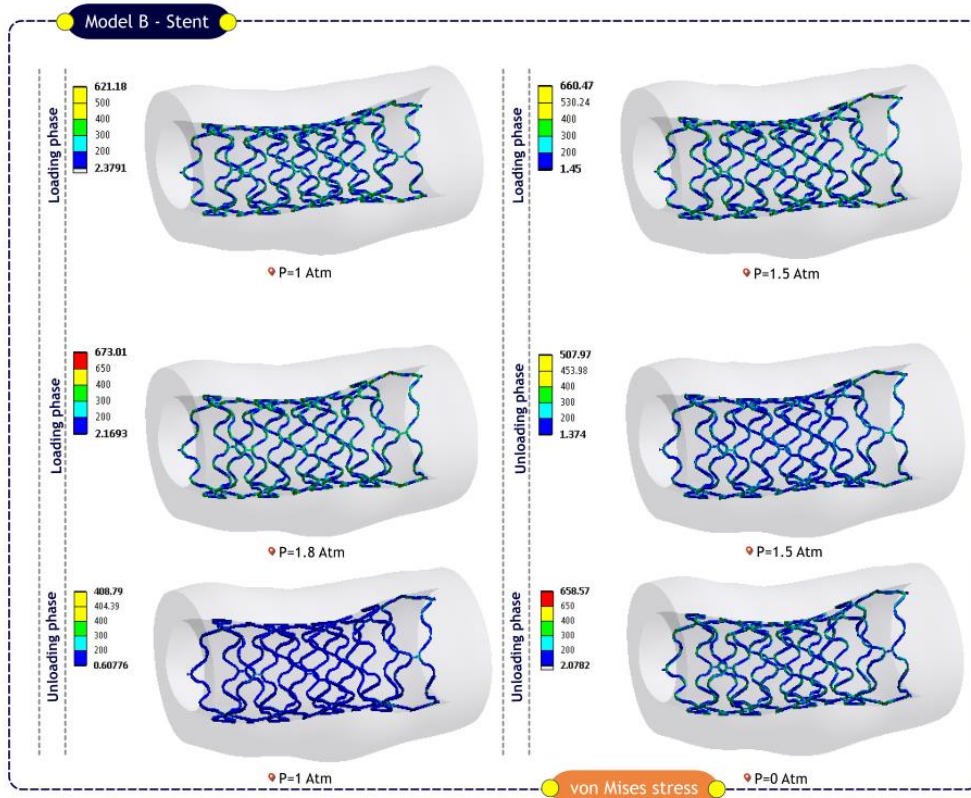


Figure 37: Von Mises stress (MPa) distribution for the stent (Model B) from the loading till the unloading phase.

Figure 38 shows the stress distribution for the stent and the artery under the inflation pressure of 1.8MPa. It is observed that the percentage of stent volume is approximately: (i) 63% for the stress range 0-200MPa, (ii) 31.47% for the stress range 200-400MPa and, (iii) 5.53% for the stress range over 400MPa. Similarly, the arterial stress is approximately: (i) 70% for the stress range 0-0.15MPa, (ii) 18% for the stress range 0.15-0.30MPa, (iii) and 12% over the range of 0.3MPa.

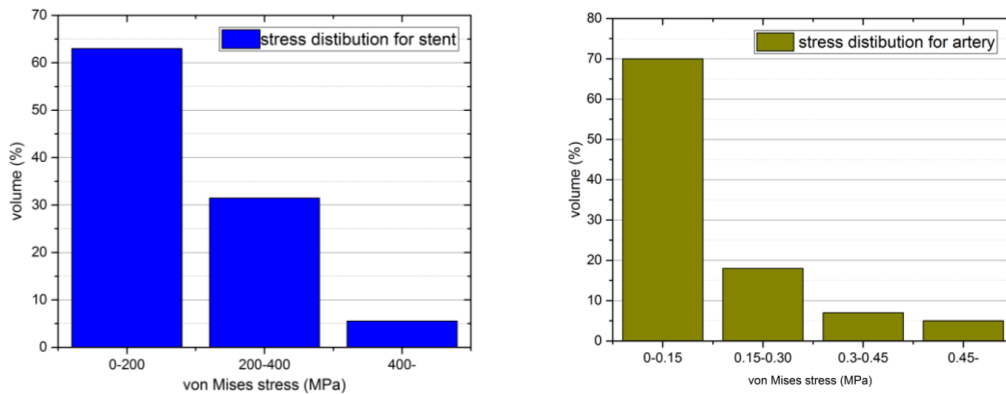


Figure 38: Von Mises stress percentage volume distribution for stent and artery of Model B (P=1.8 MPa).

Figure 39 shows the stress distribution for the stent and the artery under the deflation phase (P=0). It is observed that the percentage of stent volume is approximately: (i) 75.03% for the stress range 0-200MPa, (ii) 21.12% for the stress range 200-400MPa and, (iii) 3.85% for the stress range over 400MPa. Similarly, the arterial stress is approximately: (i) 84% for the stress range 0-0.15MPa, (ii) 13% for the stress range 0.15-0.30MPa, (iii) and in total 3% for the range over 0.3MPa.

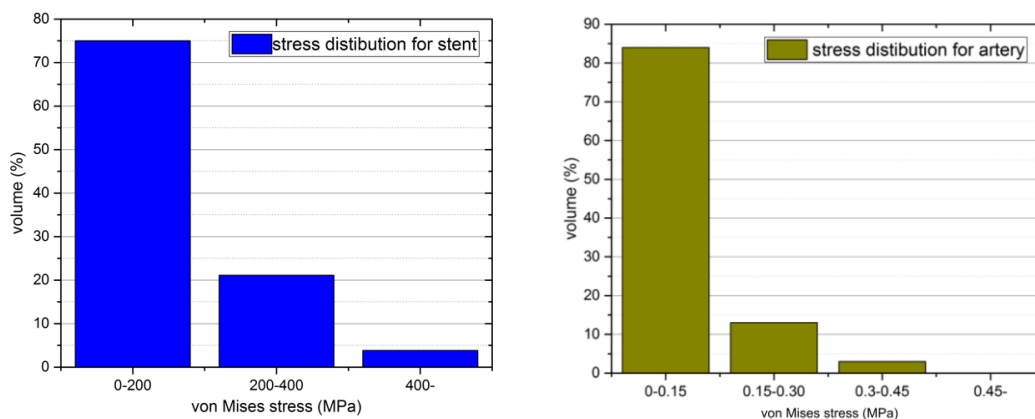


Figure 39: Von Mises stress percentage volume distribution for stent and artery of Model B (P=0 MPa).

To better understand the mechanical performance of the stent, the expanded radius against the expanding pressure was evaluated, for node 2 of the central stent cross section (Figure 40). We observe that the rate of increment of the stent radius is not

proportional to the inflation pressure. The stent radius increased slowly at inflations pressure lower than 0.4 MPa ($t=4$) and far more rapidly and significantly thereafter - plateauing at 0.67731mm at 1.8 MPa ($t=20$). The maximum radius achieved for the central node of Model A is 0.67734mm, whereas the final radius achieved for the node 2 is 0.57518mm.

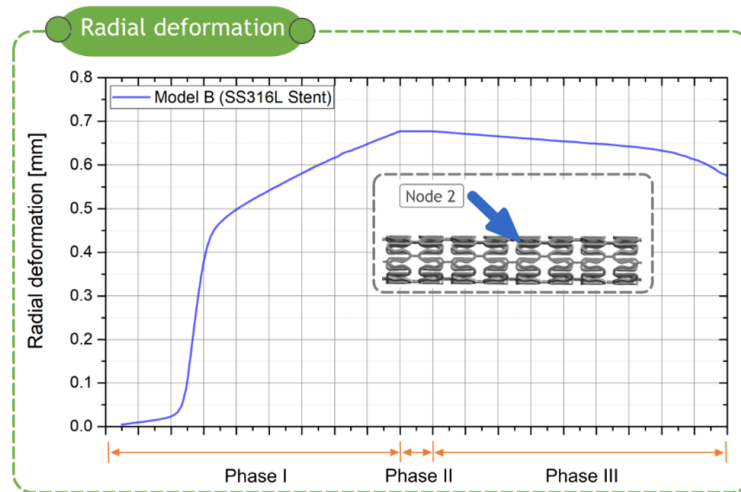


Figure 40: Plot of pressure vs radial deformation for node 2 (node existing in the stent middle cross-section) for stent (Model B).

6.5.3 Results of Model C

In this section, the results for Model C are presented. More specifically, Model C has the same geometrical characteristics for both the arterial wall and the stent, as those included in Model A. The only difference is the utilization of a different material for the stent design. More specifically, the PtCr material is used.

In Figure 41 and Figure 42, the von Mises stresses in the inner and the outer wall are depicted. In general, as expected, the area where the stent expands suffers from high stresses. It is observed that higher stresses occur in the intimal arterial area where the severity of the plaque was greatest. Specifically, the maximum von Mises in the inner arterial wall stress is approximately 0.62MPa. Regarding the outer arterial wall, the stress distribution and the stress concentration is less, reaching a maximum stress of approximately 0.19MPa. In addition, stress peaks can be locally observed behind the stent struts.

To evaluate the effect of stent deployment along the arterial segment, six (6) different cross sections perpendicular to the stent longitudinal axis were used (Figure 43). It is observed that the stress decreases when moving from the lumen to the outer wall from

all cross sections. More specifically, the highest stress occurs in section 3, followed by sections 2 and 1.

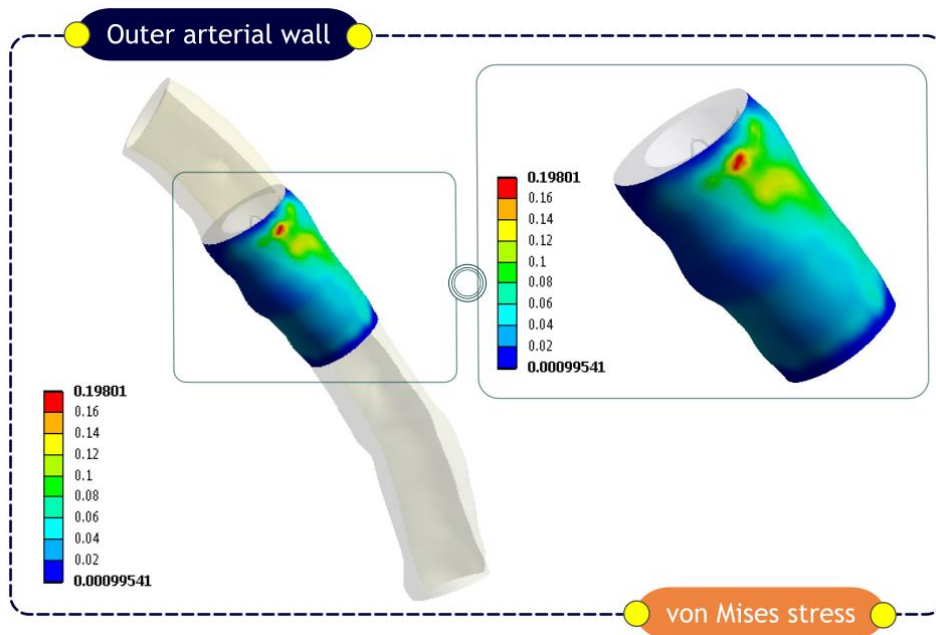


Figure 41: Von Mises stress (MPa) distribution in the outer arterial wall for Model C.

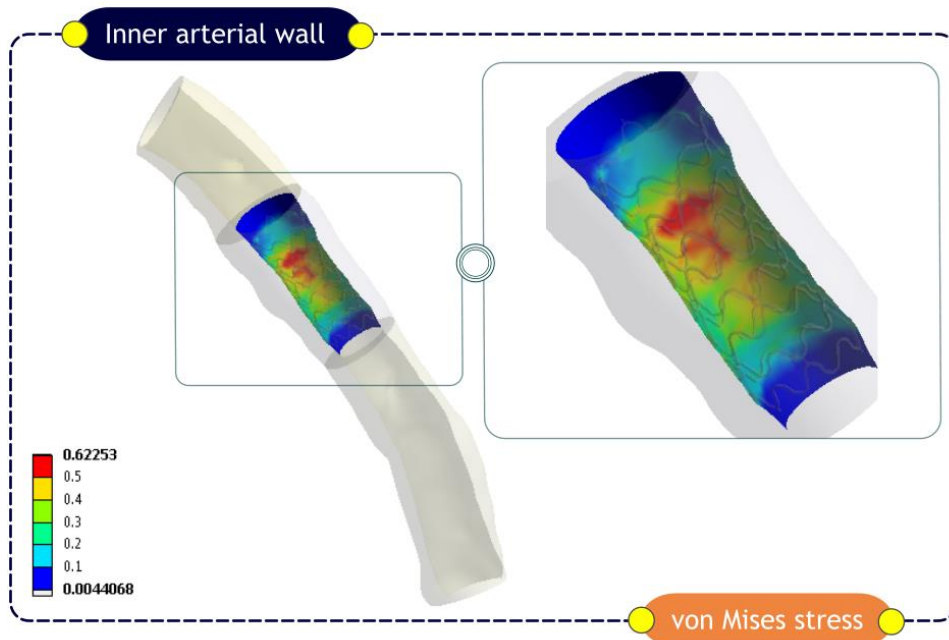


Figure 42: Von Mises stress (MPa) distribution in the inner arterial wall for Model C.

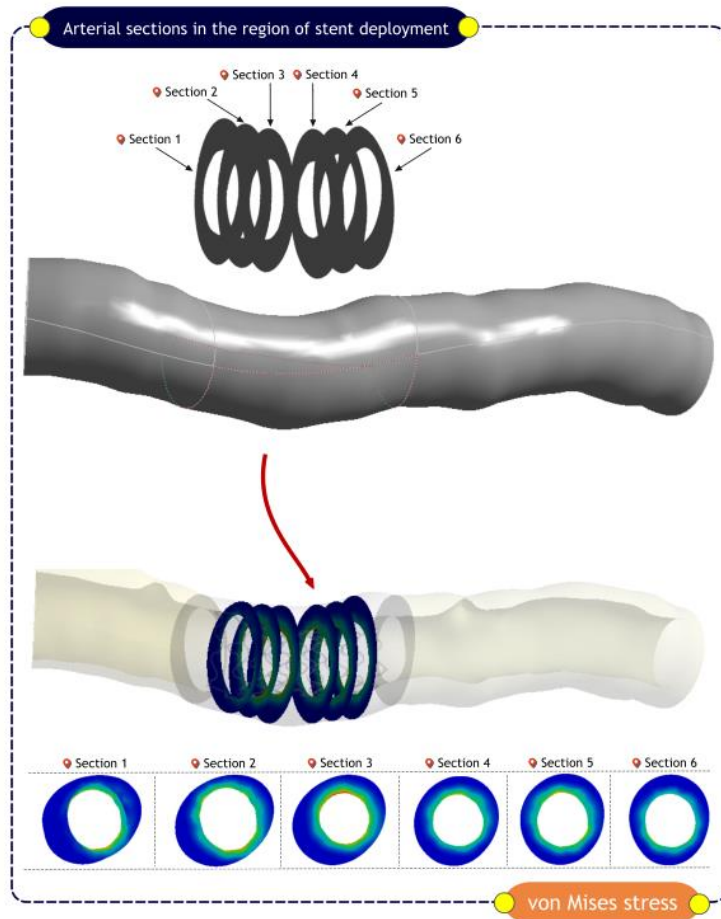


Figure 43: Von Mises stress (MPa) distribution in different cross sections along the area where the stent was deployed (Model C).

The stresses in the stent struts of Model C are shown in Figure 44. As expected, the stent expansion is affected by the degree of stenosis and does not follow a uniform expansion. Again the ends of the stent are expanded more than the middle stent area. In general, highest stresses are observed near the connection of the stent struts with a peak of approximately 709MPa. To assess how the inflation pressure affects the developing in the stent stresses, the distribution in six different inflation phases were analysed (Figure 45): (i) Inflation phase – $P=1\text{MPa}$, $P= 1.5\text{MPa}$ and $P=1.8\text{MPa}$, (ii) Deflation phase - $P=1.5\text{MPa}$, $P= 1\text{MPa}$ and $P=0\text{MPa}$. In the inflation phase, the stent stress has a stress of 662MPa ($P=1\text{MPa}$), which is increased to 721MPa ($P=1.5\text{MPa}$), reaching a maximum stress of 727MPa for $P=1.8\text{MPa}$. On the contrary, when the inflation pressure is decreased the stent stress decreases as well and reaches a value of 396MPa ($P=1\text{MPa}$). However, when the pressure is totally removed from the inner stent surface the von Mises stress increases and reaches the value of 709MPa.

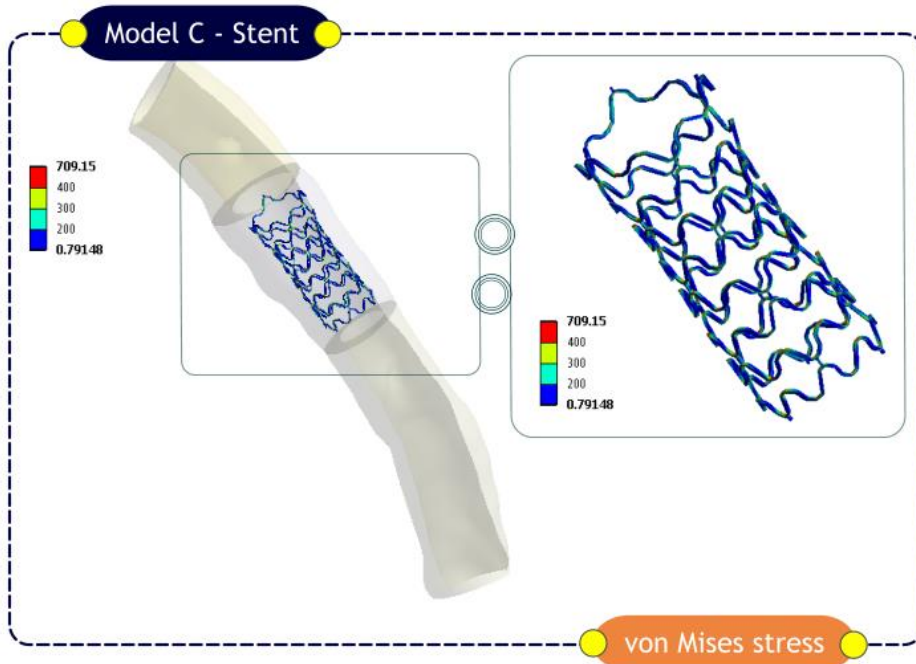


Figure 44: Von Mises stress (MPa) distribution for the stent (Model C) in the unloading phase.

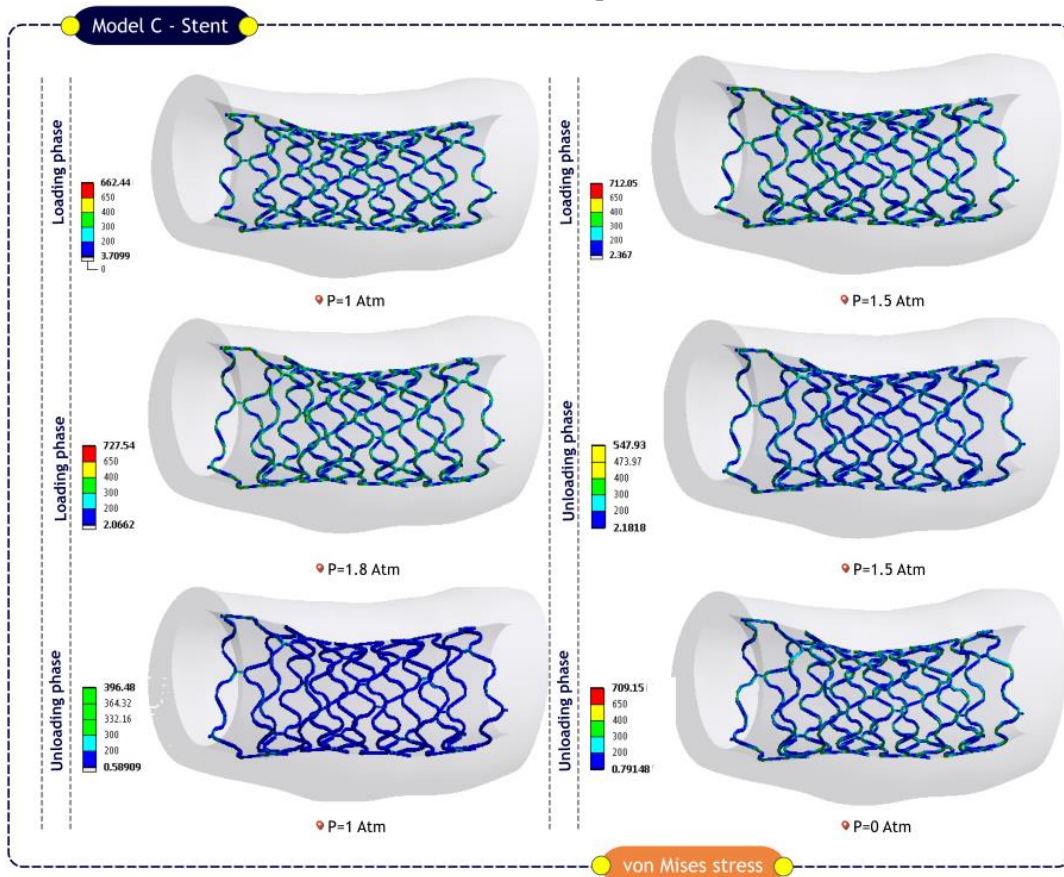


Figure 45: Von Mises stress (MPa) distribution for the stent (Model C) from the loading till the unloading phase.

Figure 46 shows the stress distribution for the stent and the artery under the inflation pressure of 1.8MPa. It is observed that the percentage of stent volume is approximately: (i) 63% for the stress range 0-200MPa, (ii) 31.47% for the stress range 200-400MPa and, (iii) 5.53% for the stress range over 400MPa. Similarly, the arterial stress is approximately: (i) 70% for the stress range 0-0.15MPa, (ii) 18% for the stress range 0.15-0.30MPa, (iii) and 12% for the range over 0.30MPa.

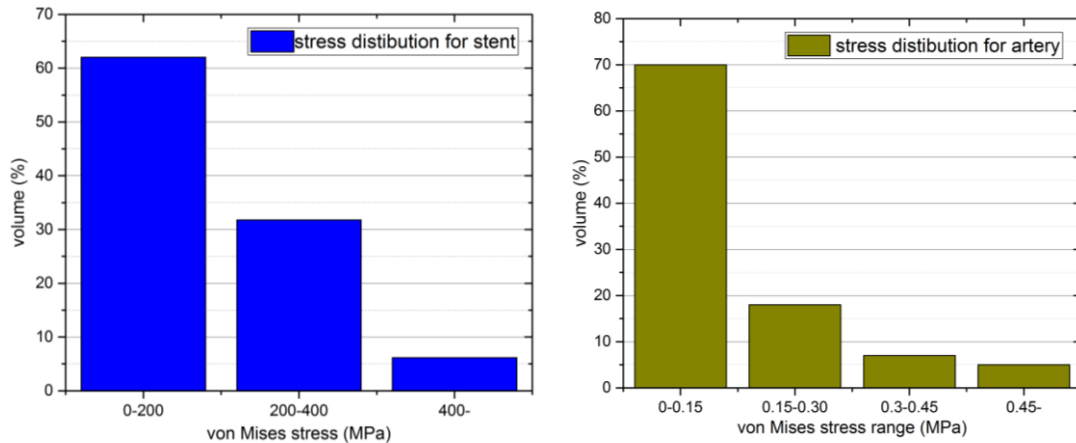


Figure 46: Von Mises stress percentage volume distribution for stent and artery of Model C (P=1.8 MPa).

Figure 47 shows the stress distribution for the stent and the artery under the deflation phase (P=0). It is observed that the percentage of stent volume is approximately: (i) 74.59% for the stress range 0-200MPa, (ii) 21.21% for the stress range 200-400MPa and, (iii) 4.2% for the stress range over 400MPa. Similarly, the arterial stress is approximately: (i) 83.10% for the stress range 0-0.15MPa, (ii) 13.3% for the stress range 0.15-0.30MPa, (iii) and 3.6% for the range over 0.3MPa.

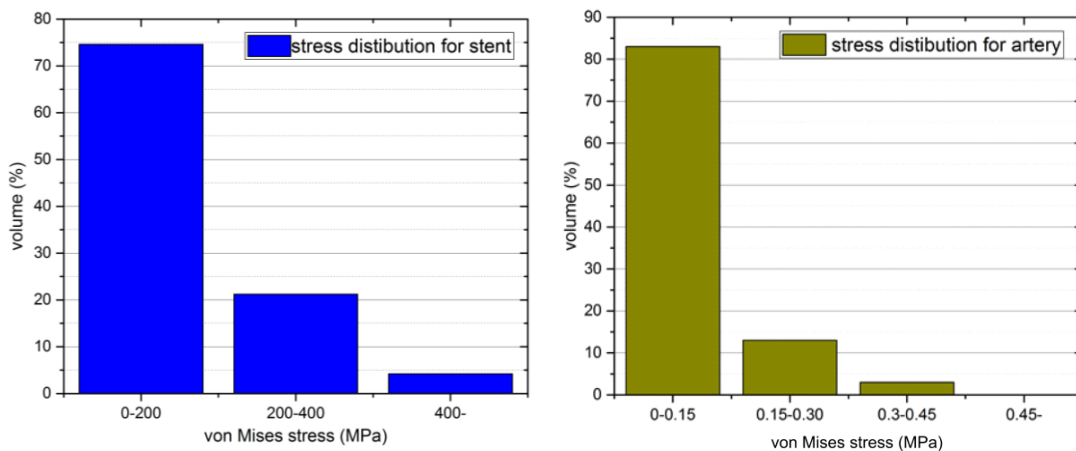


Figure 47: Von Mises stress percentage volume distribution for stent and artery of Model C (P=0 MPa).

To better understand the mechanical performance of the stent, the expanded radius against the expanding pressure was evaluated, for node 2 of the central stent cross section (Figure 48). We observe that the rate of increment of the stent radius is not proportional to the inflation pressure.

The stent radius increased slowly at inflations pressure lower than 0.5MPa and far more rapidly and significantly thereafter - plateauing at 0.67633mm at 1.8MPa (t=18). The maximum radius achieved for the central node of Model A is 0.67633mm, whereas the final radius achieved for the node 2 is 0.58117mm.

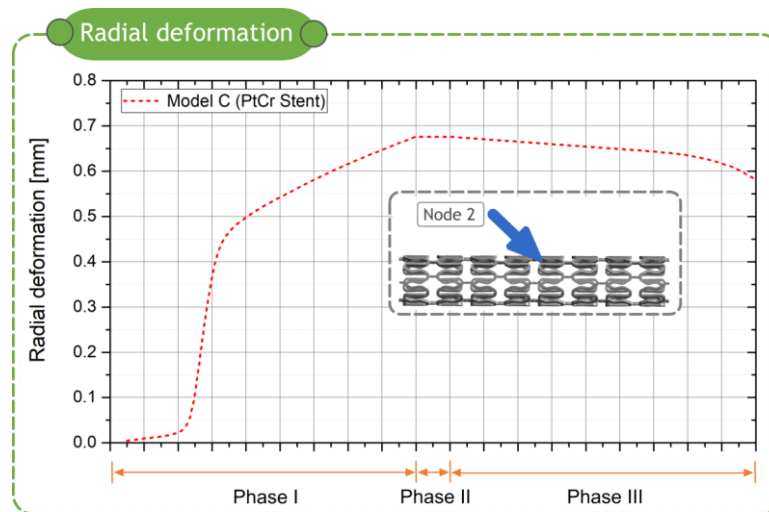


Figure 48: Plot of pressure vs radial deformation for node 2 (node existing in the stent middle cross-section) for stent (Model C).

6.6 Effect of stent design

The results of the simulations performed in this section show that the design characteristics of the stent and more specifically the strut thickness influences the resulting stress field imposed on the arterial wall. From the analysis of the models the following parameters are examined:

- **Von Mises stress in the arterial wall.** More specifically, the von Mises stress is presented in the inner and outer arterial wall of the deployment area, in the arterial ROI and in cross-sections perpendicular to the stent axis. In addition, the distribution of the von Mises stress of the arterial region of interest in different stress ranges is reported.
- **Von Mises stress in the stent scaffold.** More specifically, the von Mises stress is presented in different time points of the stent inflation and deflation.

In addition, the distribution of the von Mises stress of the stent scaffold in different stress ranges is reported.

- **Stent directional deformation.** The behavior of a specific node existing in the middle section of the stent scaffold is analysed in terms of directional deformation during the different loading phases.

6.6.1 Results of Model D

In this section, the results for Model D are presented. More specifically, in Figure 49 and Figure 50, the von Mises stresses in the inner and the outer wall are depicted. In general, as expected, the area where the stent expands suffers from high stresses. It is observed that higher stresses occur in the intimal arterial area where the severity of the plaque was greatest. Specifically, the maximum von Mises in the inner arterial wall stress is approximately 1MPa. Regarding the outer arterial wall, the stress distribution and the stress concentration is less, reaching a maximum stress of approximately 0.20MPa. In addition, stress peaks can be locally observed behind the stent struts.

To evaluate the effect of stent deployment along the arterial segment, six (6) different cross sections were created (Figure 51). Specifically, these cross sections were perpendicular to the stent longitudinal axis, starting from the one end till the other. Generally, the stress decreases when moving from the lumen to the outer wall from all cross sections. It is observed that the highest stress occurs in section 4, followed by sections 5 and 2.

The stresses in the stent struts of Model D are shown in Figure 52. As expected, the stent expansion is affected by the degree of stenosis and does not follow a uniform expansion. Again the ends of the stent are expanded more than the middle stent area. In general, highest stresses are observed near the connection of the stent struts with a peak of approximately 731MPa.

To assess how the inflation pressure affects the developing in the stent stresses, the distribution in six different inflation phases were analysed (Figure 53): (i) Inflation phase – $P=1\text{MPa}$, $P=1.5\text{MPa}$ and $P=1.8\text{MPa}$, (ii) Deflation phase - $P=1.5\text{MPa}$, $P=1\text{MPa}$ and $P=0\text{MPa}$. In the inflation phase, the stent stress has a stress of 696MPa ($P=1\text{MPa}$), which is increased to 739MPa ($P=1.5\text{MPa}$), reaching a maximum stress of 752MPa for $P=1.8\text{MPa}$. On the contrary, when the inflation pressure is decreased the

stent stress decreases as well and reaches a value of 471MPa ($P=1\text{MPa}$). However, when the pressure is totally removed from the inner stent surface the von Mises stress increases and reaches the value of 731MPa.

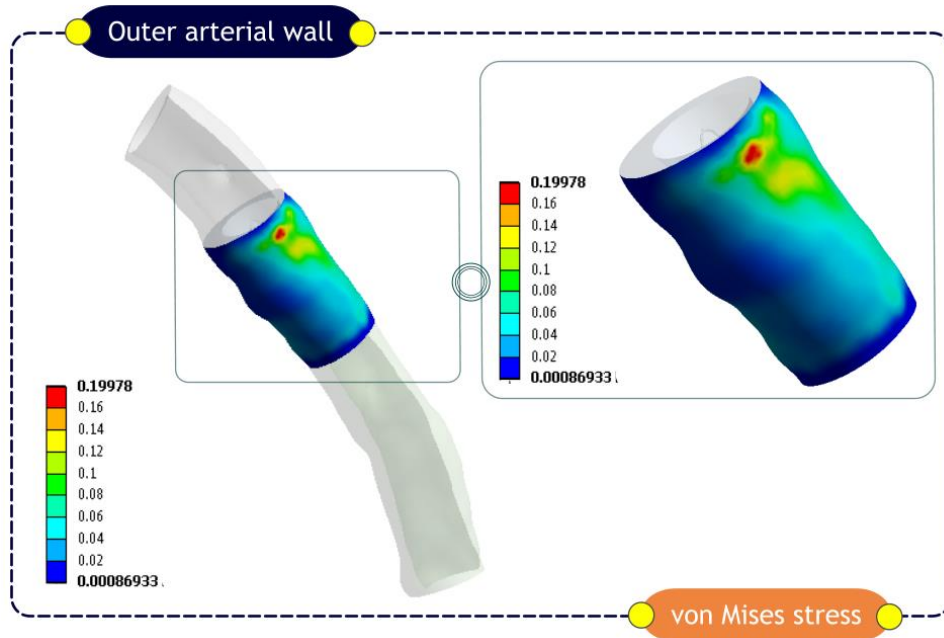


Figure 49: Von Mises stress (MPa) distribution in the outer arterial wall for Model D.

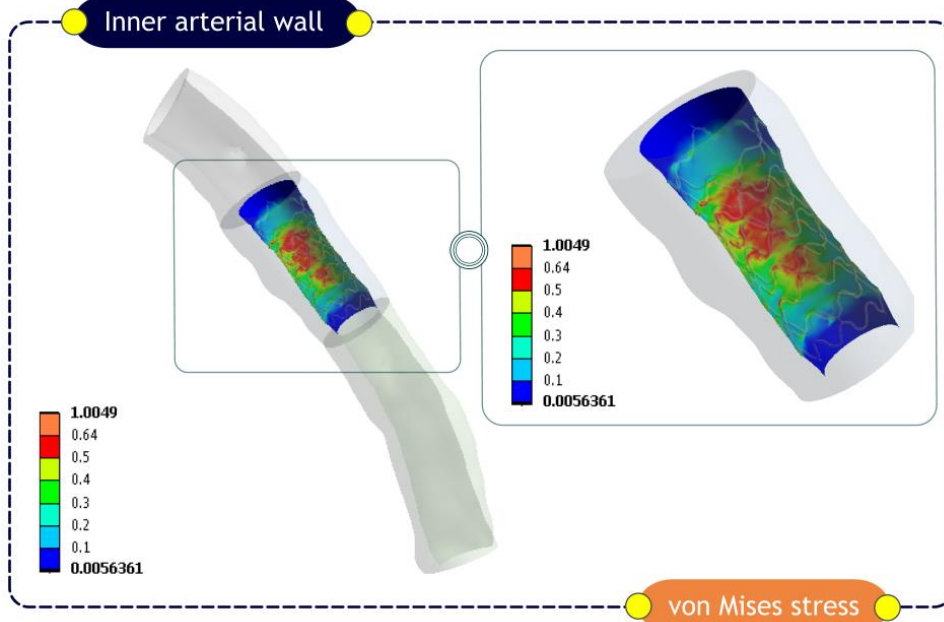


Figure 50: Von Mises stress (MPa) distribution in the inner arterial wall for Model D.

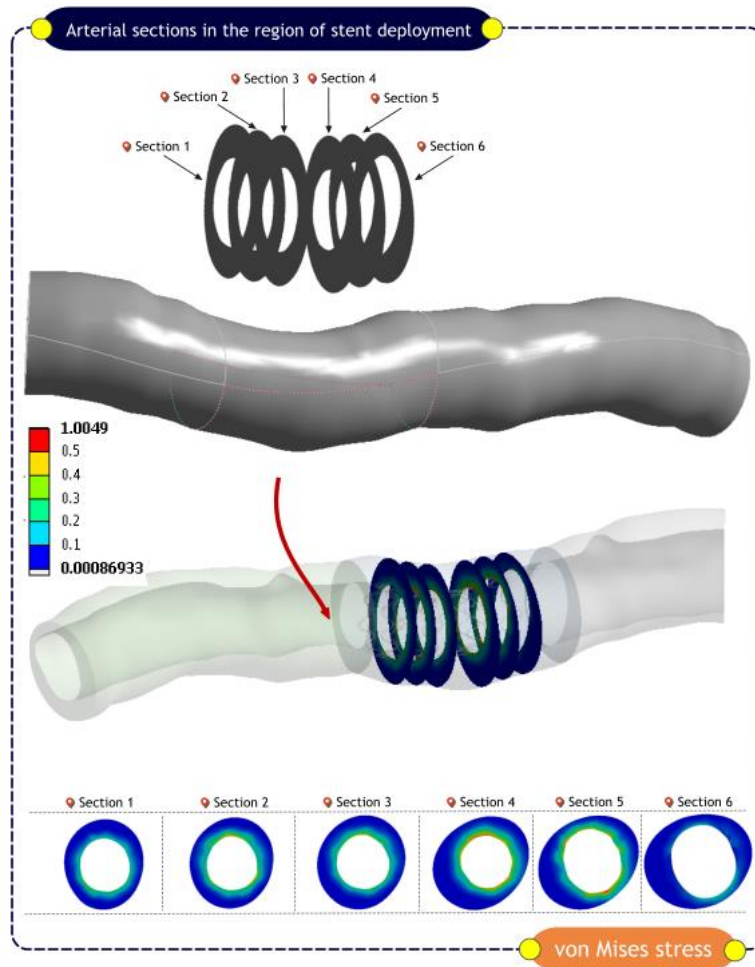


Figure 51: Von Mises stress (MPa) distribution in different cross sections along the area where the stent was deployed (Model D).

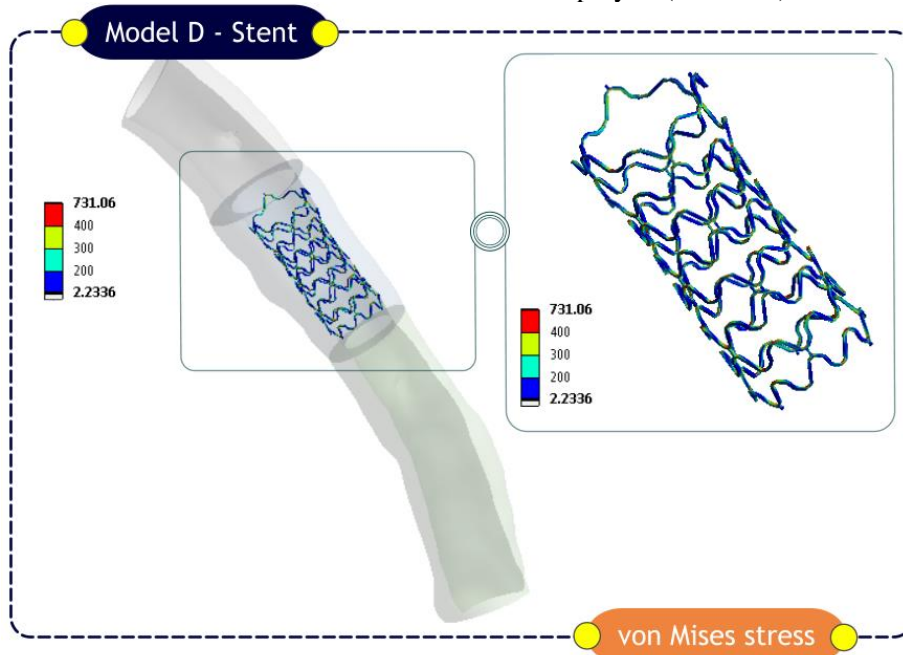


Figure 52: Von Mises stress (MPa) distribution for the stent (Model D) in the unloading phase.

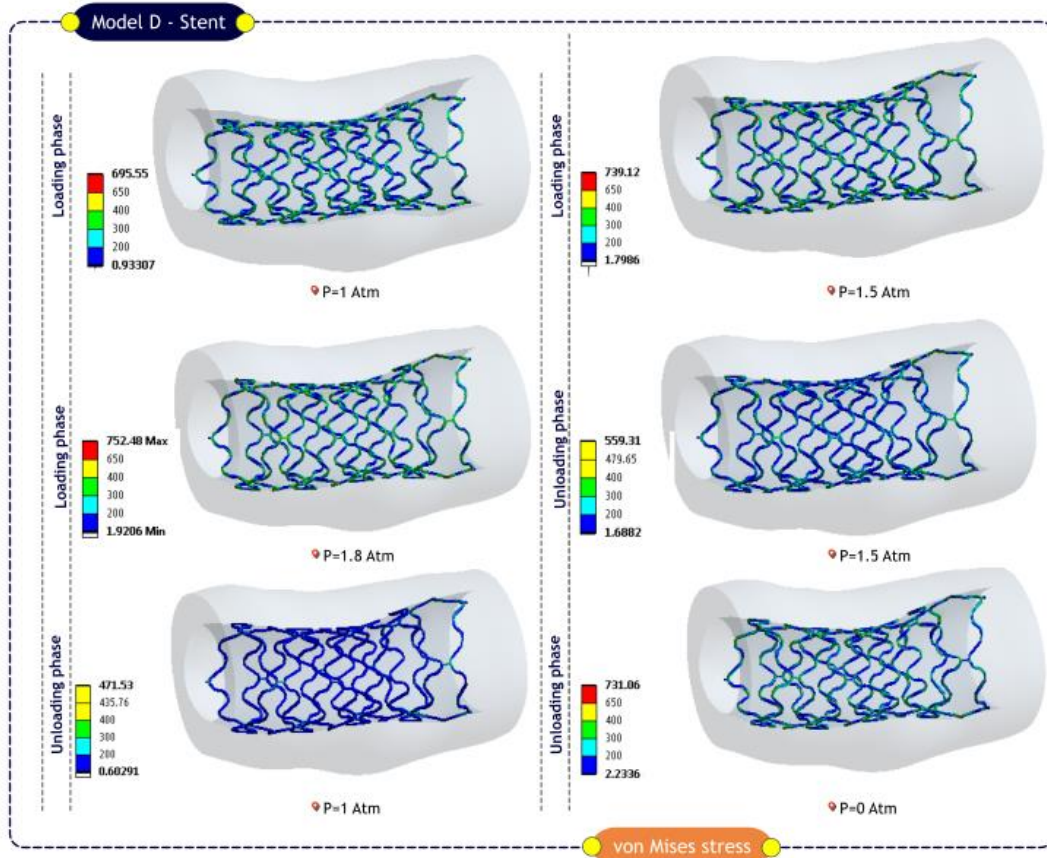


Figure 53: Von Mises stress (MPa) distribution for the stent (Model D) from the loading till the unloading phase.

Figure 54 shows the stress distribution for the stent and the artery under the inflation pressure of 1.8MPa. It is observed that the percentage of stent volume is approximately: (i) 57% for the stress range 0-200MPa, (ii) 31% for the stress range 200-400MPa and, (iii) 12% for the stress range over 400MPa. Similarly, the arterial stress is approximately: (i) 52.2% for the stress range 0-0.15MPa, (ii) 16.9% for the stress range 0.15-0.30MPa, (iii) and 30.9 for the range over 0.3MPa.

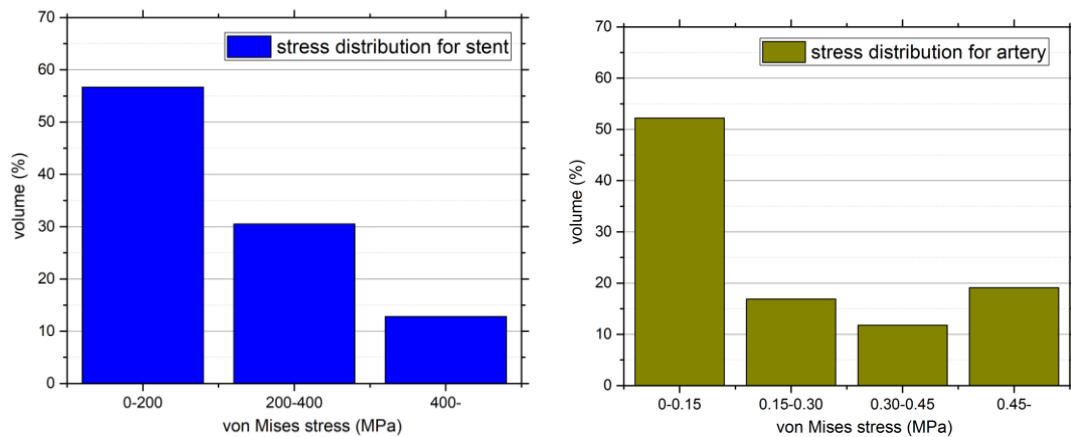


Figure 54: Von Mises stress percentage volume distribution for stent and artery of Model D (P=1.8 MPa).

Figure 55 shows the stress distribution for the stent and the artery under the deflation phase ($P=0$). It is observed that the percentage of stent volume is approximately: (i) 62.5% for the stress range 0-200MPa, (ii) 30.5% for the stress range 200-400MPa and, (iii) 7% for the stress range over 400MPa. Similarly, the arterial stress is approximately: (i) 63.8% for the stress range 0-0.15MPa, (ii) 20.9% for the stress range 0.15-0.30MPa, (iii) and in total 15.3% for the range over 0.3MPa.

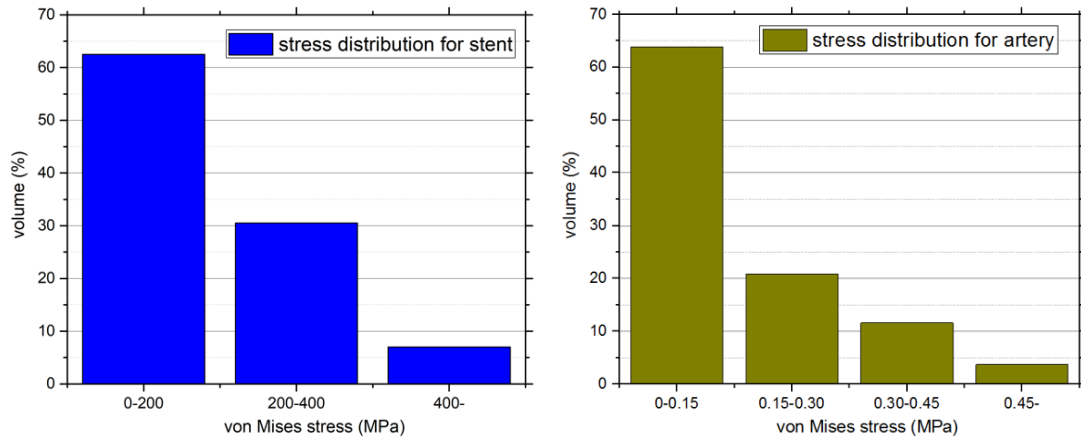


Figure 55: Von Mises stress percentage volume distribution for stent and artery of Model D ($P=0$ MPa).

To better understand the mechanical performance of the stent, the expanded radius against the expanding pressure was evaluated, for node 2 of the central stent cross section (Figure 56). We observe that the rate of increment of the stent radius is not proportional to the inflation pressure. The stent radius increased slowly at inflations pressure lower than 0.5MPa ($t=5$) and far more rapidly and significantly thereafter - plateauing at 0.6932mm at $P=1$ MPa ($t=18$). The maximum radius achieved for the central node of Model A is 0.6932mm, whereas the final radius achieved for the node 2 is 0.58842mm.

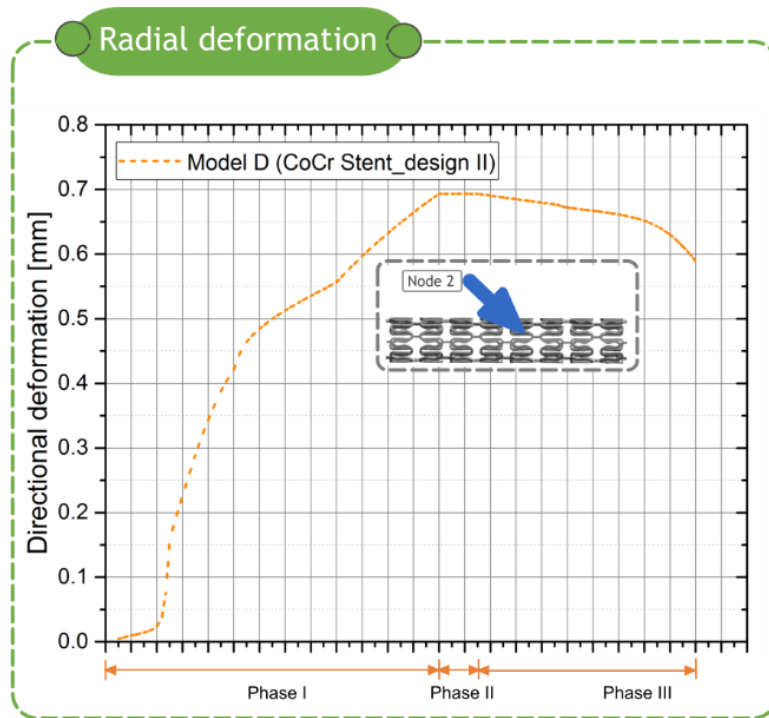


Figure 56: Plot of pressure vs radial deformation for node 2 (node existing in the stent middle cross-section) for stent (Model D).

6.6.2 Results of Model E

In this section, the results for Model E are presented. More specifically, in Figure 57 and Figure 58 the von Mises stresses in the inner and the outer wall are depicted. In general, as expected the area where the stent expands suffers from high stresses. It is observed that higher stresses occur in the intimal arterial area where the severity of the plaque was greatest. Specifically, the maximum von Mises in the inner arterial wall stress is approximately 0.91MPa. Regarding the outer arterial wall, the stress distribution and the stress concentration is less, reaching a maximum stress of approximately 0.18MPa. In addition, stress peaks can be locally observed behind the stent struts.

To evaluate the effect of stent deployment along the arterial segment, six (6) different cross sections were created (Figure 59). Specifically, these cross sections were perpendicular to the stent longitudinal axis, starting from the one end till the other. Generally, the stress decreases when moving from the lumen to the outer wall from all cross sections. It is observed that the highest stress occurs in section 4, followed by section 3.

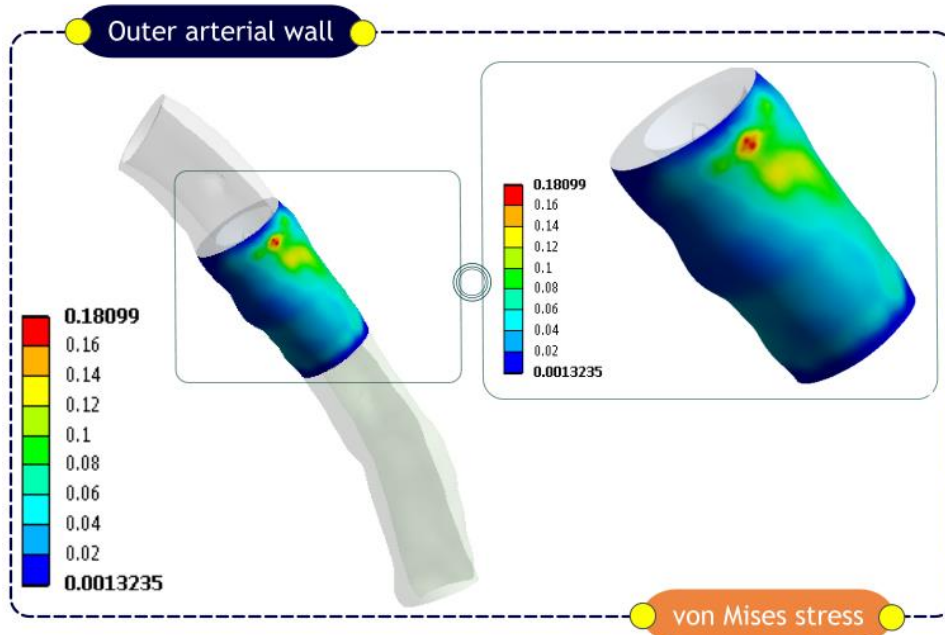


Figure 57: Von Mises stress (MPa) distribution in the outer arterial wall for Model E.

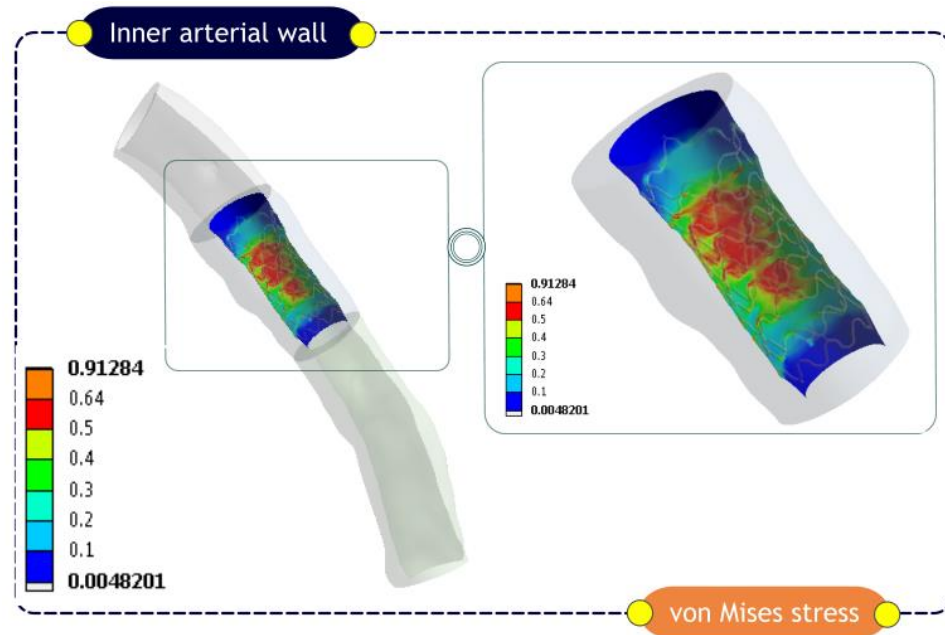


Figure 58: Von Mises stress (MPa) distribution in the inner arterial wall for Model E.

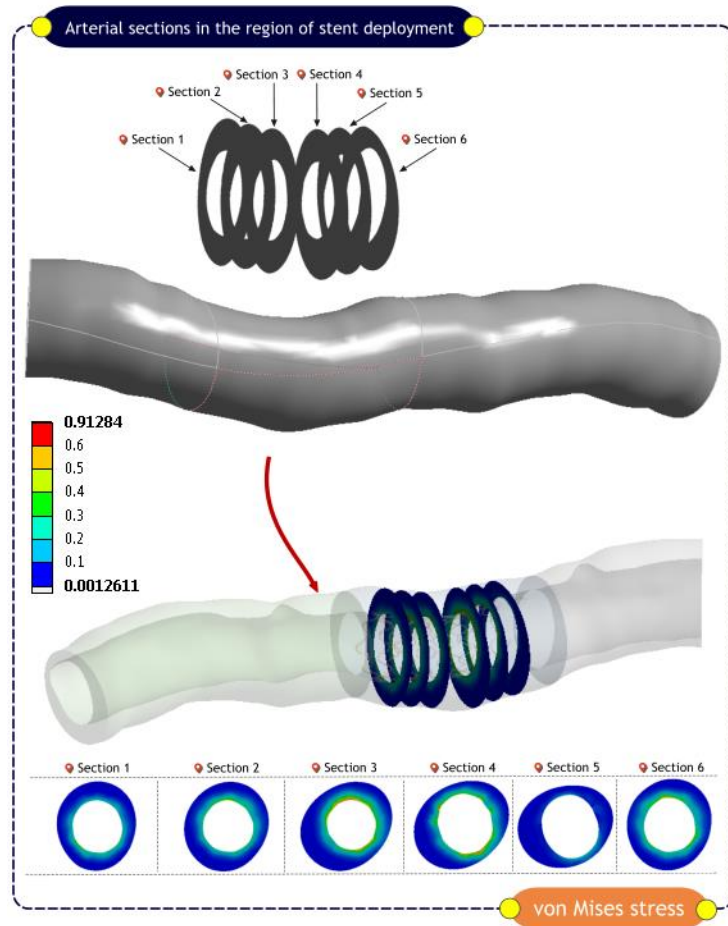


Figure 59: Von Mises stress (MPa) distribution in different cross sections along the area where the stent was deployed (Model E).

The stresses in the stent struts of Model E are shown in Figure 60. As expected, the stent expansion is affected by the degree of stenosis and does not follow a uniform expansion. Again the ends of the stent are expanded more than the middle stent area. In general, highest stresses are observed near the connection of the stent struts with a peak of approximately 729MPa.

To assess how the inflation pressure affects the developing in the stent stresses, the distribution in six different inflation phases were analysed (Figure 61): (i) Inflation phase – $P=1\text{MPa}$, $P=1.5\text{MPa}$ and $P=1.8\text{MPa}$, (ii) Deflation phase - $P=1.5\text{MPa}$, $P=1\text{MPa}$ and $P=0\text{MPa}$. In the inflation phase, the stent stress has a stress of 686MPa ($P=1\text{MPa}$), which is increased to 738MPa ($P=1.5\text{MPa}$), reaching a maximum stress of 752MPa for $P=1.8\text{MPa}$. On the contrary, when the inflation pressure is decreased the stent stress decreases as well and reaches a value of 475MPa ($P=1\text{MPa}$). However, when the pressure is totally removed from the inner stent surface the von Mises stress increases and reaches the value of 729MPa.

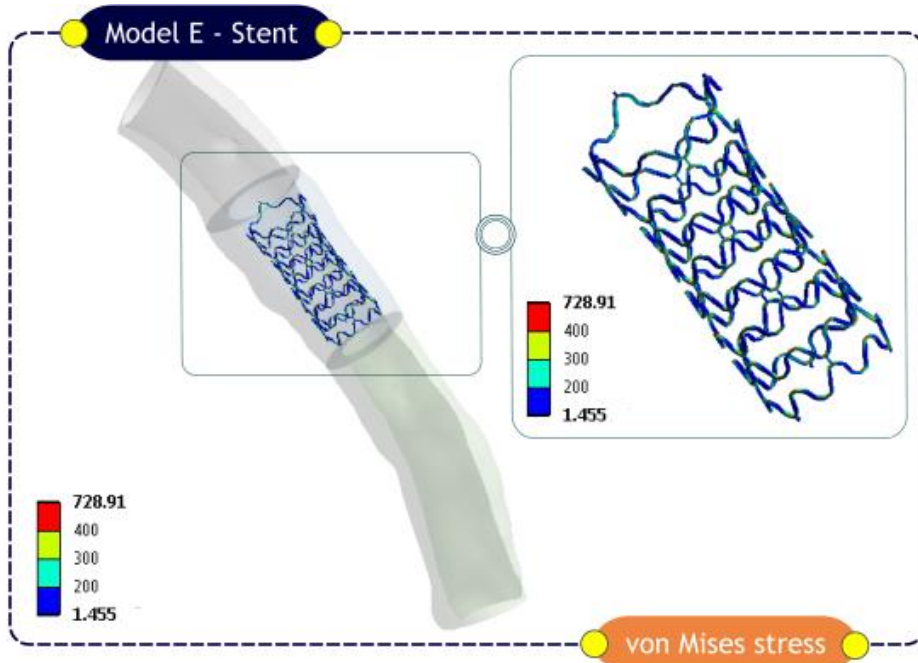


Figure 60: Von Mises stress (MPa) distribution for the stent (Model E) in the unloading phase.

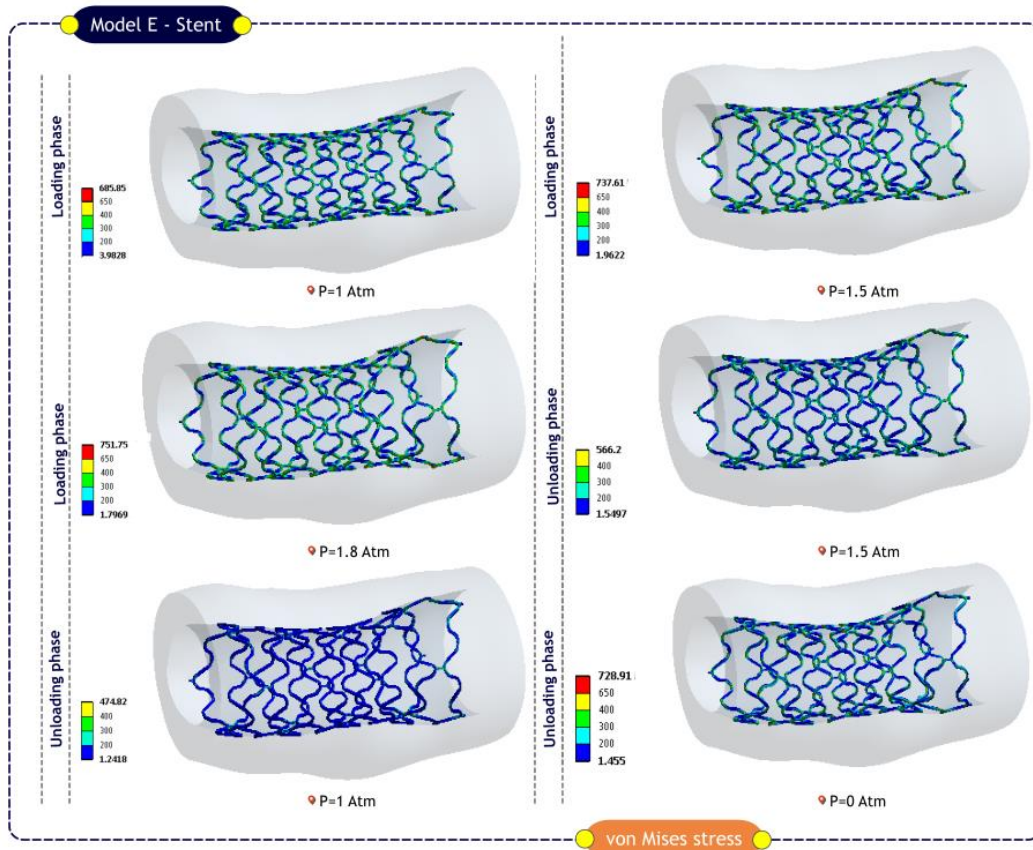


Figure 61: Von Mises stress (MPa) distribution for the stent (Model E) from the loading till the unloading phase.

Figure 62 shows the stress distribution for the stent and the artery under the inflation pressure of 1.8MPa. It is observed that the percentage of stent volume is approximately:

(i) 56.4% for the stress range 0-200MPa, (ii) 31% for the stress range 200-400MPa and, (iii) 12.6% for the stress range over 400MPa. Similarly, the arterial stress is approximately: (i) 55% for the stress range 0-0.15MPa, (ii) 16.9% for the stress range 0.15-0.30MPa, (iii) and 28.1% for the stress range over 0.3MPa.

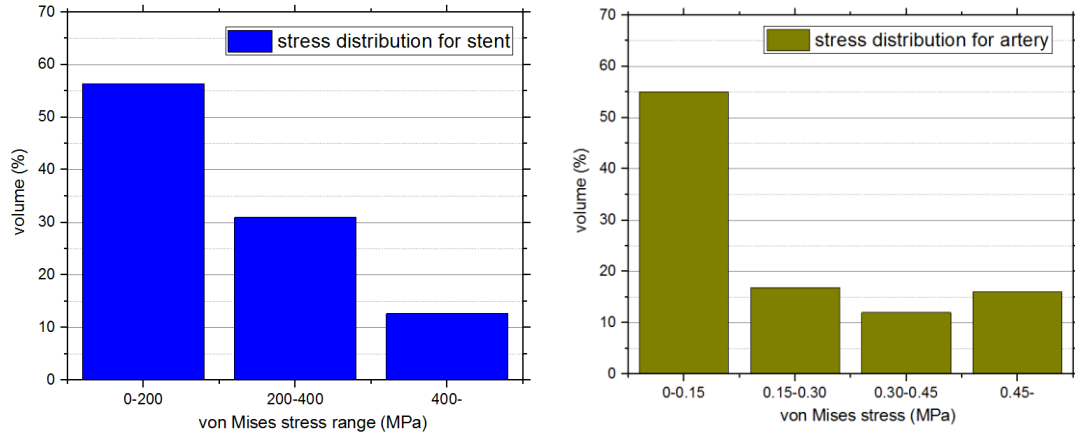


Figure 62: Von Mises stress percentage volume distribution for stent and artery of Model E (P=1.8 MPa).

Figure 63 shows the stress distribution for the stent and the artery under the inflation pressure of 1.8MPa. It is observed that the percentage of stent volume is approximately: (i) 71.28% for the stress range 0-200MPa, (ii) 23.08% for the stress range 200-400MPa and, (iii) 5.63% for the stress range over 400MPa. Similarly, the arterial stress is approximately: (i) 63.94% for the stress range 0-0.15MPa, (ii) 19.76% for the stress range 0.15-0.30MPa, (iii) and 16.29% for the stress range over 0.3MPa.

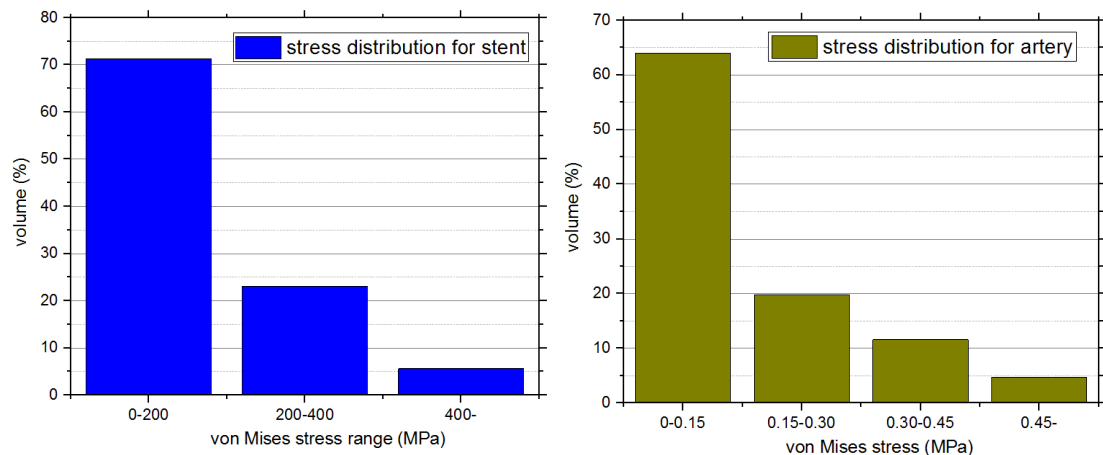


Figure 63: Von Mises stress percentage volume distribution for stent and artery of Model E (P=0 MPa).

To better understand the mechanical performance of the stent, the expanded radius against the expanding pressure was evaluated, for node 2 of the central stent cross

section (Figure 64). We observe that the rate of increment of the stent radius is not proportional to the inflation pressure.

The stent radius increased slowly at inflations pressure lower than 0.5MPa (t=5) and far more rapidly and significantly thereafter - plateauing at 0.67916mm at P=1MPa (t=18). The maximum radius achieved for the central node of Model A is 0.67916mm, whereas the final radius achieved for the node 2 is 0.60122mm.

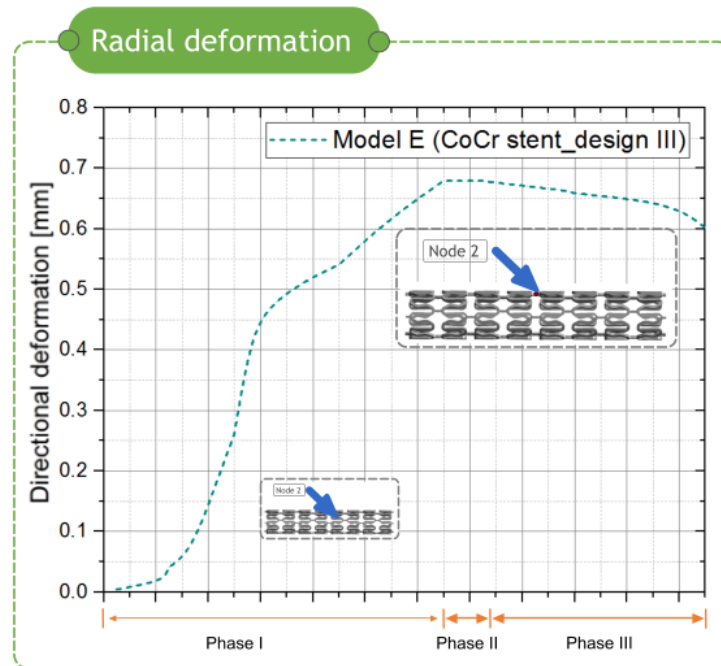


Figure 64: Plot of pressure vs radial deformation for node 2 (node existing in the stent middle cross-section) for stent (Model E).

Chapter 7: Discussion and Conclusions

7.1 Discussion of results

7.1 Discussion of results

Computational modeling has been widely used to evaluate the biomechanical performance of stents by modelling their deployment inside diseased arteries. Chua *et al.* [4] modeled the expansion of a Palmaz-Schatz stent in an artery, which included a stenotic plaque. The analysis showed the resistance ability of slotted-tube stents in the vessel recoil, preventing restenosis post expansion. Zahedmanesh *et al.* [23] used an ACS Multi-Link RX DUET stent for the deployment in a stenotic artery reconstructed based on the 3D angiography of a human coronary artery. They demonstrated that the application of pressure directly on the inner stent surface could be used as an alternative modelling strategy, in case of complex arteries. Pericevic *et al.* [196] investigated the influence of the composition of the atherosclerotic plaque (i.e., hypocellular, hypocellular and calcified). Their analysis revealed that calcified plaques are affected less in terms of stress loading and have higher resistance to expansion compared to other plaque types. Lally *et al.* [19] compared the deployment performance of two stents (i.e. S7 and NIR stents) in a stenotic artery. Tambaca *et al.* [240] examined the behaviour of different stent designs in terms of uniform compression and bending. They showed that the recent stent designs (i.e. Xience) had good radial stiffness and flexibility in bending. Gu *et al.* [241] focused on the effect of silicone coating during stent deployment and showed that the coated stent required an 30% higher pressure to expand the artery compared with the BMS. Following this, Hopkins *et al.* [180] examined the delamination of the stent coating and demonstrated that the coating thickness, the coating material and the curvature of the hinge affected the initiation of coating debonding process.

Currently, there is a lack of modelling approaches of the stent deployment process in reconstructed arterial segments, focusing on the effects of stent materials and designs. There is an ample room for understanding how the stent and the arterial stress are influenced by different stent designs and materials. In this study, a FEA has been carried out to simulate stent deployment for three representative stent materials (Model A, Model B and Model C) and three representative stent designs (Model D and Model E). Comparisons have been approached to assess the effects of design and material on stent expansion, stress distribution and occurred arterial stresses during the deployment process, inside a reconstructed diseased arterial segment.

7.1.1 Comparative analysis of stent material

In Figure 65 and Figure 66, the inner and outer arterial von Mises stresses are depicted for Model A, Model B and Model C. The results show that the stent of Model A exhibits higher arterial stresses (0.65MPa) in the arterial wall followed by Model B and Model C (0.62MPa, both). For all models, stent expansion affects the inner arterial layer but the percentage of the high arterial stress is differentiated. More specifically, Model A is highly affected whereas both Model B and Model C seem to be less affected. As far as the outer arterial wall is concerned the occurred stresses are higher for Model B (0.20MPa) and Model C (0.20MPa) and lower for Model A (0.17MPa).

As far as the distribution of the arterial stress in different stress ranges is concerned, it is demonstrated that: (i) the percentage of arterial stress in the stress range of 0-0.15MPa is higher for the arterial wall of Model B (84%) followed by Model A (83.35%) and Model C (83.10%), (ii) the percentage of arterial stress in the stress range of 0.15-0.30MPa is slightly higher for the arterial wall of Model C (13.3%) followed by Model A (13.01%) and Model B (13%), (iii) the percentage of arterial stress in the stress range over 0.3 is higher for Model A (3.64%) followed by Model C (3.6%) and Model B (3%) (Figure 67).

The stents of the three Models during the inflation and deflation phase are depicted in Figure 68. More specifically: (i) all stent models follow the same deformation pattern, (ii) for all pressures, in the stent of Model A higher von Mises stresses occur, (iii) the stent of Model B is the one in which lower von Mises stresses occur.

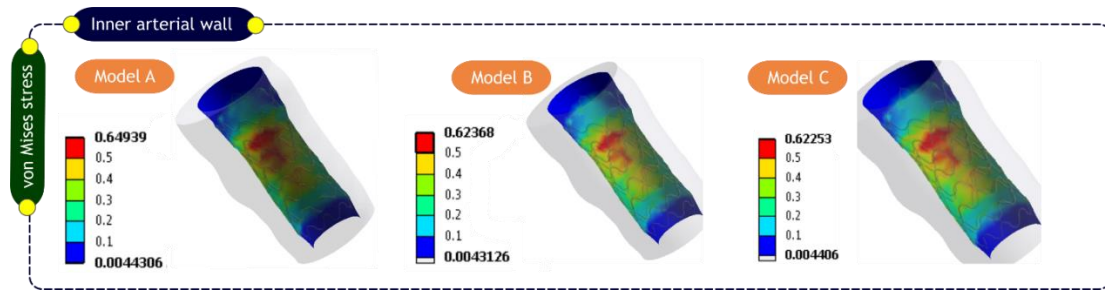


Figure 65: Von Mises stress (MPa) distribution in the inner arterial wall for Model A, Model B and Model C.

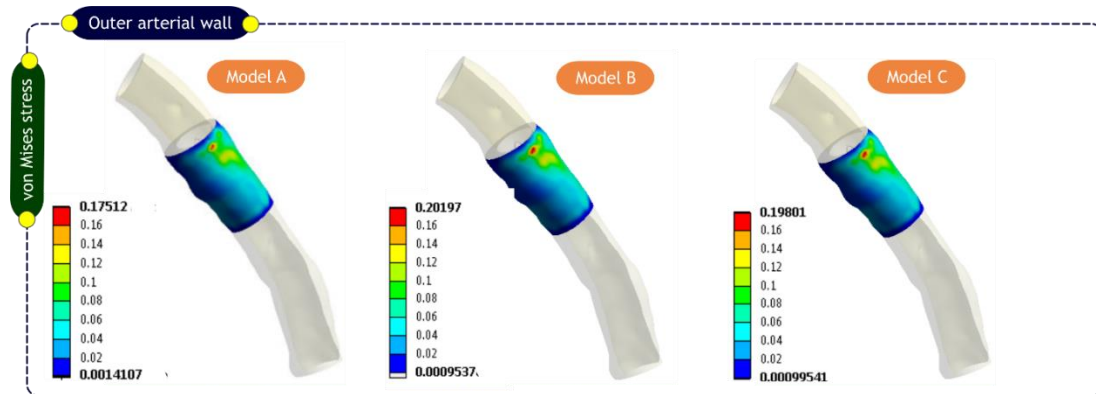


Figure 66: Von Mises stress (MPa) distribution in the outer arterial wall for Model A, Model B and Model C.

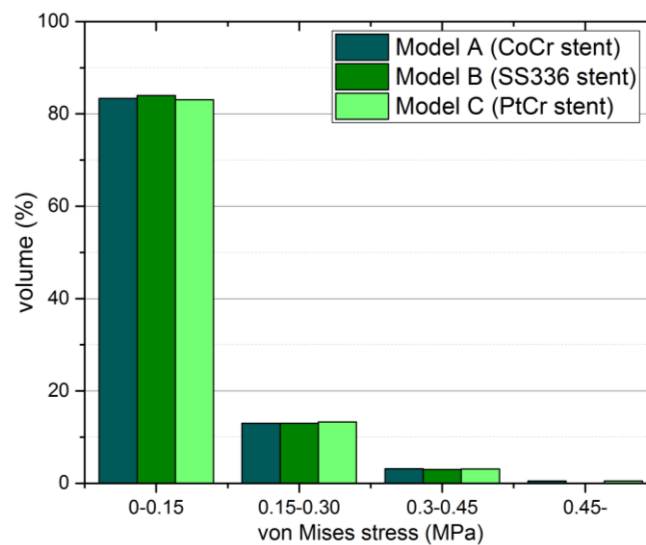


Figure 67: Von Mises stress percentage volume distribution for the artery (Model A, Model B, Model C) ($P= 0$ MPa, deflation phase).

In addition, as observed in Figure 69: (i) the percentage of the von Mises stress for the stent of Model B in the stress range of 0-200MPa is higher (75.03%) compared to Model C (74.59%) and Model A (73.98%), (ii) the percentage of the von Mises stress for the stent of Model C in the stress range of 200-400MPa is higher (21.21%) followed by Model B (21.12%) and Model A (20.83%), (iii) the percentage of the von Mises stress

the stent of Model A in the stress range over 400MPa is higher (5.19%) compared to Model B (3.85%) and Model C (4.2%).

In Figure 70, the expanded radius against the expanding pressure is plotted, for node 2 of the central stent cross section for all models. It is observed that all models follow the same pattern; (i) the radius is initially increasing slowly in Phase I followed by a sudden increase till Phase II, where the stents reach the maximum radius, (ii) during Phase II, where the inflation pressure is retained, the stent radius is plateauing, (iii) during Phase III, the stent radius continuous to slightly decrease for all models. In general, the node of the middle cross section of the stent of Model A stent is reaching a smaller radius diameter compared to the nodes of the stents of the other two models; this observation is applied for all phases (Phase I, Phase II, Phase III).

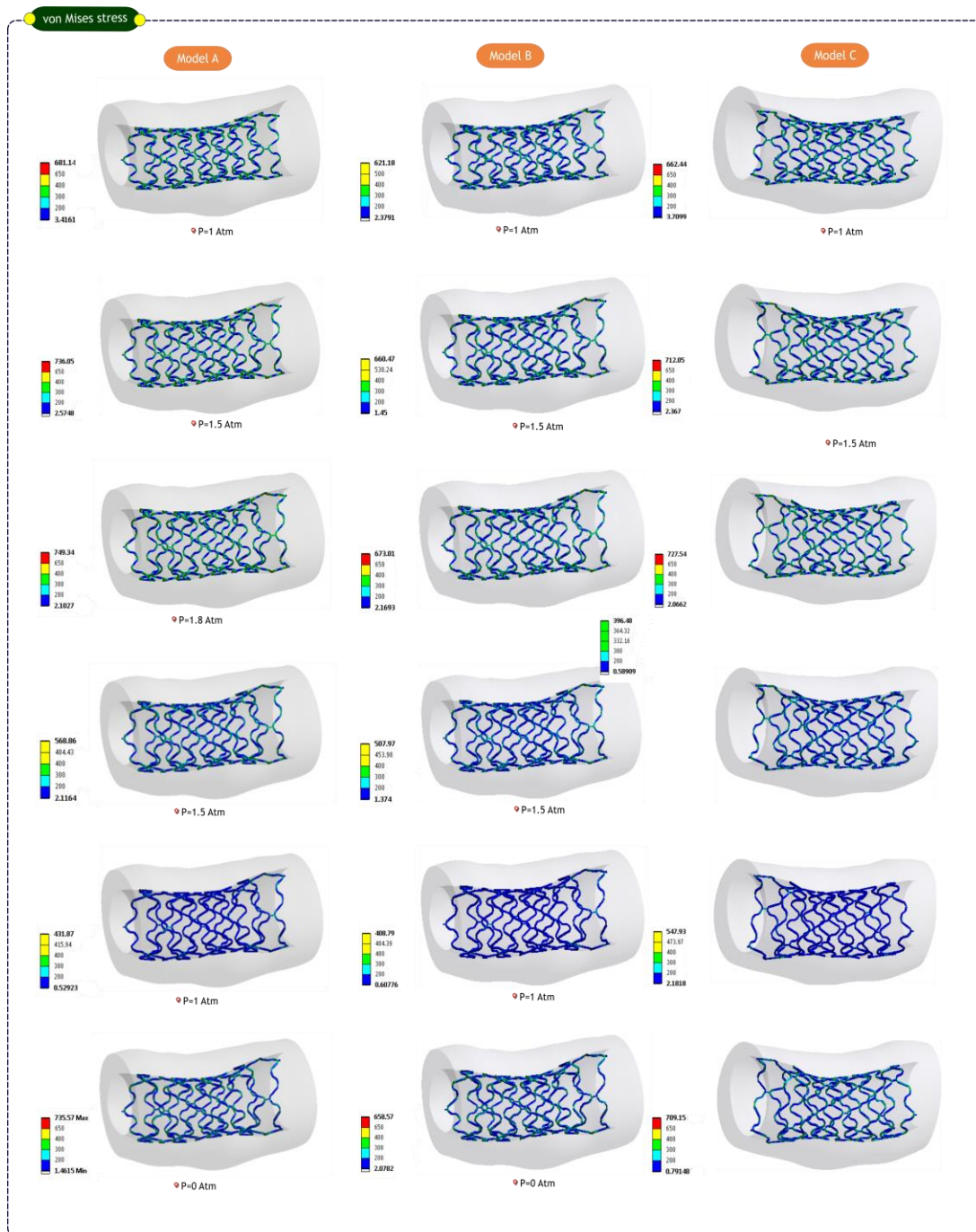


Figure 68: Von Mises stress (MPa) distribution for the stent from the loading till the unloading phase (Model A, Model B, Model C).

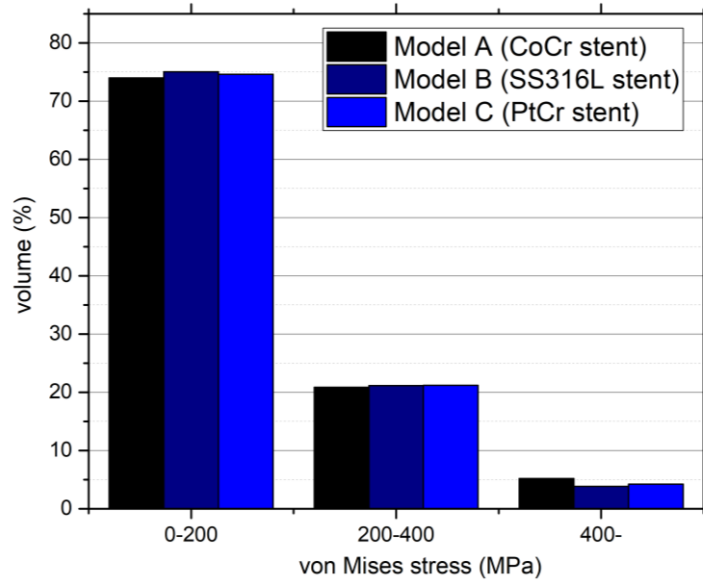


Figure 69: Von Mises stress percentage volume distribution for the stent (Model A, Model B, Model C) (P= 0 MPa, deflation phase).

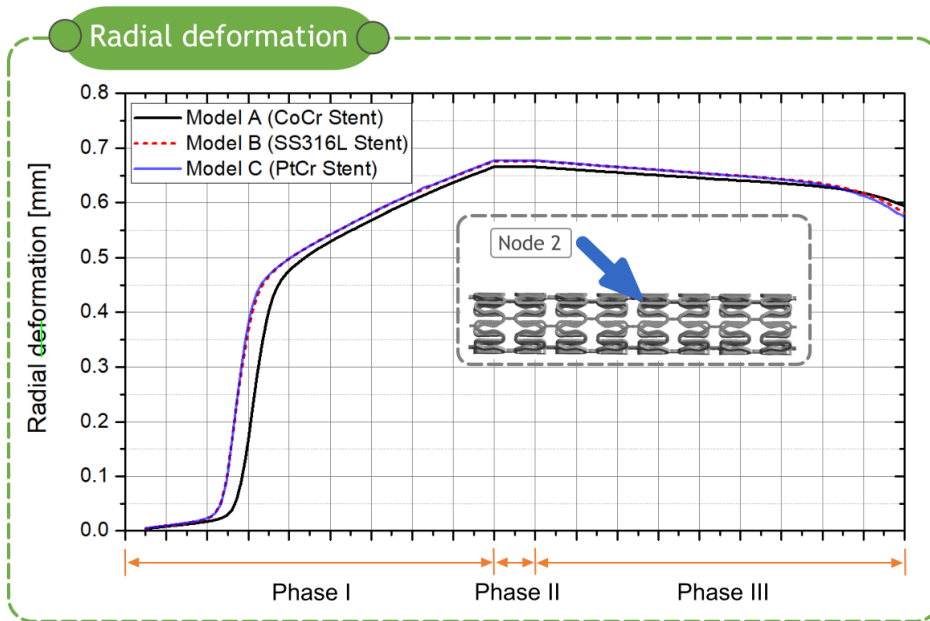


Figure 70: Plot of pressure vs radial deformation for node 2 (node existing in the stent middle cross-section) for stent (Model A, Model B, Model C).

7.1.2 Comparative analysis of stent design

In the previous sections, we have performed a qualitative and quantitative analysis for three stent designs. In the current chapter, we investigate and compare the key parameters of interest for Model D (Model_thin) and Model E (Model_thick), which have been designed with a strut thickness of 0.0702mm and 0.0774mm respectively

In Figure 71, the Principal stresses for the inner arterial wall are depicted for Model_thin and Model_thick in different views. Higher arterial stresses are located behind the region where the stent was expanded and more specifically in the region of stenosis. The slightly highest stresses in the arterial wall are observed for Model_thick compared to Model_thin. However, from the different views, it is evident that the areas of the inner arterial wall are affected from higher stresses more in the model with the thick struts. A quantitative analysis of this observation is supported by Figure 72.

It is demonstrated that: (i) the percentage of arterial principal stress in the stress range of 0-0.3 MPa is higher for Model D (67.5%) compared to Model E (66.5%), whereas the percentage of arterial principal stress in the stress range over 0.3MPa is higher for Model E with the thicker struts compared to Model D with the thinner struts. This is also in alignment with the results of the von Mises stress (Figure 73).

The stents of the two different Models during the inflation and deflation phase are depicted in Figure 74. More specifically all stent models follow the same deformation pattern, while for all pressures, in Model D (thin struts) higher von Mises stresses occur compared to Model E (thick struts).

Regarding the percentage volume of each stent model belonging to different stress ranges, as shown in Figure 75; (i) 62.5% percentage of the total von Mises stress belongs to the stress range of 0-200MPa for D and 71.28% for Model E respectively, (ii) the highest percentage in the stress range over 200MPa belongs to Model D (37.5%).

The expanded radius against the elevation of the stent pressure is presented for node 2 of the central stent cross section for Model D and Model E (Figure 76). Both models show a similar expansion performance: (i) the radius is initially increasing slowly in Phase I followed by a sudden increase till Phase II, where the stents reach the maximum radius, (ii) in all Phases (I, II and III), Model D seems to reach more quickly a radius increase compared to Model E (iii) during the deflation phase (Phase III), when the

pressure is permanently removed ($P=0$) the final radius increase is slightly higher for Model E.

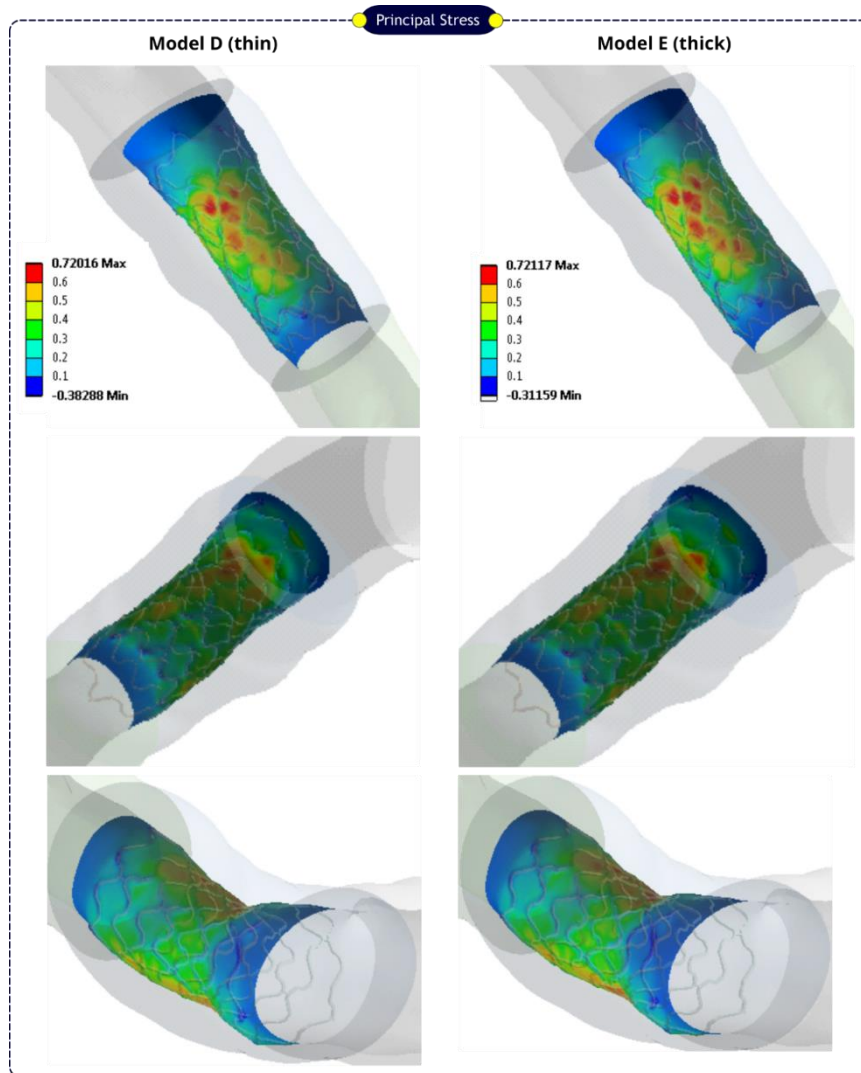


Figure 71: Principal stress in the inner arterial wall in the region of stent deployment.

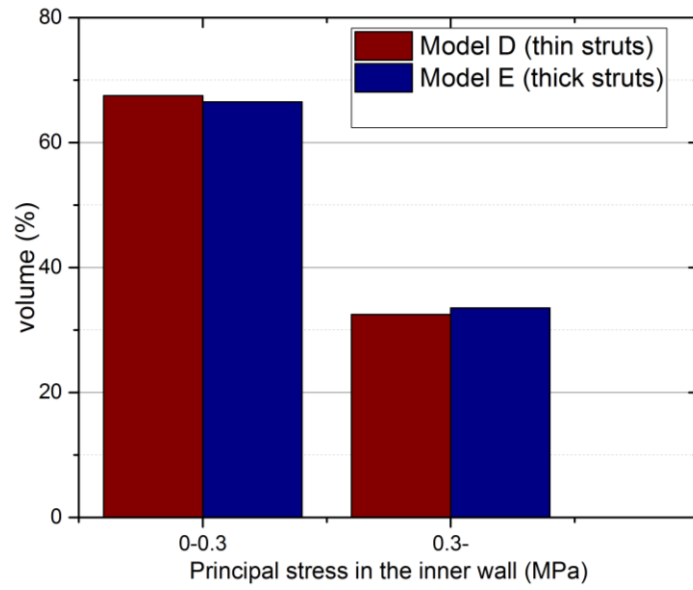


Figure 72: Principal stress percentage volume distribution for the artery (Model D, Model E) (P= 0 MPa, deflation phase).

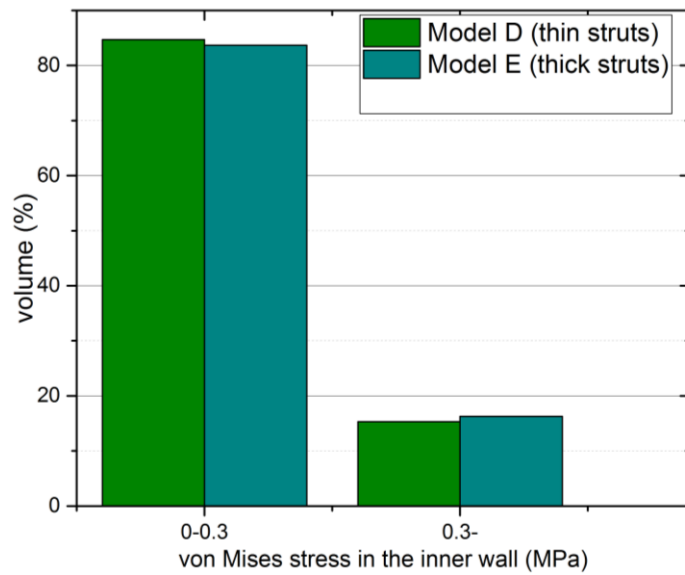


Figure 73: Von Mises stress percentage volume distribution for the artery (Model D, Model E) (P= 0 MPa, deflation phase).

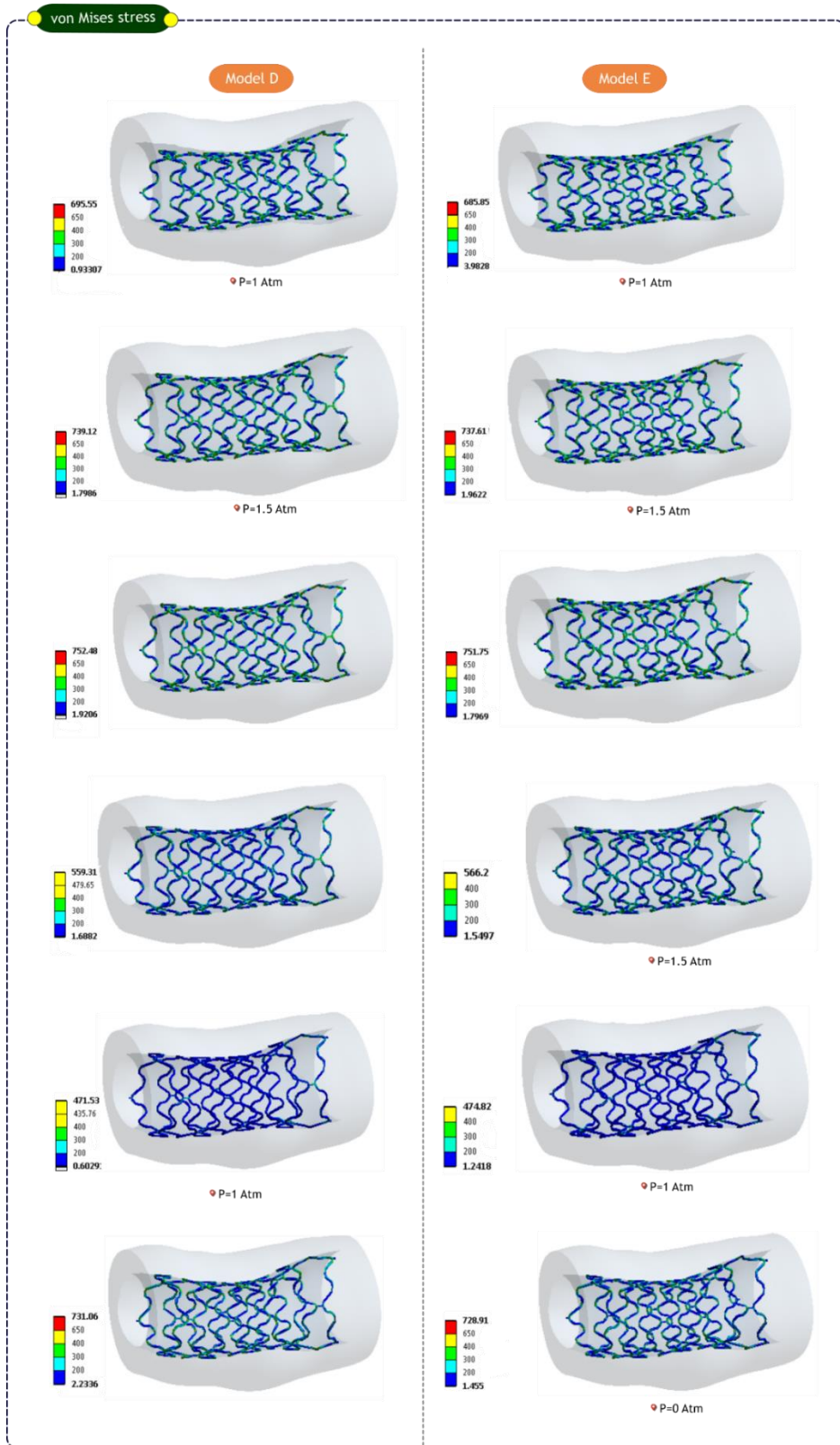


Figure 74: Von Mises stress (MPa) distribution for the stent from the loading till the unloading phase (Model D, Model E).

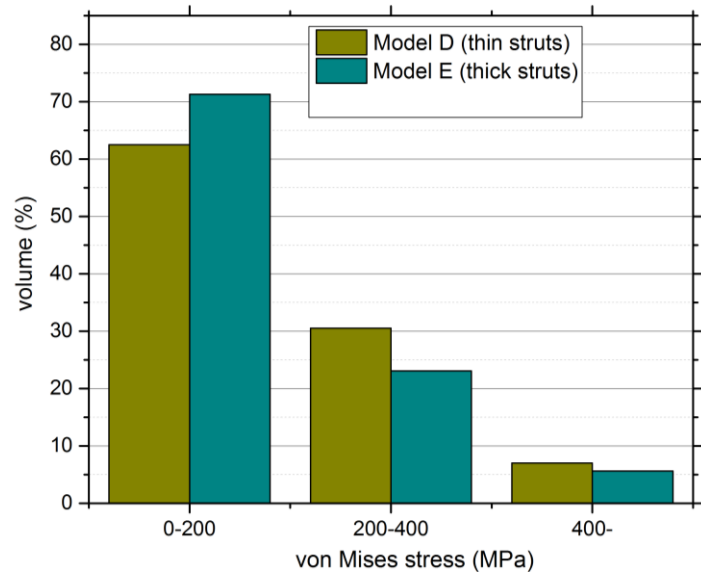


Figure 75: Von Mises stress percentage volume distribution for the stent (Model D, Model E) (P= 0 MPa, deflation phase).

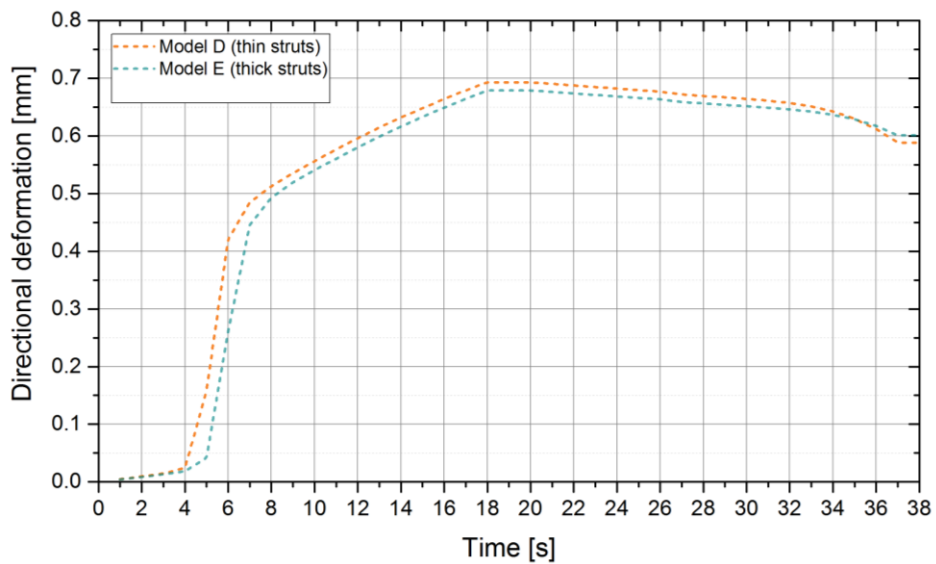


Figure 76: Plot of pressure vs radial deformation for node 2 (node existing in the stent middle cross-section) for stent (Model D, Model E).

Chapter 8: Limitations and future work

The accuracy and reliability of the results from a FE study are highly related with inputs, such as the geometry and the boundary conditions for representing adequately the problem, and the materials models used and material properties assigned to each component. Generally, stent deployment involves the interaction between a balloon, stent and atherosclerotic coronary artery. The modelling of this process through FEA could be considered as a complicated and challenging study. To completely replicate the problem, the interaction between the balloon and stent, and the stent and atherosclerotic artery should be taken into account.

The simulation of the stent expansion and the investigation of the effect of stent material and stent design presented in this study has several important features. One of the strong points is the geometrical representation of the stents and the artery. The geometric measurements of the stents were not extrapolated from a handbook of coronary stents [89], as in other similar studies. Instead, the stents were accurately described using stent dimensions obtained from the manufacturer (Rontis Corporation S.A., Zug, Switzerland). The realistic geometry of the arterial morphology and both the quantitative and qualitative evaluation of the numerical results make it a model of significant importance. In addition, even if this study targets on examining the role of stent strut thickness and materials in the generating stresses in the stented vessel and one could say that the absolute magnitude of these stresses is not the primary concern, rather the difference in the stresses generated by different stents, the reconstruction of the arterial wall and not the idealized representation of the stenotic vessel geometry represents is an asset.

However, we must recognize certain limitations in the proposed approach. An initial assumption is related to the soft tissue and the material models used. The arterial wall was represented by a Mooney-Rivlin model. Instead, ideally an anisotropic viscoelastic model could be used since this model includes the hysteresis exhibited by the arterial tissue and the anisotropy observed in the composition of the arterial wall. Another assumption is the absence of the atherosclerotic plaque component in the arterial wall. Moreover, the calcification of vulnerable plaque that harden fibrous cap layer is ignored. In addition, the soft tissue was modelled as rate independent although these tissues are most likely rate dependent and viscoelastic. One more limitation of this work

is the lack of direct experimental validation of the computational results created here. This can be mainly attributed to the difficulty in setting up sufficiently appropriate and accurate experiments. However, in the future, through the utilization of synthetic materials (eg. silicone to represent the arterial wall and gels with a range of stiffness's to represent the atherosclerotic plaque), useful experimental representations of the test-bed could be generated that would assist in validation purposes.

This study did not also include the influence of the balloon in stent expansion. The inclusion of a balloon in the stent expansion could result in a more uniform stent's structure. However, it is believed that the material of the balloon contributes largely to the uniformity of stent's expansion. Future work could investigate and assess the influence of different balloon types on the stent expansion characteristics.

Coronary stents are positioned in coronary arteries and due to the pulsatile blood the stented vessel is subjected to a dynamic pressure environment after stent implantation. The blood flow inside the arterial lumen creates a shear stress on the wall of the arteries that change upon stent implantation. In turn, stented vessels exhibit a biological response to changes in shear stresses, however the examination of fluid flow dynamics are beyond the scope of this study. In addition, since one of the most important risks, after stenting, of the artery is thrombosis, which is mainly affected by the local hemodynamics, the modelling of blood flow post-implantation could identify stent designs with the lowest risk of thrombosis.

The mesh of the stent structure could be another limitation of this study. A higher order element and finer mesh density could increase the accuracy of the magnitude of expansion and stresses found in the arterial and stent structure. However, the use of a higher order element and a finer mesh density would consequently result in the increase of the computational time and resources needed.

The assessment of the stent geometry conducted in this study considers only the radial deformation and the stresses under the expanded configuration. These are important aspects in choosing an appropriate stent type to be deployed in the treatment. Another important aspect is the stent flexibility. The flexibility of a stent could be achieved by reducing the number of bridges and using a helical arrangement of the connecting links. As a side effect, a more flexible stent may also have a greater susceptibility to deformations under specific force is applied in its longitudinal axis [14]. Therefore,

future studies could examine and identify the minimum number of bridges/connecting links for achieving optimal flexibility.

9. References

- [1] F. Migliavacca, L. Petrini, M. Colombo, F. Auricchio, and R. Pietrabissa, "Mechanical behavior of coronary stents investigated through the finite element method," *Journal of Biomechanics*, vol. 35, no. 6, pp. 803–811, 2002.
- [2] N. Li, H. Zhang, and H. Ouyang, "Shape optimization of coronary artery stent based on a parametric model," *Finite Elements in Analysis and Design*, vol. 45, no. 6–7, pp. 468–475, 2009.
- [3] S. N. D. Chua, B. J. Mac Donald, and M. S. J. Hashmi, "Finite-element simulation of stent expansion," *Journal of Materials Processing Technology*, vol. 120, no. 1–3, pp. 335–340, 2002.
- [4] S. N. David Chua, B. J. MacDonald, and M. S. J. Hashmi, "Effects of varying slotted tube (stent) geometry on its expansion behaviour using finite element method," *Journal of Materials Processing Technology*, vol. 155–156, pp. 1764–1771, 2004.
- [5] S. Lee, C. W. Lee, and C.-S. Kim, "FEA Study on the Stress Distributions in the Polymer Coatings of Cardiovascular Drug-Eluting Stent Medical Devices," *Ann Biomed Eng*, Jun. 2014.
- [6] S. N. David Chua, B. J. MacDonald, and M. S. J. Hashmi, "Finite element simulation of slotted tube (stent) with the presence of plaque and artery by balloon expansion," *Journal of Materials Processing Technology*, vol. 155–156, pp. 1772–1779, Nov. 2004.
- [7] W. Wu, W.-Q. Wang, D.-Z. Yang, and M. Qi, "Stent expansion in curved vessel and their interactions: a finite element analysis," *J Biomech*, vol. 40, no. 11, pp. 2580–2585, 2007.
- [8] C. M. Agrawal, K. F. Haas, D. A. Leopold, and H. G. Clark, "Evaluation of poly(L-lactic acid) as a material for intravascular polymeric stents," *Biomaterials*, vol. 13, no. 3, pp. 176–182, 1992.
- [9] J.-P. Nuutinen, C. Clerc, R. Reinikainen, and P. Törmälä, "Mechanical properties and in vitro degradation of bioabsorbable self-expanding braided stents," *J Biomater Sci Polym Ed*, vol. 14, no. 3, pp. 255–266, 2003.
- [10] A. Schiavone, L. G. Zhao, and A. A. Abdel-Wahab, "Dynamic simulation of stent deployment – effects of design, material and coating," *J. Phys.: Conf. Ser.*, vol. 451, no. 1, p. 012032, Jul. 2013.
- [11] C. Conway, F. Sharif, J. P. McGarry, and P. E. McHugh, "A Computational Test-Bed to Assess Coronary Stent Implantation Mechanics Using a Population-Specific Approach," *Cardiovasc Eng Tech*, vol. 3, no. 4, pp. 374–387, Dec. 2012.
- [12] A. García, E. Peña, and M. A. Martínez, "Influence of geometrical parameters on radial force during self-expanding stent deployment. Application for a variable radial stiffness stent," *J Mech Behav Biomed Mater*, vol. 10, pp. 166–175, Jun. 2012.
- [13] M. Azaouzi, A. Makradi, and S. Belouettar, "Numerical investigations of the structural behavior of a balloon expandable stent design using finite element method," *Computational Materials Science*, vol. 72, pp. 54–61, May 2013.
- [14] J. Bedoya, C. A. Meyer, L. H. Timmins, M. R. Moreno, and J. E. Moore, "Effects of stent design parameters on normal artery wall mechanics," *J Biomech Eng*, vol. 128, no. 5, pp. 757–765, Oct. 2006.
- [15] H. Zahedmanesh and C. Lally, "Determination of the influence of stent strut thickness using the finite element method: implications for vascular injury and in-stent restenosis," *Med Biol Eng Comput*, vol. 47, no. 4, pp. 385–393, Apr. 2009.
- [16] S. Xiang, Y. Hong, N. Zhonghua, and G. Xingzhong, "Optimization of coronary stent structure design for maximizing the anti-compression mechanical property," *Chin J Mech Eng*, 2008.
- [17] S. Pant, N. W. Bressloff, and G. Limbert, "Geometry parameterization and multidisciplinary constrained optimization of coronary stents," *Biomech Model Mechanobiol*, vol. 11, no. 1–2, pp. 61–82, Jan. 2012.

- [18] G. A. Holzapfel, M. Stadler, and T. C. Gasser, “Changes in the Mechanical Environment of Stenotic Arteries During Interaction With Stents: Computational Assessment of Parametric Stent Designs,” *J Biomech Eng*, vol. 127, no. 1, pp. 166–180, 2005.
- [19] C. Lally, F. Dolan, and P. J. Prendergast, “Cardiovascular stent design and vessel stresses: a finite element analysis,” *Journal of Biomechanics*, vol. 38, no. 8, pp. 1574–1581, 2005.
- [20] F. Migliavacca, L. Petrini, P. Massarotti, S. Schievano, F. Auricchio, and G. Dubini, “Stainless and shape memory alloy coronary stents: a computational study on the interaction with the vascular wall,” *Biomech Model Mechanobiol*, vol. 2, no. 4, pp. 205–217, Jun. 2004.
- [21] S. Tammareddi and Q. Li, “Effects of Material on the Deployment of Coronary Stents,” *Advanced Materials Research*, vol. 123–125, pp. 315–318, Aug. 2010.
- [22] F. Gijssen, “Simulation of stent deployment in a realistic human coronary artery.”
- [23] H. Zahedmanesh, D. John Kelly, and C. Lally, “Simulation of a balloon expandable stent in a realistic coronary artery-Determination of the optimum modelling strategy,” *J Biomech*, vol. 43, no. 11, pp. 2126–2132, Aug. 2010.
- [24] N. H. S. Choices, “UK heart disease and stroke death rates now lower than cancer - Health News - NHS Choices,” 15-Aug-2016. [Online]. Available: <http://www.nhs.uk/news/2016/08August/Pages/UK-heart-disease-and-stroke-death-rates-now-lower-than-cancer.aspx>. [Accessed: 01-Feb-2017].
- [25] G. Baltgaile, “Arterial wall dynamics,” *Perspectives in Medicine*, vol. 1, no. 1, pp. 146–151, Sep. 2012.
- [26] “WikiJournal of Medicine/Medical gallery of Blausen Medical 2014 - Wikiversity.” [Online]. Available: https://en.wikiversity.org/wiki/WikiJournal_of_Medicine/Medical_gallery_of_Blausen_Medical_2014. [Accessed: 28-Dec-2017].
- [27] P. Libby, “History of Discovery: Inflammation in Atherosclerosis,” *Arterioscler Thromb Vasc Biol*, vol. 32, no. 9, pp. 2045–2051, Sep. 2012.
- [28] A. J. Lusis, “Atherosclerosis,” *Nature*, vol. 407, no. 6801, pp. 233–241, Sep. 2000.
- [29] P. Libby, “Inflammation in Atherosclerosis,” *Arteriosclerosis, Thrombosis, and Vascular Biology*, vol. 32, no. 9, pp. 2045–2051, Sep. 2012.
- [30] “Atherosclerosis stages.”
- [31] B. Småbrekke *et al.*, “Atherosclerotic Risk Factors and Risk of Myocardial Infarction and Venous Thromboembolism; Time-Fixed versus Time-Varying Analyses. The Tromsø Study,” *PLOS ONE*, vol. 11, no. 9, p. e0163242, 2016.
- [32] K. Jesionek, A. Slapik, and M. Kostur, “Low-density lipoprotein transport through an arterial wall under hypertension – A model with time and pressure dependent fraction of leaky junction consistent with experiments,” *Journal of Theoretical Biology*, vol. 411, pp. 81–91, Dec. 2016.
- [33] A. Kratzer, H. Giral, and U. Landmesser, “High-density lipoproteins as modulators of endothelial cell functions: alterations in patients with coronary artery disease,” *Cardiovasc Res*, vol. 103, no. 3, pp. 350–361, Aug. 2014.
- [34] R. Baumgartner, “Biglycan: Unpuzzling the causal links between tobacco-smoking and atherosclerosis?,” *Atherosclerosis*, vol. 237, no. 2, pp. 809–810, Dec. 2014.
- [35] F. Lovren, H. Teoh, and S. Verma, “Obesity and atherosclerosis: mechanistic insights,” *Can J Cardiol*, vol. 31, no. 2, pp. 177–183, Feb. 2015.
- [36] R. Hallmark, J. T. Patrie, Z. Liu, G. A. Gaesser, E. J. Barrett, and A. Weltman, “The Effect of Exercise Intensity on Endothelial Function in Physically Inactive Lean and Obese Adults,” *PLoS One*, vol. 9, no. 1, Jan. 2014.
- [37] H. C. Stary *et al.*, “A Definition of Advanced Types of Atherosclerotic Lesions and a Histological Classification of Atherosclerosis,” *Circulation*, vol. 92, no. 5, pp. 1355–1374, Sep. 1995.
- [38] J. M. Tarkin *et al.*, “Imaging Atherosclerosis,” *Circulation Research*, vol. 118, no. 4, pp. 750–769, Feb. 2016.
- [39] V. Kočka, “The coronary angiography – An old-timer in great shape,” *Cor et Vasa*, vol. 57, no. 6, pp. e419–e424, Dec. 2015.

- [40] P. J. Scanlon *et al.*, “ACC/AHA Guidelines for Coronary Angiography: Executive Summary and Recommendations: A Report of the American College of Cardiology/American Heart Association Task Force on Practice Guidelines (Committee on Coronary Angiography) Developed in collaboration with the Society for Cardiac Angiography and Interventions,” *Circulation*, vol. 99, no. 17, pp. 2345–2357, May 1999.
- [41] N. E. Green, S.-Y. J. Chen, J. C. Messenger, B. M. Groves, and J. D. Carroll, “Three-dimensional vascular angiography,” *Curr Probl Cardiol*, vol. 29, no. 3, pp. 104–142, Mar. 2004.
- [42] “Stress cardiac MR matches 320-row CCTA results,” *AuntMinnie.com*. [Online]. Available: <http://www.auntminnie.com/index.aspx?sec=ser&sub=def&pag=dis&ItemID=105318>. [Accessed: 28-Dec-2017].
- [43] S. Çimen, A. Gooya, M. Grass, and A. F. Frangi, “Reconstruction of coronary arteries from X-ray angiography: A review,” *Medical Image Analysis*, vol. 32, no. Supplement C, pp. 46–68, Aug. 2016.
- [44] “Assessment of three dimensional quantitative coronary analysis by using rotational angiography for measurement of vessel length and diameter.” [Online]. Available: <https://www.ncbi.nlm.nih.gov/pmc/articles/PMC3473188/>. [Accessed: 28-Dec-2017].
- [45] L. Sarry and J. Y. Boire, “Three-dimensional tracking of coronary arteries from biplane angiographic sequences using parametrically deformable models,” *IEEE Trans Med Imaging*, vol. 20, no. 12, pp. 1341–1351, Dec. 2001.
- [46] C. Cañero, F. Vilariño, J. Mauri, and P. Radeva, “Predictive (un)distortion model and 3-D reconstruction by biplane snakes,” *IEEE Trans Med Imaging*, vol. 21, no. 9, pp. 1188–1201, Sep. 2002.
- [47] S. Zheng, T. Meiying, and S. Jian, “Sequential reconstruction of vessel skeletons from X-ray coronary angiographic sequences,” *Computerized Medical Imaging and Graphics*, vol. 34, no. 5, pp. 333–345, Jul. 2010.
- [48] J. Yang, W. Cong, Y. Chen, J. Fan, Y. Liu, and Y. Wang, “External force back-projective composition and globally deformable optimization for 3-D coronary artery reconstruction,” *Phys Med Biol*, vol. 59, no. 4, pp. 975–1003, Feb. 2014.
- [49] S. J. Chen and J. D. Carroll, “3-D reconstruction of coronary arterial tree to optimize angiographic visualization,” *IEEE Trans Med Imaging*, vol. 19, no. 4, pp. 318–336, Apr. 2000.
- [50] K. R. Hoffmann, A. Sen, L. Lan, K.-G. Chua, J. Esthappan, and M. Mazzucco, “A system for determination of 3D vessel tree centerlines from biplane images,” *Int J Cardiovasc Imaging*, vol. 16, no. 5, pp. 315–330, Oct. 2000.
- [51] S. Y. J. Chen and J. D. Carroll, “Kinematic and deformation analysis of 4-D coronary arterial trees reconstructed from cine angiograms,” *IEEE Trans Med Imaging*, vol. 22, no. 6, pp. 710–721, Jun. 2003.
- [52] G. Shechter, F. Devernay, E. Coste-Manière, A. Quyyumi, and E. R. McVeigh, “Three-Dimensional Motion Tracking of Coronary Arteries in Biplane Cineangiograms,” *IEEE Trans Med Imaging*, vol. 22, no. 4, pp. 493–503, Apr. 2003.
- [53] A. Andriotis *et al.*, “A new method of three-dimensional coronary artery reconstruction from X-ray angiography: validation against a virtual phantom and multislice computed tomography,” *Catheter Cardiovasc Interv*, vol. 71, no. 1, pp. 28–43, Jan. 2008.
- [54] P. Fallavollita and F. Cheriet, “Optimal 3D reconstruction of coronary arteries for 3D clinical assessment,” *Comput Med Imaging Graph*, vol. 32, no. 6, pp. 476–487, Sep. 2008.
- [55] U. Jandt, D. Schäfer, M. Grass, and V. Rasche, “Automatic generation of 3D coronary artery centerlines using rotational X-ray angiography,” *Med Image Anal*, vol. 13, no. 6, pp. 846–858, Dec. 2009.
- [56] U. Jandt, D. Schäfer, M. Grass, and V. Rasche, “Automatic generation of time resolved motion vector fields of coronary arteries and 4D surface extraction using rotational x-ray angiography,” *Phys Med Biol*, vol. 54, no. 1, pp. 45–64, Jan. 2009.

- [57] J. Yang, Y. Wang, Y. Liu, S. Tang, and W. Chen, "Novel approach for 3-d reconstruction of coronary arteries from two uncalibrated angiographic images," *IEEE Trans Image Process*, vol. 18, no. 7, pp. 1563–1572, Jul. 2009.
- [58] R. Liao, D. Luc, Y. Sun, and K. Kirchberg, "3-D reconstruction of the coronary artery tree from multiple views of a rotational X-ray angiography," *Int J Cardiovasc Imaging*, vol. 26, no. 7, pp. 733–749, Oct. 2010.
- [59] X. Liu, F. Hou, A. Hao, and H. Qin, "A parallelized 4D reconstruction algorithm for vascular structures and motions based on energy optimization," *Vis Comput*, vol. 31, no. 11, pp. 1431–1446, Nov. 2015.
- [60] H. S. Hecht, "Coronary artery calcium scanning: past, present, and future," *JACC Cardiovasc Imaging*, vol. 8, no. 5, pp. 579–596, May 2015.
- [61] V. I. Kigka *et al.*, "3D reconstruction of coronary arteries and atherosclerotic plaques based on computed tomography angiography images," *Biomedical Signal Processing and Control*, vol. 40, pp. 286–294, Feb. 2018.
- [62] S. Kato *et al.*, "Assessment of Coronary Artery Disease Using Magnetic Resonance Coronary Angiography: A National Multicenter Trial," *Journal of the American College of Cardiology*, vol. 56, no. 12, pp. 983–991, Sep. 2010.
- [63] M. Stuber and R. G. Weiss, "Coronary magnetic resonance angiography," *J. Magn. Reson. Imaging*, vol. 26, no. 2, pp. 219–234, Aug. 2007.
- [64] A. Chiribiri, R. M. Botnar, and E. Nagel, "Magnetic Resonance Coronary Angiography: Where Are We Today?," *Curr Cardiol Rep*, vol. 15, no. 2, 2013.
- [65] H. Sakuma, "Coronary CT versus MR Angiography: The Role of MR Angiography," *Radiology*, vol. 258, no. 2, pp. 340–349, Feb. 2011.
- [66] A. Nair, M. P. Margolis, B. D. Kuban, and D. G. Vince, "Automated coronary plaque characterisation with intravascular ultrasound backscatter: ex vivo validation," *EuroIntervention*, vol. 3, no. 1, pp. 113–120, May 2007.
- [67] M. Terashima, H. Kaneda, and T. Suzuki, "The Role of Optical Coherence Tomography in Coronary Intervention," *Korean J Intern Med*, vol. 27, no. 1, pp. 1–12, Mar. 2012.
- [68] E. A. Osborn and F. A. Jaffer, "Imaging Atherosclerosis and Risk of Plaque Rupture," *Curr Atheroscler Rep*, vol. 15, no. 10, Oct. 2013.
- [69] A. Sakellarios, G. Rigas, T. Exarchos, and D. Fotiadis, "A methodology and a software tool for 3D reconstruction of coronary and carotid arteries and atherosclerotic plaques," *Conference on Imaging Systems and Techniques (IST)*, 2016.
- [70] P. I. Tsompou, P. K. Siogkas, A. I. Sakellarios, P. A. Lemos, L. K. Michalis, and D. I. Fotiadis, "Non-invasive Assessment of Coronary Stenoses and Comparison to Invasive Techniques: A Proof-of-Concept Study," in *2017 IEEE 30th International Symposium on Computer-Based Medical Systems (CBMS)*, 2017, pp. 328–331.
- [71] D. Ochijewicz, M. Tomaniak, L. Koltowski, A. Rdzanek, A. Pietrasik, and J. Kochman, "Intravascular imaging of coronary artery disease: recent progress and future directions," *J Cardiovasc Med (Hagerstown)*, vol. 18, no. 10, pp. 733–741, Oct. 2017.
- [72] "Next Generation IVUS and OCT: HD-IVUS, Heartbeat-OCT, Micro-OCT, Combination Devices, and More," *tctmd.com*. [Online]. Available: <https://www.tctmd.com/videos/next-generation-ivus-and-oct-hdivus-heartbeat-oct-microoct-combination-devices-and-more.690015fbadbe4d79ade403664be57a66>. [Accessed: 23-Nov-2017].
- [73] S. C. Bergheanu, M. C. Bodde, and J. W. Jukema, "Pathophysiology and treatment of atherosclerosis," *Neth Heart J*, vol. 25, no. 4, pp. 231–242, Apr. 2017.
- [74] Y. Soto *et al.*, "Antiatherosclerotic effect of an antibody that binds to extracellular matrix glycosaminoglycans," *Arterioscler. Thromb. Vasc. Biol.*, vol. 32, no. 3, pp. 595–604, Mar. 2012.
- [75] T. English, "The Evolution of Cardiac Surgery," *Ann Surg*, vol. 219, no. 1, p. 105, Jan. 1994.
- [76] G.-W. He, *Arterial Grafting for Coronary Artery Bypass Surgery*. Springer Science & Business Media, 2006.

- [77] T. Gaziano, K. S. Reddy, F. Paccaud, S. Horton, and V. Chaturvedi, "Cardiovascular Disease," in *Disease Control Priorities in Developing Countries*, 2nd ed., D. T. Jamison, J. G. Breman, A. R. Measham, G. Alleyne, M. Claeson, D. B. Evans, P. Jha, A. Mills, and P. Musgrove, Eds. Washington (DC): World Bank, 2006.
- [78] J. T. Stewart *et al.*, "Percutaneous transluminal coronary angioplasty in chronic coronary artery occlusion," *Journal of the American College of Cardiology*, vol. 21, no. 6, pp. 1371–1376, May 1993.
- [79] V. Farooq, B. D. Gogas, and P. W. Serruys, "Restenosis: delineating the numerous causes of drug-eluting stent restenosis," *Circ Cardiovasc Interv*, vol. 4, no. 2, pp. 195–205, Apr. 2011.
- [80] T. Simard, B. Hibbert, F. D. Ramirez, M. Froeschl, Y.-X. Chen, and E. R. O'Brien, "The evolution of coronary stents: a brief review," *Can J Cardiol*, vol. 30, no. 1, pp. 35–45, Jan. 2014.
- [81] U. Sigwart, J. Puel, V. Mirkovitch, F. Joffre, and L. Kappenberger, "Intravascular stents to prevent occlusion and restenosis after transluminal angioplasty," *N. Engl. J. Med.*, vol. 316, no. 12, pp. 701–706, Mar. 1987.
- [82] D. E. Cutlip *et al.*, "Clinical restenosis after coronary stenting: perspectives from multicenter clinical trials," *J. Am. Coll. Cardiol.*, vol. 40, no. 12, pp. 2082–2089, Dec. 2002.
- [83] M.-C. Morice *et al.*, "A randomized comparison of a sirolimus-eluting stent with a standard stent for coronary revascularization," *N. Engl. J. Med.*, vol. 346, no. 23, pp. 1773–1780, Jun. 2002.
- [84] J. W. Moses *et al.*, "Sirolimus-eluting stents versus standard stents in patients with stenosis in a native coronary artery," *N. Engl. J. Med.*, vol. 349, no. 14, pp. 1315–1323, Oct. 2003.
- [85] G. W. Stone *et al.*, "A Polymer-Based, Paclitaxel-Eluting Stent in Patients with Coronary Artery Disease," *New England Journal of Medicine*, vol. 350, no. 3, pp. 221–231, 2004.
- [86] C. Spaulding *et al.*, "Four-year follow-up of TYPHOON (trial to assess the use of the CYPHer sirolimus-eluting coronary stent in acute myocardial infarction treated with Balloon angioplasty)," *JACC Cardiovasc Interv*, vol. 4, no. 1, pp. 14–23, Jan. 2011.
- [87] G. Lewis, "Materials, fluid dynamics, and solid mechanics aspects of coronary artery stents: A state-of-the-art review," *J. Biomed. Mater. Res.*, vol. 86B, no. 2, pp. 569–590, Aug. 2008.
- [88] A. Mattesini *et al.*, "ABSORB biodegradable stents versus second-generation metal stents: a comparison study of 100 complex lesions treated under OCT guidance," *JACC Cardiovasc Interv*, vol. 7, no. 7, pp. 741–750, Jul. 2014.
- [89] P. W. Serruys *et al.*, "Comparison of an everolimus-eluting bioresorbable scaffold with an everolimus-eluting metallic stent for the treatment of coronary artery stenosis (ABSORB II): a 3 year, randomised, controlled, single-blind, multicentre clinical trial," *The Lancet*, vol. 388, no. 10059, pp. 2479–2491, Nov. 2016.
- [90] C. von Birgelen *et al.*, "Very thin strut biodegradable polymer everolimus-eluting and sirolimus-eluting stents versus durable polymer zotarolimus-eluting stents in allcomers with coronary artery disease (BIO-RESORT): a three-arm, randomised, non-inferiority trial," *The Lancet*, vol. 388, no. 10060, pp. 2607–2617, Nov. 2016.
- [91] M. C. Alraies, F. Darmoch, R. Tummala, and R. Waksman, "Diagnosis and management challenges of in-stent restenosis in coronary arteries," *World Journal of Cardiology*, vol. 9, no. 8, pp. 640–651, Aug. 2017.
- [92] A. Kastrati *et al.*, "Sirolimus-eluting stents vs paclitaxel-eluting stents in patients with coronary artery disease: meta-analysis of randomized trials," *JAMA*, vol. 294, no. 7, pp. 819–825, Aug. 2005.
- [93] P. A. Lemos *et al.*, "Unrestricted utilization of sirolimus-eluting stents compared with conventional bare stent implantation in the 'real world': the Rapamycin-Eluting Stent Evaluated At Rotterdam Cardiology Hospital (RESEARCH) registry," *Circulation*, vol. 109, no. 2, pp. 190–195, Jan. 2004.

- [94] M. Joner *et al.*, “Endothelial cell recovery between comparator polymer-based drug-eluting stents,” *J. Am. Coll. Cardiol.*, vol. 52, no. 5, pp. 333–342, Jul. 2008.
- [95] A. V. Finn *et al.*, “Vascular responses to drug eluting stents: importance of delayed healing,” *Arterioscler. Thromb. Vasc. Biol.*, vol. 27, no. 7, pp. 1500–1510, Jul. 2007.
- [96] P. K. Kuchulakanti *et al.*, “Correlates and long-term outcomes of angiographically proven stent thrombosis with sirolimus- and paclitaxel-eluting stents,” *Circulation*, vol. 113, no. 8, pp. 1108–1113, Feb. 2006.
- [97] S. Garg and P. W. Serruys, “Coronary Stents: Current Status,” *Journal of the American College of Cardiology*, vol. 56, no. 10 Supplement, pp. S1–S42, Aug. 2010.
- [98] F. Otsuka, A. V. Finn, S. K. Yazdani, M. Nakano, F. D. Kolodgie, and R. Virmani, “The importance of the endothelium in atherothrombosis and coronary stenting,” *Nat Rev Cardiol*, vol. 9, no. 8, pp. 439–453, May 2012.
- [99] Y. Suzuki, A. C. Yeung, and F. Ikeno, “The importance of pre-clinical animal testing in interventional cardiology,” *Arquivos Brasileiros de Cardiologia*, vol. 91, no. 5, pp. 348–360, Nov. 2008.
- [100] R. Virmani, F. D. Kolodgie, A. Farb, and A. Lafont, “Drug eluting stents: are human and animal studies comparable?,” *Heart*, vol. 89, no. 2, pp. 133–138, Feb. 2003.
- [101] A. K. Mitra and D. K. Agrawal, “In stent restenosis: Bane of the stent era,” *Journal of Clinical Pathology*, vol. 59, no. 3, pp. 232–239, 2006.
- [102] F. G. P. Welt *et al.*, “Leukocyte recruitment and expression of chemokines following different forms of vascular injury,” *Vasc Med*, vol. 8, no. 1, pp. 1–7, 2003.
- [103] N. Kipshidze *et al.*, “Role of the endothelium in modulating neointimal formation: vasculoprotective approaches to attenuate restenosis after PCIs,” *J. Am. Coll. Cardiol.*, vol. 44, no. 4, pp. 733–739, Aug. 2004.
- [104] C. Chaabane, F. Otsuka, R. Virmani, and M.-L. Bochaton-Piallat, “Biological responses in stented arteries,” *Cardiovasc Res*, vol. 99, no. 2, pp. 353–363, Jul. 2013.
- [105] J. H. Campbell and G. R. Campbell, “Smooth muscle phenotypic modulation--a personal experience,” *Arterioscler. Thromb. Vasc. Biol.*, vol. 32, no. 8, pp. 1784–1789, Aug. 2012.
- [106] T. N. Wight and S. Potter-Perigo, “The extracellular matrix: an active or passive player in fibrosis?,” *Am. J. Physiol. Gastrointest. Liver Physiol.*, vol. 301, no. 6, pp. G950-955, Dec. 2011.
- [107] B. Zwart, T. C. Godschalk, J. C. Kelder, and J. M. Ten Berg, “High risk of stent thrombosis in the first 6 months after coronary stenting: Do not discontinue clopidogrel early after ACS,” *J Interv Cardiol*, vol. 30, no. 5, pp. 421–426, Oct. 2017.
- [108] A. J. Kirtane and G. W. Stone, “How to Minimize Stent Thrombosis,” *Circulation*, vol. 124, no. 11, pp. 1283–1287, Sep. 2011.
- [109] B. E. Claessen, J. P. S. Henriques, F. A. Jaffer, R. Mehran, J. J. Piek, and G. D. Dangas, “Stent Thrombosis,” *JACC: Cardiovascular Interventions*, vol. 7, no. 10, pp. 1081–1092, Oct. 2014.
- [110] A. J. Kirtane *et al.*, “Safety and efficacy of drug-eluting and bare metal stents: comprehensive meta-analysis of randomized trials and observational studies,” *Circulation*, vol. 119, no. 25, pp. 3198–3206, Jun. 2009.
- [111] G. W. Stone *et al.*, “Safety and Efficacy of Sirolimus- and Paclitaxel-Eluting Coronary Stents,” *New England Journal of Medicine*, vol. 356, no. 10, pp. 998–1008, Mar. 2007.
- [112] K. Kolandaivelu *et al.*, “Stent Thrombogenicity Early in High Risk Interventional Settings is Driven by Stent Design and Deployment, and Protected by Polymer-Drug Coatings,” *Circulation*, vol. 123, no. 13, pp. 1400–1409, Apr. 2011.
- [113] T. Tada *et al.*, “Impact of stent strut thickness on arterial healing after drug-eluting stents implantation assessed by optical coherence tomography,” *Eur Heart J*, vol. 34, no. suppl_1, Aug. 2013.
- [114] “Global Markets for Coronary Stent Devices - HLC111A.” [Online]. Available: <http://www.bccresearch.com/market-research/healthcare/coronary-stent-devices-global-market-hlc111a.html>. [Accessed: 24-Mar-2017].

- [115] “Coronary stent market Size To Reach \$15.2 Billion By 2024.” [Online]. Available: <https://www.grandviewresearch.com/press-release/global-coronary-stent-industry>. [Accessed: 14-Mar-2017].
- [116] “CORONARY STENTS –GLOBAL ANALYSIS AND MARKET FORECASTS.”
- [117] A. Shafer, C. Zhou, P. A. Gehrig, J. F. Bogges, and V. L. Bae-Jump, “Rapamycin potentiates the effects of paclitaxel in endometrial cancer cells through inhibition of cell proliferation and induction of apoptosis,” *Int J Cancer*, vol. 126, no. 5, pp. 1144–1154, Mar. 2010.
- [118] A. Wadood, “Brief Overview on Nitinol as Biomaterial,” *Advances in Materials Science and Engineering*, 2016. [Online]. Available: <https://www.hindawi.com/journals/amse/2016/4173138/>. [Accessed: 08-Aug-2018].
- [119] S. Saghaian *et al.*, “Effects of Ni content on the shape memory properties and microstructure of Ni-rich NiTi-20Hf alloys,” *Smart Materials and Structures*, vol. 25, p. 095029, Sep. 2016.
- [120] B. O’Brien, H. Zafar, A. Ibrahim, J. Zafar, and F. Sharif, “Coronary Stent Materials and Coatings: A Technology and Performance Update,” *Ann Biomed Eng*, vol. 44, no. 2, pp. 523–535, Feb. 2016.
- [121] R. Köster *et al.*, “Nickel and molybdenum contact allergies in patients with coronary in-stent restenosis,” *Lancet*, vol. 356, no. 9245, pp. 1895–1897, Dec. 2000.
- [122] B. AL-Mangour and R. Mongrain, “Coronary Stents Fracture: An Engineering Approach,” *Mater. Sci. Appl*, pp. 606–621, 2013.
- [123] “Platinum as a Metallic Material - Chemgapedia.” [Online]. Available: http://www.chemgapedia.de/vsengine/vlu/vsc/en/ch/25/heraeus/pt_als_werkstoff/platin.vlu/Page/vsc/en/ch/25/heraeus/pt_als_werkstoff/pt_werkstoff06.vscml.html. [Accessed: 27-Mar-2017].
- [124] J. B. Park and J. D. Bronzino, *Biomaterials : principles and applications*. Boca Raton : CRC Press, 2003.
- [125] Y. Zheng, X. Xu, Z. Xu, J.-Q. Wang, and H. Cai, *Metallic Biomaterials: New Directions and Technologies*. John Wiley & Sons, 2017.
- [126] “Corrosion Resistance of High-Performance Materials: Titanium, Tantalum, Zirconium | Industrial Chemistry | Chemistry | Subjects | Wiley.” [Online]. Available: <https://www.wiley.com/en-us/Corrosion+Resistance+of+High+Performance+Materials%3A+Titanium%2C+Tantalum%2C+Zirconium-p-9783527334353>. [Accessed: 08-Aug-2018].
- [127] D. CRISTEA, I. GHIUȚĂ, and D. MUNTEANU, “TANTALUM BASED MATERIALS FOR IMPLANTS AND PROSTHESES APPLICATIONS,” vol. 8, no. 2, p. 8, 2015.
- [128] A. Adam, R. Dondelinger, and P. Mueller, *Textbook of Metallic Stents*. CRC Press, 1997.
- [129] Y. X. Leng, J. Y. Chen, P. Yang, H. Sun, J. Wang, and N. Huang, “The biocompatibility of the tantalum and tantalum oxide films synthesized by pulse metal vacuum arc source deposition,” *Nuclear Instruments and Methods in Physics Research Section B: Beam Interactions with Materials and Atoms*, vol. 242, no. 1–2, pp. 30–32, 2006.
- [130] P. P. Karjalainen, A. S. Ylitalo, and K. E. Juhani Airaksinen, “Real world experience with the TITAN(R) stent: a 9-month follow-up report from The Titan PORI Registry,” *EuroIntervention*, vol. 2, no. 2, pp. 187–191, Aug. 2006.
- [131] G. Manivasagam and D. Dhinasekaran, “Biomedical Implants: Corrosion and its Prevention - A Review,” *40 Recent Patents on Corrosion Science*, vol. 2, pp. 40–54, 2010.
- [132] W. Haider and N. Munroe, “Assessment of Corrosion Resistance and Metal Ion Leaching of Nitinol Alloys,” *J Mater Eng Perform*, vol. 20, no. 4, pp. 812–815, Jul. 2011.
- [133] A. Sciahbasi *et al.*, “Closed versus open cell stent for high-risk PCIs in ST-elevation acute myocardial infarction: The Closed versus Open Cells stent for High risk PCIs in ST-Elevation acute myocardial infarction (COCHISE) pilot study,” *American Heart Journal*, vol. 165, no. 3, pp. 415–420, 2013.
- [134] A. W. Martinez and E. L. Chaikof, “Microfabrication and Nanotechnology in Stent Design,” *Wiley Interdiscip Rev Nanomed Nanobiotechnol*, vol. 3, no. 3, pp. 256–268, 2011.

- [135] “Medical devices - Council Directive 93/42/EEC,” *Growth*. [Online]. Available: https://ec.europa.eu/growth/single-market/european-standards/harmonised-standards/medical-devices_en. [Accessed: 08-Feb-2017].
- [136] “Medical devices - Directive 2007/47/EC.” [Online]. Available: <http://eur-lex.europa.eu/legal-content/en/ALL/?uri=CELEX%3A32007L0047>. [Accessed: 08-Feb-2017].
- [137] A. G. Fraser *et al.*, “Clinical evaluation of cardiovascular devices: principles, problems, and proposals for European regulatory reform. Report of a policy conference of the European Society of Cardiology,” *Eur. Heart J.*, vol. 32, no. 13, pp. 1673–1686, Jul. 2011.
- [138] R. Byrne, P. Serruys, A. Baumbach, J. Escaned, J. Fajadet, and S. James, “Report of a European Society of Cardiology-European Association of Percutaneous Cardiovascular Interventions task force on the evaluation of coronary stents in Europe: executive summary,” *European Heart Journal Advance*, 2015.
- [139] N. D. Nam, S. H. Lee, J. G. Kim, J. W. Yi, and K. R. Lee, “Effect of stress on the passivation of Si-DLC coating as stent materials in simulated body environment,” *Diamond and Related Materials*, vol. 18, no. 9, pp. 1145–1151, 2009.
- [140] C.-T. Zhou and H.-Y. Dong, “Stability and dynamic deforming process for structure of coronary artery stents,” *Current Applied Physics*, vol. 5, no. 5, pp. 458–462, 2005.
- [141] D. Vassilev, “Changes in Coronary Bifurcations after Stent Placement in the Main Vessel and Balloon Opening of Stent Cells. Theory and Practical Verification on a Bench-Test Model,” *Journal of Geriatric Cardiology*, 2008.
- [142] M. Pitney *et al.*, “Major stent deformation/pseudofracture of 7 Crown Endeavor/Micro Driver stent platform: incidence and causative factors,” *EuroIntervention*, vol. 7, no. 2, pp. 256–262, Jun. 2011.
- [143] S. Zhao, L. Gu, and S. R. Froemming, “Experimental investigation of the stent-artery interaction,” *J Med Eng Technol*, vol. 37, no. 7, pp. 463–469, Oct. 2013.
- [144] J. Iqbal, J. Chamberlain, S. E. Francis, and J. Gunn, “Role of Animal Models in Coronary Stenting,” *Ann Biomed Eng*, vol. 44, no. 2, pp. 453–465, Feb. 2016.
- [145] M. Chinikar and P. Sadeghipour, “Coronary Stent Fracture: A Recently Appreciated Phenomenon with Clinical Relevance,” *Curr Cardiol Rev*, vol. 10, no. 4, pp. 349–354, Nov. 2014.
- [146] W. Y. Kang, W. Kim, H. G. Kim, and W. Kim, “Drug-eluting stent fracture occurred within 2 days after stent implantation,” *International Journal of Cardiology*, vol. 120, no. 2, pp. 273–275, 2007.
- [147] J.-S. Park, D.-G. Shin, Y.-J. Kim, G.-R. Hong, and I.-H. Cho, “Acute myocardial infarction as a consequence of stent fracture and plaque rupture after sirolimus-eluting stent implantation,” *International Journal of Cardiology*, vol. 134, no. 2, pp. e79–e81, May 2009.
- [148] T. Okamura *et al.*, “Late giant coronary aneurysm associated with a fracture of sirolimus eluting stent: A case report,” *Journal of Cardiology*, vol. 51, no. 1, pp. 74–79, 2008.
- [149] S.-H. Lee *et al.*, “Frequency of stent fracture as a cause of coronary restenosis after sirolimus-eluting stent implantation,” *Am. J. Cardiol.*, vol. 100, no. 4, pp. 627–630, Aug. 2007.
- [150] F. Shaikh, R. Maddikunta, M. Djelmami-Hani, J. Solis, S. Allaqaband, and T. Bajwa, “Stent fracture, an incidental finding or a significant marker of clinical in-stent restenosis?,” *Catheter Cardiovasc Interv*, vol. 71, no. 5, pp. 614–618, Apr. 2008.
- [151] F. Williamson, “Richard courant and the finite element method: A further look,” *Historia Mathematica*, vol. 7, no. 4, pp. 369–378, Nov. 1980.
- [152] S. H. Lo and C. K. Lee, “On using meshes of mixed element types in adaptive finite element analysis,” *Finite Elements in Analysis and Design*, vol. 11, no. 4, pp. 307–336, Aug. 1992.
- [153] F. Migliavacca, L. Petrini, V. Montanari, I. Quagliana, F. Auricchio, and G. Dubini, “A predictive study of the mechanical behaviour of coronary stents by computer modelling,” *Med Eng Phys*, vol. 27, no. 1, pp. 13–18, Jan. 2005.

- [154] C. Dumoulin and B. Cochelin, "Mechanical behaviour modelling of balloon-expandable stents," *Journal of Biomechanics*, vol. 33, no. 11, pp. 1461–1470, 2000.
- [155] L. B. Tan, D. C. Webb, K. Kormi, and S. T. Al-Hassani, "A method for investigating the mechanical properties of intracoronary stents using finite element numerical simulation," *Int. J. Cardiol.*, vol. 78, no. 1, pp. 51–67, Mar. 2001.
- [156] F. Etave, G. Finet, M. Boivin, J. C. Boyer, G. Rioufol, and G. Thollet, "Mechanical properties of coronary stents determined by using finite element analysis," *J Biomech*, vol. 34, no. 8, pp. 1065–1075, Aug. 2001.
- [157] S. N. David Chua, B. J. Mac Donald, and M. S. J. Hashmi, "Finite element simulation of stent and balloon interaction," *Journal of Materials Processing Technology*, vol. 143–144, pp. 591–597, 2003.
- [158] L. Petrini, F. Migliavacca, F. Auricchio, and G. Dubini, "Numerical investigation of the intravascular coronary stent flexibility," *Journal of Biomechanics*, vol. 37, no. 4, pp. 495–501, Apr. 2004.
- [159] J. P. McGarry, B. P. O'Donnell, P. E. McHugh, and J. G. McGarry, "Analysis of the mechanical performance of a cardiovascular stent design based on micromechanical modelling," *Computational Materials Science*, vol. 31, no. 3–4, pp. 421–438, 2004.
- [160] W. Walke, Z. Paszenda, and J. Filipiak, "Experimental and numerical biomechanical analysis of vascular stent," *Journal of Materials Processing Technology*, vol. 164–165, pp. 1263–1268, 2005.
- [161] K. Mori and T. Saito, "Effects of Stent Structure on Stent Flexibility Measurements," *Ann Biomed Eng*, vol. 33, no. 6, pp. 733–742, Jun. 2005.
- [162] G. J. Hall and E. P. Kasper, "Comparison of element technologies for modeling stent expansion," *J Biomech Eng*, vol. 128, no. 5, pp. 751–756, Oct. 2006.
- [163] W. Wu, D.-Z. Yang, M. Qi, and W.-Q. Wang, "An FEA method to study flexibility of expanded coronary stents," *Journal of Materials Processing Tech.*, vol. 1–3, no. 184, pp. 447–450, 2007.
- [164] P. Mortier, M. De Beule, S. G. Carlier, R. Van Impe, B. Verheghe, and P. Verdonck, "Numerical study of the uniformity of balloon-expandable stent deployment," *J Biomech Eng*, vol. 130, no. 2, p. 021018, Apr. 2008.
- [165] J. F. X. Z. and S. K., "On the finite element modelling of balloon-expandable stents.," *J Mech Behav Biomed Mater*, vol. 1, no. 1, pp. 86–95, Jan. 2008.
- [166] W. Park, "Evaluation of Stent Performances using FEA considering a Realistic Balloon Expansion," 2011. .
- [167] W.-Q. Wang, D.-K. Liang, D.-Z. Yang, and M. Qi, "Analysis of the transient expansion behavior and design optimization of coronary stents by finite element method," *Journal of Biomechanics*, vol. 39, no. 1, pp. 21–32, 2006.
- [168] E. W. Donnelly, M. S. Bruzzi, T. Connolley, and P. E. McHugh, "Finite element comparison of performance related characteristics of balloon expandable stents," *Comput Methods Biomech Biomed Engin*, vol. 10, no. 2, pp. 103–110, Apr. 2007.
- [169] Z. Xia, F. Ju, and K. Sasaki, "A general finite element analysis method for balloon expandable stents based on repeated unit cell (RUC) model," *Finite Elements in Analysis and Design*, vol. 43, no. 8, pp. 649–658, 2007.
- [170] M. De Beule, P. Mortier, S. G. Carlier, B. Verheghe, R. Van Impe, and P. Verdonck, "Realistic finite element-based stent design: The impact of balloon folding," *Journal of Biomechanics*, vol. 41, no. 2, pp. 383–389, 2008.
- [171] D. Lim *et al.*, "Suggestion of potential stent design parameters to reduce restenosis risk driven by foreshortening or dogboning due to non-uniform balloon-stent expansion," *Ann Biomed Eng*, vol. 36, no. 7, pp. 1118–1129, Jul. 2008.
- [172] F. Ju, Z. Xia, and K. Sasaki, "On the finite element modelling of balloon-expandable stents," *Journal of the Mechanical Behavior of Biomedical Materials*, vol. 1, no. 1, pp. 86–95, 2008.
- [173] M. Pochrzast, W. Walke, and M. Kaczmarek, "Biomechanical characterization of the balloon-expandable slotted tube stents," *Journal of Achievements of Materials and Manufacturing Engineering*, 2009.

- [174] S. Tammareddi, G. Sun, and Q. Li, “Computational design analysis for deployment of cardiovascular stents,” *IOP Conf. Ser.: Mater. Sci. Eng.*, vol. 10, no. 1, p. 012123, 2010.
- [175] H.-M. Hsiao, Y.-H. Chiu, K.-H. Lee, and C.-H. Lin, “Computational modeling of effects of intravascular stent design on key mechanical and hemodynamic behavior,” *CAD Computer Aided Design*, vol. 44, no. 8, pp. 757–765, 2012.
- [176] C. W. Park and H. S. Joe, “FEM for Design of Balloon Expandable Stent for Coronary Artery Using Co-Cr Alloy,” *Journal of Mechanics Engineering and Automation*, 2012.
- [177] A. Ciekot, A. Idziak-Jabłońska, and P. Lacki, “OPTIMIZATION OF DOGBONING PHENOMENON OF THE CORONARY ARTERY STENT,” *Scientific Research of the Institute of Mathematics and Computer Science*, 2012.
- [178] T. Roy and A. Chanda, “Computational Modelling and Analysis of Latest Commercially Available Coronary Stents During Deployment,” *Procedia Materials Science*, vol. 5, pp. 2310–2319, 2014.
- [179] Y. Levy, D. Mandler, J. Weinberger, and A. J. Domb, “Evaluation of drug-eluting stents’ coating durability—Clinical and regulatory implications,” *J. Biomed. Mater. Res.*, vol. 91B, no. 1, pp. 441–451, 2009.
- [180] C. G. Hopkins, P. E. McHugh, and J. P. McGarry, “Computational Investigation of the Delamination of Polymer Coatings During Stent Deployment,” *Ann Biomed Eng*, vol. 38, no. 7, pp. 2263–2273, Jul. 2010.
- [181] F. Auricchio, M. D. Loreto, and E. Sacco, “Finite-element Analysis of a Stenotic Artery Revascularization Through a Stent Insertion (PDF Download Available),” *Computer Methods in Biomechanics and Biomedical Engineering*, vol. 4, pp. 249–263, 2001.
- [182] P. D. Ballyk, “Intramural Stress Increases Exponentially with Stent Diameter: A Stress Threshold for Neointimal Hyperplasia,” *Journal of Vascular and Interventional Radiology*, vol. 17, no. 7, pp. 1139–1145, 2006.
- [183] C. Flege *et al.*, “Development and characterization of a coronary polylactic acid stent prototype generated by selective laser melting,” *J Mater Sci Mater Med*, vol. 24, no. 1, pp. 241–255, Jan. 2013.
- [184] Y. Onuma and P. W. Serruys, “Bioresorbable scaffold: the advent of a new era in percutaneous coronary and peripheral revascularization?,” *Circulation*, vol. 123, no. 7, pp. 779–797, Feb. 2011.
- [185] R. Waksman, “Biodegradable stents: they do their job and disappear,” *J Invasive Cardiol*, vol. 18, no. 2, pp. 70–74, Feb. 2006.
- [186] W. Wu *et al.*, “Finite Element Shape Optimization for Biodegradable Magnesium Alloy Stents,” *Ann Biomed Eng*, vol. 38, no. 9, pp. 2829–2840, Sep. 2010.
- [187] D. K. Liang, D. Z. Yang, M. Qi, and W. Q. Wang, “Finite element analysis of the implantation of a balloon-expandable stent in a stenosed artery,” *Int. J. Cardiol.*, vol. 104, no. 3, pp. 314–318, Oct. 2005.
- [188] G. I. N. Rozvany, “Aims, scope, methods, history and unified terminology of computer-aided topology optimization in structural mechanics,” *Struct Multidisc Optim*, vol. 21, no. 2, pp. 90–108, Apr. 2001.
- [189] C. Y. Lin, N. Kikuchi, and S. J. Hollister, “A novel method for biomaterial scaffold internal architecture design to match bone elastic properties with desired porosity,” *Journal of Biomechanics*, vol. 37, no. 5, pp. 623–636, 2004.
- [190] L. H. Timmins, M. R. Moreno, C. A. Meyer, J. C. Criscione, A. Rachev, and J. E. Moore, “Stented artery biomechanics and device design optimization,” *Med Biol Eng Comput*, vol. 45, no. 5, pp. 505–513, May 2007.
- [191] K. Takashima, T. Kitou, K. Mori, and K. Ikeuchi, “Simulation and experimental observation of contact conditions between stents and artery models,” *Medical Engineering & Physics*, vol. 29, no. 3, pp. 326–335, 2007.
- [192] L. H. Timmins, C. A. Meyer, M. R. Moreno, and J. E. Moore, “Effects of stent design and atherosclerotic plaque composition on arterial wall biomechanics,” *J. Endovasc. Ther.*, vol. 15, no. 6, pp. 643–654, Dec. 2008.
- [193] X. Qian, “Full analytical sensitivities in NURBS based isogeometric shape optimization,” *Computer Methods in Applied Mechanics and Engineering*, 2010.

- [194] D. Kelliher, R. Clune, J. Campbell, J. Robinson, and B. Appelbe, "Sensitivity of shape change on the performance of stainless steel cardio-vascular stents.," *Proceedings of the 7th ASMO UK conference on engineering design optimization*, 2008.
- [195] A. Kastrati *et al.*, "[Intracoronary Stenting and Angiographic Results Strut Thickness Effect on Restenosis Outcome (ISAR-STEREO) Trial]," *Vestn Rentgenol Radiol*, no. 2, pp. 52–60, Apr. 2012.
- [196] I. Pericevic, C. Lally, D. Toner, and D. J. Kelly, "The influence of plaque composition on underlying arterial wall stress during stent expansion: The case for lesion-specific stents," *Medical Engineering & Physics*, vol. 31, no. 4, pp. 428–433, May 2009.
- [197] M. Early, C. Lally, P. J. Prendergast, and D. J. Kelly, "Stresses in peripheral arteries following stent placement: a finite element analysis," *Comput Methods Biomech Biomed Engin*, vol. 12, no. 1, pp. 25–33, Feb. 2009.
- [198] C. Capelli, F. Gervaso, L. Petrini, G. Dubini, and F. Migliavacca, "Assessment of tissue prolapse after balloon-expandable stenting: influence of stent cell geometry," *Med Eng Phys*, vol. 31, no. 4, pp. 441–447, May 2009.
- [199] S. Pant, G. Limbert, N. P. Curzen, and N. W. Bressloff, "Multiobjective design optimisation of coronary stents," *Biomaterials*, vol. 32, no. 31, pp. 7755–7773, 2011.
- [200] "A Matlab Kriging Toolbox." [Online]. Available: <http://www2.imm.dtu.dk/projects/dace/dace.pdf>. [Accessed: 28-Apr-2017].
- [201] H. Li, T. Qiu, B. Zhu, J. Wu, and X. Wang, "Design Optimization of Coronary Stent Based on Finite Element Models," *ScientificWorldJournal*, vol. 2013, Oct. 2013.
- [202] S. M. Imani, A. M. Goudarzi, S. E. Ghasemi, A. Kalani, and J. Mahdinejad, "Analysis of the stent expansion in a stenosed artery using finite element method: application to stent versus stent study," *Proc Inst Mech Eng H*, vol. 228, no. 10, pp. 996–1004, Oct. 2014.
- [203] A. Schiavone, L. G. Zhao, and A. A. Abdel-Wahab, "Effects of material, coating, design and plaque composition on stent deployment inside a stenotic artery—Finite element simulation," *Materials Science and Engineering: C*, vol. 42, pp. 479–488, 2014.
- [204] R. Clune, D. Kelliher, J. C. Robinson, and J. S. Campbell, "NURBS modeling and structural shape optimization of cardiovascular stents," *Struct Multidisc Optim*, vol. 50, no. 1, pp. 159–168, Jul. 2014.
- [205] A. Schiavone, T.-Y. Qiu, and L.-G. Zhao, "Crimping and deployment of metallic and polymeric stents -- finite element modelling," *Vessel Plus*, 2017.
- [206] D. Martin and F. J. Boyle, "Computational structural modelling of coronary stent deployment: a review," *Comput Methods Biomech Biomed Engin*, vol. 14, no. 4, pp. 331–348, Apr. 2011.
- [207] S. Zhao, L. Gu, and S. R. Froemming, "Effects of arterial strain and stress in the prediction of restenosis risk: Computer modeling of stent trials," *Biomed. Eng. Lett.*, vol. 2, no. 3, pp. 158–163, Sep. 2012.
- [208] G. A. Holzapfel, "Determination of material models for arterial walls from uniaxial extension tests and histological structure," *Journal of Theoretical Biology*, vol. 238, no. 2, pp. 290–302, 2006.
- [209] G. A. Holzapfel, G. Sommer, C. T. Gasser, and P. Regitnig, "Determination of layer-specific mechanical properties of human coronary arteries with nonatherosclerotic intimal thickening and related constitutive modeling," *Am. J. Physiol. Heart Circ. Physiol.*, vol. 289, no. 5, pp. H2048–2058, Nov. 2005.
- [210] C. A. J. Schulze-Bauer, P. Regitnig, and G. A. Holzapfel, "Mechanics of the human femoral adventitia including the high-pressure response," *Am. J. Physiol. Heart Circ. Physiol.*, vol. 282, no. 6, pp. H2427–2440, Jun. 2002.
- [211] G. A. Holzapfel, P. Regitnig, and G. Sommer, "Anisotropic Mechanical Properties of Tissue Components in Human Atherosclerotic Plaques," *J Biomech Eng*, vol. 126, no. 5, pp. 657–665, 2004.
- [212] G. A. Holzapfel, M. Stadler, and C. A. J. Schulze-Bauer, "A layer-specific three-dimensional model for the simulation of balloon angioplasty using magnetic resonance imaging and mechanical testing," *Ann Biomed Eng*, vol. 30, no. 6, pp. 753–767, Jun. 2002.

- [213] D. E. Kioussis, T. C. Gasser, and G. A. Holzapfel, "A Numerical Model to Study the Interaction of Vascular Stents with Human Atherosclerotic Lesions," *Ann Biomed Eng*, vol. 35, no. 11, pp. 1857–1869, Nov. 2007.
- [214] T. C. Gasser and G. A. Holzapfel, "Modeling plaque fissuring and dissection during balloon angioplasty intervention," *Ann Biomed Eng*, vol. 35, no. 5, pp. 711–723, May 2007.
- [215] P. Mortier *et al.*, "A novel simulation strategy for stent insertion and deployment in curved coronary bifurcations: comparison of three drug-eluting stents," *Ann Biomed Eng*, vol. 38, no. 1, pp. 88–99, Jan. 2010.
- [216] F. Gervaso, C. Capelli, L. Petrini, S. Lattanzio, L. Di Virgilio, and F. Migliavacca, "On the effects of different strategies in modelling balloon-expandable stenting by means of finite element method," *J Biomech*, vol. 41, no. 6, pp. 1206–1212, 2008.
- [217] "Ansys Mechanical." [Online]. Available: <http://www.ansys.com>.
- [218] "Rontis Medical Device Co." [Online]. Available: <http://www.rontis-ag.com/>.
- [219] C. V. Bourantas *et al.*, "ANGIOCARE: an automated system for fast three-dimensional coronary reconstruction by integrating angiographic and intracoronary ultrasound data," *Catheter Cardiovasc Interv*, vol. 72, no. 2, pp. 166–175, Aug. 2008.
- [220] R. H. Cox, "Comparison of arterial wall mechanics using ring and cylindrical segments," *Am. J. Physiol.*, vol. 244, no. 2, pp. H298–303, Feb. 1983.
- [221] R. H. Cox, "Changes in arterial wall properties during development and maintenance of renal hypertension," *American Journal of Physiology - Heart and Circulatory Physiology*, vol. 242, no. 3, pp. H477–H484, Mar. 1982.
- [222] P. B. Dobrin and J. M. Doyle, "Vascular smooth muscle and the anisotropy of dog carotid artery," *Circ. Res.*, vol. 27, no. 1, pp. 105–119, Jul. 1970.
- [223] P. B. Dobrin and T. R. Canfield, "Elastase, collagenase, and the biaxial elastic properties of dog carotid artery," *Am. J. Physiol.*, vol. 247, no. 1 Pt 2, pp. H124–131, Jul. 1984.
- [224] C. M. Abshire *et al.*, "Importance of Axial Length in the Detection of Carotid Artery Stiffness Induced by a High Fat Diet," *The FASEB Journal*, vol. 31, no. 1_supplement, pp. 1068.1–1068.1, Apr. 2017.
- [225] N. Stergiopoulos, A. Pannatier, A. Rachev, S. E. Greenwald, and J.-J. Meister, "Assessment of Mechanical Homogeneity of the Arterial Wall by an Artery-Inversion Test," *Cardiovascular Engineering*, vol. 1, no. 1, pp. 31–36, Mar. 2001.
- [226] W. W. von Maltzahn, D. Besdo, and W. Wiemer, "Elastic properties of arteries: a nonlinear two-layer cylindrical model," *J Biomech*, vol. 14, no. 6, pp. 389–397, 1981.
- [227] P. Vito and H. Demiray, "A two layered model for arterial wall mechanics," *Proceedings of the 35th Annual conference on Engineering in Medicine and Biology (ACEMB)*, p. 1982.
- [228] D. J. Patel and D. L. Fry, "The elastic symmetry of arterial segments in dogs," *Circ. Res.*, vol. 24, no. 1, pp. 1–8, Jan. 1969.
- [229] G. A. Holzapfel, T. C. Gasser, and R. W. Ogden, "A New Constitutive Framework for Arterial Wall Mechanics and a Comparative Study of Material Models," *Journal of Elasticity*, vol. 61, no. 1–3, pp. 1–48, Jul. 2000.
- [230] M. Griffin, Y. Premakumar, A. Seifalian, P. E. Butler, and M. Szarko, "Biomechanical Characterization of Human Soft Tissues Using Indentation and Tensile Testing," *J Vis Exp*, no. 118, Dec. 2016.
- [231] M. Mooney, "A Theory of Large Elastic Deformation," *Journal of Applied Physics*, vol. 11, no. 9, pp. 582–592, Sep. 1940.
- [232] L. R. G. Treloar, "Stress-strain data for vulcanised rubber under various types of deformation," *Trans. Faraday Soc.*, vol. 40, no. 0, pp. 59–70, Jan. 1944.
- [233] "Large Elastic Deformations of Isotropic Materials. IV. Further Developments of the General Theory | Philosophical Transactions of the Royal Society of London A: Mathematical, Physical and Engineering Sciences." [Online]. Available: <http://rsta.royalsocietypublishing.org/content/241/835/379>. [Accessed: 23-May-2017].

- [234] R. S. Rivlin, “Large Elastic Deformations of Isotropic Materials,” in *Collected Papers of R.S. Rivlin*, G. I. Barenblatt and D. D. Joseph, Eds. Springer New York, 1997, pp. 90–108.
- [235] G. Puglisi and G. Saccomandi, “Multi-scale modelling of rubber-like materials and soft tissues: an appraisal,” *Proc Math Phys Eng Sci*, vol. 472, no. 2187, Mar. 2016.
- [236] *Biomechanics - Motion, Flow, Stress, and Growth* | Y.C. Fung | Springer. .
- [237] “Large Deformation Isotropic Elasticity - On the Correlation of Theory and Experiment for Incompressible Rubberlike Solids | Proceedings of the Royal Society of London A: Mathematical, Physical and Engineering Sciences.” [Online]. Available: <http://rspa.royalsocietypublishing.org/content/326/1567/565>. [Accessed: 23-May-2017].
- [238] R. W. Ogden, G. Saccomandi, and I. Sgura, “Fitting hyperelastic models to experimental data,” *Computational Mechanics*, vol. 34, no. 6, pp. 484–502, Nov. 2004.
- [239] “Nonlinear Solid Mechanics: a Continuum Approach for Engineering.” [Online]. Available: <https://www.abebooks.com/book-search/isbn/0471823198/>. [Accessed: 23-May-2017].
- [240] J. Tambaca, S. Canic, M. Kosor, R. D. Fish, and D. Paniagua, “Mechanical behavior of fully expanded commercially available endovascular coronary stents,” *Tex Heart Inst J*, vol. 38, no. 5, pp. 491–501, 2011.
- [241] L. Gu, S. Santra, R. A. Mericle, and A. V. Kumar, “Finite element analysis of covered microstents,” *J Biomech*, vol. 38, no. 6, pp. 1221–1227, Jun. 2005.

A. APPENDIX

A1. Detailed list of clinical trials in coronary stenting [135].

Study title/Device	Description
SYNERGY China: Assess SYNERGY Stent in China/ SYNERGY MONORAIL Everolimus-Eluting Platinum Chromium Coronary Stent System	Prospective, multicenter, single-arm study in no more than 10 sites across China, the primary endpoint is Technical success.
Safety Study to Assess the Feasibility of Use in Humans of the TAXUS Petal Bifurcation Coronary Stent System/ TAXUS® Petal™ Paclitaxel-Eluting Coronary Stent.	The purpose of this study is to determine the safety and feasibility of use in humans of the TAXUS Petal Paclitaxel-Eluting Bifurcation Coronary Stent System in the treatment of de novo lesions in native coronary arteries involving a major side branch.
TAXUS ARRIVE 2: A Multi-Center Safety Surveillance Program/ TAXUS™ Express2™ Paclitaxel-Eluting Coronary Stent System	The TAXUS ARRIVE 2 study is a multi-center safety and surveillance study designed to to compile safety surveillance and clinical outcomes data for the TAXUS™ Express2™ Paclitaxel-Eluting Coronary Stent System in routine clinical practice and to identify low frequency TAXUS related clinical events.
RESOLUTE International Registry: Evaluation of the Resolute Zotarolimus-Eluting Stent System in a 'Real-World' Patient Population/ Endeavor Resolute Zotarolimus-Eluting Coronary Stent System	The primary objective of the RESOLUTE international registry is to document the safety and overall clinical performance of the Resolute Zotarolimus-Eluting Coronary Stent System in a 'real-world' patient population requiring stent implantation.
A Prospective, Randomized Trial of BVS Veruss EES in Patients Undergoing Coronary Stenting for MI/ Bioresorbable vascular scaffold (ABSORB) vs Durable polymer everolimus-eluting metallic stent (Xience)	The aim of the current study is to test the clinical performance of the everolimus-eluting BVS compared with that of the durable polymer everolimus-eluting stent in patients undergoing PCI in the setting of acute MI.
RESOLUTE Japan SVS: The Clinical Evaluation of the MDT-4107 DES in the Treatment of De Novo Lesions in Small Diameter Native Coronary Arteries/ Device: MDT-4107 Zotarolimus-Eluting Coronary Stent	The objective of the study is to verify the safety and efficacy of the MDT-4107 Drug-Eluting Coronary Stent in the treatment of de novo lesions in native coronary arteries with a reference vessel diameter (RVD) that allows the use of 2.25mm diameter stents.
RESOLUTE Japan - The Clinical Evaluation of the MDT-4107 Drug-Eluting Coronary Stent/ MDT-4107 Drug Eluting Stent Implantation of a MDT-4107 Zotarolimus-Eluting Coronary Stent	The objective of the study is to verify the safety and efficacy of the MDT-4107 Drug-Eluting Coronary Stent for the treatment of de novo lesions in native coronary arteries.
Acute Safety, Deliverability and Efficacy of the Medtronic Resolute Integrity™ Zotarolimus-Eluting Coronary Stent System in the Treatment of Suitable Patients According to Indication for Use (CHINA RESOLUTE INTEGRITY STUDY)/ Resolute Integrity™ Zotarolimus-Eluting Coronary Stent System.	The purpose of this study is to conduct a prospective, multi-center, single arm, non-randomized evaluation of acute outcomes in Chinese subjects with the Medtronic Resolute Integrity™ Zotarolimus-Eluting Coronary Stent System.
IRIS-Onyx Cohort in the IRIS-DES Registry (IRIS-Onyx)/ Device: Onyx Drug Eluting Stent group	

The purpose of this study is to evaluate the relative effectiveness and safety of Onyx stent compared to other (drug eluting stents) DES.

China Resolute Integrity 34/38 mm Study/ Device: Resolute Integrity™ Zotarolimus-Eluting Coronary Stent System(34/38 mm)

To evaluate the clinical safety and efficacy in Chinese subjects, eligible for percutaneous transluminal coronary angioplasty (PTCA) in lesions amenable to treatment with a 34/38 mm Medtronic Resolute Integrity™ Zotarolimus-Eluting Coronary Stent System.

An Observational Registry Using Drug Eluting Stents (DES) in Patients in a Real-World Setting (DESCover Registry)/ Cypher Stent

The DESCover Registry is designed to observe the results of using Drug Eluting Stents (DES) in patients in a real-world setting.

RESOLUTE China Randomized Clinical Trial (RCT)/ Taxus Liberte Paclitaxel-Eluting Coronary Stent System

Device: Resolute Zotarolimus-Eluting Coronary Stent System

The primary objective of this study is to evaluate the in-stent late lumen loss (LLL) at 9 months, defined as the difference between the post-procedure MLD and the follow-up angiography MLD, of the Resolute Zotarolimus-Eluting Coronary Stent System compared to Taxus Liberte Paclitaxel-Eluting Coronary Stent System.

RESOLUTE ONYX China RCT Study/ Resolute Onyx™ Zotarolimus-Eluting Coronary Stent System

vs Resolute Integrity™ Zotarolimus-Eluting Coronary Stent System

It is a randomized controlled trial to evaluate the safety and efficacy of the Medtronic Resolute Onyx™ Zotarolimus-Eluting Coronary Stent System in comparison with the Medtronic Resolute Integrity™ Zotarolimus-Eluting coronary stent system.

RESOLUTE ONYX China Single Arm Study/ Resolute Onyx™ Zotarolimus-Eluting Coronary Stent System.

It is a single arm clinical evaluation of safety and efficacy of the Medtronic Resolute Onyx™ zotarolimus-eluting coronary stent system in subjects who are eligible for percutaneous transluminal coronary angioplasty (PTCA) in de novo lesions amenable to treatment with Resolute Onyx™ Stent System in China.

RESOLUTE Asia: Evaluation of the Endeavor Resolute Zotarolimus-Eluting Stent System in a Patient Population With Long Lesion(s) and/or Dual Vessels in Asia/ DES treatment.

The purpose of this study is to document the safety and overall clinical performance of the Endeavor Resolute Zotarolimus-Eluting Coronary Stent System in a patient population with long lesion(s) and/or dual vessels requiring stent implantation.

SPIRIT FIRST Clinical Trial of the Abbott Vascular XIENCE V® Everolimus Eluting Coronary Stent System/ Coronary artery drug eluting stent placement

The SPIRIT FIRST clinical trial will assess the feasibility and performance of the XIENCE V® Everolimus Eluting Coronary Stent System in the treatment of patients with de novo native coronary artery lesions. In this trial, the XIENCE V® Everolimus Eluting Coronary Stent System will be compared to the MULTI-LINK VISION® metallic stent which is CE marked and FDA approved and is available for commercial use in Europe and in the United States.

XIENCE PRIME Everolimus Eluting Coronary Stent System (EECSS) China Single-Arm Study/ XIENCE PRIME Everolimus Eluting Coronary Stent System (EECSS).

This prospective, observational, open-label, multi-center, single-arm, post-approval study is designed to evaluate the continued safety and effectiveness of the XIENCE PRIME EECSS in a cohort of real-world patients receiving the XIENCE PRIME EECSS during commercial use in real-world settings in China.

Galaxy Rapamycin Drug-Eluting Bioresorbable Coronary Stent System First-in-man Study/ Rapamycin Drug-Eluting Bioresorbable Coronary Stent System.

The Galaxy First-in-man study is a small pilot. The goal is to assess the feasibility, safety and efficacy of Rapamycin Drug-Eluting Bioresorbable Coronary Stent System in the treatment of patients with de novo coronary lesion.

Safety Study of a Bioresorbable Coronary Stent/ Bioresorbable ReZolve Stent.

To evaluate the safety of a new bioresorbable (non-permanent) stent platform in native coronary arteries.

BIONICS - Pharmacokinetics (PK) Trial/ BioNIR Ridaforolimus Eluting Coronary Stent.

This study will to evaluate the pharmacokinetic parameters of ridaforolimus release from the BioNIR stent.

Late Stent Strut Apposition and Coverage After Drug-Eluting Stent Implantation by OCT in Patients With AMI/ everolimus-eluting stent (EES) with bioabsorbable polymer (SYNERGY™ vs

Zotarolimus-Eluting stent with permanent polymer.

The purpose of this study is to evaluate the incidence of late incomplete stent apposition (ISA) and un-coverage following everolimus-eluting stent (EES) with bioabsorbable polymer (SYNERGY™, Boston Scientific, Natick, MA, USA) versus zotarolimus-eluting stent (ZES) with permanent polymer (Resolute Onyx™, Medtronic, Santa Rosa, CA, USA) implantation in patients with AMI at 12 months.

Efficacy Study of Drug-eluting and BMS in Bypass Graft Lesions/ Sirolimus-eluting stent vs paclitaxel-eluting stent vs biodegradable-polymer-based sirolimus-eluting stent vs bare metal stents.

The aim of this study is to compare the efficacy of DESs and bare metal stents to reduce reblockage of bypass grafts after coronary stenting.

ORSIRO sirolimus-eluting stent NOBORI biolimus-eluting stent/ vs Drug-eluting stent.

The aim of the Danish Organization for Randomized Trials with Clinical Outcome (SORT OUT) is to compare the safety and efficacy of the sirolimus eluting ORSIRO stent and the biolimus-eluting NOBORI stent.

Helistent Titan2 (Titanium coated stent) Titan2/ vs Endeavor™ (Zotarolimus-Eluting Stent) Endeavor.

A Randomized Comparison of a Titanium-Nitride-Oxide Coated Stent (Helistent Titan2, Hexacath) With a Zotarolimus-Eluting Stent (Endeavor™, Medtronic) for PCI.

Safety and Efficacy of Everolimus - Eluting Bioresorbable Vascular Scaffold for Cardiac Allograft Vasculopathy/ Everolimus-Eluting Bioresorbable Vascular Scaffold (ABSORB)

The CART Pilot study will evaluate the performance at one year of second-generation ABSORB Bioresorbable Vascular Scaffold (BVS), the Everolimus Eluting Bioresorbable Vascular Scaffold, in heart transplant recipients affected by cardiac allograft vasculopathy (CAV) and significative coronary stenosis.

Test Safety of Biodegradable and Permanent Limus-Eluting Stents Assessed by Optical Coherence Tomography/ Biodegradable polymer limus-eluting stents due randomization biodegradable polymer limus-eluting stents will be implanted vs Xience-V®

The objective of the study is to assess the superiority of the biodegradable polymer based limus-eluting stent (Nobori®) compared with the permanent polymer based everolimus-eluting stent (XIENCE V®) regarding absolute percentage of uncovered stent strut segments.

Trial to Demonstrate the Safety and Effectiveness of the MiStent II for the Revascularization of Coronary Arteries/ MiStent II coronary artery stent vs Xience or Promus coronary artery stents

To compare MiStent to either the Xience or Promus stents with the primary objective being to assess the safety and efficacy of the MiStent in a patient population.

Trial on Safety & Performance of TAXUS Element vs. XIENCE Prime Stent in Treatment of Coronary Lesion in Diabetics/ TAXUS Element™ Paclitaxel-Eluting Stent System vs Xience PRIME Everolimus-Eluting Stent System

The TUXEDO-India is a prospective, single blind, multi-center randomized clinical trial to assess the TAXUS Element™ in a consecutive population of diabetic patients with coronary artery disease undergoing coronary revascularization.

Test of Long-Term Safety and Efficacy of Sirolimus-Permanent-Polymer Eluting Stent (Cypher)- and Sirolimus-Polymer-free Eluting Stents (PPS/PFS) Assessed by Optical Coherence Tomography/ Sirolimus-Permanent-Polymer Eluting Stent vs Sirolimus-Polymer-free Eluting Stent

The objective of this pilot study is to compare the PFS-eluting stent (ISAR Rapa G1) with the PPS-eluting stent (Cypher®) regarding uncovered stent strut segments at 5 years.

Test Safety and Efficacy of Zotarolimus- and Everolimus-Eluting Stents (ZES/EES) Assessed by Optical Coherence Tomography/ Everolimus-Eluting-Stent vs Zotarolimus-Eluting-Stent

The objective of the study is to assess the superiority of the everolimus-eluting stent (Endeavor Resolute®) compared with the everolimus-eluting stent (XIENCE V®) regarding uncovered stent strut segments.

TAXUS® Element™ Paclitaxel-Eluting Coronary Stent System European Post-Approval Surveillance Study (TE-Prove).

The goal of the TAXUS™ Element™ Paclitaxel-Eluting Coronary Stent System European Post-Approval Surveillance Study is to evaluate real world clinical outcomes data for the TAXUS™ Element™ Coronary Stent System in unselected patients in routine clinical practice.

Optical Coherence Tomography Assessment of Intimal Tissue and Malapposition/ Biolimus-eluting stent vs Everolimus-eluting coronary stent

The purpose of this study is to use a high-resolution intracoronary imaging modality, called optical coherence tomography (OCT) to examine two different types of coronary artery stents used to treat patients with coronary artery disease.

Optimized Stenting Using Intravascular Ultrasound (IVUS) in Long Lesion: Rationale for Simplified criteria/ TAXUS™ Element long stent

OTELLO study is an ongoing trial sponsored by Boston Scientific Inc, to determine Major Adverse Cardiac Event with the new TAXUS Element stent.

Rapamycin-Eluting Stents With Different Polymer Coating to Reduce Restenosis (ISAR-TEST-3), Rapamycin-eluting stent with biodegradable polymer vs polymer-free, rapamycin-eluting stent vs rapamycin-eluting Stent with permanent polymer

The purpose of this study is to evaluate the efficacy of 3 different rapamycin-eluting-stent platforms to reduce coronary artery reblockage after stent implantation

The First-In-Man Pilot Study of Firehawk/ Rapamycin target-eluting Coronary Stent System

This is a small-scale pilot clinical study of the Rapamycin-Eluting Coronary Stent System of Microport for the first time to assess the preliminary safety and feasibility used in the human body.

Yonsei OCT (Optical Coherence Tomography) Registry for Evaluation of Efficacy and Safety of Coronary Stenting/ e.g. Sirolimus eluting stent, Paclitaxel-eluting stent, Zotarolimus-eluting stent, Everolimus-eluting stent, Biolimus eluting stent, EPC(endothelial progenitor cell) Capture stent, etc

We will evaluate the appropriateness of currently using coronary stents (e.g. Sirolimus eluting stent, Paclitaxel-eluting stent, Zotarolimus-eluting stent, Everolimus-eluting stent, Biolimus eluting stent, EPC(endothelial progenitor cell) Capture stent, etc) based on the findings of OCT.

3 Limus Agent Eluting Stents With Different Polymer Coating/ Biodegradable polymer Rapamycin-eluting stent vs permanent polymer rapamycin-eluting stent (Cypher) vs permanent polymer everolimus-eluting stent (Xience, Promus)

The aim of this study is to determine whether biodegradable polymer based rapamycin-eluting stent performs equal to permanent polymer based everolimus- and rapamycin-eluting stents regarding reduction of adverse cardiac events at one year.

Clinical Trial on the Efficacy and Safety of Sirolimus-Eluting Stent (MiStent® System)/ MiStent vs

TIVOLI

To evaluate the safety and efficacy of MiStent drug (sirolimus)-eluting stent system in the treatment of coronary heart disease (CHD) in patients with primary in situ CHD (de novo); To evaluate operating performance of the MiStent drug (sirolimus)-eluting coronary stent system.

Test Efficacy of Biodegradable and Permanent Limus-Eluting Stents/ Nobori® (Biodegradable polymer limus-eluting stents) vs Xience-V® (Permanent polymer limus-eluting stent)

The aim of this prospective, randomized study is to compare the efficacy and safety of biodegradable polymer based limus-eluting stents (BPDES) with permanent polymer based everolimus eluting stents (PPDES).

PROMUS™ Element™ Everolimus-Eluting Coronary Stent System European Post-Approval Surveillance Study/ PROMUS™ Element™ Everolimus Eluting Coronary Stent System

The goal of the PROMUS™ Element™ Everolimus-Eluting Coronary Stent System European Post- Approval Surveillance Study is to evaluate real world clinical outcomes data for the PROMUS™ Element™ Coronary Stent System in unselected patients in routine clinical practice.

PCI With the Angiolite Drug-eluting Stent: an Optical Coherence Tomography Study/ Angiolite stent

The purpose of this study is to perform a first-in-man assessment of feasibility, exploratory efficacy and clinical performance of the novel Angiolite DES (iVascular, Barcelona, Spain).

Firebird2 Cobalt-Chromium Alloyed Sirolimus-Eluting Stent Registry Trial/ Firebird2

A multi-center, prospective, non-controlled, non-randomized, single-arm clinical registry trial. The study will enroll 5,000 patients who receive the Firebird2™ Cobalt-Chromium Alloyed Sirolimus-Eluting Stent implantation.

Study of the Xience V Everolimus-eluting Stent in Saphenous Vein Graft Lesions/ Xience V coronary stent

The specific aim of the SOS-Xience V study is to examine the 12-month incidence of binary angiographic ISR after implantation of the Xience V stent in aortocoronary saphenous vein bypass graft lesions.

Sirolimus-eluting Stent CALYPSO vs Everolimus-eluting Stent XIENCE/ DES "Calypso" vs "Xience Prime"

The aim of the study is to evaluate the efficacy and safety of sirolimus-eluting coronary stent "Calypso" (Angioline, Russia) in comparison with everolimus-eluting coronary stent "Xience" (Abbott Vascular, USA).

Sirolimus-Eluting Versus Paclitaxel-Eluting Stents for Coronary Revascularization/ Sirolimus-eluting stent vs Paclitaxel-eluting stent

To determine differences in safety and efficacy between sirolimus and paclitaxel eluting stents.

Evaluation of New Specifications (38mm) of Firehawk™ in the Treatment of Coronary Heart Disease/ Rapamycin target-eluting coronary stent systems (38mm)

The purpose of this study is to evaluate the clinical safety and effectiveness of released specification (38mm) of Firehawk™ Sirolimus target-eluting coronary stent system.

Optimal Drug Eluting Stents Implantation Guided By Intravascular Ultrasound and Optical coherence tomography ORENBURG/ Xience Prime", "Xience V", "Promus Element", "Resolute Integrity", "Biomatrix Flex", "Nobori", "Orsiro".

The objective of this research is to assess the clinical results of implantation of different drug eluting stents under "aggressive" intravascular ultrasound (IVUS) guided all the way up to 24 months after operation and to establish the significance of the data of an optical coherent tomography (OCT) for the assessment of direct results of stenting and the degrees of endothelialization of stent after 6 months.

Efficacy and Safety of the YUKON Drug Eluting Stent in Diffuse Coronary Artery Disease/ High dose rapamycin stent vs Low dose rapamycin stent

This prospective, multicenter, randomized controlled clinical trials aimed to explore efficacy and safety of the YUKON drug eluting stent in diffuse coronary artery disease.

Soluble Receptors for Advanced Glycation End-Products and PCI/ Drug Eluting Stent vs Bare Metal Stent

The purpose of this pilot study is to afford invasive cardiologists with additional evidenced based information to guide their decision as to which patients should receive a BMS or DES for coronary implantation.

Cortisone or Drug Eluting Stents (DES) as Compared to BMS to Eliminate Restenosis/ Bare metal coronary stent vs Stenting with DES (Cypher or Taxus), Drug: Prednisone Bare metal stenting with administration of oral prednisone as described in the protocol

The aim of our study is to perform a multicenter, randomized study to assess the clinical efficacy and safety of the oral prednisone therapy after PCI as a possible systemic alternative to currently available BMS and DES.

A Prospective Evaluation in a Randomized Trial of TAXUS in the Treatment of De Novo Coronary Artery Lesions/ TAXUS Element Stent or TAXUS Express Stent

This study is to compare the safety and performance of two stents coated with the same drug (the TAXUS Element Paclitaxel-Eluting Coronary Stent System and the TAXUS Express2 Paclitaxel-Eluting Coronary Stent System).

Harmonizing Optimal Strategy for Treatment of Coronary Artery Stenosis - Safety & Effectiveness of Drug-Eluting Stents & Anti-platelet Regimen/ Everolimus-eluting coronary stenting system (EECSS, Promus Element) vs Zotarolimus-eluting coronary stenting system (ZECSS, Endeavor Resolute)

To compare the safety and long-term effectiveness of coronary stenting with the new platform Everolimus-Eluting coronary stenting system (EECSS, Promus Element) compared with the Zotarolimus-Eluting coronary stenting system (ZECSS, Endeavor Resolute) in patients with coronary heart disease (CHD)

Stent Coverage and Neointimal Tissue Characterization After Extra Long Everolimus - Eluting Stent implantation/ SYNERGY 48 mm

The objective of this study is to evaluate the rate of SYNERGY 48 mm stent strut coverage and assess neointimal progression via OCT measurement in patients who underwent PCI.

Relation Among Shear Stress Distribution, Stent Design, and Subsequent Vessel Healing After Drug-eluting Stent Implantation (SHEAR DES)/ Promus element vs Xience prime vs Nobori

The purpose of this study is to evaluate the differences of wall shear stress distribution among different types of DESs and its impact on vessel healing evaluated by intravascular optical coherence tomography evaluation.

ORSIRO Stents Versus Xience PRIME Stents Assessed by Optical Coherence Tomography/ ORSIRO vs XIENCE PRIME DES

This prospective, randomized trial will compare the extent of covered stent strut segments by assessed by Optical Coherence Tomography (OCT) of the ORSIRO DES with that of the XIENCE PRIME DES, which is the standard of choice of contemporary drug eluting stents (DES).

The Study of Active Transfer of Plaque Technique for Non-Left Main Coronary Bifurcation Lesions/ Sirolimus Drug-eluting Stent via Active Transfer of Plaque vs Sirolimus Drug-eluting Stent implantation via Provisional T Stenting

A Prospective Multi-center Randomized Trial Assessing the Efficacy and Safety of Active Transfer of Plaque vs. Provisional T Stenting for the Treatment of Non-Left-Main Coronary Bifurcation Lesions.

Efficacy of Everolimus-Eluting Versus Zotarolimus-Eluting Stent for Coronary Lesions in Acute MI/ Everolimus eluting stent vs Zotarolimus eluting stent

Comparison of the Efficacy of Everolimus-Eluting Versus Zotarolimus-Eluting Stent for Coronary Lesions in Acute MI

Prospective Assessment of Efficacy and Safety of Drug Eluting Stents

This study will examine the prognosis in groups with different brands of DES, and various real-life factors, that may affect patients recovery after the procedure.

Dexamethasone-Eluting Stent in Acute Coronary Syndrome to Prevent Restenosis/ Dexamethasone-Eluting Stent

In this study, by a special-designed, phosphorylcholine-coated stent, dexamethasone could be readily absorbed and then gradually released locally even 4 weeks after deployment.

A reduction of In-stent restenosis in ACS patient was expected by the method with no or few systemic adverse effect of steroid; and angiographic follow-up as well as intra-vascular ultrasound assessment would be performed according to pur protocol.

DXR Stent for Vascular Healing and Thrombus Formation: OCT Study/ DUAL Drug-eluting Stent (DXR Stent)

Evaluation of DUAL Drug-eluting Stent (DXR Stent) for Vascular Healing and Thrombus Formation

A Study Comparing Two Stent on the Degree of Early Stent Healing and Late Lumen Loss.The OCT-ORION Study/ Resolute Integrity Stent VS Biomatrix stent

In this study, stent coverage and neo-intimal growth between zotarolimus-eluting stents (ZES) and biolimus-eluting stents (BES) will be compared by using OCT at 9 month and specific post-intervention re-study intervals. The investigators objective is to investigate the clinical impact and OCT difference on early stent healing and late lumen loss between the two new-generation limus-eluting-stents - Resolute Integrity and Biomatrix, which differ in stent design, eluting drug and coating polymer.

Everolimus-eluting(PROMUS-ELEMENT) vs. Biolimus A9-Eluting(NOBORI) Stents for Long-Coronary Lesions/ Biolimus A9-eluting stentVS Everolimus-eluting stent

This randomized study is a multi-center, randomized, study to compare the efficacy of biolimus A9-eluting stent (Nobori) vs. everolimus-eluting stent (Promus Element) for long coronary lesions.

Procedural Advantages of a Novel Drug-Eluting Coronary Stent/ Synergy Stent VS Currently common DES

This study sought to compare procedural performance of a new coronary stent generation that is already available in Germany, with hitherto established current DESs

Everolimus Stent in Patients With Coronary Artery Disease/ XIENCE V drug eluting stent vs Abbot Vascular USA (Cypher drug eluting stent)

The aim of the study is to compare the everolimus eluting stent and sirolimus eluting stent in all comers PCI eligible patients

SERIES III RUN-IN Clinical Trial: A Comparison of the Supralimus® Stent With the Xience V™ Stent/ Supralimus(R) Sirolimus-Eluting Coronary Stent System vs Xience V™ Everolimus Eluting Coronary Stent

The objective of Series III Run-In Trial is to compare the performance and efficacy of the Supralimus® sirolimus-eluting stent with the Xience V™ everolimus-eluting stent with respect to in-stent luminal late loss at 9 months as assessed by off-line QCA. Ninety percent power to reject the null hypothesis that the Supralimus® stent is inferior to Xience V™ in favor of the alternative hypothesis that the Supralimus® stent is not inferior to Xience V™.

Randomized Study Comparing Endeavor With Cypher Stents (PROTECT)/ Medtronic Endeavor® Zotarolimus Eluting Coronary Stent System

The PROTECT TRIAL is a randomized stent trial with 8800 patients in approximately 200 hospitals, which is designed to evaluate whether the Endeavor stent PROTECTS against late stent thrombosis resulting in less deaths and myocardial infarctions.

OBORI Biolimus-Eluting Versus XIENCE/PROMUS Everolimus-eluting Stent Trial/ Biolimus-eluting stent vs Everolimus-eluting stent

The purpose of this study is to evaluate whether the newly-approved biolimus-eluting stent is not inferior to the everolimus-eluting stent in terms of the rate of target-lesion revascularization at 1-year and death or myocardial infarction at 3-year after stent implantation in the real world clinical practice.

OCT Evaluation of Early Healing of EPC Capturing (GENOUS) Stent (EGO Study)/ Coronary Intervention (GENOUS stent)

Evaluation of Endothelial Progenitor Cell (EPC) Capturing (GENOUS) Stent After Coronary Stenting Utilizing Optical Coherence Tomography (OCT): the EGO Study

Apposition Assessed Using Optical Coherence Tomography of Chromium Stents Eluting Everolimus From Cobalt Versus Platinum Alloy Platforms/ Cobalt Chromium Everolimus-

eluting stent (Xience Prime) VS Platinum Chromium Everolimus-eluting stent (Promus Element)

The purpose of the trial is to directly compare the Cobalt Chromium platform everolimus-eluting stent, Xience Prime™, with the Platinum Chromium platform everolimus-eluting stent, Promus Element™, in relation to stent scaffolding shape, position with the heart blood vessel and extent of tissue coverage (at 6 months) using optical coherence tomography.

Prospective Registry to Assess the Long-term Safety and Performance of the Combo Stent/ Combo stent

The REMEDEE REGISTRY evaluates the long-term safety and performance of the Combo stent in routine clinical practice. In total 1000 patients will be registered and followed for five years.

Non-inferiority Study Comparing Firehawk Stent With Abbott Xience Family Stent (TARGET-AC)/ Firehawk™ stent system vs Abbott Xience family Everolimus-Eluting Stent

The TARGET All comers trial is a prospective, multicenter, randomized, two-arm, non-inferiority, open-label study with 1656 patients at 20 centers in Europe.

Everolimus-eluting SYNERGY Stent Versus Biolimus-eluting Biomatrix NeoFlex Stent - SORT-OUT VIII/ Biomatrix NeoFlex coronary stent vs SYNERGY stent

The purpose of this study is to perform a randomised comparison between the SYNERGY and the Biomatrix NeoFlex stents in treatment of unselected patients with ischemic heart disease.

BioMime Vs. Xience Randomised Control Clinical Study/ Sirolimus Eluting Coronary Stent vs Everolimus-eluting Coronary stent

A Prospective, Active Control Open Label, Multicentre Randomized Clinical Trial for Comparison Between BioMime Sirolimus Eluting Stent and Xience Everolimus Eluting Stent to Evaluate Efficacy and Safety in Coronary Artery Disease.

Comparison of Zotarolimus-Eluting Stent vs Sirolimus-Eluting Stent for Diabetic Patients/ Endeavor Resolute stent vs Cypher stent

The purpose of this study is to establish the safety and effectiveness of coronary stenting with the Zotarolimus-Eluting stent compared to the Sirolimus-Eluting stent in the treatment of de novo coronary stenosis in patients with diabetic patients.

Safety and Efficacy Study of Kaname Coronary Stent System for the Treatment of Patients With Coronary Artery Disease/ Kaname cobalt-chromium coronary stent

The purpose of this study is to assess whether the new Kaname coronary stent is safe and effective for the treatment of patients with coronary artery disease.

Treatment of Coronary ARtery bifurcation Narrowing by AXxess Stent Implantation/ Axxess™ Biolimus A9™ Eluting Coronary Bifurcation Stent System

The Axxess™ Biolimus A9™ Eluting Coronary Bifurcation Stent System is a dedicated bifurcation stent, designed to cover the lesion at the level of the carina. In the present registry the investigators report the performance and the efficacy of the self-expanding biolimus-eluting Axxess™ stent for the treatment of bifurcation lesions in a real-world population.

European Multicenter, Randomized, Comparative Efficacy/Safety Study of the Mar-Tyn TiN-Coated Stent/ Mar-Tyn TiN coated CoCr Numen stent VS Vision CoCr stent implant

The main objective of this study is to assess the safety and effectiveness of the TiN-coated MAR-Tyn stent in maintaining minimum lumen diameter in de novo native coronary artery lesions as compared to an uncoated control cobalt-chromium balloon-expandable stent (Vision, Abbott Vascular). Both stents are mounted on a Rapid Exchange Stent Delivery System.

Firebird 2 Versus Excel Sirolimus-eluting Stent in Treating Real-world Patients With Coronary Artery Disease/ Firebird 2 sirolimus-eluting stent vs Excel sirolimus-eluting stent

Sirolimus-eluting stent (SES) has been world-widely used in clinical practice in treating patients with coronary artery disease. The efficacy and safety of Excel SES (JW Medical, Shandong, China, MA) with biodegradable polymer has been proved by several clinical trials. Here the investigators design a prospective, multicenter, randomized clinical study in purpose of identifying the non-inferiority in the efficacy and safety in treating coronary artery

disease patients by Firebird 2 SES (Microport, Shanghai) with durable polymer, comparing with Excel SES.

Efficacy and Safety of RESOLUTE Zotarolimus-Eluting Stent in Treatment of Chinese Diabetic Coronary Lesions/ Resolute stent treatment

This study sets out a multicenter, non-inferiority study: the efficacy and safety of RESOLUTE zotarolimus-eluting stents in treatment of Chinese diabetes (RESOLUTE-DIABETES CHINA) in purpose of identifying the efficacy and safety in Asia coronary artery disease correlated with diabetic population.

A Study to Examine the Implantation Characteristics of Two Drug-Eluting Stents/ Coronary Stent
Cypher vs

Coronary stent Xience

This study will use OCT to examine how two different types of commonly used DESs relate to the artery wall. The Xience V (Abbott Vascular, USA) stent has thinner struts and a more open frame than the Cypher (Cordis, USA) stent.

The TRIMAXX Coronary Stent Trial/ TriMaxx Coronary Stent placement

The primary objective of the trial is to demonstrate the safety and feasibility of treating coronary artery lesions which have not been previously treated with the TRIMAXX Coronary stent system as compared to the reported results for commercially available non-drug eluting coronary stent systems which are indicated for the same treatments.

Comparison of Biolimus-eluting Biodegradable Polymer, Everolimus-eluting and Sirolimus-eluting Coronary Stents/ Everolimus-eluting stent (Promus Element®) and biolimus-eluting stent with biodegradable polymer (Nobori®)

To compare the safety and efficacy of coronary stenting with everolimus-eluting stent (Promus Element®) and biolimus-eluting stent with biodegradable polymer (Nobori®)

The Treatment of Coronary Artery Lesions Using the PRO-Kinetic Energy Cobalt-Chromium, Bare-Metal Stent/ PRO-Kinetic Energy Stent Bare-metal stent

The purpose of this study is to assess the clinical performance of the BIOTRONIK PRO-Kinetic Energy stent in subjects with atherosclerotic disease of native coronary arteries.

Wall Shear Stress and Neointimal Healing Following PCI in Angulated Coronary Vessels/ Device: Resolute Integrity Zotarolimus eluting stent vs Xience Xpedition everolimus eluting stent

This study will evaluate the effects of 2 FDA-approved metallic stents with different designs that may have important effects on regional plaque response and blood flow dynamics immediately after stent deployment and stent healing at 12 months follow up.

Self-apposing Stentys Stents Registry/ Drug-eluting stent

The aim of this study is to assess the feasibility, the effectiveness and the safety of the implantation of self-apposing, drug-eluting Stentys stents for PCI.

The Initial Double-Blind Drug-Eluting Stent vs Bare-Metal Stent Study./ Sirolimus coated Bx Velocity™ vs Bare metal Bx Velocity™

The main objective of this study is to assess the safety and effectiveness of the sirolimus coated Bx VELOCITY stent in reducing angiographic in-stent late loss in de novo native coronary lesions as compared to the bare metal Bx VELOCITY balloon-expandable stent.

Study Examining the PROMUS Element Everolimus-eluting Stent in Multi-center Coronary Intervention of Complex Arterial Lesion Subsets/ Platinum chromium everolimus-eluting stent

Study Examining the PROMUS Element Everolimus-eluting Stent in Multi-center Coronary Intervention of Complex Arterial Lesion Subsets

Intra-Individual Comparison of Sirolimus and Paclitaxel Coated Stent (FRE-RACE Study)/ Paclitaxel-eluting TAXUS™ vs Sirolimus eluting Cypher Select(TM)

The main objective of this study is to assess the safety and effectiveness of the Sirolimus eluting Cypher Select(TM) stent in reducing angiographic in-stent late loss in de novo native coronary lesions as compared to the TAXUS(TM) Paclitaxel-eluting stent in patients presenting with two or more coronary artery stenoses (prospective, randomized, intra-individual comparison).

OCT Evaluation 3 Months After Sirolimus Eluting Stent Implantation/ Sirolimus Eluting Stent Inspiron vs Bare Metal Stent

Prospective, single center, randomized and non-inferiority study for evaluating the Sirolimus eluting stent.

Japan-Drug Eluting Stents Evaluation; a Randomized Trial/ TAXUS stent vs Cypher stent

To evaluate the procedural, short and long term clinical outcomes of the TAXUS stent compared to Cypher stent in coronary arteries of ≥ 2.5 and ≤ 3.75 mm.

Nordic Bifurcation Study. How to Use Drug Eluting Stents (DES) in Bifurcation Lesions?/ Drug Eluting Stents (DES)

How to use drug eluting stents (DES) in bifurcation lesions. A strategy of routine stenting of both main vessel and side branch versus a strategy of routine main vessel stenting and optional treatment of side branch.

The Medtronic Endeavor III Drug Eluting Coronary Stent System Clinical Trial/ Endeavor Drug Eluting Coronary Stent System coated with ABT-578 vs Cypher Sirolimus-Eluting Coronary Stent

To demonstrate the equivalency in in-segment late lumen loss at 8 months between the Endeavor Drug Eluting Coronary Stent System coated with ABT-578 (10 micrograms/mm) and the Cypher Sirolimus-Eluting Coronary Stent System for the treatment of single de novo lesions in native coronary arteries.

The ENDEAVOR IV Clinical Trial: A Trial of a Coronary Stent System in Coronary Artery Lesions/ Endeavor stent is equivalent in safety and efficacy to the Taxus stent

The purpose of this study is to assess the equivalence in safety and efficacy of the Endeavor Drug Eluting Coronary Stent System when compared to the Taxus Paclitaxel-Eluting Coronary Stent System for the treatment of single de novo lesions in native coronary arteries.

Registry to Evaluate the Efficacy of Zotarolimus-Eluting Stent/ Endeavor Resolute stent vs Endeavor Sprint stent

The objective of this study is to evaluate the safety and long-term effectiveness of coronary stenting with the zotarolimus eluting stent (ZES) and to determine clinical device and procedural success during commercial use of ZES.

Treatment of Bifurcated Coronary Lesions With Cypher™-Stent/ PCI of bifurcated coronary lesions using sirolimus coated stents in modified T-Stenting -Technique

This study is a prospective, randomized, single-center evaluation of the Cypher™ Sirolimus eluting coronary stent system in the treatment of de novo bifurcated coronary lesions comparing provisional modified T stenting with systematic modified T-stenting.

Efficacy of Xience/Promus Versus Cypher in rEducating Late Loss After stenting/ Everolimus-eluting stent (Xience or Promus) vs Sirolimus-eluting stent (Cypher)

To evaluate the safety and long-term effectiveness of coronary stenting with the Everolimus-eluting coronary stent system (EECSS) (XIENCETM V, Abbott Vascular, Santa Clara, CA, PromusTM, Boston Scientific, Natick, MA), compared with the sirolimus-eluting coronary stent system (SECSS) (CypherTM, Cordis Johnson & Johnson, Warren, NJ) in the treatment of coronary stenosis. To evaluate the safety and efficacy of 6-month clopidogrel therapy compared with 12-month clopidogrel therapy.

Evaluation of Sirolimus-Eluting, Heparin-Coated CoCr Stent in the Treatment of de Novo Coronary Artery Lesions in Small Vessels (EVOLUTION)/ Sirolimus eluting vs Heparin coated CoCr stent

The objective of this study is to assess the performance and safety of a sirolimus-eluting, heparin-coated, cobalt chromium balloon-expandable stent (Small Vessel Stent) in patients with de novo native coronary artery lesions in small vessels as compared to historical data from small vessel patients in the RAVEL trial receiving the Sirolimus-eluting Bx VELOCITY™ stent.

BIOTRONIK Orsiro Pre-Marketing Registration

The clinical investigation is a non-inferiority, multicenter, blinding evaluation, randomized, parallel controlled clinical study. All subjects will receive the BIOTRONIK Orsiro SES or the Abbott Xience Prime™ EES to evaluate the efficacy and safety of the SES drug eluting stent in the treatment of coronary artery disease.

A Study of the Cypher SES to Treat Restenotic Native Coronary Artery Lesions./ Cypher™ sirolimus-eluting stent.

The main objective of this study is to assess the safety and effectiveness of the Cypher™ sirolimus-eluting stent in reducing angiographic in-lesion late loss in patients with an in-stent restenotic native coronary artery lesion.

FIM-NL - First-in-Man Study (Netherlands Part) With Sirolimus Coated Modified Bx Velocity Stent/ Sirolimus-coated Bx VELOCITY Stent

The objective of this study is to assess the performance and safety of a formulation of the antiproliferative agent, sirolimus coated on modified Bx VELOCITY Balloon-Expandable Stent mounted on the Raptor Over The Wire (OTW) Stent Delivery System (SDS) in patients with de novo coronary artery lesions.

First-in-man Trial Examining the Safety and Efficacy of BuMA Supreme and Resolute Integrity in Patients With de Novo Coronary Artery Stenosis/ BuMA Supreme Biodegradable drug coating coronary stent vs Resolute Integrity durable polymer stent system.

Prospective, multi-center, randomized 1:1, single blind trial using BuMA Supreme versus Resolute Integrity conducted in approximately 14 interventional cardiology centers.

First-In-Human Trial of the MiStent Drug-Eluting Stent (DES) in Coronary Artery Disease/ Sirolimus-eluting MiStent SES.

The DESSOLVE I clinical trial is to assess the safety and performance of the sirolimus-eluting MiStent SES.

Sirolimus-Eluting Stents for Chronic Total Coronary Occlusions/ Sirolimus-eluting stent
Sirolimus-Eluting Stents for Chronic Total Coronary Occlusions: A Randomized Comparison of Bare Metal Stent Implantation With Sirolimus-Eluting Stent Implantation for the Treatment of Chronic Total Coronary Occlusions (PRISON II)

A Safety and Efficacy of Supralimus™ Core™ Sirolimus Eluting Stent at MAX DDHV Institute/ Supralimus-Core™

The primary objective of this study is to assess the safety and efficacy of the Supralimus - Core™ Sirolimus Eluting Stent in de novo native vessel obstructive coronary artery disease.
Multicenter Comparison of Early and Late Vascular Responses to Everolimus-eluting Cobalt-CHromium Stent/ Everolimus-eluting cobalt- chromium stent (everolimus-eluting stent: EES, Xience Prime, Xpedition)

To treat patients with stable coronary artery disease, elective PCI (PCI) will be performed with the use of an everolimus-eluting cobalt- chromium stent (everolimus-eluting stent: EES, Xience Prime, Xpedition), which is the current standard DES. Vascular responses at the site of stent placement will be evaluated by optical coherence tomography (OCT) at 1 or 3 months and at 12 months after stent placement, along with observation of changes over time in the target vessel. The relationships between OCT findings and the time course of platelet aggregation and between OCT findings and the occurrence of major cardio- cerebrovascular events will also be elucidated.

Orsiro™ Drug Eluting Stent in Routine Clinical Practice/ Orsiro™ Drug Eluting Stent group
The purpose of this study is to evaluate effectiveness and safety of Orsiro™ Drug Eluting Stent in Routine Clinical Practice

Comparison of Neointimal Coverage Between Zotarolimus Eluting Stent and Everolimus Eluting Stent/ Zotarolimus eluting stent (Endeavor resolute - ZES resolute) vs Everolimus eluting stent (Xience - EES)

This study will investigate the pattern of neointimal coverage over stent in ZES resolute and EES at 9 months after stent implantation.

Resolute Integrity US Extended Length Sub-Study(RI US XL)/ Resolute Integrity Stent DES

The purpose of this postapproval study is to conduct a prospective, multi-center evaluation of the procedural and clinical outcomes of subjects that are treated with the commercially available 34 mm and 38 mm Medtronic Resolute Integrity Zotarolimus-Eluting Coronary Stent System.

Study of Sirolimus-Coated BX VELOCITY Balloon-Expandable Stent in Treatment of de Novo Native Coronary Artery Lesions (SIRIUS)/ CYPHER Sirolimus-Eluting Stent vs Uncoated BX VELOCITY Balloon-Expandable Stent

The main objective of this study is to assess the safety and effectiveness of the sirolimus-coated Bx VELOCITY™ stent in reducing target vessel failure in de novo native coronary artery lesions as compared to the uncoated Bx VELOCITY™ balloon-expandable stent.

Evaluation of a Thin Strut Metallic Stent: DynamX Stent Clinical Study/ DynamX Novolimus-eluting coronary stent system

The DynamX stent study is a consecutive enrolling, prospective, multicenter clinical trial recruiting up to 50 patients at up to 10 international sites.

Spot Drug-Eluting Stenting for Long Coronary Stenoses/ Drug-eluting stents (Cypher and Taxus)

We hypothesized that an approach based on spot-stenting with the use of DES might result in superior clinical outcomes compared to full cover of atheromatic lesions with long or multiple stents. We are therefore conducting a randomized comparison of spot versus multiple overlapping stenting on consecutive patients with long (>20 mm) lesions and indications for PCI.

Study of the 4.0mm Sirolimus-Eluting Stent in the Treatment of Patients With Coronary Artery Lesions/ Device: 4.0 CYPHER Sirolimus-Eluting Coronary Stent

The main objective of this study is to assess the safety and effectiveness of the sirolimus-eluting Bx VELOCITY™ stent in reducing in-lesion late loss in patients with de novo native coronary artery lesions.

Medtronic RevElution Trial/ Polymer-free DES (Drug Eluting Stent)

The purpose of this trial is to evaluate the clinical safety and efficacy of the Polymer-Free Drug-Eluting coronary stent system for the treatment of de novo lesions in native coronary arteries with a reference vessel diameter (RVD) that allows use of stents between 2.25 and 3.50 mm in diameter.

In Stent ELUTES Study/ DES coronary stent

This trial will compare the long term safety and effectiveness of the V Flex Plus PTX Drug Eluting coronary stent with conventional treatment for ISR for coronary arteries.

First in Man Experience With a Drug Eluting Stent in De Novo Coronary Artery Lesions/ ORSIRO - Drug Eluting Coronary Stent

The objective of this trial is to assess the safety and clinical performance of the ORSIRO drug eluting stent in patients with single de-novo coronary artery lesions.

Evaluation of Everolimus-Eluting Stents (The K-XIENCE Registry)/ Xience

The objective of this study is to evaluate effectiveness and safety of everolimus-eluting stents (XIENCE, Abbott) in the "real world" daily practice as compared with first-generation DESs (sirolimus-eluting stents).

ACROSS-Cypher Total Occlusion Study of Coronary Arteries 4 Trial/ Cypher sirolimus eluting coronary stent

ACROSS-Cypher® is a prospective, multi-center, open label, single arm study of the Cypher® sirolimus eluting coronary stent in native total coronary occlusion revascularization. The primary endpoint is binary angiographic restenosis at 6 months. The hypothesis is that compared with TOSCA-1 patients who were treated with the heparin-coated Palmaz Schatz stent, treatment with the Cypher® sirolimus eluting coronary stent will result in a >50% relative reduction in 6 month restenosis within the treated segment of the target vessel.

PREVENT: Promus BTK/ Everolimus-Eluting Stent (PROMUS ELEMENT)

This is a single-arm, prospective, multi-center monitored trial recruiting patients with critical limb ischemia and with one or more lesions in the arteries below the knee. The immediate and long-term (up to 12 months) outcome of the PROMUS ELEMENT Everolimus-Eluting Stent System (Boston Scientific) and the PROMUS ELEMENT PLUS Everolimus-Eluting Stent System (Boston Scientific) will be evaluated.

The Nordic-Baltic Bifurcation Study IV/ Implantation of coronary stent in bifurcation lesion

The 2-stent strategy is superior to the 1-stent strategy regarding occurrence of cardiac death, non-procedure related myocardial infarction and re-revascularization with PCI or coronary artery bypass grafting (CABG).

Comparison of Neointimal coverage between ZES and EES Using OCT at 3 Months/
Device: ZES resolute (Endeavor Resolute) Device: EES (Xience)

This study will evaluate the neointimal coverage and malapposition at 3 month after new zotarolimus eluting stent (Endeavor resolute) and everolimus eluting stent (Xience) implantation and compare them between ZES resolute and EES at 3 months (early period) after stent implantation.

BES, EES, and ZES-R in Real World Practice/ Biolimus-eluting stent vs Everolimus-eluting stent vs Zotarolimus-eluting stent

The primary objective of this study is to compare the rate of device-oriented composite consisted of cardiac death, myocardial infarction not clearly attributable to a nontarget vessel, and clinically indicated TLR among the patients treated with EES, ZES-R, or BES at 24-month clinical follow-up post-index procedure. The hypothesis is that BES is equivalent to EES or BES is equivalent to ZES-R at the primary end point.

RESOLUTE ONYX Post-Approval Study/ Resolute Onyx™ Zotarolimus-Eluting Coronary Stent System

To observe the continued performance of the Medtronic Resolute Onyx™ Zotarolimus-Eluting Coronary Stent System in a real-world more-comer population.

The OMEGA Clinical Trial/ OMEGA™ Monorail Coronary Stent System

The purpose of this study is to evaluate the safety and effectiveness of the OMEGA Coronary Stent System for the treatment of subjects with a de novo atherosclerotic coronary artery lesion.

TAXUS PERSEUS Workhorse/ Paclitaxel-eluting stent (TAXUS Element) vs Paclitaxel-eluting stent (TAXUS Express)

The purpose of the TAXUS PERSEUS Workhorse trial is to evaluate the safety and efficacy of the next-generation Boston Scientific TAXUS paclitaxel-eluting coronary stent system (TAXUS® Element™) for the treatment of de novo atherosclerotic lesions of up to 28 mm in length in native coronary arteries of 2.75 mm to 4.0 mm diameter.

MASCOT - Post Marketing Registry/ Combo Bio-Engineered Sirolimus Eluting Stent

To collect post marketing surveillance data on patients receiving at least one Combo Bio-Engineered Sirolimus Eluting Stent when used according to the Instructions for Use.

V-Flex Plus PTX Drug Eluting Coronary Stent/ DES

The study is intended to collect data to evaluate effectiveness and safety of drug eluting stent devices in a dose ranging assessment.

DELIVER Study: DELiverability of the Resolute Integrity Stent in All-Comer Vessels and Cross-Over Stenting

The primary objective of the DELIVER Study is to assess the deliverability of the Resolute Integrity Stent as primary stent or as a secondary cross-over stent following delivery failure of another stent type in real world patients.

A Study to Evaluate the Efficacy and Safety of BuMA Supreme Drug Eluting Stent(DES)/ BuMA Supreme Drug Eluting Stent(DES)

PIONEER-II OPC trial is a prospective, multicenter, single-arm registry trial which will evaluate the TLF as the primary endpoint at 1 year.

Bifurcation Stenting Using 2 Link Stent Nobori Versus 3 Link Stent Xience/ DESs with different link number (2-link Nobori and 3-link Xience)

The primary objective of this study is to make a comparison of safety and efficacy of DESs with different link number (2-link Nobori and 3-link Xience) in patients with de novo true bifurcation lesions.

Medtronic Resolute Onyx 2.0 mm Clinical Study/ Device: Resolute Onyx Stent - 2.0 mm

The purpose of this trial is to assess the safety and efficacy of the Resolute Onyx Zotarolimus-Eluting Coronary Stent System for the treatment of de novo lesions in native coronary arteries that allows the use of a 2.0 mm diameter stent.

Evaluation of Effectiveness and Safety of BIOMATRIX Stent (IRIS-BIOMATRIX)/ BioMatrix Biolimus A9-eluting coronary stent

The objective of this study is to evaluate the effectiveness and safety of BioMatrix stent in the "real world" daily practice as compared with first-generation DESs (sirolimus- or paclitaxel-eluting stents).

Retrospective Study of the Impact of Drug Eluting Stents/ Drug Eluting Stents

The purpose of this study is to determine whether the use of drug eluting stents is associated with higher rates of death, myocardial infarction, and major bleeding.

Clinical Investigation of the MiStent Drug Eluting Stent (DES) in Coronary Artery Disease/ MiStent DES vs Endeavor DES

The DESSOLVE II clinical trial is to assess the safety and performance of the sirolimus-eluting MiStent for the treatment for improving coronary luminal diameter in patients with symptomatic ischemic heart disease due to discrete de novo lesions in the native coronary arteries.

Direct Stenting of TAXUS Liberté™-SR Stent for the Treatment of Patients With de Novo Coronary Artery Lesions/ TAXUS™ Liberté™ Paclitaxel-Eluting Coronary Stent

The primary objective is to compare outcomes of direct stenting with balloon catheter predilatation.

Everolimus-Eluting Bioresorbable Scaffolds Versus Everolimus-Eluting Metallic Stents for Diffuse Long Coronary Artery Disease/ Everolimus-eluting bioresorbable vascular (Absorb) scaffold

vs everolimus-eluting cobalt-chromium (Xience) stent

The purpose of this study is to determine whether ABSORB bioresorbable vascular scaffold is non-inferior to XIENCE everolimus-eluting cobalt-chromium stent with respect to TLF at 1 year.

Clinical Trial of Abluminus DES+ Sirolimus Eluting Stent Versus Everolimus-eluting DES/ Abluminus DES vs Everolimus-eluting DES

The objective of the study is to compare angiographic and clinical performance of Abluminus DES+ versus Everolimus-eluting DES in patients with diabetes mellitus.

Korean Nationwide Multicenter Pooled Registry of Drug-Eluting Stents/ Biomatrix vs Biomatrix Flex vs Nobori vs Xience Prime vs Xience V/Promus vs Cypher vs DP-ZES-RI vs Endeavor Resolute

The objective of this study is to evaluate the long-term efficacy and safety of coronary stenting with the various types of DES and to determine clinical device and procedural success during commercial use of DES in the real world.

CYPHER™ Stent Post-Marketing Surveillance Registry (US-PMS)/ Device: CYPHER Sirolimus-Eluting Coronary Stent

The purpose of the e-CYPHER Stent Registry is to collect post marketing surveillance data on the CYPHER™ Sirolimus-eluting Coronary Stent following marketing approval, when used in normal clinical practice within the labeled indications.

BIOFLOW-III UK Satellite Registry Orsiro Stent System/ Orsiro Drug-Eluting Stent

Clinical evaluation of the Orsiro LESS in subjects requiring coronary revascularization with Drug Eluting Stents (DES).

The ELUTES Clinical Trial/ Paclitaxel Eluting V-Flex Plus coronary stent

ELUTES is a European multicenter, randomized, controlled, triple-blinded study designed to evaluate the ability of the Paclitaxel Eluting V-Flex Plus coronary stent to reduce restenosis in the coronary artery.

The PzF Shield Trial/ COBRA PzF NanoCoated cobalt chromium stent platform

This is a prospective, multi-center, non-randomized, single arm clinical trial that will be conducted at up to 40 sites. This study will enroll patients with symptomatic ischemic heart disease due to a single de novo lesion contained within a native coronary artery with reference vessel diameter between 2.5 mm and 4.0 mm and lesion length ≤ 24 mm that is amenable to PCI (PCI) and stent deployment.

Registry to Evaluate Efficacy of Xience/Promus Versus Cypher in Reducing Late Loss After Stenting/ Xience, Promus vs Cypher

The objective of this study is to evaluate the safety and long-term effectiveness of coronary stenting with the everolimus-eluting stent (EES) and to determine clinical device and procedural success during commercial use of EES in the real world. The investigators will compare EES (Xience/Promus, prospective arm) with sirolimus-eluting stent (SES, Cypher, retrospective arm).

LEADERS FREE II: BioFreedom™ Pivotal Study/ BioFreedom™ Drug Coated Stent vs Gazelle™ Bare Metal Stent

This study aims to confirm non-inferiority of the BioFreedom™ Drug Coated Stent to the Gazelle™ Bare Metal Stent arm of the Leaders Free study in high bleeding risk patients.

The Medtronic RESOLUTE Clinical Trial/ Endeavor Resolute Zotorolimus Eluting Coronary Stent

To evaluate the clinical safety, efficacy, and pharmacokinetics (PK) of the Endeavor Resolute Zotorolimus Eluting Coronary Stent System for the treatment of single de novo lesions in native coronary arteries with a reference vessel diameter (RVD) between 2.5 and 3.5 mm in diameter.

A Registry To Evaluate Safety And Effectiveness Of Everolimus Drug Eluting Stent For Coronary Revascularization/ Everolimus Drug Eluting Stent

This is a prospective, multi-center registry to evaluate safety and effectiveness of the Everolimus Drug Eluting Stent for treatment coronary revascularization in Chinese patients with long lesion, small vessel or multi-vessel diseases.

XIENCE V® Everolimus Eluting Coronary Stent System USA Post-Approval Study (XIENCE V® USA Long Term Follow-up Cohort)/ XIENCE V® EECSS

XIENCE V USA is a prospective, multi-center, multi-cohort post-approval study. The objective of this study is to evaluate the XIENCE V EECSS continued safety and effectiveness during commercial use in real world settings, and to support the FDA DAPT initiative.

BIOTRONIK - BIOFLOW-III Registry French Satellite/ Orsiro less Drug Eluting Stent (DES)

This observational registry has been designed to investigate and collect clinical evidence for the clinical performance and safety of the Orsiro Drug Eluting Stent System in an all-comers patient population in daily clinical practice.

XIENCE V: SPIRIT WOMEN Sub-study/ XIENCE PRIME™ vs CYPHER SELECT

The purpose of this Clinical Evaluation is the assessment of the XIENCE Everolimus Eluting Coronary Stent System (XIENCE V® and XIENCE PRIME™ EECSS) with the primary focus on clinical outcomes in the treatment of female patients with de novo coronary artery lesions, and the characterization of the female population undergoing stent implantation with a XIENCE stent.

Randomized Trial Evaluating Slow-Release Formulation TAXUS Paclitaxel-Eluting Coronary Stents to Treat De Novo Coronary Lesions/ TAXUS Paclitaxel-Eluting Coronary Stent vs Slow-Formulation

The primary objective of this study is to further evaluate the safety and effectiveness of the TAXUS Express2 Paclitaxel-Eluting Coronary Stent System in long lesion lengths, small and large vessel diameters and with multiple overlapping stents in the treatment of de novo coronary artery lesions

China Made Sirolimus Eluting Stent for Intermediate Lesion/ China-made SES (Firebird 2 and Excel)

Sirolimus-eluting stent (SES) has been proven to improve outcomes in patients with significant coronary artery disease (> 70% lumen diameter narrowing). But, acute coronary syndrome may occur in those with intermediate lesions (50%-70% lumen diameter narrowing), and the effect of SES in these patients remains unclear. Here the investigators hypothesize that application of China-made SES may improve the clinical outcomes in these setting.

A Study of the TAXUS Liberté Stent for the Treatment of de Novo Coronary Artery Lesions in Small Vessels/ TAXUS Liberté-SR vs TAXUS™ Express2

The objective of the study is to evaluate clinical and angiographic outcomes of TAXUS Liberté-SR 2.25 mm stent in de novo lesions. The hypothesis is that the TAXUS Liberté-SR stent has non-inferior safety and efficacy to the TAXUS Express-SR stent in the treatment of de novo lesions in small coronary vessels.

A Multi-center Post-Market Surveillance Registry/ Drug-eluting stent

This multicenter, prospective, observational registry will evaluate the safety and performance of the CYPHER SELECT™ Sirolimus-eluting Coronary Stent, and of all future generation of commercially approved Cordis Sirolimus-eluting Stents (SES), in routine clinical practice. Single Long vs Two Short Overlapping Bioabsorbable Polymer DES/ Bioabsorbable polymer DES

The study is a spontaneous randomized multicenter open-label study. The long stent group (Group A) will be treated by a single 44mm Biomime DES (II generation DES with bioabsorbable polymer, Meril Life Sciences Pvt. Ltd., Gujarat, India). The short stent group (Group B) will be treated by 2 short Biomime DES positioned with minimal overlapping. The primary end-point of the study will be the 6 month in-stent late lumen loss. Secondary end-points will be 1, 6 and 12 month overall mortality, myocardial infarction, target vessel revascularization, stent thrombosis and MACE (combination of the 3 previous clinical end-points).

Xience, Promus for Long Coronary Lesion Registry/ Everolimus-eluting coronary stents

The utilization of everolimus-eluting coronary stents in a coronary artery diseases is effective in reducing both repeat revascularization and major adverse cardiac events within two year follow-up. To evaluate the procedural, short and long term clinical outcomes of multiple everolimus-eluting coronary stent implantation in long (>30mm) coronary lesions.

The Study to Compare Cypher Versus Cypher Select in Treating Coronary Artery Lesions./ Cypher Select vs Cypher

The main objective of this study is to assess the safety and effectiveness of the CYPHER SELECT™ Sirolimus-eluting Coronary Stent in reducing angiographic in-stent late loss in de novo native coronary lesions as compared to the CYPHER™ Sirolimus-eluting Coronary Stent.

NEXUS Study for the Treatment of de Novo Native Coronary Artery Lesions/ CYPHER NxT SES ON BX SONIC OTW STENT DELIVERY SYSTEM (SDS)

The objective of this study is to evaluate the effectiveness and safety of the CYPHER NxT Sirolimus-eluting Coronary Stent on the BX SONIC Over-the-Wire (OTW) Stent Delivery System (SDS) in patients with de novo native coronary artery lesions.

Excel Drug-Eluting Stent Pilot Clinical Registry/ Excel Drug-eluting stent

The Trial aims to evaluate long-term efficiency of Excel stent in the inhibition of restenosis as well as the safety after the cessation of the 6-month anti-platelet drug treatment.

A Prospective Multicenter Post Approval Study to Evaluate the Long-term Safety and Efficacy of the Resolute Integrity in the Japanese All-comers Patients With Coronary Artery Disease (PROPEL)/ Zotarolimus-eluting resolute stents vs Everolimus-eluting xience V

This is a prospective, multicenter, historical controlled study. The selected historical control is the Xience V arm from RESOLUTE All-Comer clinical study, that study is a prospective, multicenter, randomized, two-arm, international, open-label study.

Cynergy: the CYPHER-NEVO Registry/ CYPHER Select® Plus Sirolimus-eluting Coronary Stent (SES)

The purpose of this registry is to compare the safety and the performance of the NEVO™ Sirolimus-eluting Coronary Stent, to the CYPHER Select® Plus Sirolimus-eluting Coronary Stent in complex subjects presenting with acute STEMI for primary intervention, diabetes mellitus or multi vessel disease. The second purpose of this registry is to evaluate the safety and performance of the NEVO™ Sirolimus-eluting Coronary Stent, once commercially available and the CYPHER Select® Plus Sirolimus-eluting Coronary Stent in complex subjects diagnosed with acute STEMI for primary intervention, diabetes mellitus and/or multi vessel disease.

Comparison of BuMA eG Based BioDegradable Polymer Stent With EXCEL Biodegradable Polymer Sirolimus-eluting Stent in "Real-World" Practice/ BuMA eG Based BioDegradable Polymer Stent vs EXCEL Biodegradable Polymer Sirolimus-eluting

PANDA III is sought to investigate the safety and efficacy of a PLGA-polymer with electro-grafting base layer sirolimus-eluting stent (SES) versus a PLA-polymer SES at 12 months follow-up.

Evaluation of the GTX™ 5126 DES Coronary Stent System in the Treatment of Patients With a Lesion in the Coronary Artery/ GTX™ Drug Eluting Coronary Stent

The GTX™ Drug Eluting Coronary Stent System is intended for the treatment of patients with a lesion in the coronary artery.

A Study of the TAXUS Liberté Stent for the Treatment of Long De Novo Coronary Artery Lesions/ TAXUS Liberté-SR vs TAXUS™ Express

TAXUS ATLAS is a global, multi-center, single-arm, non-inferiority trial comparing results from patients treated with the TAXUS Liberté 38 mm stent to an historical TAXUS Express control. The objective of the study is to evaluate clinical outcomes of TAXUS Liberté-SR 38 mm stent in de novo lesions and to assess the non-inferiority of TAXUS Liberté versus TAXUS Express.

ABSORB II Randomized Controlled Trial/ Device: XIENCE Everolimus Eluting Coronary Stent S vs Abbott Vascular ABSORB Everolimus Eluting Bioresorbable Vascular Scaffold System

Prospective, randomized (2:1), active control, single blinded, parallel two-arm, multi-center clinical investigation using Abbott Vascular ABSORB Everolimus Eluting Bioresorbable Vascular Scaffold System (ABSORB BVS); compared to Abbott Vascular XIENCE Everolimus Eluting Coronary Stent System (XIENCE)

Elixir Medical Clinical Evaluation of the DESolve Myolimus Eluting Bioresorbable Coronary Stent System - DESolve I Trial/ Device: Novolimus Eluting Bioresorbable Coronary Scaffold

This prospective, consecutive enrolment, single-arm study will enroll up to 15 patients with single de novo, Type A lesions < 10 mm in length and located in a native coronary artery with a reference vessel diameter of 2.75 mm - 3.0 mm as measured by both offline QCA and IVUS. All patients will receive a 3.0 x 14mm DESolve Stent loaded with approximately 40 mcg of Myolimus.

The Impact of Stent Deployment Techniques on Clinical Outcomes of Patient Treated With the CYPHER® Stent (S.T.L.L.R.)/ CYPHER® Bx Velocity™ stent (sirolimus-eluting)

1500 eligible patients will be treated with the commercially available CYPHER® sirolimus-eluting Bx Velocity™ stent. Patients will be followed to twelve months post-procedure, watching for patients that require a repeat procedure on the same diseased area of the coronary artery.

IRIS-Synergy Cohort in the IRIS-DES Registry (IRIS Synergy)/ Synergy™ Stent

The purpose of this study is to evaluate the relative effectiveness and safety of Synergy stent compared to other drug eluting stents.

BIOFLOW III Satellite-Italy Orsiro Stent System/ Limus Eluting Orsiro Stent

Clinical evaluation of the Orsiro LESS in subjects requiring coronary revascularization with Drug Eluting Stents (DES).

Study of the Orsiro Drug Eluting Stent System/ Xience Prime DES vs Orsiro DES

The purpose of this study is to compare the BIOTRONIK Orsiro Drug Eluting Stent System with the Abbott Xience Prime™ Drug Eluting Stent System with respect to in-stent Late Lumen Loss in a non-inferiority study in de novo coronary lesions at 9 months.

TAXUS ATLAS: TAXUS Liberté™-SR Stent for the Treatment of de Novo Coronary Artery Lesions/ TAXUS Liberté-SR vs TAXUS™ Express

TAXUS ATLAS is a global, multi-center, single-arm, non-inferiority trial comparing results from patients treated with the TAXUS Liberté stent to an historical TAXUS Express control.

The BRIDGE Registry: Safety and Efficacy Registry of Bx Cypher Stent/ Bx Cypher stent

The objective of this study is to establish the safety and efficacy of the treatment with Cypher DES in diabetic patients with documented ischemia due to stenosis (small coronary artery 2.5 -3 mm in lumen diameter, with lesion between 15 mm 30 mm in length) in native coronary arteries.

BIOFLOW-III VIP Russia Registry Orsiro Stent System/ ORSIRO LESS

Clinical evaluation of the Orsiro LESS in subjects requiring coronary revascularization with Drug Eluting Stents (DES). Along with it, an explanatory (hypothesis-finding) problem will be investigated, whether the patient's body inflammation status correlates with the clinical outcome.

Evaluation of Effectiveness and Safety of PROMUS Element Stent (IRIS-ELEMENT)/ PROMUS Element stent with first-generation DES

This study is a non-randomized, prospective, open-label registry to compare the efficacy and safety of Promus Element stents versus first-generation DES in patients with coronary artery disease.

PEPCAD III Substudy: Stem Cell Mobilization/ Device: DEBlue vs Cypher vs BMS

The aim of the PEPCAD III substudy is to assess the efficacy of the Paclitaxel-eluting DEBlue stent system in the treatment of stenoses in native coronary arteries compared to the Sirolimus-eluting Cypher stent by intravascular ultrasound (IVUS) and to study the influence of both devices on endothelial function, coronary flow reserve, and stem cell mobilization.

The EVOLVE China Clinical Trial/ SYNERGY vs PE Plus Investigational Device

The purpose of this study is to assess the safety and effectiveness of the SYNERGY™ Coronary Stent System for the treatment of subjects with atherosclerotic lesion(s) ≤ 34 mm in length (by visual estimate) in native coronary arteries ≥ 2.25 mm to ≤ 4.0 mm in diameter (by visual estimate)

The Promus Element Rewards Study/ Cypher vs Taxus Express vs Endeavor vs Promus/Xience vs Promus Element vs Element stent

The objective of this study is to analyse the stent deformation on persons with de novo coronary lesions to determine how much deformation takes place and how often. The information gathered from the group that receives the Promus element stent will be compared to other groups that receive other contemporary drug eluting stents.

DXR Stent(Previous Cilotax) Implantation Registry/ DXR(Previous Cilotax) Stent

Registry of cilotax stent(Dual drug eluting stent) implantation for coronary artery disease patients

Prospective, Randomized, Multicenter Study to Assess the Safety and Effectiveness of the Orsiro Sirolimus-eluting Stent/ Biotronik Orsiro drug eluting stent vs Xience Prime

The purpose of this trial is to compare the Biotronik Orsiro drug eluting stent system with the Xience Prime / Xience Xpedition (Xience)drug eluting stent system in de novo coronary lesions.

Promus - Registry Experience at the Washington Hospital Center, Drug-eluting Stent (DES)/ Promus® DES

Single-center registry of patients treated with at least one Promus, everolimus-eluting, Stent, with the primary objective to assess clinical success and safety at 30 days, 6 months and 1 year post-implantation.

The BIFSORB Pilot Study II/ Magmaris Sirolimus Eluting Bioresorbable Magnesium Stent

The purpose of this study is to investigate the feasibility and safety of the Magmaris BRS for treatment of coronary bifurcation lesions.

Comparison of Biomatrix and Orsiro Drug Eluting Stent/ Orsiro drug eluting stent vs Biomatrix drug eluting stent

The primary objective of the BIODEGRADE study is to evaluate clinical efficacy of the Orsiro DES compared with Biomatrix DES, both of which have biodegradable polymer for the treatment of all-comers' coronary artery diseases.

Registry of Patients With a Bioabsorbable Magnesium Stent Implant MAGMARIS in Usual Clinical Practice/ Magmaris Sirolimus Eluting Bioresorbable Magnesium Stent

The objective is to evaluate the efficacy and safety of the bioabsorbable stent MAGMARIS in the percutaneous treatment of severe coronary disease (in vessels between 2.7mm and 3.75 mm) in routine clinical practice in poorly selected populations.

DES for diabetic patients in coronary artery disease treatment/ ABLUMINUS® sirolimus eluting stent

Investigational Device ABLUMINUS® sirolimus eluting stent consists of four components; a bare metal stent (BMS), a delivery system, the bio absorbable polymer delivery matrix and Abluminal surface coating on stent and parts of balloon in Pre-crimped condition the anti-proliferative drug, Sirolimus.

European Bifurcation Club Trial - Two-stent Versus One-stent Technique for Large Bifurcation Lesions/ Single stent vs two stent

This study will examine the use of two-stent versus one-stent techniques for patients with large calibre bifurcation lesions including significant side branch disease

SWISS Evaluation of Bioabsorbable Polymer-coated Everolimus-eluting Coronary sTent/ Third-generation Synergy everolimus-eluting stent (sEES)

Bioresorbable polymer drug eluting stents (DES) are an indisputable improvement over first-generation DES with promising results on long-term adverse events.

Test Efficacy With Bioresorbable Polymer Coating Versus Bioresorbable Polymer Backbone (ISAR-RESORB)/ SYNERGY EES vs ABSORB [BVS]

The objective is to study the bioresorbable polymer SYNERGY EES and compare it with the ABSORB bioresorbable vascular scaffold in terms of antirestenotic efficacy as assessed by angiography at 6-8 months.

A Clinical Evaluation of the XIENCE PRIME Small Vessel Everolimus Eluting Coronary Stent System in Japanese Population/ XIENCE PRIME SV EECSS

The purpose of this study is to evaluate the safety and effectiveness of the AVJ-09-385 Small Vessel Everolimus Eluting Coronary Stent System (EECSS) in treatment of subjects with ischemic heart disease caused by de novo lesions.

French Post-Marketing Surveillance Survey/ Cypher stent™ vs Cypher Select™

To assess the safety and efficacy of the Cypher stent™ & Cypher Select™ in the normal use of medical practices, within the labeled indications.

"JACTAX" Trial Drug Eluting Stent Trial/ JACTAX paclitaxel-eluting stent

Prospective, multi-center, non-randomized registry. The results of this study will be compared to the TAXUS™ ATLAS clinical trial to evaluate the safety of the product.

Cost-Effectiveness Study in the Reduction of Coronary Restenosis With Sirolimus-Eluting Stents/ Bare metal stent vs Cypher sirolimus-eluting stent

This study examines the effectiveness of sirolimus-eluting stents (SES) compared to bare-metal stents (BMS) in patients with coronary stenosis.

SEA-SIDE: Sirolimus Versus Everolimus-eluting Stent Randomized Assessment in Bifurcated Lesions and Clinical Significance of Residual siDE-branch Stenosis/ Sirolimus eluting stent

vs Everolimus eluting stent

The aims of the present study are to compare in a prospective randomized study the acute 3D angiographic results and the late clinical outcome of Sirolimus-eluting (SES) vs Everolimus-eluting stent (EES) obtained using a provisional TAP-stenting technique.

SPIRIT II: A Clinical Evaluation of the XIENCE V® Everolimus Eluting Coronary Stent System/ XIENCE V® Everolimus Eluting Coronary Stent vs TAXUS™ EXPRESS2™ Paclitaxel Eluting Coronary Stent

Prospective, randomized, active-control, single blind, parallel two-arm multi-center clinical trial comparing XIENCE V® Everolimus Eluting Coronary Stent System to the approved commercially available active control TAXUS™ EXPRESS2™ Paclitaxel Eluting Coronary Stent System.

The Bioresorbable Implants for Scaffolding Obstructions in Randomized Bifurcations (BIFSORB) Study/ Absorb stent vs Desolve stent

The purpose of this study is to compare the safety and vessel healing after treatment of simple bifurcation lesions with the CE-marked bioresorbable stents Absorb and Desolve.

Z-SEA-SIDE: Sirolimus Versus Everolimus Versus Zotarolimus-eluting Stent Assessment in Bifurcated Lesions and Clinical Significance of Residual side-branch Stenosis/ Sirolimus eluting stent vs Everolimus eluting stent vs Zotarolimus eluting stent

The aims of the present study are to compare in a prospective study the acute 3D angiographic results and the late clinical outcome of Sirolimus-eluting (SES) vs Everolimus-eluting (EES) vs Zotarolimus eluting stent (ZES) obtained using a provisional TAP-stenting technique.

Safety and Efficacy Study Comparing 3 New Types of Coronary Stents/ Everolimus-eluting stent vs

Bare-metal stent vs Biodegradable Polymer-DES

The primary objective is to demonstrate non-inferiority of the Nobori DES stent compared to the Xience Prime DES stent on safety and efficacy in patients requiring stents ≥ 3.0 mm in diameter on the background of contemporary DAPT with prasugrel and aspirin

China Endeavor Registry: A Registry With The Endeavor Zotarolimus Eluting Coronary Stent in China/ Endeavor(TM) Zotarolimus Eluting Coronary stent

The primary objective is to document the acute and mid-term safety and overall clinical performance of the Endeavor(TM) Zotarolimus Eluting Coronary stent system in a "real world" Chinese patient population requiring stent implantation.

The REALITY Study - Head-to-Head Comparison Between Cypher and Taxus/ Cypher Sirolimus-Eluting Stent vs Taxus Paclitaxel-Eluting Stent

The main objective of this study is to compare the performance of the Cypher sirolimus-eluting and the Taxus paclitaxel-eluting stent systems in a prospective, multi-center, randomized clinical study.

SPIRIT III Clinical Trial of the XIENCE V® Everolimus Eluting Coronary Stent System (EECSS)/ XIENCE V® Everolimus Eluting Coronary Stent vs TAXUS® EXPRESS2™ Paclitaxel Eluting Coronary Stent

This RCT will compare the XIENCE V® Everolimus Eluting Coronary Stent System (CSS) (2.5, 3.0, 3.5 mm diameter stents) with the approved commercially available active control TAXUS® EXPRESS2™ Paclitaxel Eluting Coronary Stent (TAXUS® EXPRESS2™ PECS) System.

An Evaluation of BioMime™ - Sirolimus Eluting Coronary Stent in a Multi- Centre Study./ BioMime™ - Sirolimus Eluting Coronary Stent

This is a multi-centre, prospective trial. 250 patients will be enrolled in the study.

XIENCE V: SPIRIT WOMEN/ XIENCE V®/ XIENCE PRIME™

The purpose of this Clinical Evaluation is the assessment of the XIENCE Everolimus Eluting Coronary Stent System (XIENCE V® and XIENCE PRIME™ EECSS) with the primary focus on clinical outcomes in the treatment of female patients with de novo coronary artery lesions, and the characterization of the female population undergoing stent implantation with a XIENCE stent.

ProStent Coronary Drug-Eluting Stent/ ProStent rapamycin-eluting stent system vs Firebird DESs

A single blind, multi-center, randomized study is performed to compare ProStent DESs with Firebird DESs from MicroPort Medical (Shanghai) Co., Ltd. to evaluate the safety and efficacy of ProStent DES in treating coronary artery lesions.

Study Comparing the MiStent SES Versus the XIENCE EES Stent/ MiStent DES vs XIENCE EES

The primary objective of this study is to compare the performance of MISTENT to that of XIENCE in an all-comers patient population with symptomatic ischemic heart disease.

SPIRIT V: Post-marketing Evaluation of the XIENCE V® Everolimus Eluting Coronary Stent System in Europe/ XIENCE V® Everolimus Eluting Coronary Stent

The purpose of this Clinical Evaluation is a continuation in the assessment of the performance of the XIENCE V® Everolimus Eluting Coronary Stent System (XIENCE V® EECSS) in the treatment of patients with de novo coronary artery lesions.

Comparison of the Conor Sirolimus-eluting Coronary Stent to the Taxus Liberte Paclitaxel-eluting Coronary Stent in the Treatment of Coronary Artery Lesions/ NEVO™ Sirolimus-eluting Coronary Stent System vs TAXUS Liberte Paclitaxel-eluting Coronary Stent System

The purpose of this study is to evaluate the safety and effectiveness of the Conor Sirolimus-eluting Coronary Stent System in the treatment of coronary artery disease (a single atherosclerotic lesion) in native coronary arteries. The study will evaluate the outcomes of a new DES compared to an approved DES.

Thin Strut Sirolimus-eluting Stent in All Comers Population vs Everolimus-eluting Stent/ SUPRAFLEX Drug Eluting Stent vs XIENCE

The primary objective of this study is to compare the performance of SUPRAFLEX to that of XIENCE in an all-comers patient population with symptomatic ischemic heart disease.

Drug-eluting Stents to Treat Unprotected Coronary Left Main Disease/ Everolimus-eluting stent (Xience) vs Zotarolimus-eluting stent (Endeavor Resolute)

The purpose of this study is to evaluate the efficacy of two different DESs (Everolimus and Zotarolimus-eluting) for treatment of unprotected left main coronary artery disease.

Limus Eluted From A Durable Versus ERodable Stent Coating/ Cypher SELECT Sirolimus-Eluting stent

Compare the safety and efficacy of the BioMatrix Flex (Biolimus A9-Eluting) stent system with the Cypher SELECT (Sirolimus-Eluting) stent system in a prospective, multi-center, randomized, controlled, non-inferiority trial in patients undergoing PCI in routine clinical practice.

Evaluation of HealinG of Polymer-Free Biolimus A9-Coated Stent by Optical Coherence Tomography (EGO-BIOFREEDOM)/ Polymer-Free Biolimus A9-Coated Stent

Biolimus A9 is the therapeutic agent used in the BioFreedom drug coated stent. Biolimus A9 is a proprietary semi-synthetic sirolimus derivative. It is highly lipophilic, rapidly absorbed in tissues, and able to reversibly inhibit growth factor-stimulated cell proliferation. In this study, we use intracoronary optical coherence tomography (OCT) to evaluate the BioFreedom Stents after implantation regarding endovascular healing over time.

Long Term Efficacy and Safety of Firebird Sirolimus-Eluting Stent In Complex Coronary Lesions/ Firebird(TM) Sirolimus-Eluting Stent

The purpose of this study is to investigate the long term efficacy and safety of firebird sirolimus-eluting stent for treatment of complex coronary Lesions.

XIENCE V® Everolimus Eluting Coronary Stent System India Post-marketing Single-arm Study/ XIENCE V® Everolimus Eluting Coronary Stent

XIENCE V® India is a prospective, open-label, multi-center, observational, single-arm study to evaluate XIENCE V® EECSS continued safety and effectiveness during commercial use in real world settings.

Evaluate Safety And Effectiveness Of The Tivoli® DES and The Firebird2® DES For Treatment Coronary Revascularization/ TIVOLI Biodegradable polymer Rapamycin-Eluting Stent comparing with The FIREBIRD2™ Rapamycin-eluting Stent (DES)

This is a prospective, multi-center, open label, randomized study to evaluate the efficacy and safety of The TIVOLI Biodegradable polymer Rapamycin-Eluting Stent comparing with The FIREBIRD2™ Rapamycin-eluting Stent (DES) for Treatment Coronary Revascularization.

Korean Coronary Overlapping Stenting Registry/ Drug-eluting stent overlap

The Korean Coronary Overlapping Stenting Registry is a multicenter database which includes percutaneous intervention using DESs from cardiovascular centers in eight affiliated hospitals of The Catholic University of Korea.

A Randomized, Multi-Center Study of the Pimecrolimus-Eluting and Pimecrolimus/Paclitaxel-Eluting Coronary Stent Systems (GENESIS)/ Corio™ Pimecrolimus-Eluting Coronary Stent vs SymBio™ Pimecrolimus/Paclitaxel-Eluting Coronary Stent vs Costar™ Paclitaxel-Eluting Coronary Stent

The objective of this study is to demonstrate non-inferiority in 6-month angiographic in-stent late lumen loss of the pimecrolimus-eluting coronary stent (Corio) compared to the CoStar coronary stent control arm and the dual pimecrolimus/paclitaxel-eluting (Symbio) coronary stent compared to the CoStar coronary stent control arm for the treatment of single de novo lesions <25 mm in length in native coronary arteries 2.5 - 3.5 mm in diameter.

XIENCE V Everolimus Eluting Coronary Stent System (EECSS) China: Post-Approval Randomized Control Trial (RCT)/ XIENCE V EECSS vs CYPHER SELECT PLUS SECSS

This is a prospective, randomized, active-controlled, open label, parallel two-arm, multi-center, post-approval study descriptively comparing the XIENCE V EECSS to the CYPHER SELECT PLUS Sirolimus-Eluting Coronary Stent System (SECSS) ("CYPHER SELECT PLUS") during commercial use in China.

COMPETE: A Clinical Evaluation of Chrono Carbostent Carbofilm™ Coated Stent/ Chrono Carbostent Carbofilm™ Coated Coronary Stent vs Driver Cobalt Alloy Coronary Stent

The COMPETE study is a prospective, randomized, two-arm multi-center clinical trial comparing two commercially available coronary stents: Chrono Carbostent Carbofilm™ Coated vs Driver/Micro-Driver Coronary Stent System. In this study, 204 subjects will be included (2:1 randomization Chrono: Driver/Micro Driver) in 6 Italian sites.

Comparison of Strut Coverage With OPTIMAX Versus SYNERGY Stents/ Titanium-nitride-oxide-coated OPTIMAX™ Bio-active-stent (BAS) Stent vs SYNERGY™ Everolimus-Eluting Stent (EES)

The purpose of this study is to compare vascular healing of the stented segment after deployment of titanium-nitride-oxide coated cobalt-chromium OPTIMAX™ bio-active stent (BAS) and SYNERGY™ everolimus-eluting stent (EES) in patients with acute coronary syndromes requiring PCI.

Nonpolymer- and Polymer-Based Drug-Eluting Stents for Restenosis (ISAR-TEST-1)/ Paclitaxel-eluting stent (Taxus) vs Rapamycin-eluting stent

The purpose of this study is to assess the efficacy of nonpolymer-based rapamycin-eluting stent compared to standard polymer-based paclitaxel-eluting stent to reduce reblockage of coronary arteries.

In-stent Restenosis in Patients With Patent Previous Bare Metal Stent/ Bare metal stent vs DES

The objective of this study is to investigate whether in patients with previously deployed bare metal stent and no evidence of in-stent re-stenosis there will be a significant difference in the rates of in-stent between drug eluting stents and bare metal stents deployed within de-novo stenotic lesions.

Thrombogenicity Assessment in Patients Treated With Bioresorbable Vascular Scaffolds/ Bioresorbable Vascular Scaffold vs Drug Eluting Stent

Platelet activation and aggregation, intrinsic thrombogenicity, and biomarkers (fibrinogen, C-reactive protein, platelet endothelial cell adhesion molecule, von Willebrand factor, p-selectin) will be measured and compared following the implantation of Bioreabsorbable Vascular Scaffolds and Drug Eluting Stents.

The Real-world Firebird 2 Versus Cypher Sirolimus-eluting Stent in Treating Patients With Coronary Artery Disease/ Firebird 2 SES vs Cypher SES

The efficacy and safety of Cypher SES (Cordis, MA) has been proved by several randomized clinical trials. Here the investigators design a prospective, multicenter, randomized clinical study in purpose of identifying the non-inferiority in the efficacy and safety in treating coronary artery disease patients by Firebird 2 SES (Microport, Shanghai), comparing with Cypher SES.

Evaluation of Effectiveness and Safety of the GENOUS STENT (IRIS-GENOUS STEMI)/ GENOUS EPC-coated drug eluting stent

The objective of this study is to evaluate the effectiveness and safety of GENOUS EPC-coated stent in patients with STEMI with other DESs.

Cobalt Chromium Stent With Antiproliferative for Restenosis II Trial (COSTAR II)/ CoStar Paclitaxel Drug Eluting Coronary Stent vs TAXUS™ Express2™ Paclitaxel-Eluting Coronary Stent

The purpose of this study is to evaluate the safety and effectiveness of the investigational stent CoStar™ Paclitaxel-Eluting Coronary Stent- a reservoir based DES system in comparison to a surface coated DES stent (TAXUS™ Express2™ Paclitaxel-Eluting

Coronary Stent) in the treatment of single-vessel (one blood vessel) and multi-vessel (two or three blood vessels) coronary artery disease.

SPIRIT V: A Clinical Evaluation of the XIENCE V® Everolimus Eluting Coronary Stent System in the Treatment of Patients With de Novo Coronary Artery Lesions (Diabetic Sub-Study)/ TAXUS® Liberté™ vs XIENCE V® EECSS

The purpose of this Clinical Evaluation is a continuation in the assessment of the performance of the XIENCE V® Everolimus Eluting Coronary Stent System (XIENCE V® EECSS) in the treatment of patients with de novo coronary artery lesions in patients (Diabetic sub-study).

Prospective, Multi-Center, Random. Study of CoStar Paclitaxel-Eluting Coronary Stent(Direct Stenting vs. Pre-Dilatation)/ CoStar Paclitaxel-eluting coronary stent

The primary objective of this study is to evaluate the safety and effectiveness of a direct stenting technique compared to conventional stenting with pre-dilatation strategy using the CoStar Paclitaxel-eluting coronary stent system for the treatment of a single de novo lesion in a native coronary artery ≤ 25 mm long in a native coronary artery 2.5-3.5 mm diameter.

Safety and Efficacy Study of the Nile PAX Drug-Eluting Coronary Bifurcation Stent/ Nile PAX® paclitaxel-eluting coronary stent

The purpose of this trial is to assess the safety and efficacy of the Nile PAX® Drug Eluting Coronary Bifurcation Stent System for the treatment of single de novo bifurcation lesions in native coronary arteries with a main branch reference vessel diameter of 2.5-3.5 mm and side branch reference vessel diameter of 2.0-3.0 mm.

Drug-eluting-stents for Unprotected Left Main Stem Disease (ISAR-LEFT-MAIN)/ Sirolimus-eluting stent vs Paclitaxel-eluting stent

The purpose of this study is to evaluate the efficacy of sirolimus- and paclitaxel-eluting stents for treatment of unprotected left main coronary artery disease.

Safety and Efficacy of the ZoMaxx™ Drug-Eluting Stent System in Coronary Arteries/ ZoMaxx™ Drug-Eluting Coronary Stent System vs TAXUS™ EXPRESS2™ Paclitaxel Eluting Coronary Stent

The purpose of this study is to demonstrate the safety and efficacy of the ZoMaxx DES in patients with blockage of native coronary arteries. The study is designed to demonstrate non-inferiority to the TAXUS Express2 Paclitaxel-Eluting Stent that has proven superior to bare metal stents and is a recognized standard of care.

XIENCE V Everolimus Eluting Coronary Stent System (EECSS) China: Post-Approval, Single-Arm Study/ XIENCE V® Everolimus Eluting Coronary Stent

The purpose of this study is to evaluate the continued safety and effectiveness of the XIENCE V EECSS in a cohort of real-world patients receiving the XIENCE V EECSS during commercial use.

Conor Cobalt Chromium Reservoir Based Stent With Sirolimus Elution in Native Coronary Artery Lesions/ NEVO™ Sirolimus-eluting Coronary Stent

The primary objective of this study is to evaluate the TLF rate of the NEVO Sirolimus-eluting Coronary Stent System.

Coroflex ISAR 2000 Extended Registry (ISAR2000 Extended)/ Sirolimus-eluting Coroflex ISAR Stent

The aim of the study is to assess the safety and efficacy of elective deployment of the Sirolimus-eluting Coroflex ISAR Stent for the treatment of "real world" de-novo and restenotic lesions after stand-alone angioplasty in coronary arteries of 2.0 mm up to 4.0 mm in diameter and up to 30 mm in length for procedural success and preservation of vessel patency.

PROMUS Element Japan Small Vessel Trial/ PROMUS Everolimus-Eluting Coronary Stent

A non-randomized, small vessel (SV) trial at approximately 15 sites in Japan to enroll 60 patients with a de novo lesion ≤ 28 mm in length (by visual estimate) in a native coronary artery ≥ 2.25 mm to < 2.50 mm in diameter (by visual estimate).

Coroflex ISAR 2000 Registry/ Sirolimus-eluting Coroflex ISAR Stent

Postmarket surveillance in terms of the safety and efficacy of Sirolimus-eluting Coroflex ISAR Stent for the treatment of "real world" patients with de-novo and restenotic lesions after stand-alone angioplasty in coronary arteries.

The Efficacy of Three Different Limus Agent-Eluting Stents to Prevent Restenosis/ Rapamycin-eluting Stent vs Zotarolimus-eluting Stent

The purpose of this study is to evaluate the efficacy of 3 different DES platforms to reduce coronary artery reblockage after stent implantation.

Sirolimus- and Paclitaxel-Eluting Stents for Small Vessels (ISAR-SMART-3)/ Sirolimus-eluting stent (Cypher) vs Paclitaxel-eluting stent (Taxus)

The purpose of this study is to compare the efficacy of paclitaxel- and sirolimus-eluting stents to prevent re-blockage of small coronary arteries.

Intra-stent Tissue Evaluation Within BMS and DES > 3 Years Since Implantation

This study aims to test the hypothesis that plaque composition differs within a stent between bare metal stents and drug eluting stents (DES). It is possible that a difference in plaque composition seen within a stent may be contributory to the late thrombotic events seen more frequently with DES.

ABSORB Clinical Investigation, Cohort B/ Bioabsorbable Everolimus Eluting Coronary Stent

The purpose of this study is to assess the safety and performance of the BVS Everolimus Eluting Coronary Stent System (EECSS) in the treatment of patients with a maximum of two de novo native coronary artery lesions located in two different major epicardial vessels.

JACTAX LD Drug Eluting Stent Trial/ JACTAX LD DES vs TAXUS™ Libertè™ DES

The objective of this study is the evaluation of the efficacy of the JACTAX LD stent or the TAXUS™ Libertè™ stent.

ABSORB Clinical Investigation, Cohort A (ABSORB A) Everolimus Eluting Coronary Stent System Clinical Investigation/ Bioabsorbable Everolimus Eluting Coronary Stent

Prospective, open-labeled First in Man Clinical Investigation enrolling patients with visually estimated nominal vessel diameter of 3.0 mm receiving a single 3.0 x 12 mm or 3.0 x 18 mm BVS EECSS containing 98 microgramme per cm² of surface area.

REWARDS- In-stent Restenosis/ PCI with Commercially available DES

To define the long-term incidence and frequency of ISR follow DES implantation. Compare the clinical presentation, treatment and intervention success among de novo coronary artery stenosis and DES ISR. Compare short- and long-term outcomes of de novo coronary artery stenosis and DES ISR, assessed by incidence of mortality, MACE, MI, and TLR/TVR at index hospitalization, 30 days, 6 months, 1 year, 3 years, and 5 years, if available.

The XLIMUS-DES in Very Complex Lesions/ XLIMUS Sirolimus-eluting Coronary Stent

This is a prospective, non-randomized, single-center pilot study, aiming to evaluate the performance of the XLIMUS DES in severely complex coronary lesions in real-world clinical practice.

Study of MeRes100 in the Treatment of Patient With Coronary Artery Disease./ MeRes100 Sirolimus-Eluting BioResorbable Vascular Scaffold vs Xience EES Everolimus Eluting Coronary Stent

This is a Multi Center Randomized (MeRes:XIENCE=1:1) Control Study of MeRes100 Sirolimus Eluting BioResorbable Vascular Scaffold System. The post marketed XIENCE Everolimus Eluting Coronary Stent System will serve as the control device, to evaluate the safety and efficacy of MeRes100 Sirolimus Eluting BioResorbable Vascular Scaffold System in coronary artery disease.

TAXUS ARRIVE: TAXUS Peri-Approval Registry: A Multi-Center Safety Surveillance Program/ TAXUS Express 2™

The TAXUS ARRIVE study is a multi-center safety and surveillance study designed to to compile safety surveillance and clinical outcomes data for the TAXUS™ Express2™ Paclitaxel-Eluting Coronary Stent System in routine clinical practice and to identify low frequency TAXUS related clinical events.

Vascular Healing After Deployment of Titanium-nitride-oxide-coated OPTIMAX™ Stent and PROMUS-ELEMENT™ Everolimus-Eluting Stent/ Titanium-nitride-oxide coated cobalt-chromium Optimax™-stent stent and Promus-Element™ everolimus-eluting stent

The purpose of this study is to compare vascular healing of the stented segment after deployment of titanium-nitride-oxide coated cobalt-chromium Optimax™-stent stent and Promus-Element™ everolimus-eluting stent in patients with acute coronary syndromes requiring PCI.

Trial of MiStent Compared to Xience in Japan/ MiStent (MT005) Coronary Artery Stent vs Xience Stent

To compare the MT005 (MiStent) with the XIENCE with respect to TLF at 12 months in a non-inferiority trial in a "real world" patient population and to confirm that the domestic extrapolation of the DESSOLVE III study results is valid.

Clinical Evaluation of Patients With Everolimus-eluting Stent Xience V® Implanted in the Treatment of Restenosis in Non-coated Metallic Stent (BMS In-stent Restenosis) During a 2 Year Clinical Follow-up Period/ Xience V® stent

Interventional, prospective, non-randomized, non-comparative, open and multicentric study of patients with everolimus-eluting stent "Xience V® " implanted in the treatment of restenosis in non-coated metallic stent (BMS ISR) during a 2 year clinical follow-up period.

Study of BioNIR Drug Eluting Stent System in Coronary Stenosis/ BioNIR ridaforolimus eluting stent vs Resolute stent

The BioNIR study aims to show that the BioNIR ridaforolimus eluting stent is non-inferior to the Resolute zotarolimus-eluting stent for the primary clinical endpoint of TLF at 12 months; that it is non-inferior to the Resolute for the secondary endpoint of angiographic in-stent late loss at 13 months; and that it is more cost-effective.

Per-cutaneous Intervention Based Paclitaxel and Sirolimus-Eluting Versus Bare Stents for the Treatment of de Novo Coronary Lesions (PAINT)/ Millennium Matrix® vs Infinium® vs Supralimus®

To compare the in-stent late loss at 9 months of paclitaxel- and sirolimus- eluting stents with the late loss of bare metal control stents.

XIENCE PRIME SV Everolimus Eluting Coronary Stent Post Marketing Surveillance (XIENCE PRIME SV PMS)/ XIENCE PRIME SV Everolimus Eluting Coronary Stent

The objective of the study is to evaluate the safety and efficacy of XIENCE PRIME SV in real world practice in Japanese hospitals.

Comparison of Cilotax Stent and Everolimus -Eluting Stent With Diabetes Mellitus (ESSENCE-DM III)/ Xience Prime stent vs Cilotax stent

The purpose of this study is to examine the safety and effectiveness of coronary stenting with the Cilotax stent compared to the Xience Prime stent in the treatment of diabetic patients.

SORT-OUT VI - Randomized Clinical Comparison of Biomatrix Flex® and Resolute Integrity®/ DES

To perform a randomized comparison between the BioMatrix Flex™ and the Resolute Integrity® stents in the treatment of unselected patients with ischemic heart disease.

Randomized "All-comer" Evaluation of a Permanent Polymer Resolute Integrity Stent Versus a Polymer Free Cre8 Stent/ Cre8 Stent vs Resolute Integrity stent

The study objective is to assess the safety and efficacy of the Permanent Polymer Zotarolimus-Eluting Stent Resolute Integrity™ to the Polymer Free Amphilimus-Eluting Stent Cre8™ compared in an all-comer patient population.

The Real-World Endeavor Resolute Versus XIENCE V Drug-Eluting Stent Study in Twente/ Endeavor Resolute (Biolinx-based Zotarolimus-eluting stent) vs Xience V (Everolimus-eluting stent)

The TWENTE Study is a single center prospective single-blinded randomized study. Randomization will involve the type of Drug-Eluting Stent (DES) used in study population. Patients will be blinded to the type of DES they will receive.

Reservoir-Based Polymer-Free Amphilimus-Eluting Stent Versus Polymer-Based Everolimus-Eluting Stent in Diabetic Patients/ Polymer-Based Everolimus-Eluting Stent vs Polymer-Free Amphilimus-Eluting Stent

The purpose of this study is to determine whether Polymer-Free Amphilimus-Eluting Stent implantation is effective in reducing neointimal hyperplasia as compared to Polymer-Based Everolimus-Eluting Stent in diabetic patients, using Optical Coherence Tomography (OCT) as the primary imaging modality.

REal World Advanced Experience of BioResorbable Scaffold by SMart Angioplasty Research Team (SMART REWARD)/ Bioresorbable scaffold (BRS)

The objective of this study is to test the feasibility and safety of BRS in these complex lesion subsets. Bioresorbable scaffold (BRS) is known to disappear 2 to 3 years after the implantation, which may result in the more favorable very long-term clinical outcomes compared with metallic stents. The initial clinical experiences of BRS in relatively simple lesion subsets were comparable to DESs. BRS, however, is limited by the disadvantageous mechanical characteristics such as thick strut and the risk of fracture by overdilation. There is concern that BRS is less optimal for complex lesion subsets such as bifurcation lesions, calcified tortuous lesions, or diffuse long lesions.

Comparison of Cypher Select and Taxus Express Coronary Stents/ DES

Randomized nine months clinical comparison of implantation of Taxol eluting (Taxus Express) and Sirolimus eluting (Cypher Select) stents in non-selected patients with coronary artery disease.

Brazil Xience V Everolimus-Eluting Coronary Stent System "Real-World" Outcomes Registry/ Xience V everolimus-eluting coronary stent system (EECSS)

To evaluate the performance and long-term clinical outcomes of the Xience V everolimus-eluting coronary stent system (EECSS) in the treatment of minimally selective, high risk patients in the real-world clinical practice.

Intimal Hyperplasia Evaluated by Optical Coherence Tomography (OCT) in de Novo Coronary Lesions Treated by Drug-eluting Balloon and Bare-metal Stent/ Device: drug (paclitaxel)-eluting balloon (DEB) vs bare-metal stent (BMS) vs Drug (paclitaxel)-eluting balloon (DEB)

The aim of this open label prospective, randomized trial is to evaluate neointimal hyperplasia in patients undergoing bare-metal stent (BMS) implantation alone compared to those receiving additional DEB use and to assess if the technique of DEB use may affect the degree of neointimal hyperplasia.

A Randomized Clinical Evaluation of the BioFreedom™ Stent/ Biofreedom™ Drug Coated Stent (DCS) vs Gazelle™ Bare Metal Coronary Stent (BMS)

The purpose of this study is to demonstrate that a BioFreedom™ Drug Coated Stent is non-inferior to a bare metal stent at one year as measured by the composite safety endpoint of cardiovascular death, myocardial infarction and definite/probable stent thrombosis, and that its efficacy is superior to a bare metal stent as measured by clinically driven TLR at one year.

A Clinical Evaluation of the ProNOVA XR Polymer Free Drug Eluting Coronary Stent System/ ProNOVA Drug Eluting Coronary Stent System

The objective of this study is the assessment of the performance, safety and efficacy of the ProNOVA XR Polymer Free Drug Eluting Stent System in the treatment of patients with de novo native coronary artery lesions.

Safety and Efficacy Study of the Amaranth Medical APTITUDE Bioresorbable Drug-Eluting Coronary Stent/ AmM APTITUDE Bioresorbable Drug-Eluting Coronary Scaffold

The purpose of this study is to evaluate the safety and performance of a new version of a coronary artery stent for treating blockages in the arteries supplying blood to the heart muscle. The Amaranth Medical APTITUDE scaffold releases a drug (sirolimus) to reduce the likelihood of the treated blood vessel developing a new blockage.

Safety and Effectiveness of the Orsiro Sirolimus Eluting Coronary Stent System in Subjects With Coronary Artery Lesions/ Orsiro DES vs Xience DES

The objective of this study is to assess the safety and efficacy of the Orsiro Sirolimus Eluting Coronary Stent System in the treatment of subjects with up to three native de novo or restenotic (standard PTCA only) coronary artery lesions compared to the Xience coronary stent system.

SORT OUT X - Combo Stent Versus ORSIRO Stent/ COMBO vs ORSIRO stent

The aim of the Danish Organisation for randomised trials with clinical outcome (SORT OUT) is to compare the safety and efficacy of the Combo™ stent and Orsiro™ stent in the treatment of unselected patients with ischemic heart disease, using registry detection of clinically driven events.

Second-generation Drug-eluting Stents in Diabetes/ Polymer-free amphiphilic-eluting stent vs

Biolinx Polymer-based zotarolimus-eluting stent

It is a multicenter, international, parallel, randomized 1:1 (amphiphilic-eluting stents vs zotarolimus-eluting stents) clinical trial performed exclusively in patients with diabetes mellitus.

Safety and Efficacy Study of the Amaranth Medical FORTITUDE Bioresorbable Drug-Eluting Coronary Stent/ AmM FORTITUDE Bioresorbable Drug-Eluting Coronary Scaffold

The purpose of this study is to evaluate the safety and performance of a new coronary artery stent for treating blockages in the arteries supplying blood to the heart muscle. The Amaranth FORTITUDE scaffold releases a drug (sirolimus) to reduce the likelihood of the treated blood vessel developing a new blockage.

Comparison of the Angiographic Result of the Orsiro Hybrid Stent With Resolute Integrity Stent/ Orsiro Hybrid Drug-Eluting Stent vs Resolute Integrity

The purpose of this multicenter, randomized, open label, parallel arm study whether the newest 3rd generation stent - Orsiro hybrid sirolimus-eluting stent is noninferior to the newest 2nd generation stent - Resolute Integrity zotarolimus-eluting stent in terms of 9 months in-stent late lumen loss.

Safety and Efficacy Study of the Amaranth Medical MAGNITUDE Bioresorbable Drug-Eluting Coronary Stent (RENASCENT III)/ AmM MAGNITUDE Bioresorbable Drug-Eluting Coronary Scaffold

The purpose of this study is to evaluate the safety and performance of a new version of a coronary artery stent for treating blockages in the arteries supplying blood to the heart muscle. The Amaranth Medical MAGNITUDE scaffold releases a drug (sirolimus) to reduce the likelihood of the treated blood vessel developing a new blockage.

Closed Versus Open Cells Stent for Acute MI/ Open cells stent vs Closed Cells Stent

The aim of this study is to determine whether a closed cell stent design may reduce distal embolization and no reflow during primary PCI (PPCI) for acute ST-elevation acute myocardial infarction (STEMI) compared to an open cell stent design.

Comparison of Stent Graft, Sirolimus Stent, and Bare Metal Stent Implanted in Patients With Acute Coronary Syndrome/ Sirolimus Stent vs Bare Metal Stent

The objective of this study is to evaluate the sirolimus stent vs a Bare Metal Stent.

NeoVas Bioresorbable Coronary Scaffold Randomized Controlled Trial/ NeoVas BCS vs XIENCE PRIME EECSS

The NeoVas Bioresorbable Coronary Scaffold Randomized Controlled Trial is a prospective, multi-center, randomized trial that compares NeoVas sirolimus-eluting bioresorbable coronary scaffold with XIENCE PRIME Everolimus Eluting Coronary Stent System (EECSS) to evaluate the safety and efficacy of NeoVas in the treatment of patients with de novo coronary lesion.

Bioresorbable Polymer ORSIRO Versus Durable Polymer RESOLUTE ONYX Stents/ Orsiro vs

Resolute Onyx

The objective of this study is to compare the bioresorbable polymer DES with a contemporary highly flexible new generation permanent polymer coated DES.

Sirolimus-eluting Stents With Biodegradable Polymer Versus an Everolimus-eluting Stents/ Sirolimus-eluting stent with a bioresorbable polymer (Orsiro) vs Everolimus-eluting stent with a durable polymer

The objective of the study is to compare the safety and efficacy of a sirolimus-eluting stent with a biodegradable polymer with an everolimus-eluting stent with a durable polymer in a

prospective multicenter randomized controlled non-inferiority trial in patients undergoing PCI in routine clinical practice.

Multi-Center Clinical Trial: Evaluation of Effectiveness and Safety/ CoStar Paclitaxel Drug-Eluting Coronary Stent

This trial aims to demonstrate the non-inferiority of the CI-CMS-005 Coronary Stent System to the study device as well as to the TAXUS™ Express2™ Drug-Eluting Coronary Stent System in in-segment late lumen loss at 9 months after treatment of a single de novo lesion per vessel.

DUrable Polymer-based STent CHallenge of Promus ElemEnt Versus ReSolute Integrity/ Resolute Integrity® vs Promus Element®

To investigate whether the clinical outcome is similar after implantation of the Promus Element versus the Resolute Integrity stent (non-inferiority hypothesis).

Everolimus Stent in MI/ Xience Everolimus eluting stent vs Cypher sirolimus eluting stent

Randomized trial to test the efficacy and safety of newer Drug Eluting Stent generation in patient with acute myocardial infarction treated with primary PCI (PCI)

To Evaluate Safety and Efficacy of CGBIO Stent Compared to Biomatrix Flex Stent/ CGBio CoCr biodegradable polymer DES Sirolimus DRUG Ascorbic Acid vs Biomatrix abluminal biodegradable polymer DES BA9™ (BIOLIMUS A9™) DRUG

The objective of this study is to evaluate the safety and efficacy of CGBIO stent(DES) compared to Biomatrix flex stent(DES)

HARMONEE - Japan-USA Harmonized Assessment by Randomized, Multi-Center Study of OrbusNEich's Combo StEnt/ OrbusNeich Combo DES stent vs Everolimus Eluting Stent (EES)

This study is intended to demonstrate that the Combo stent platform shows superiority to an imputed BMS performance goal, noninferior effectiveness and safety vs best-in-class second-generation everolimus-eluting stent (EES) (Xience V, Xience Prime, Xience Xpedition stents; [Abbott Vascular/Abbott Vascular Japan]), and evidence of mechanistic activity of the anti-CD34-Ab EPC capture technology with healthy level of intimal tissue coverage superior to that of the best-in-class EES.

SORT-OUT V - Randomised Clinical Comparative Study of the Nobori and the Cypher Stent./ Cypher Select vs Nobori stent

The objective of this study is to perform a randomized comparison between the Cypher Select+ stent and the Nobori stent in the treatment of unselected patients with ischaemic heart disease.

Comparison of Everolimus-Eluting Stent vs Sirolimus-Eluting Stent in Patients With DIABETES Mellitus/ XIENCE V vs CYPHER stent

The purpose of this study is to establish the safety and effectiveness of coronary stenting with the Everolimus- Eluting stent compared to the Sirolimus-Eluting stent in the treatment of de novo coronary stenosis in patients with diabetic patients.

Safety and Efficacy Study of CYPHER® Sirolimus Stent and ENDEAVOR® Zotarolimus Stent in Patients With Acute ST Elevation Myocardial Infarction (STEMI) and Analysis of Current Status of Emergency PCI Green Channel for STEMI Patients in China/ Drug eluting CYPHER® stent vs ENDEAVOR® stent

This study is to compare the clinical effect of CYPHER® stent and ENDEAVOR® stent in patients with acute ST elevation myocardial infarction.

Strut Coverage With SYNERGY Stents and Bioresorbable Vascular Scaffold in Acute MI/ SYNERGY (Platinum chromium coronary stent) vs ABSORB (Everolimus-eluting Bioresorbable Vascular Scaffold)

To assess strut coverage in patients presenting an acute myocardial infarction and treated either with the SYNERGY stent or the Bioresorbable Vascular Scaffold, through a parallel group design.

Comparison of Biolimus A9 and Everolimus Drug-Eluting Stents in Patients With ST Segment Elevation MI/ Biolimus A9 DES vs Everolimus DES.

The primary objective of this study is to compare the safety and effectiveness of third generation DES (biolimus A9 and everolimus) in patients with STEMI treated by primary PCI with OCT guidance.

BioFreedom US IDE Feasibility Trial/ BioFreedom drug coated coronary stent

The purpose of this study is to collect additional safety and effectiveness data for on the Biosensors BioFreedom™ BA9 Drug Coated Coronary Stent in patients with native, de novo coronary artery disease.

XIENCE PRIME Japan Post-Marketing Surveillance (PMS)/ XIENCE PRIME - Long Length (LL) vs XIENCE PRIME - Core Size

The objectives of the PMS are to observe the frequency, type, and degree of device deficiency to assure the safety of the new medical device (XIENCE PRIME) as well as to collect information on evaluation of the efficacy and safety for re-evaluation.

Six-month Coverage and Vessel Wall Response of the Zotarolimus Drug-eluting Stent Implanted in AMI Assessed by Optical Coherence Tomography/ ENDEAVOR® DES vs DRIVER bare metal stent vs Bare Metal Coronary Stent

The objective of this study is to evaluate the completeness of struts coverage and vessel wall response (strut malapposition, neointima disomogeneities in texture) to the ENDEAVOR DES vs the DRIVER stent (bare metal stent of identical metallic platform) implanted for the treatment of the culprit lesion in ST-elevation acute myocardial infarction (STEMI). To investigate the completeness of the coverage as well as the number of uncovered stent struts per section (embedded, uncovered, malapposed) and the neointima texture, high resolution (~ 10-15 µm axial) intracoronary optical coherence tomography (OCT) will be used.

Effect and Efficacy of Onyx™, Zotarolimus-eluting Stent for Coronary Atherosclerosis/ Resolute Onyx

The objectives of this study is to compare the long-term efficacy and safety of coronary stenting between the Resolute Onyx™ stent and other contemporary DESs which had established their own registry.

BioFreedom QCA Study in coronary artery disease Patients/ BioFreedom™ CoCr Biolimus A9™ stent vs BioFreedom™ SS Biolimus A9™ stent

This study aims to demonstrate that the BioFreedom™ Cobalt Chromium Drug Coated Stent is non-inferior to the market authorized BioFreedom™ Stainless Steel Stent with respective to efficacy and shows a similar safety profile.

Randomized Clinical Comparison of the Endeavor and the Cypher Coronary Stents in Non-selected Angina Pectoris Patients/ Endeavor vs Cypher Select

Randomized clinical comparison of the sirolimus eluting Cypher stent and the zotarolimus eluting Endeavor stent.

MAGnesium-based Bioresorbable Scaffold in ST Segment Elevation MI/ MAGMARIS Sirolimus Eluting Bioresorbable Vascular Scaffold System (M-BRS) vs Biotronik ORSIRO Sirolimus Eluting Coronary Stent System

This is a prospective, randomized, active control, single-blind, non-inferiority, multicenter clinical trial. All eligible patients (STEMI < 12 hours from onset of chest pain) will be randomized to Biotronik MAGMARIS™ Sirolimus Eluting Bioresorbable Vascular Scaffold System (M-BRS) or Biotronik ORSIRO Sirolimus Eluting Coronary Stent System

Comparison of Titanium-Nitride-Oxide Coated Bio-Active-Stent (Optimax™) to the Drug (Everolimus) -Eluting Stent (Synergy™) in Acute Coronary Syndrome/ Titanium-Nitride-Oxide Coated Bio-Active-Stent (Optimax™) vs Drug (Everolimus) -Eluting Stent (Synergy™)

The purpose of the prospective, randomized and a multicenter trial is to compare clinical outcome in patients presenting with ACS, treated with PCI using Optimax-BAS versus Synergy-EES.

Drug Eluting Stent (DES) in Primary Angioplasty/ Drug Eluting Stent (DES)

Stent implantation is the best treatment in patients with acute myocardial infarction (STEMI) referred for primary angioplasty (pPCI). However the occurrence of ISR is responsible for the need of repeat intervention. Both Sirolimus-eluting stents (SES) and Paclitaxel-eluting

stents (PES) have been proven to virtually abolish ISR in elective patients in simple e more complex lesions. Both SES and PES have raised concerns regarding occurrence of late stent thrombosis, especially in complex lesion subsets or in high risk patients. The PaclitAxel or Sirolimus-Eluting Stent vs Bare Metal Stent in primary angioplasty (PASEO) trial was a prospective, single-center, randomized trial evaluating the benefits of SES or PES as compared to BMS implantation in patients undergoing primary angioplasty for acute STEMI.

The OCT SORT-OUT VIII Study/ Everolimus eluting bioresorbable polymer stent vs Biolimus eluting bioresorbable polymer stent

The purpose of this study is to compare early vessel healing after implantation of SYNERGY drug eluting stent (DES) or BioMatrix NeoFlex DES at one and three months in two cohorts.

A Trial of Everolimus-eluting Stents and Paclitaxel-eluting Stents for Coronary Revascularization in Daily Practice: The COMPARE Trial/ everolimus stent vs paclitaxel stent

The main objective of the study is to compare the everolimus coated XIENCE-V™ stent with the paclitaxel coated TAXUS™ stent in order to observe whether there is a difference in clinical outcome between both stents.

The SCRIPPS DES REAL WORLD Registry/ Cypher™ Sirolimus-Eluting Stent

The registry is conducted for the evaluation of the impact of Cypher™ Sirolimus-eluting stent implantation in the "real world" of interventional cardiology.

Trial of Drug Eluting Stent Versus Bare Metal Stent to Treat Coronary Artery Stenosis/ BMS vs DES

The purpose of this trial is to compare the long-term effects on MI and total mortality of BMS vs DES. The patients will be randomized to treatment with BMS or DES. Clinical events will be registered for 5 years after treatment.

Coronary Microcirculatory and Bioresorbable Vascular Scaffolds/ Bioresorbable Vascular Scaffolds Versus Metallic Drug-eluting Stents

These narrowings can be opened using a balloon and stent (angioplasty). Traditionally, stents are constructed from metal and are permanent. However, newer stents are being constructed from carbohydrate polymers (scaffolds), which allow them to reabsorb over time leaving no permanent implant. New data has suggested that these scaffolds appear to reduce recurrent angina and may alter the blood flow down the artery. However, it is not known whether this is due to the scaffolds themselves or the way the scaffolds are inserted. In this study we hope to measure the blood flow to the heart and assess changes in that flow during stent and scaffold insertion. It is also important to know whether these effects are durable and thus, a cohort of patients will return at 3-months to be restudied. These data are important to help us understand why blood flow is affected by stent/scaffold selection or device implantation technique and whether this results in better long-term outcomes.

Everolimus-EIUtInG BioresorbAble VasculaR Scaffolds vErsus EVerolimus-Eluting Stents in Patients With Diabetes Mellitus/ Absorb GT1 EverolimuS-EIUtInG BioresorbAble VasculaR Scaffolds vs

Promus everolimus-eluting stent

Prospective, randomized, controlled, multicenter, open-label study to compare everolimus-eluting bioresorbable vascular scaffolds to everolimus-eluting stents in patients with diabetes mellitus.

The Effect of Prolonged Inflation Time During Stents Deployment for ST-elevation MI

The purpose of this study is to determine whether prolonged inflation time on DESs deployment for ST-elevation myocardial Infarction was better than conventional stents deployment.

Safety and Effectiveness Evaluation of COBRA PzF Coronary Stent System: A Post Marketing Observational Registry/ Deploying the Drug-eluting Stents with a prolonged time vs deploying the Drug-eluting Stents with a conventional time COBRA PzF Cobalt Chromium stent Coronary Stent System

A multi-center, prospective, consecutive enrolled, observational registry with patients in whom the COBRA PzF coronary stent was implanted.

Biofreedom Prospective Multicenter Observational Registry/ Biofreedom drug-coated stent

LEADERS-FREE trial demonstrated the safety and efficacy of polymer-free drug-coated stent in patients with high bleeding risk. The purpose of this registry is to evaluate the safety and efficacy of Biofreedom stent in patients with coronary artery disease.

Zotarolimus-Versus Sirolimus-Versus PacliTaxel-Eluting Stent for Acute MI Patients/ Endeavor vs Cypher, vs Taxus Liberte

To compare the safety and effectiveness of primary acute MI intervention with ABT 578-eluting balloon expandable stent vs. sirolimus-eluting balloon expandable stent vs. paclitaxel-eluting stent.

Leaders Free III: BioFreedom™ Clinical Trial/ BioFreedom™ BA9™ drug-coated stent

A study evaluating the safety and efficacy of the BioFreedom™ Biolimus A9™ coated Cobalt Chromium coronary stent system in patients at high risk of bleeding

The Direct III Post Market Study/ SLENDER IDS Sirolimus-Eluting Coronary Stent

The primary objective of this multicenter, single-arm, observational study is to evaluate the feasibility of a systematic direct stenting strategy with the Svelte SLENDER IDS Sirolimus-Eluting Coronary Stent-on-a-Wire Integrated Delivery System (SLENDER IDS) in an all-comers, real-world population.

Comparison of Diabetes Mellitus and Non-diabetes Mellitus Patients for DES Surface COVERage by OCT/ Polymer-based sirolimus-eluting Cypher stent vs Polymer-free paclitaxel-eluting YinYi stent

The aim of this study was to analyze the surface coverage and late malapposition after two types of DES implantation in DM patients compared with non-DM patients by using OCT and IVUS.

Assessment of Surface Coverage of Two Types of DES in Diabetes Mellitus and Non-Diabetes Mellitus/ Polymer-based sirolimus-eluting Cypher stent vs Polymer-free paclitaxel-eluting YinYi stent

The aim of this study was to analyze the surface coverage and late malapposition after two types of DES implantation in DM patients compared with non-DM patients by using OCT and IVUS.

EXCELLA Post-Approval Study/ DESyne Novolimus Eluting CSS

The aim of this study is to evaluate the long-term safety and performance of the DESyne Novolimus Eluting Coronary Stent System and the DESyne BD Novolimus Eluting Coronary Stent System.

DURable Polymer-based STent CHallenge of Promus Element Versus ReSolute Integrity in an All Comers Population/ Resolute Integrity Zotarolimus-eluting stent vs Promus Everolimus-eluting stent

The introduction of DES in the treatment of coronary artery disease has led to a significant reduction in morbidity but there are further demands on DES performance. Such demands are an optimized performance in very challenging coronary lesions; third generation DES were developed in an effort to further improve DES performance in such challenging lesions. Two CE-certified third generation DES (Resolute Integrity and Promus Element stents) are currently available; there are no data that indicate an advantage of one of these DES over the other.

Absorb IV Randomized Controlled Trial/ Absorb BVS vs XIENCE stent

The ABSORB IV Randomized Controlled Trial (RCT) is designed to continue to evaluate the safety and effectiveness as well as the potential short and long-term benefits of Abbott Vascular Absorb™ Bioresorbable Vascular Scaffold (BVS) System, and the Absorb GT1™ BVS System (once commercially available), as compared to the commercially approved, control stent XIENCE.

A First-in-Man Study of the Firesorb BVS (FUTURE-I)/ Sirolimus Target Eluting Bioresorbable Vascular Scaffold

This study is a small scale pilot trial for Sirolimus Target Eluting Bioresorbable Vascular Scaffold (Firesorb) in Patients with Coronary Artery Disease for the first time. The goal is to assess the preliminary safety and efficacy of Firesorb implantation in the human body, and to provide evidence for subsequent large-scale, multi-center, randomized controlled clinical trials.

Italian Diffuse/Multivessel Disease ABSORB Prospective Registry: IT-Disappears/ ABSORB stent

The purpose of this study is to determine whether patients with diffuse or multivessel coronary artery disease may benefit from the percutaneous implantation of the device ABSORB in larger extent with respect to the general population of patients undergoing percutaneous treatment of coronary artery disease.

ABSORB III RCT/ Absorb BVS vs XIENCE stent

The ABSORB III RCT is a prospective randomized, single-blind, multi-center trial. It is the pivotal trial to support the US pre-market approval (PMA) of Absorb™ Bioresorbable Vascular Scaffold (BVS).

AVJ-301 Clinical Trial: A Clinical Evaluation of AVJ-301 (Absorb™ BVS) in Japanese Population/ XIENCE PRIME® vs XIENCE Xpedition™ vs Absorb™ BVS

Prospective, Randomized (2:1), active control, single-blind, non-inferiority, multicenter, Japanese Clinical Trial to evaluate the safety and effectiveness of Absorb™ BVS (AVJ-301) in the treatment of subjects with ischemic heart disease caused by de novo native coronary artery lesions in Japanese population by comparing to approved metallic drug eluting stent.

First in Man Study of the DREAMS 2nd Generation Drug Eluting Absorbable Metal Scaffold (BIOSOLVE-II)/ Drug Eluting Absorbable Metal Scaffold (DREAMS 2nd Generation)

BIOSOLVE-II is a prospective, international, multicenter, First in Man study. The purpose of this study is to assess the safety and clinical performance of the drug eluting absorbable metal scaffold (DREAMS 2nd Generation).

Feasibility and Outcomes of Complete Coronary Revascularization Using BVS in All-comer Patients With Angina/ Bioresorbable vascular scaffold (BVS)

The aim of the study is feasibility of complete coronary revascularization with bioresorbable vascular scaffold (BVS) implantation and assessment of treatment outcomes in a group of consecutive patients with stable and unstable angina in Russian population.

Vascular Healing After BVS-implantation/ Absorb-BVS

Evaluation of coronary artery vessel wall healing at different time points in patients undergoing implantation of bioresorbable vascular scaffold by using intravascular imaging.

ABSORB FIRST is a Registry Designed to Evaluate the Safety and Performance of Absorb Bioresorbable Vascular Scaffold (Absorb BVS) Used in Real-world Patients./ Absorb Bioresorbable Vascular Scaffold

ABSORB FIRST is a prospective, multi-center registry. The objectives of the study are: (i) to provide ongoing post-market surveillance for documentation of safety, performance and clinical outcomes of the Absorb BVS (Bioresorbable Vascular Scaffold) System in daily PCI (PCI) practice per Instructions for Use (IFU, on-label use). (ii) to evaluate the safety and performance of 12 mm or shorter Absorb BVS in single or overlapping use (bailout, optimization of long lesion treatment) for the treatment of patients with ischemic heart disease caused by de novo native coronary artery lesion(s). (iii) to collect additional information (e.g. acute success) to evaluate handling and implantation of Absorb BVS by physicians under a wide range of commercial use conditions and following routine clinical practice.

NeoVas Bioresorbable Coronary Scaffold First-in-Man Study/ NeoVas Bioresorbable Sirolimus-eluting Coronary Scaffold

The hypothesis of the NeoVas First-in-Man study study is to evaluate clinical feasibility, safety, and efficacy of NeoVas sirolimus-eluting bioresorbable coronary scaffold in the treatment of patients with de novo coronary lesion.

IRIS-PREMIER REGISTRY/ Promus PREMIER™ Drug-Eluting Coronary Stent

The purpose of this study is to evaluate effectiveness and safety of Promus PREMIER in Routine Clinical Practice

Bifurcation ABSORB OCT Trial/ ABSORB BVS

The Bifurcation ABSORB OCT Trial is a prospective, randomized (1:1) evaluation of the efficacy and performance of single ABSORB everolimus eluting bioresorbable vascular scaffold provisional strategy in the treatment of (a) coronary bifurcation lesion(s) in consecutive subjects with and without fenestration towards the side branch.

NeoVas Bioresorbable Coronary Scaffold Registry Study/ NeoVas sirolimus-eluting bioresorbable coronary scaffold

The NeoVas Bioresorbable Coronary Scaffold Registry Trial is a prospective, multi-center, single arm registry trial based on the NeoVas FIM study which verified the safety and effectiveness of NeoVas initially. This study is to evaluate the safety and effectiveness of NeoVas sirolimus-eluting bioresorbable coronary scaffold in the treatment of patients with de novo coronary lesion.

A2. Stent design

In the following section, the main steps used in the creation of the 3D stent model are presented. The geometrical pattern of the “Reference Model” is depicted in Figure A2.1.

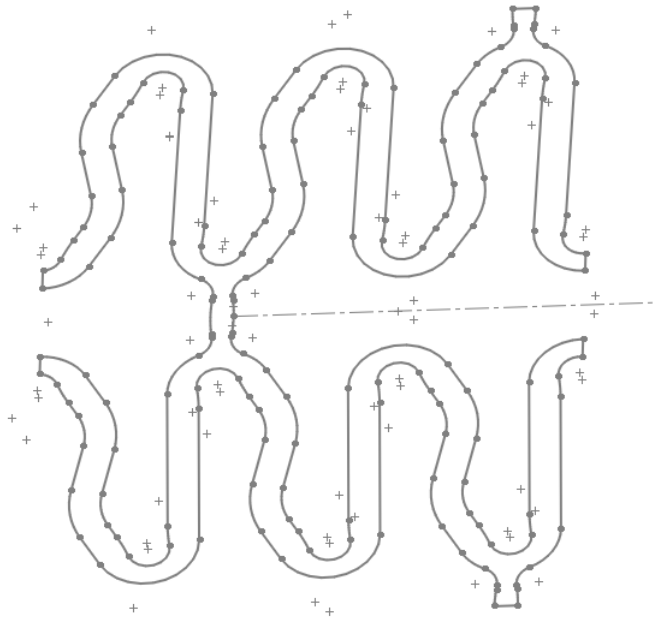


Figure A2.1 Geometrical pattern of the reference model.

STEP 1. We create another plane, where we make a sketch of two circles. The outer circle has a diameter of 1.39993mm whereas the thickness is 0.078mm. With the help of the “Extrude”  (2D to 3D) we extruded the base sketch

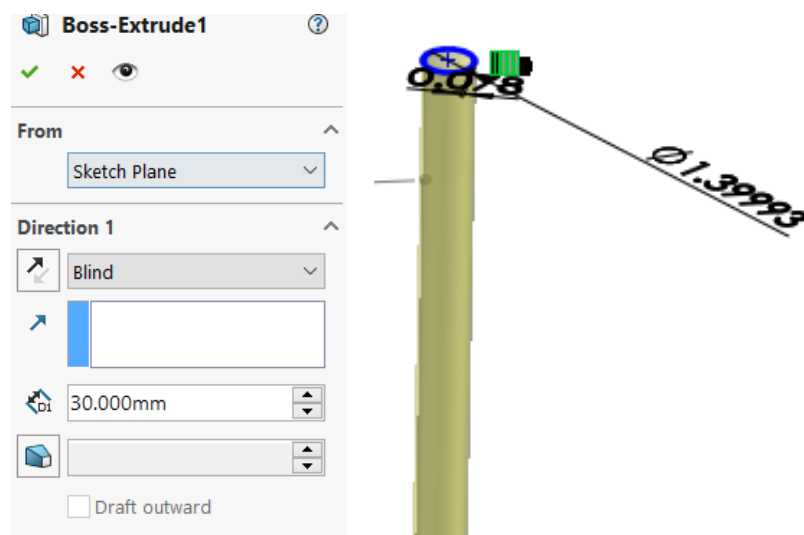


Figure A2.2 Boss extrude.

STEP 2. The wrap feature  supports contour selection and sketch reuse since it allows the projection onto the 3D cylinder (Figure A2.3).

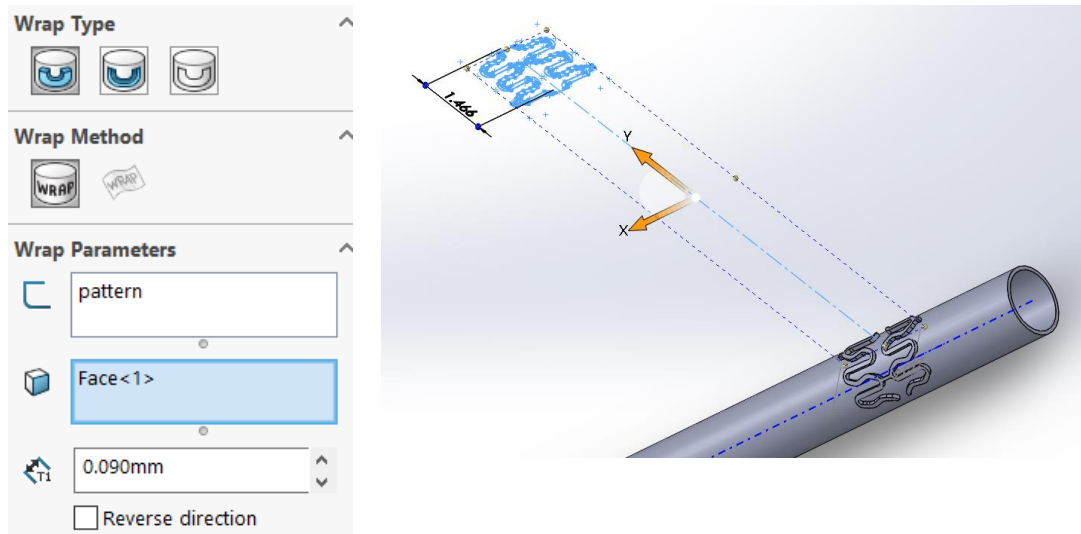


Figure A2.3 Wrap feature.

STEP 3. To create the extruded and revolved cut feature in this assembly the “Cut-Extrude” feature was selected.

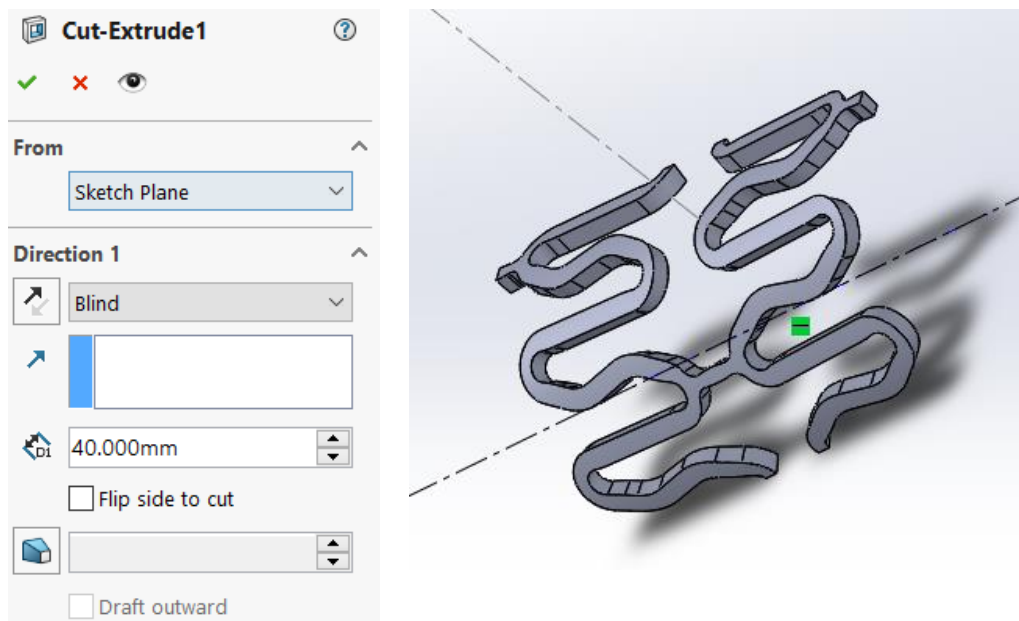


Figure A2.4 Cut- Extrude feature.

STEP 4. The Circular Pattern feature  was selected to pattern the 3D design of Figure 7 to four features around an axis.

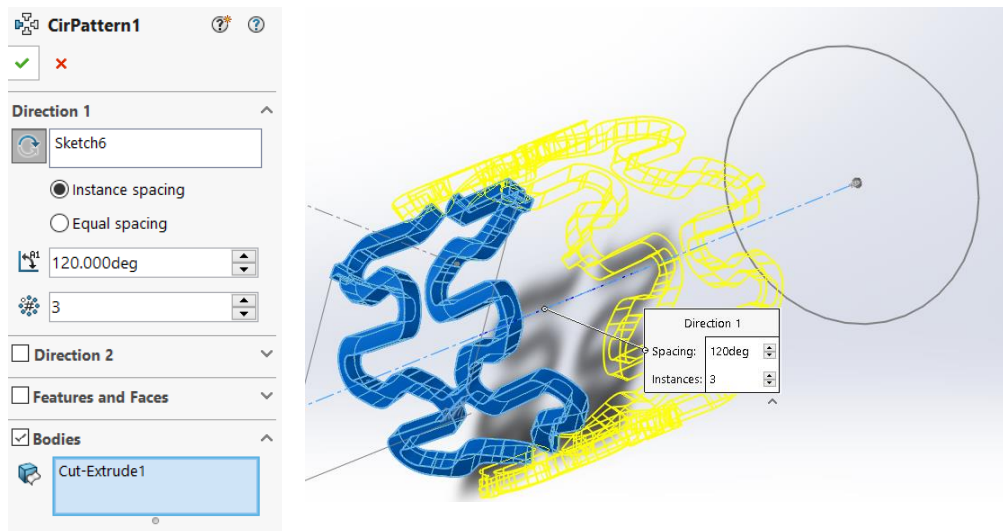


Figure A2.5 Circular pattern of the 3D design.

STEP 5. To create the 3D design (of Figure 8) along the linear path, the feature "Linear Pattern"  is used.

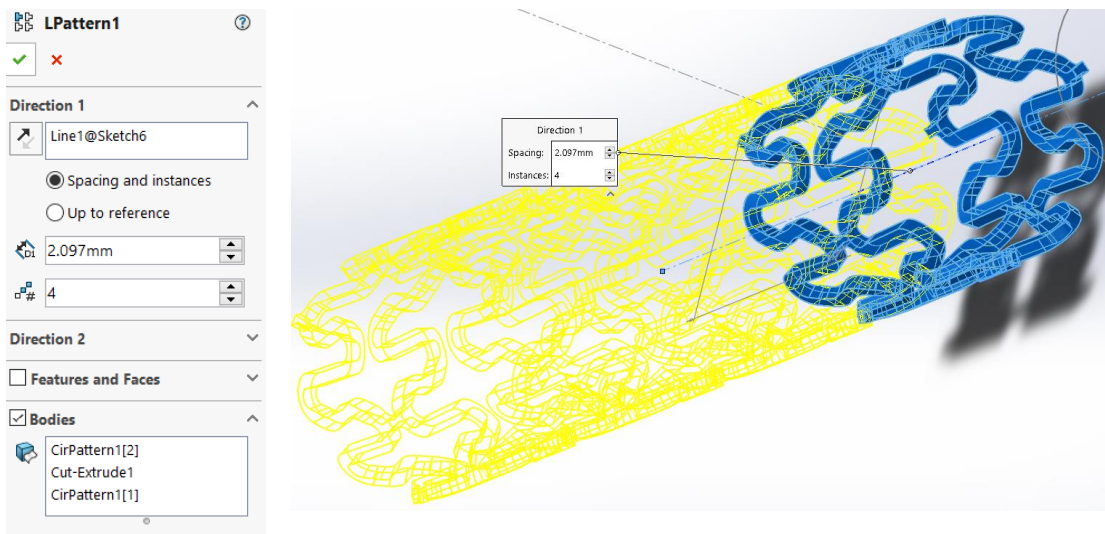


Figure A2.6 Linear pattern of the 3D design.

STEP 6. To create a unified geometry of the stent design the "Combine" feature  is utilised.

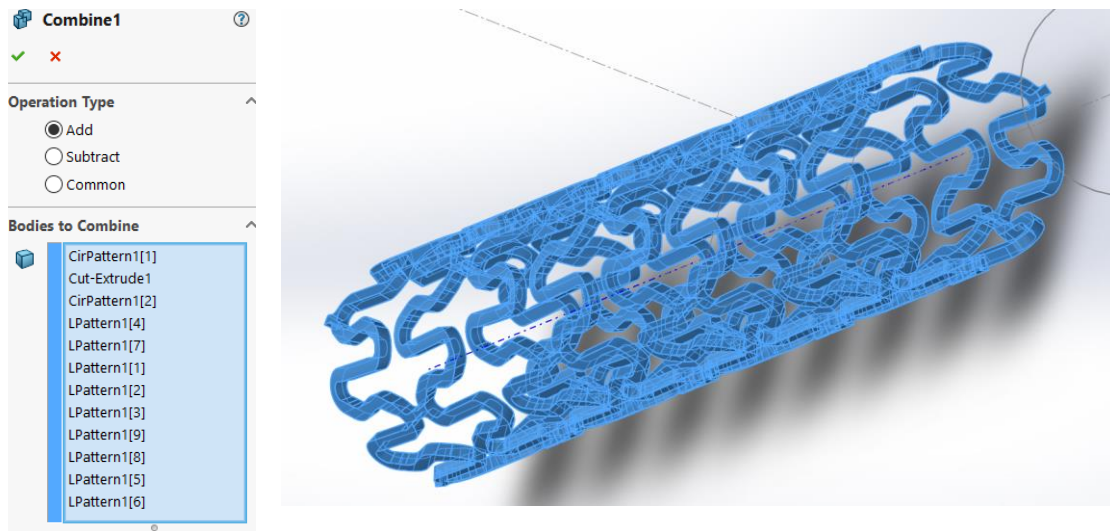


Figure A2.7 Combine all parts to one part.

A3. Mesh sensitivity

Details of the mesh used in the Mesh Sensitivity Analysis is presented below.

	Mesh A	Mesh B	Mesh C	Mesh D
Nodes	65202	129645	261794	227779
Elements	267702	611367	258373	203557
Stent Element Size	5.e-002 mm	5.e-002 mm	5.e-002 mm	5.e-002 mm
Artery part I Element size	0.2 mm	0.15 mm	0.25 mm	0.28 mm
Artery part II Element size	0.3 mm	0.2 mm	0.25 mm	0.28 mm
Face sizing	2.5e-002 mm	2.5e-002 mm	-	-
Midside nodes	No	No	Yes	Yes

Author's Publications

Journal publications

1. **G. Karanasiou**, M. Papafaklis, C. Conway, L. Michalis, R. Tzafiri, E. Edelman, D. Fotiadis, Stents: Biomechanics, Biomaterials, and Insights from Computational Modeling, *Ann Biomed Eng.* 2017 Apr;45(4):853-872. doi: 10.1007/s10439-017-1806-8. Epub 2017 Feb 3.
2. A. Sakellarios, **G. Karanasiou**, P. Siogkas, V. Kigka, T. Exarchos, G. Rigas, L. Michalis, D. Fotiadis, Available Computational Techniques to Model Atherosclerotic Plaque Progression Implementing a Multi-Level Approach, *Computational Biomechanics for Medicine*, pp 39-55, 2017.
3. **G. Karanasiou**, N. Tachos, L. Michalis, E. Edelman, D. Fotiadis, Effect of stent design and material on stent deployment., to be submitted.

Conference publications

1. A. Sakellarios, N. Tachos, E. Georga, G. Rigas, V. Kigka, P. Siogkas, S. Kyriakidis, **G. Karanasiou**, P. Tsompou, I. Andrikos, S. Rocchiccioli, G. Pelosi, O. Parodi, D. Fotiadis, A novel concept of the management of coronary artery disease patients based on machine learning risk stratification and computational biomechanics: Preliminary results of SMARTool project, *World Congress on Medical Physics and Biomedical Engineering 2018*, pp 629-633.
2. **G. Karanasiou**, N. Tachos, A. Sakellarios, C. Conway, G. Pennati, L. Petrini, L. Michalis, E. Edelman, D. Fotiadis, *In silico* analysis of stent deployment - effect of stent design, *Proceedings of 40th International Engineering in Medicine and Biology Conference*.
3. A. Sakellarios, P. Siogkas, E. Georga, N. Tachos, V. Kigka, P. Tsompou, I. Andrikos, **G. Karanasiou**, S. Rocchiccioli, J. Correia, G. Pelosi, P. Stofella, N. Filipovic, O. Parodi, D. Fotiadis, A Clinical Decision Support Platform for the Risk Stratification, Diagnosis, and Prediction of Coronary Artery Disease Evolution, *Proceedings of 40th International Engineering in Medicine and Biology Conference*.
4. **G. Karanasiou**, G. Rigas, S. Kyriakidis, N. Tachos, A. Sakellarios, D. Fotiadis, InSilc: 3D Reconstruction and plaque characterization tool, *Proceedings of 40th International Engineering in Medicine and Biology Conference*.
5. A. Sakellarios, G. Rigas, V. Kigka, P. Siogkas, P. Tsompou, **G. Karanasiou**, T. Exarchos, I. Andrikos, N. Tachos, G. Pelosi, O. Parodi, D. Fotiaids, SMARTool: A Tool for Clinical Decision Support for the Management of Patients with Coronary Artery Disease Based on Modeling of Atherosclerotic Plaque Process, *Conf Proc IEEE Eng Med Biol Soc.* 2017 Jul;2017:96-99. doi: 10.1109/EMBC.2017.8036771.
6. **G. Karanasiou**, N. Tachos, A. Sakellarios, C. Conway, E. Edelman, L. Michalis, D. Fotiadis, *In silico* assessment of the effects of material on stent deployment, 17th annual IEEE international conference on bioinformatics and bioengineering, 2017 IEEE 17th International Conference on Bioinformatics and Bioengineering (BIBE), DOI: 10.1109/BIBE.2017.00-11.
7. **G. Karanasiou**, C. Conway, M. Papafaklis, A. Lopes, K. Stefanou, L. Athanasiou, L. Michalis, E. Edelman, D. Fotiadis, Finite Element Analysis of Stent Implantation in a Three-Dimensional Reconstructed Arterial Segment, *Conf Proc IEEE Eng Med Biol Soc.* 2014;2014:5623-6. doi: 10.1109/EMBC.2014.6944902.
8. **G. Karanasiou**, A. Sakellarios, E. Tripoliti, E. Petrakis, M. Zervakis, F. Migliavacca, G. Dubini, E. Dordoni, L. Michalis, D. Fotiadis, Modeling stent deployment in realistic arterial segment geometries: the effect of the plaque composition, 13th international conference on bioinformatics and bioengineering, BIBE 2013, DOI: 10.1109/BIBE.2013.6701537.
9. **G. Karanasiou**, A. Sakellarios, E. Tripoliti, M. Petrakis, M. Zervakis, F. Migliavacca, G. Dubini, E. Dordoni, L. Michalis, D. Fotiadis, Modeling of stent implantation in a human stenotic artery, XIII Mediterranean Conference on Medical and Biological Engineering and Computing 2013 pp 1045-1048.

Book Chapters

1. **G. Karanasiou**, E. Tripoliti, E. Edelman, L. Michalis, D. Fotiadis, Stent deployment computer based simulations for health care treatment of diseased arteries, *Concepts and Trends in Healthcare Information Systems*, pp 143-167.

Short CV

Georgia S. Karanasiou received her diploma from the Dept. of Mechanical Engineering & Aeronautics in the University of Patras. She participated in the European research project entitled "Real Time Simulation for Safer vascular Stenting - KAE 80252", in which she performed the computational modeling of the angioplasty procedure (stent) in obstructed coronary arterial segments. She also participated in the HORIZON2020 project SMARTool – Simulation Modeling of coronary ARtery disease: a tool for clinical decision support (GA 689068) and she is currently participating in the HORIZON2020 project InSilc - In-silico trials for drug-eluting BVS development and evaluation (GA 777119). Georgia S. Karanasiou has published 2 journal articles, 9 conference papers and 1 book chapter.